GEOMETRIC METHODS FOR EFFICIENT AND EXPLAINABLE

CONTROL OF UNDERACTUATED ROBOTIC SYSTEMS

Jake Welde

A DISSERTATION

in

Mechanical Engineering and Applied Mechanics

Presented to the Faculties of the University of Pennsylvania

in

Partial Fulfillment of the Requirements for the

Degree of Doctor of Philosophy

2025

Supervisor of Dissertation

Vijay Kumar

Professor of Mechanical Engineering and Applied Mechanics

Graduate Group Chairperson

Jordan R. Raney

Associate Professor of Mechanical Engineering and Applied Mechanics

Dissertation Committee

Daniel E. Koditschek, Alfred Fitler Moore Professor of Electrical and Systems Engineering

Michael Posa, Associate Professor of Mechanical Engineering and Applied Mechanics

Muruhan Rathinam, Professor of Mathematics and Statistics, University of Maryland, Baltimore County

James P. Ostrowski, Chief Technology Officer, Blue River Technology

ACKNOWLEDGEMENTS

I have often imagined writing these acknowledgements, and yet I hardly know where to begin to capture the incredible support that I have enjoyed during my time here at Penn. The PhD itself is an improbable exercise, seemingly bordering on a fool's errand—that a novice should create new knowledge for humanity. Such a task becomes feasible only through the guidance, mentorship, and encouragement of so many others, as well as the time, space, and security in which to explore freely. Having started here as an undergrad, Penn has been my home for my entire adult life—a period of intense transformation for me, both personally and professionally. I am filled with immense gratitude, and I will miss this place dearly.

I am so thankful to my advisor, Vijay Kumar, who first welcomed me into his lab as a wide-eyed freshman and agreed to let me stick around as a graduate student. Vijay has always made his trust in me clear—encouraging me to take leaps where I would have hesitated—and his calm confidence has provided an essential counterpoint to my own doubts and anxieties at so many points along the road. The incredible agency Vijay has given me to explore my own interests, and to dabble in areas that may not lead immediately to publications, has been essential in cultivating my own research tastes and discovering which questions really keep me up at night. Vijay has opened doors for me at every turn, always knowing what paper to read or which person to ask any question. His extraordinary breadth and depth of experience have ensured that my own wandering was always guided and grounded by his wisdom.

Justin Thomas was my first direct research mentor, who gladly spent hours teaching me the basics of quadrotor control and differential flatness (long before I had any business doing either of those things). Seeing his work in the lab convinced me that grad school seemed like a pretty fun idea (even though I had no plans to become an academic). Justin also modeled remarkable work-life harmony as a grad student, showing me that great research should be complemented by a great life outside the lab. I cherish the friendship that has grown out of what began as an impactful mentor-mentee relationship.

I owe an enormous amount to Matthew Kvalheim, who I first began working with after he replied to my (very niche) post-seminar question with several pages of detailed LaTeX notes, a mere three days later. Matthew's fathomless technical depth is rivaled only by his generosity with his time. His patient mentorship took my vague and bumbling interest in geometry to the point of publishing my first mathematically rigorous work, and I haven't looked back since. Some of my best memories of research in grad school were hours spent on Zoom learning from Matthew and working through research questions together. His frequent advice on all things academic (from attention to detail, to working one's way into new professional communities, to the job market) has been a constant resource. In many ways, Matthew has been almost like a second advisor to me, and I eagerly look forward to seeing the success of his own PhD students.

I sincerely thank my thesis committee for their thought-provoking questions and helpful criticisms. Michael Posa's grounded critiques have helped me learn to communicate better and align my abstract interests to practical impact, a goal I continue to strive towards with his guidance in mind. I deeply appreciate Dan

Nicole Luna, and Eshan Singhal) get an early taste of academic research was another rewarding outlet. In my forays into hardware, Fernando Cladera has always been ready to lend masterful advice or just the right piece of equipment. Many thanks also to Jeremy Wang and Britny Major for their skillful fabrication assistance, and to Matt Piccoli and Luca Scheuer for help with the finer points of brushless motor control.

MEAM and GRASP are strong communities. They operate smoothly thanks to the efforts of skilled and compassionate administrators, and I am grateful that any issue I encountered could be quickly resolved by Peter Litt, Charity Payne, Jill Mallon, or Justin Nachea. I am also enormously thankful for the many friends I have found along the way within these communities—from early days in our MEAM cohort with Spencer Folk, Greg Campbell, and Parker LaMascus, to lab ski trips planned by Anish Bhattacharya and the unofficial GRASP volleyball team captained by Matt Malencia. Anusha Srikanthan has always been ready for a heartfelt conversation about life, research, career, or nothing much at all, and Fridays have long been my favorite day of the week, thanks to weekly lunches with my labmates. Parker and Kennedy McAlister have become lifelong friends—the first time I really felt like grad school was coming to an end was when they moved away. To those not mentioned by name, know that I value you all the same.

Grad school is full of backtracks and meanders (case in point—the chapters in this thesis were written in the following order: 4, 2, 3, 6, 5, 7, 1, 8). The ups and downs of my life and the world at large over the last six years included a global pandemic, family illness and death, and far greater self-doubt than I'd ever encountered before. It is my family who got me through this, and their contributions began long before I arrived at Penn and will continue long after departing—thank you. To my mom, for supporting and enabling my education and growth at every juncture for nearly three decades, and for never doubting me once—even when I am my own harshest critic. To my dad, for nurturing my early interest in programming and computers. To my grandma, whose day-to-day role in my life was a blessing, and whose absence is felt acutely. To my sister Megan, for sharing your unique brand of humor and knowing "where I come from" like no one else. Lastly, to my fiancée Anna, who has witnessed every (and I mean *every*) up and down of this journey—you have helped me become better at riding these waves without letting them consume me. I cherish your delight in my attempts to describe to you the details of my work or my latest research hunch, and your support has been constant and unfailing. It is a joy to be your partner in life!

<div align="right">

Jake Welde

July 21, 2025

Philadelphia, PA

</div>

ABSTRACT

GEOMETRIC METHODS FOR EFFICIENT AND EXPLAINABLE CONTROL OF UNDERACTUATED ROBOTIC SYSTEMS

Jake Welde

Vijay Kumar

Robots are complex, high-dimensional systems governed by nonlinear, underactuated dynamics evolving on non-Euclidean manifolds, posing numerous challenges for control synthesis and analysis. While optimization-based methods of control can flexibly accommodate diverse dynamics, costs, and constraints, they often demand coarse approximations or powerful onboard processors due to their relatively poor computational efficiency. Meanwhile, learning-based controllers require offline training that is often brittle and computationally burdensome. Conversely, explicit, analytical control laws with negligible computational overhead often perform robustly, but they are typically only applicable to individual systems (or a narrow class), limiting their broader usefulness.

However, robots are not black-box nonlinear control systems—rather, their dynamics enjoy powerful properties (*e.g.*, symmetry and mechanical structure) that can provide traction on control design problems. In this thesis, we explore the role of geometric methods in mitigating many of the above drawbacks, across both analytical and data-driven methods. We study the role of symmetry in systematically identifying effective abstractions for trajectory planning ("flat outputs") in underactuated mechanical systems and explore applications to aerial manipulation. We also synthesize explicit tracking controllers for mechanical systems evolving on homogeneous Riemannian manifolds, and certify the almost global asymptotic stability of cascades (commonly seen in the closed-loop dynamics of hierarchical controllers). Lastly, we accelerate the training of tracking controllers via reinforcement learning using symmetry reduction, also improving the converged policy.

In each method, a geometric perspective enables us to explainably construct abstractions that reduce dimensionality, enforce structure, and capture essential features, ultimately representing the system or problem in a form more convenient for analysis or design. Such reduced representations typically improve computational efficiency, while also encouraging generality over a broader class of systems and affording insight into *why* prior handcrafted approaches succeeded. Such realizations can also guide mechanical design, closing the control-morphology feedback loop and leading to synergies between a robot's embodiment and its controller. By combining explainable abstractions with scalable computation, such methods build towards a future in which robotic systems move through their surroundings as capably and dynamically as their counterparts in Nature.

TABLE OF CONTENTS

LIST OF TABLES

LIST OF ILLUSTRATIONS

Car c'est une remarque que nous pouvons faire dans toutes nos recherches mathé-matiques : ces quantités auxiliaires, ces calculs longs et difficiles où l'on se trouve entrainé, y sont presque toujours la preuve que notre esprit n'a point, dès le com-mencement, considérés les choses en elles-mêmes et d'une vue assez directe, puisqu'il nous faut tant d'artifices et de détours pour y arriver; tandis que tout s'abrége et se simplifie sitôt qu'on se place au vrai point de vue.

For we may remark generally of our mathematical researches, that these auxiliary quantities, these long and difficult calculations into which we are often drawn, are almost always proofs that we have not in the beginning considered the objects themselves so thoroughly and directly as their nature requires, since all is abridged and simplified, as soon as we place ourselves in a right point of view.

—**Louis Poinsot**, *Théorie nouvelle de la rotation des corps*, 1851.

Translation by Charles Thomas Whitley.

CHAPTER 1

INTRODUCTION

Robots are *embodied* systems—in order to deliver the practical benefits that our discipline has promised society, they must move capably and intelligently through the world. Inherent to this challenge is the problem of *control synthesis*—in short, how can we design algorithms that choose the appropriate actuator commands to autonomously and reliably achieve a desired robot behavior?

1.1 Fundamental Challenges in the Control of Robotic Systems

Such control design problems can be very challenging. In particular, robotic systems evolve on high-dimensional non-Euclidean manifolds, governed by complex, nonlinear dynamics and subject to underactuation constraints. In consideration of these attributes, and in admiration of the incredible capabilities that animals exhibit in Nature, we consider several fundamental challenges that emerge in the design of control algorithms for these systems:

1. **Computational Efficiency:** As the complexity robotic systems draws ever nearer to the richness of Nature, our approach to control synthesis must scale gracefully as well, renouncing brute computational force in favor of solutions that can accommodate complex, high-dimensional systems with ease. In particular, agile systems like aerial and space robots are typically outfitted with lightweight or radiation-hardened processors, requiring controllers that adhere to stringent computational budgets in order to achieve real-time operation. Additionally, the rapidly escalating computational cost of training data-driven control policies raises concerns over environmental impact as well as egalitarianism in scientific research. Finally, computationally efficient algorithms can run on inexpensive processors, improving societal access to robotic innovation, facilitating the deployment of large swarms, and enabling economical use of robots in dangerous environments with high risk of damage.

2. **Generality Across Morphologies:** The extraordinary morphological variation we observe in Nature reflects the diversity of ecological niches occupied by disparate species. In much the same manner, as we develop robotic systems capable of performing ever more varied tasks, their morphological variety will also increase rapidly, requiring generalized methods that can accommodate this diversity, instead of handcrafting solutions for individual systems. However, "good general theory does not search for the maximum generality, but for the right generality", in the words of Mac Lane [1]. Thus, we seek methods of control synthesis that improve efficiency, robustness, or performance by leveraging the structure enjoyed by a well-defined class of systems (even if this may exclude others). We aim to renounce ad hoc or bespoke solutions in favor of understanding the essential characteristics underlying a method's success, thereby expanding its domain of applicability.

3. **Global Performance:** Applying linear analysis and synthesis techniques to nonlinear systems requires "zooming in" on a local operational domain of interest. However, in order to exploit a system's full hypothetical performance envelope, performing dynamically over a wide range of conditions (as in Nature), we require techniques that can accommodate the changing, nonlinear character of the system over its full state space. Moreover, the state spaces of robotic systems are typically non-Euclidean, and thus globally valid formulations must be fundamentally compatible with the system's topological and geometric characteristics.

Broadly speaking, the objective of this thesis is the development of methods for the control of underactuated robotic systems that exhibit these favorable characteristics.

1.2 The Role of Abstraction

A central theme will be the development of *abstractions* that are particularly amenable to control design or analysis. A good abstraction eliminates extraneous details while still capturing all essential features of the problem, thereby "giving the same name to different things", in the words of Poincaré [2]. Thus, we study properties that persist across systems, leading to broadly-useful abstractions that afford understanding, beget efficient algorithms, and obviate bespoke methods. Most crucially, abstraction is a means of changing our "point of view" on a problem. This notion of perspective is perhaps best captured in our chosen epigraph (due to Poinsot, whose geometric characterization of the unforced motion of a freely-rotating rigid body was a founding result in geometric mechanics [3]).

Of course, it's worth recognizing that Poinsot wrote these words some decades prior to the first inklings of computational complexity theory, and thus lacked a formal understanding that many computational problems are (simply put) *hard* on a more fundamental level. Nonetheless, his words are at a minimum an ideal to which we should aspire. In many of the solutions presented in this thesis, the success of the method relies on finding an alternative representation of the system (a "right point of view") in which the problem ends up being easier to solve. Such an abstraction may be of lower dimension, of simpler (*e.g.*, linear) structure, free of constraints, or independent of time variation. Abstraction may also allow us to decompose the problem into smaller, decoupled subproblems that are more easily addressed. Nonetheless, in each case, such abstractions must fundamentally preserve those characteristics of the original system that are essential to the problem at hand.

1.3 Geometric Control of Robotic Systems

In this thesis, we use a range of analytical tools to develop such abstractions, but a particularly central role is played by differential geometry, a natural language for describing systems evolving over time while subject to smooth structural constraints. By working natively on the non-Euclidean manifolds where such systems evolve, we also innately ensure validity throughout the entire state space. In addition, we

draw from decision and control theory (in order to to develop solutions for a class of systems, instead of just one example) and dynamical systems theory (to characterize a system's long-term behavior, even when its exact trajectory is unknown), as well as learning and optimization (to take full advantage of the computational resources available when closed-form solutions are not viable).

When tackling a problem via abstraction (and therein, creating a *new* problem to solve), the burden of proof is on *us* to demonstrate that we ultimately obtain a meaningful solution to the *original* problem (*i.e.*, the abstraction should be "lossless", or losses should at least be bounded or quantified). Thus, mathematical rigor is essential in order to relate our abstract solutions to the concrete problem we originally faced. However, for the complexity and diversity of robotic systems to ultimately reach even a fraction of the splendor of Nature, we believe that as a community, our methods of control synthesis will need to systematically leverage *both* formal insights *and* scalable computational tools. Finally, as robots of diverse morphologies proliferate, exiting the laboratory into the real world, it seems more crucial than ever to develop *explainable* algorithms—we must understand *why* and *when* our methods work, so they can be applied broadly and with confidence.

1.4 Roadmap and Contributions

The subsequent chapters in this thesis make up three parts. First, in Chapter 2, we provide a crash course in certain essential aspects of differential geometry. While this overview is limited and cannot cover all topics in detail, it is hopefully enough to give the reader some basic familiarity with the mathematical toolkit that will be used throughout the thesis. Second, in Chapters 3 and 4, we consider aspects of trajectory planning, in particular related to the property of "differential flatness". We develop methods for systematically identifying "flat outputs" that both exploit and respect a natural symmetry of the system, and such abstractions aid in more conveniently representing the family of dynamically feasible trajectories of the system. Third, in Chapters 5, 6, and 7, we develop methods relevant to the design and certification of "tracking controllers" that drive a system asymptotically towards the planned reference trajectory. Towards those goals, we design explicit control laws suitable for fully-actuated systems and develop compositional stability certificates which could (in principle) extend such methods to a hierarchical setting, suitable for many underactuated systems. To close this section, we explore how symmetry-informed methods can accelerate learning algorithms for tracking controller synthesis. Finally, we discuss the limitations of these contributions and identify opportunities for future work in Chapter 8. In the remainder of this introduction, we describe in greater detail the contributions of each chapter in the body of this thesis.

1.4.1 Geometric Flat Outputs of Mechanical Systems with Symmetry

The evolution of a mechanical system can be described on a "principal bundle" arising from its inherent symmetries, and the ensuing factorization of the configuration manifold into a "symmetry group" and an internal "shape space" has provided deep insights into the locomotion of many robotic and biological

systems. On the other hand, the property of "differential flatness" has enabled efficient, effective planning and control algorithms for various robotic systems, yet a practical means of finding a flat output for an arbitrary robotic system (or ensuring that it preserves the fundamental symmetries of the system) remains an open question. In Chapter 3, we demonstrate new connections between these two domains, directly employing symmetry to construct a flat output. We provide sufficient conditions for the existence of a trivialization of the bundle in which the group variables themselves are a flat output, which we call a "geometric flat output", to underscore connections with the geometric mechanics literature. Moreover, when the system's symmetry is of a sufficiently strong flavor, we can ensure that the mappings both to and from the flat space preserve this symmetry (*i.e.*, they are equivariant). In such a trivialization, the motion planning problem is easily solved, since a given trajectory for the group variables will fully determine the trajectory for the shape variables that exactly achieves this motion.

A central hypothesis of our sufficient condition is the knowledge of a so-called "orthogonal section", a certain kind of smooth function which is orthogonal to a certain computable distribution. Closed form solutions for such a section often exist, and sometimes yield flat outputs in agreement with those previously discovered through ad hoc means. However, in general, determining such a section amounts to solving an underdetermined system of nonlinear partial differential equations. Thus, we develop computational tools which approximate such solutions numerically, ultimately showing close numerical agreement with known closed-form solutions for certain example systems.

1.4.2 Dynamically Feasible Task Space Planning for Underactuated Aerial Manipulators

In Chapter 4, we address the problem of planning dynamically feasible trajectories for underactuated aerial manipulators (consisting of an underactuated quadrotor equipped with an n-joint manipulator arm) that achieve a desired trajectory for the end effector. In particular, we show that the combined underactuated system is differentially flat—however, the flat outputs obtained do not, in general, correspond directly to the motion of the end effector (whose prescription is the obvious task of interest). We therefore develop a method which determines the family of flat output trajectories which will exactly produce any desired task trajectory, even in the case of dynamic maneuvers. We also give criteria on the manipulator geometry which will ensure certain important stability properties in our planning algorithms, informing hardware design. The proposed approach is demonstrated in simulation for aerial manipulators of varying geometry and number of joints performing several different tasks. The simultaneous resolution of the kinematic and dynamic constraints allows these tasks to be performed dynamically without sacrificing accuracy.

1.4.3 Almost Global Asymptotic Tracking on Homogeneous Riemannian Manifolds

In Chapter 5, we address the design of explicit tracking controllers that drive a mechanical system's state asymptotically towards a reference trajectory. In particular, we consider fully-actuated systems evolving

on the broad class of homogeneous Riemannian manifolds (encompassing all vector spaces, Lie groups, and spheres of any finite dimension, among other cases). In this setting, the transitive action of a Lie group on the configuration manifold enables an intrinsic description of the tracking error as an element of the state space, even in the absence of a group structure on the configuration manifold itself (*e.g.*, for $\mathbb{S}^2$). Such an error state facilitates the design of a generalized control policy depending smoothly on state and time, which drives the geometric tracking error to a designated origin from almost every initial condition, thereby guaranteeing almost global convergence to the reference trajectory. Moreover, the proposed controller simplifies elegantly when specialized to a Lie group or the n-sphere. The proposed approach is a unified, intrinsic controller guaranteeing almost global asymptotic trajectory tracking for fully-actuated mechanical systems evolving on a broad class of manifolds. In particular, we demonstrate the method as applied to reduced attitude tracking for an axisymmetric satellite and to position and orientation tracking for an omnidirectional aerial robot.

1.4.4 Almost Global Asymptotic Stability of Cascades

In Chapter 6, we give sufficient conditions for the almost global asymptotic stability of a cascade in which the subsystems are almost globally asymptotically stable. (In fact, the main results can essentially be understood as a generalization of classical results on the stability of cascades whose subsystems are *globally* asymptotically stable.) In particular, if the decoupled subsystems are almost globally asymptotically stable and their only chain recurrent points are hyperbolic equilibria, then the boundedness of forward trajectories is sufficient for the almost global asymptotic stability of the full system. We show that unboundedness of such cascades is prohibited by growth rate conditions on the interconnection term and on a Lyapunov function for the restriction of the driven subsystem to the stable equilibrium of the driving subsystem.

In particular, a chain recurrent set of the required kind is enjoyed by several classes of systems common in geometric control (*e.g.*, gradient systems and dissipative mechanical systems), including the closed-loop dynamics of the tracking controllers proposed in Chapter 5. Our results stand in contrast to prior works that require either time scale separation, prohibitively strong disturbance robustness properties, or *global* asymptotic stability in the subsystems. Moreover, we believe these results (or perhaps extensions theoreof) have a role to play for underactuated systems in the design and certification of hierarchical controllers, whose closed-loop dynamics can often be expressed in cascade form.

1.4.5 Symmetry-Accelerated Reinforcement Learning for Trajectory Tracking Control

In prior chapters, particular structural properties (*e.g.*, full actuation, differential flatness, cascade structure, etc.) enabled us to develop particularly efficient or convenient methodologies for analysis and control of a certain class of systems. However, other systems may lack these properties entirely. In such settings, we may choose to turn towards more flexible techniques, in spite of their greater computational cost or lack of formal guarantees. In particular, reinforcement learning (RL) has shown promise in the synthesis

of controllers for systems with complex dynamics and modest online compute budgets. However, the poor sample efficiency of RL and the challenges of reward design make training slow and sometimes unstable, especially for high-dimensional systems.

In Chapter 7, we mitigate these challenges when training a tracking controller via reinforcement learning by leveraging the inherent Lie group symmetries of robotic systems with a floating base. We model a general tracking problem as a Markov decision process (MDP) that captures the evolution of both the physical and reference states. Next, we prove that symmetry in the underlying dynamics and running costs leads to an "MDP homomorphism", a mapping that allows a policy trained on a lower-dimensional "quotient" MDP to be lifted to a tracking controller for the original system (with value equivalence guarantees). We compare such a symmetry-informed approach to an unstructured baseline (trained directly on the original MDP), using Proximal Policy Optimization (PPO) to learn tracking controllers for three systems: the `Particle` (a forced point mass), the `Astrobee` (a fully-actuated space robot), and the `Quadrotor` (an underactuated system). Results show that a symmetry-aware approach both accelerates training and reduces tracking error at convergence.

CHAPTER 2

ASPECTS OF DIFFERENTIAL GEOMETRY

In this chapter, we review some essential aspects of differential geometry that will furnish the technical language of this thesis. We will assume that the reader has a moderate familiarity with smooth manifolds (providing only a brief review), and present a limited exposition of Riemannian geometry and Lie group theory, followed by a brief exploration of the structures induced a the action of Lie group on a smooth manifold with certain properties. The hope is to provide a "crash course" in the most relevant topics, so that a reader with some prior exposure to manifolds and Lie groups can acquire here a basic familiarity with our notation and those aspects of our toolkit less widely known in the robotics community. A reader with a comprehensive background in differential geometry may wish to skip ahead and reference the chapter only when needed.

Throughout this chapter (and the thesis more broadly), we will make considerable use of *commutative diagrams*, such as the following:

$$X \xrightarrow{f} Y \atop \searrow_{h} \downarrow_{g} \atop Z \tag{2.1}$$

We say that a diagram *commutes* if, for any pair of vertices in the directed graph of the diagram, traversing any path from the first vertex to the second vertex will yield the same result, when applied to any element of the space at the start vertex. To traverse a path, we evaluate the map given by the successive composition of the maps along each edge in the path. For example, the diagram in (2.1) commutes if and only if $(g \circ f)(x) = h(x)$ for all $x \in X$. Note that every node in the diagram also has an implicit "self-looping" edge back to itself, labeled with the identity map. Commutative diagrams thus provide a compact and illustrative means of describing relationships between maps, which we will use extensively.

2.1 Smooth Manifolds

We will give only a brief and relatively informal overview of smooth manifolds, mainly to make our notation clear. In particular, we have made an effort to unify the notation throughout the entire text, but we will also sometimes deliberately define multiple notations for the same concept, which will be more or less convenient depending on the point of view we wish to emphasize. We direct the less experienced reader to [4], which gives a thorough introduction to smooth manifolds (requiring little more background than undergraduate calculus), and [5, 6], which also explore advanced topics. Many of these concepts can also be found in texts more specically focused on geometric mechanics, such as [7–9]. In this thesis, we will consider control systems whose state spaces are, in general, smooth manifolds (not necessarily $\mathbb{R}^n$).

Roughly speaking, a space Q is a *smooth manifold* if it can be locally "thought of" as a Euclidean space $\mathbb{R}^n$ (whereas the *global* structure of Q may perhaps be very different). Perhaps the most familiar example is the sphere $\mathbb{S}^2$—in particular, any local region of the Earth's surface can be drawn on a paper map as a subset of $\mathbb{R}^2$, despite the fact that the Earth as a whole is not flat, but rather shaped roughly like $\mathbb{S}^2$. More precisely, the neighborhood of any point $q \in Q$ must be diffeomorphic to a local region of $\mathbb{R}^n$ (with the same n for all neighborhoods), where a *diffeomorphism* is a smooth, invertible map. We denote the set of all smooth maps from M to N (both manifolds) by $\mathsf{C}^\infty(M, N)$.

2.1.1 The Tangent and Cotangent Bundles

The *tangent space* at each point $q \in Q$ is given by

$$T_q Q = \left\{ \dot{\gamma}(0) : \gamma : (-\varepsilon, \varepsilon) \to Q \ \text{s.t.} \ \gamma(0) = q \right\}, \tag{2.2}$$

where each tangent vector can thus be thought of as an equivalence class of curves in "first-order contact". The *tangent bundle* is the collection of all the tangent spaces, namely,

$$TQ = \{(q, v_q) : q \in Q, v_q \in T_q Q\}, \tag{2.3}$$

where elements of the tangent bundle are often written with a subscript denoting their basepoint (*i.e.*, $v_q \in T_q Q$). Moreover, the *tangent bundle projection* is the map $\pi_Q : TQ \to Q, v_q \mapsto q$. Thus, the instantaneous velocity $\dot{q}$ of a smooth curve $q : \mathbb{R} \to Q$ lives in the tangent bundle TQ (and effectively encompasses both position and velocity *simultaneously*). We will sometimes write $(q, \dot{q}) \in TQ$ to further emphasize this point, but we try to avoid this notation since in general, $TQ \not\cong Q \times T_p Q$ for any point $p \in Q$.

Moreover, at each point $q \in Q$, the *cotangent space* $T_q^* Q$ is the dual of the tangent space, namely, the set of all linear maps $f_q : T_q Q \to \mathbb{R}$, and the *cotangent bundle* $T^* Q$ is the collection of all such cotangent spaces. The *natural pairing* allows us to compose any tangent and cotangent vectors at a given point, as $\langle f_q ; v_q \rangle := f_q(v_q) \in \mathbb{R}$. In mechanics, the velocity v_q live in the tangent bundle of the configuration manifold, while the force f_q live in the cotangent bundle, and their pairing gives the instantaneous rate at which mechanical work is being done on the system.

2.1.2 Vector Fields

A *vector field* on Q is a smooth map $V : Q \to TQ$ such that the following diagram commutes:

$$
\begin{array}{ccc}
 & & TQ \\
 & \overset{V}{\nearrow} & \downarrow \pi_Q \\
Q & \underset{\mathrm{id}}{\longrightarrow} & Q
\end{array}
\tag{2.4}
$$

where id is the identity map— in other words, $\pi_Q \circ V(q) = q$ for all $q \in Q$ (*i.e.*, the base point is preserved). $\mathfrak{X}(Q)$ denotes the set of all vector fields on Q, and $\mathfrak{X}^*(Q)$, the set of all covector fields on Q, is defined analogously. A *complete* vector field V is one for which unique solutions to the initial value problem

$$\dot{q}(t) = V\big(q(t)\big), \quad q(0) = q_0 \tag{2.5}$$

exist for all $t \in \mathbb{R}$ and from all initial conditions $q_0 \in Q$ (although unique solutions always exist on a sufficiently small interval). A complete vector field generates a flow Φ^V, where for each for $q_0 \in Q$, the curve $t \mapsto \Phi_t^V(q_0)$ is the solution to the corresponding initial value problem. The *Lie bracket* of vector fields is the operation $[\,\cdot\,,\,\cdot\,] : \mathfrak{X}(Q) \times \mathfrak{X}(Q) \to \mathfrak{X}(Q)$ defined such that

$$[V,W](q) := \tfrac{\mathrm{d}}{\mathrm{d}t}\big|_{t=0} \big(\Phi_{-\sqrt{t}}^W \circ \Phi_{-\sqrt{t}}^V \circ \Phi_{\sqrt{t}}^W \circ \Phi_{\sqrt{t}}^V\big)(q), \tag{2.6}$$

where Φ^X and Φ^Y are the (perhaps local) flows induced by X and Y. Moreover, the *Lie derivative* of a smooth function $f : Q \to \mathbb{R}$ along a vector field V is the smooth function $\nabla_V f : Q \to \mathbb{R}$ given by

$$\big(\nabla_V f\big)(q) := \tfrac{\mathrm{d}}{\mathrm{d}t}\big|_{t=0} f \circ \Phi_t^V(q). \tag{2.7}$$

2.1.3 The Differential of a Smooth Map

Assuming for simplicity that smooth manifolds $M, N \subseteq \mathbb{R}^k$ are embedded in an ambient Euclidean space (although these concepts can also be defined completely intrinsically), for any smooth map $f : M \to N$, we can define a map $\mathrm{d}f : TM \to TN$, called the *differential* (or *tangent map*, or *derivative*) of f, by

$$\mathrm{d}f\big(v_m\big) := \frac{\mathrm{d}}{\mathrm{d}t}\bigg|_{t=0} \big(f \circ \gamma(t)\big) = \lim_{\Delta t \to 0} \frac{f\big(\gamma(\Delta t)\big) - f\big(\gamma(0)\big)}{\Delta t} \tag{2.8}$$

for *any* smooth curve $\gamma : (-\varepsilon, \varepsilon) \to M$ such that $\gamma(0) = m$ and $\dot{\gamma}(0) = v_m$. It can be verified that the result is independent of the particular choice of γ.

For any map $f : X \times Y \to Z$, $(x, y) \mapsto f(x, y)$, we define the maps $f_x : y \mapsto f(x, y)$ and $f^y : x \mapsto f(x, y)$ by respectively holding the first and second argument constant. Then, we may define the partial derivative

$$\partial_x f : TX \times Y \to TZ, \; (v_x, y) \mapsto \big(\mathrm{d}(f^y)\big)(v_x) \tag{2.9}$$

and likewise for $\partial_y f$, where the non-vector argument is sometimes thought of as a temporarily fixed parameter. We define partial derivatives for functions with more than two arguments analogously.

Given a smooth, real-valued function $P : M \to \mathbb{R}$, the differential $\mathrm{d}P : TM \to T\mathbb{R}$ can also be thought of as a covector field $\mathrm{d}P : M \to T^*M$ via the identification $T\mathbb{R} \cong \mathbb{R} \times \mathbb{R}$ (and thus, $\nabla_V P = \langle \mathrm{d}P; V \rangle$).

For a smooth map $f : M \to N$, the *dual* of $\mathrm{d}f$ is the unique map $\mathrm{d}f^* : T^*N \to T^*M$ defined such that

$$\langle \omega_n ; \mathrm{d}f(v_m) \rangle = \langle \mathrm{d}f^*(\omega_n) ; v_m \rangle \text{ for all } v_m \in TM \text{ and all } \omega_n \in T^*_{f(m)}N. \tag{2.10}$$

Moreover, the kernel of $\mathrm{d}f$ is the set of all vectors mapped to a zero tangent vector, namely,

$$\ker \mathrm{d}f = \left\{ v_m \in TM : \mathrm{d}f(v_m) = 0_{f(m)} \right\}. \tag{2.11}$$

2.1.4 Distributions

A *distribution* D (respectively, a codistribution F) on a smooth manifold Q is a smooth assignment of a linear subspace $D_q \subseteq T_qQ$ (resp. $F_q \subseteq T^*Q$) to each point $q \in Q$. A distribution (respectively, a codistribution) can also be thought of as a *distribution* of the tangent bundle TQ (respectively, the cotangent bundle T^*Q). The rank of D (respectively, F) at a point $q \in Q$ is the dimension of D_q (respectively, F_q). In this thesis, we will mostly consider *regular* distributions, which are those of constant rank. The annihilator of D and coannihilator of F, denoted $\operatorname{ann} D$ and $\operatorname{coann} F$, are the codistribution and distribution given by

$$(\operatorname{ann} D)_q = \left\{ f_q \in T^*_q Q : \langle f_q ; v_q \rangle = 0 \text{ for all } v_q \in D_q \right\}, \tag{2.12}$$

$$(\operatorname{coann} F)_q = \left\{ v_q \in T_q Q : \langle f_q ; v_q \rangle = 0 \text{ for all } f_q \in F_q \right\}. \tag{2.13}$$

A *basis of vector fields* for a regular distribution D of rank k is a set of vector fields $\{X_1, \ldots, X_k\}$ such that

$$D_q = \operatorname{span} \left\{ X_1(q), \ldots, X_k(q) \right\}, \tag{2.14}$$

and a local basis is defined similarly over a local region. Also, we denote the set of vector fields in $\mathfrak{X}(Q)$ that take values uniformly in D by $\Gamma(D)$. Analogous concepts are defined for codistributions, and of course, TQ (respectively T^*Q) can be thought of, in particular, as a distribution (respectively, a codistribution). We also call a basis of vector fields for TQ a *frame*, and a basis of covector fields for T^*Q a *coframe*.

2.1.5 Notational Miscellanea

We close this section with some miscellaneous notation. In a product manifold $M_1 \times M_2 \times \cdots \times M_k$, the ith *canonical projection* is the map $\operatorname{pr}_i : (m_1, m_2, \ldots, m_n) \mapsto m_i$. When working with coordinates $(q^1, q^2, \ldots, q^n)$ for a smooth manifold Q, the symbol ∂_i (or sometimes, ∂_{q^i}) denotes the locally-defined "coordinate vector field" associated with the coordinate q^i, such that $\{\partial_i\}$ is a local frame. Frequently, we use index notation with the Einstein summation convention, and thus will denote the quantity $\sum_i a^i b_i$ more concisely by simply suppressing the sum notation, yielding $a^i b_i$ (where the sum is implied).

2.2 Riemannian Geometry

In this section, we present some basic facts of Riemannian geometry, which extends many familiar aspects of Euclidean geometry to arbitrary smooth manifolds by equipping the manifold with some additional structure. Riemannian geometry will ultimately furnish a concise and powerful means to describe the dynamics of mechanical systems, particularly in the absence of nonholonomic constraints. For more detailed presentations, we refer to [10], [5], and [9].

2.2.1 Riemannian Metrics

Any smooth manifold can be equipped with additional geometric structure in the following manner.

Definition 2.1. A *Riemannian metric* (or simply a *metric*) κ is a smoothly-varying assignment of a bilinear, positive definite inner product

$$\langle\langle\,\cdot\,,\,\cdot\,\rangle\rangle_q : T_qQ \times T_qQ \to \mathbb{R} \tag{2.15}$$

on the tangent space T_qQ at each point q on a manifold Q. When convenient, we also denote the metric as a whole by $\kappa(\cdot,\cdot)$. We say that the pair (Q,κ) is a *Riemannian manifold*. $\bullet$

Just as an inner product on a vector space induces a norm and a notion of the angle between vectors, a metric extends similar notions to the non-Euclidean setting, as follows.

Definition 2.2. The *Riemannian norm* is given by

$$\|\cdot\|_\kappa : TQ \to \mathbb{R},\ v_q \mapsto \sqrt{\langle\langle v_q, v_q\rangle\rangle}, \tag{2.16}$$

which also induces a norm on covectors, denoted in the same manner and defined by

$$\|\cdot\|_\kappa : T^*Q \to \mathbb{R},\ f_q \mapsto \sup_{\|v_q\|_\kappa = 1}\ \langle f_q; v_q\rangle, \tag{2.17}$$

since covectors are just linear functionals on their corresponding tangent space. The *angle* between two tangent vectors in the same tangent space is given by

$$\angle(\,\cdot\,,\cdot\,) : (v_q, w_q) \mapsto \arccos\left(\frac{\langle\langle v_q, w_q\rangle\rangle}{\|v_q\|_\kappa\,\|w_q\|_\kappa}\right), \tag{2.18}$$

and two vectors $v_q, w_q \in T_qQ$ are called *orthogonal* whenever $\langle\langle v_q, w_q\rangle\rangle = 0$. $\bullet$

We may also formalize the notion of the length of a curve as follows.

Definition 2.3. Let $\mathsf{A}(Q)$ consist of all piecewise curves $\gamma : [0,1] \to Q$ made up of smooth segments with nonvanishing velocity on the interior of each segment, called *admissible curves*. On the space of admissible

curves, we may define the Riemannian *length functional*, given by

$$\ell : \mathsf{A}(Q) \to \mathbb{R}, \ \gamma \mapsto \int_0^1 \sqrt{\langle\langle \dot{\gamma}(t), \dot{\gamma}(t) \rangle\rangle} \, dt. \tag{2.19}$$

Let us define the set of admissible curves from p to q, given by $\mathsf{A}_p^q = \{\gamma \in \mathsf{A}(Q) : \gamma(0) = p, \gamma(1) = q\}$. Then, we may define the *Riemannian distance* as

$$\mathrm{dist}_\kappa : Q \times Q \to \mathbb{R}, \ (p, q) \mapsto \inf_{\gamma \in \mathsf{A}_p^q} \ell(\gamma), \tag{2.20}$$

which makes any connected Riemannian manifold into a metric space. ●

Perhaps the most familiar (nontrivial) example of a Riemannian manifold is the following.

Example 2.1 *(The n-Sphere).* A classic example of a Riemannian manifold is $(\mathbb{S}^n, \rho)$, namely the n-sphere embedded in $\mathbb{R}^{n+1}$, where

$$\mathbb{S}^n = \left\{ x \in \mathbb{R}^{n+1} : x^\mathsf{T} x = 1 \right\}, \tag{2.21}$$

and ρ is the obvious "round" metric, given by

$$\langle\langle \, \cdot \, , \, \cdot \, \rangle\rangle_x : (v_x, w_x) \mapsto v_x^\mathsf{T} w_x. \tag{2.22}$$

Thus, the Riemannian norm under ρ is the restriction of the usual Euclidean norm to each tangent space. ●

The manifold in the previous example is embedded in a Euclidean space and inherits the metric from the Euclidean inner product. A similar construction works even when the ambient space is non-Euclidean.

Definition 2.4. An *isometric immersion* $i : (R, \mu) \hookrightarrow (Q, \kappa)$ is an immersion $i : R \hookrightarrow Q$ such that

$$\mu(v_r, w_r) = \kappa\big(\mathrm{d}i(v_r), \mathrm{d}i(w_r) \big) \text{ for all } v_r, w_r \in TR, \tag{2.23}$$

where R and Q are called the *immersed* and *ambient* manifolds respectively. Given a metric on Q and an immersion, the *induced metric* on R is the unique metric which makes the immersion isometric. ●

However, metrics can also be defined intrinsically, without any reference to an ambient space.

2.2.2 The Musical Isomorphisms

The designation of a metric induces a canonical isomorphism between the tangent and cotangent bundles.

Definition 2.5. Each Riemannian metric κ induces a pair of *musical isomorphisms*

$$\kappa^\sharp : T^*Q \to TQ \ \text{ and } \ \kappa^\flat : TQ \to T^*Q, \tag{2.24}$$

which are defined such that for all $f_q \in T^*Q$ and $v_q, w_q \in TQ$, we have

$$\langle\langle \kappa^\sharp(f_q), v_q \rangle\rangle = \langle f_q ; v_q \rangle \ \text{ and } \ \langle\langle w_q, v_q \rangle\rangle = \langle \kappa^\flat(w_q) ; v_q \rangle. \tag{2.25}$$

When the metric κ is clear from context, we may sometimes write $v_q{}^\flat := \kappa^\flat(v_q)$ and $f_q{}^\sharp := \kappa^\sharp(f_q)$.   ●

It is easily verified that $(\kappa^\flat)^{-1} = \kappa^\sharp$, and the restriction of $\kappa^\flat$ (respectively, $\kappa^\sharp$) to a given tangent (respectively, cotangent) space is a linear isomorphism.

In vector calculus, the gradient of a real-valued function is a vector field, whose definition makes no explicit reference to a metric (but in fact implicitly relies on the canonical Euclidean metric). In the absence of a canonical metric, an explicit choice is necessary to formalize the notion of the gradient, as follows.

Definition 2.6. In a Riemannian manifold (Q, κ), for any smooth function $f : Q \to \mathbb{R}$, the vector field

$$\operatorname{grad} f : Q \to TQ, \ q \mapsto \kappa^\sharp\big(\mathrm{d}f(q)\big) \tag{2.26}$$

is called the *gradient* vector field.   ●

2.2.3 Affine Connections

We now define a class of vector field operations that plays a key role in Riemannian geometry (and beyond).

Definition 2.7. An *affine connection* is an operation[1] $\nabla : \mathfrak{X}(Q) \times \mathfrak{X}(Q) \to \mathfrak{X}(Q)$ with the following properties, for all vector fields $X, Y, Z \in \mathfrak{X}(Q)$, constants $\alpha, \beta \in \mathbb{R}$, and functions $f, g \in C^\infty(Q, \mathbb{R})$:

1. *Linearity over $\mathbb{R}$ in the second argument:* $\nabla_X\big(\alpha Y + \beta Z\big) = \alpha \, \nabla_X Y + \beta \, \nabla_X Z$,

2. *Linearity over $C^\infty(Q, \mathbb{R})$ in the first argument:* $\nabla_{(fX+gY)} Z = f \, \nabla_X Z + g \, \nabla_Y Z$, and

3. *Leibniz rule:* $\nabla_X(fY) = f \, \nabla_X Y + (\nabla_X f) \, Y$,

where by abuse of notation, $\nabla_X f$ is a Lie derivative (*i.e.*, $\nabla_X f = \langle \mathrm{d}f ; X \rangle$).   ●

We call $\nabla_X Y$ the *covariant derivative of Y along X*. It should also be clear from the above properties that ∇ is $\mathbb{R}$-bilinear. A given manifold admits many affine connections, so it will be useful to consider special properties possessed by certain affine connections which may distinguish them from others.

Definition 2.8. An affine connection ∇ is *compatible* with a given metric $\langle\langle \, \cdot \, , \, \cdot \, \rangle\rangle$ if

$$\nabla_Z \langle\langle X, Y \rangle\rangle = \langle\langle \nabla_Z X, Y \rangle\rangle + \langle\langle X, \nabla_Z Y \rangle\rangle \tag{2.27}$$

---

[1]Note our use of the notational convention (almost universally adopted) that writes $\nabla_X Y$ in place of $\nabla(X, Y)$. Except for a suppressed set of parentheses around Y, this is in keeping with our standard notation for "currying" functions of two arguments.

for all $X, Y, Z \in \mathfrak{X}(Q)$. Also, the *torsion* of an affine connection ∇ is a vector field operation given by

$$\mathrm{T}^{\nabla} : \mathfrak{X}(Q) \times \mathfrak{X}(Q) \to \mathfrak{X}(Q), \ (X, Y) \mapsto \nabla_X Y - \nabla_Y X - [X, Y], \tag{2.28}$$

and we say that ∇ is *torsion-free* when $\mathrm{T}^{\nabla}(X, Y)$ is identically zero for all $X, Y \in \mathfrak{X}(Q)$.   ●

The following establishes a canonical choice of affine connection in the presence of a Riemannian metric.

Fact 2.1 (Levi-Civita Theorem). *For any Riemannian manifold, there exists a unique affine connection that is both compatible with the metric and torsion-free, known as the* Riemannian (*or* Levi-Civita) connection.

For the remainder, ∇ will always denote the Riemannian connection unless stated otherwise.

2.2.4 Covariant Differentiation Along Curves

Although we described affine connections in terms of vector fields defined over the entire Riemannian manifold, it will be useful to establish a notion of covariant differentiation for data defined only along a curve in the manifold. We will need some additional constructions to make this precise.

Definition 2.9. Given a curve $\gamma \in \mathsf{A}(Q)$, a *vector field along* γ is a piecewise smooth map $X : [0, 1] \to TQ$ such that the following diagram commutes:

$$
\begin{array}{ccc}
 & & TQ \\
 & \overset{X}{\nearrow} & \downarrow \pi_Q \\
[0, 1] & \underset{\gamma}{\longrightarrow} & Q
\end{array}
\tag{2.29}
$$

The set of all vector fields along γ is denoted $\mathfrak{X}(\gamma)$.   ●

In other words, a vector field along a curve assigns to each time in the interval an element of the tangent space of the value of the curve at that point in time, such as the curve's velocity $\dot{\gamma} \in \mathfrak{X}(\gamma)$. Note that a vector field in $\mathfrak{X}(\gamma)$ cannot always be extended (even locally) to a vector field in $\mathfrak{X}(Q)$. For example, a self-intersecting curve may visit the same point repeatedly but with a different velocity.

Definition 2.10. The *covariant derivative along* γ induced by an affine connection ∇ is the unique operation $\nabla_{\dot{\gamma}} : \mathfrak{X}(\gamma) \to \mathfrak{X}(\gamma)$ with the following properties:

1. *Distributive Property:* $\nabla_{\dot{\gamma}}(X + Y) = \nabla_{\dot{\gamma}} X + \nabla_{\dot{\gamma}} Y$,

2. *Liebniz Rule:* $\nabla_{\dot{\gamma}}(fX) = f \nabla_{\dot{\gamma}} X + \dot{f} X$, and

3. *Extension Invariance:* $\nabla_{\dot{\gamma}} X = \left(\nabla_{\dot{\gamma}} \tilde{X} \right) \circ \gamma$

where $X, Y \in \mathfrak{X}(\gamma)$, $f : [0, 1] \to \mathbb{R}$, and $\tilde{X} \in \mathfrak{X}(Q)$ is any vector field satisfying $X = \tilde{X} \circ \gamma$.   ●

The third property is well-defined, since an affine connection is tensorial in its subscripted argument (*i.e.*, it depends only on point values). The following allows us to pass from a covariant derivative along the curve to derivatives of real-valued functions of time and covariant derivatives of regular vector fields.

Lemma 2.1 (Covariant Derivatives Along a Curve in a Local Frame). *Consider a local frame* $\{X_i\}$, *a smooth curve* $\gamma : [0,1] \to Q$ *remaining within the domain of this local frame, and a smooth vector field* $Y \in \mathfrak{X}(\gamma)$. *Then, there exist unique smooth coefficient functions* $u^i, v^i : [0,1] \to \mathbb{R}$ *such that*

$$\dot{\gamma}(t) = u^i(t)\, X_i \circ \gamma(t) \ \ and \ \ Y(t) = v^i(t)\, X_i \circ \gamma(t), \tag{2.30}$$

and furthermore the covariant derivative of Y *along* γ *satisfies*

$$\left(\nabla_{\dot{\gamma}} Y\right)(t) = \left(\dot{v}^i(t)\, X_i + u^i(t)\, v^j(t)\, \nabla_{X_i} X_j\right) \circ \gamma(t). \tag{2.31}$$

Proof. The existence of the coefficient functions is trivial, since a local frame evaluated at a particular point yields a basis for the tangent space, and all relevant quantities are smooth. Then, the result follows directly from a careful application of the properties of $\nabla_{\dot{\gamma}}$:

$$\left(\nabla_{\dot{\gamma}} Y\right)(t) = \left(\nabla_{u^i(t)\, X_i} v^j(t)\, X_j\right) \circ \gamma(t) \tag{2.32}$$

$$= \left(\dot{v}^j(t)\, X_j + v^j(t)\, \nabla_{u^i(t) \cdot X_i} X_j\right) \circ \gamma(t) \tag{2.33}$$

$$= \left(\dot{v}^j(t)\, X_j + u^i(t)\, v^j(t)\, \nabla_{X_i} X_j\right) \circ \gamma(t), \tag{2.34}$$

where all vector fields are evaluated only along the curve, in harmony with extension invariance. ∎

2.2.5 Parallel Transport and Geodesics

The Riemannian connection gives us an intrinsic notion of acceleration in a Riemannian manifold.

Definition 2.11. Given a curve $\gamma \in \mathsf{A}(Q)$, a vector field $V \in \mathfrak{X}(\gamma)$ is said to be *parallel along* γ if $\nabla_{\dot{\gamma}} V = 0$, and the *geometric acceleration* of γ is the vector field $\nabla_{\dot{\gamma}} \dot{\gamma} \in \mathfrak{X}(\gamma)$. Moreover, γ is called a *geodesic* curve if its velocity is self-parallel (*i.e.*, its geometric acceleration is identically zero: $\nabla_{\dot{\gamma}} \dot{\gamma} = 0$). ●

Since a point traveling through Euclidean space with zero acceleration follows a straight line, geodesics generalize the notion of "straight lines" from Euclidean space to general Riemannian manifolds. Although a straight line is always the shortest path between two points in Euclidean space, in the general case, geodesics do not necessarily minimize length.

Fact 2.2. *Geodesics are stationary curves of the length functional under variations with fixed endpoints.*

Thus, curves which locally maximize or minimize the length of a curve between two points are geodesics.

Definition 2.12. Consider a given curve $\gamma \in \mathsf{A}(Q)$. For any $v_q \in T_{\gamma(0)}Q$, let $X^{v_q} \in \mathfrak{X}(\gamma)$ denote the unique parallel vector field along γ with $X^{v_q}(0) = v_q$. Then, the *parallel transport along* γ is the linear map given by

$$\tau_\gamma : T_{\gamma(0)}Q \to T_{\gamma(1)}Q, \ v_q \mapsto X^{v_q}(1), \tag{2.35}$$

where the existence and uniqueness of X^{v_q} for each $v_q \in TQ$ follows from standard existence and uniqueness results for solutions of ordinary differential equations. $\bullet$

The parallel transport map allows us to "move" vectors from one tangent space to another; however, in general, the outcome depends on the path along which the vector is transported.

2.3 Lie Group Theory

In this section, we review some aspects of Lie group theory, which will provide a language to describe the continuous symmetries of physical systems. We also refer the reader to [11] for a relatively informal but very accessible introduction for readers in robotics, or [12] and [5] for more rigorous, in-depth treatments.

Definition 2.13. A *group* $(G, \cdot)$ is a set G equipped with a *group operation*

$$\cdot : G \times G \to G, \ (a, b) \mapsto a \cdot b \tag{2.36}$$

with the following properties (known as the *group axioms*):

1. *Associativity:* for all $a, b, c \in G$, $(a \cdot b) \cdot c = a \cdot (b \cdot c)$,

2. *Identity:* there exists a unique *identity* element $e \in G$ such that $e \cdot a = a \cdot e = a$ for all $a \in G$, and

3. *Inverse:* for each $a \in G$, there exists a unique *inverse* element $a^{-1} \in G$ such that $a^{-1} \cdot a = a \cdot a^{-1} = e$.

A group is *Abelian* if the group operation is symmetric (*i.e.*, $a \cdot b = b \cdot a$); otherwise, it is *non-Abelian*. $\bullet$

In a context where the group operation is clear, we will often denote the group solely by the set G without the operator, and we will often write the operation $g \cdot h$ as simply gh. The group operation also induces several other maps from the group back to itself.

Definition 2.14. The families of maps indexed by $g \in G$ and given by

$$\mathrm{L}_g : G \to G, \ h \mapsto gh, \quad \mathrm{R}_g : G \to G, \ h \mapsto hg \tag{2.37}$$

are called the *left* and *right automorphisms* of G, while the family of maps given by

$$\mathrm{I}_g : G \to G, \ h \mapsto ghg^{-1}. \tag{2.38}$$

is called the *inner automorphisms.* ●

Clearly, if G is Abelian, then $\mathrm{L}_g = \mathrm{R}_g$ and $\mathrm{I}_g = \mathrm{id}$.

2.3.1 Lie Groups

While groups of various kinds have broad and important applications, we will be particularly interested in the following class.

Definition 2.15. A *Lie group* is a group for which:

1. the set G is a smooth manifold, and

2. the group operation $(a, b) \mapsto ab$ and the inverse operation $a \mapsto a^{-1}$ are smooth. ●

Lie groups play a major role in describing the symmetries of the spaces inhabited by robotic systems.

Example 2.2 *(Euclidean Space).* Euclidean space can be understood as the Lie group $(\mathbb{R}^n, +)$, since $\mathbb{R}^n$ is a smooth manifold and vector addition satisfies the group axioms:

1. *Associativity:* $(a + b) + c = a + (b + c)$,

2. *Identity:* $a + b = b + a = a \implies b = 0$, and

3. *Inverse:* $a + b = 0 \implies b = -a$.

Furthermore, the group operation $(a, b) \mapsto a + b$ and the inverse $a \mapsto -a$ are both smooth. ●

Example 2.3 *(The General Linear Group).* The space of $n \times n$ invertible matrices[2]

$$\mathrm{GL}(n) = \left\{ A \in \mathbb{R}^{n \times n} : \det A \neq 0 \right\} \tag{2.39}$$

is a Lie group under the operation of matrix multiplication. In particular, this set can be shown to be a smooth manifold, and matrix multiplication satisfies the group axioms:

1. *Associativity:* $(AB)C = A(BC)$,

2. *Identity:* $AB = BA = A \implies B = I_{n \times n}$, and

3. *Inverse:* $A^{-1}A = AA^{-1} = I_{n \times n}$.

Furthermore, the operation $(A, B) \mapsto AB$ and the inverse $A \mapsto A^{-1}$ are both smooth. ●

Several other specific Lie groups of interest in robotics will also be described later.

---

[2]This group is often denoted $\mathrm{GL}(\mathbb{R}, n)$ to distinguish it from $\mathrm{GL}(\mathbb{C}, n)$ (the group of $n \times n$ invertible matrices with complex entries), but in this thesis, we consider only invertible matrices with real entries.

2.3.2 Lie Algebras

Definition 2.16. A *Lie algebra* is a vector space $\mathfrak{g}$ endowed with a map

$$[\,\cdot\,,\,\cdot\,] : \mathfrak{g} \times \mathfrak{g} \to \mathfrak{g} \tag{2.40}$$

called the *Lie bracket*, such that the following properties hold for all $\xi, \eta, \omega \in \mathfrak{g}$:

1. *Bilinearity:* $[a\eta, b\xi] = ab\,[\eta, \xi]$ for all $a, b \in \mathbb{R}$,

2. *Skew Symmetry:* $[\xi, \eta] = -[\eta, \xi]$, and

3. *Jacobi Identity:* $[\xi, [\eta, \omega]] + [\omega, [\xi, \eta]] + [\eta, [\omega, \xi]] = 0.$ •

For any Lie group G, let $\mathfrak{g} := T_e G$. For each $\xi \in \mathfrak{g}$, define a vector field in $\mathfrak{X}(G)$ given by

$$\xi_G : g \mapsto \mathrm{d}\mathrm{L}_g(\xi), \tag{2.41}$$

called a *left-invariant vector field*. In fact, $\mathfrak{g}$ is a Lie algebra (induced by G), endowed with the Lie bracket

$$[\,\cdot\,,\,\cdot\,]_{\mathfrak{g}} : \mathfrak{g} \times \mathfrak{g} \to \mathfrak{g},\ (\xi, \eta) \mapsto \big([\xi_G, \eta_G]_G\big)(e), \tag{2.42}$$

where $[\,\cdot\,,\,\cdot\,]_G$ denotes the Lie bracket of vector fields on G (as a smooth manifold). In particular, it is clear that $\mathfrak{g} = T_e G$ is a vector space and $\mathrm{d}\mathrm{L}_g$ is a linear isomorphism on each tangent space for any $g \in G$. Moreover, it can be shown that the commutator of vector fields possesses precisely the three properties that we need to verify for the proposed Lie bracket: bilinearity, skew symmetry, and the Jacobi identity, and thus $[\,\cdot\,,\,\cdot\,]_{\mathfrak{g}}$ given in (2.42) is a valid Lie bracket.

Going forward, $\mathfrak{g}$ will always denote the Lie algebra of G in the previous manner. Also, we note that because $[\,\cdot\,,\,\cdot\,]_{\mathfrak{g}}$ is bilinear, given a basis for $\mathfrak{g}$, we can express brackets in closed form in terms of the brackets of basis vectors (called the "structure coefficients" of $\mathfrak{g}$), so we need only compute $[\,\cdot\,,\,\cdot\,]_G$ finitely many times. Another convenient feature of Lie groups is that any tangent vector can be associated to a particular element of the Lie algebra, using either of the following two maps.

Definition 2.17. The *left* and *right Maurer-Cartan forms* are respectively given by

$$\lambda : TG \to \mathfrak{g},\ v_g \mapsto \mathrm{d}\mathrm{L}_{g^{-1}}(v_g), \qquad \rho : TG \to \mathfrak{g},\ v_g \mapsto \mathrm{d}\mathrm{R}_{g^{-1}}(v_g). \tag{2.43}$$

For any smooth curve $\gamma : [0, 1] \to G$, the curves $\xi_b, \xi_s : [0, 1] \to \mathfrak{g}$ given by

$$\xi_b : t \mapsto \lambda\big(\dot{\gamma}(t)\big), \qquad \xi_s : t \mapsto \rho\big(\dot{\gamma}(t)\big). \tag{2.44}$$

are respectively called the *body velocity* and *spatial velocity* of γ. ●

The following map permits us to convert between the body and spatial representations of the velocity.

Definition 2.18. The *adjoint representation* of G on $\mathfrak{g}$ is given by

$$\mathrm{Ad}_g : \mathfrak{g} \to \mathfrak{g}, \ \xi \mapsto \mathrm{d}\mathrm{L}_g \circ \mathrm{d}R_{g^{-1}}(\xi), \tag{2.45}$$

which amounts to the restriction of $\mathrm{d}\mathrm{I}_g$ to T_eG. ●

It is straightforward to verify that $\xi_s = \mathrm{Ad}_g(\xi_b)$. Finally, there is also a natural way to relate elements of the Lie algebra to elements of the group itself, in the following manner.

Definition 2.19. The *exponential map* of $\mathfrak{g}$ into G is given by

$$\xi \mapsto \Phi_1^{\xi_G}(e), \tag{2.46}$$

where Φ^{ξ_G} is the flow of $\xi_G \in \mathfrak{X}(G)$. The *logarithmic map* from (a region of) G back to $\mathfrak{g}$ is defined only over the maximal neighborhood of $e \in G$ for which $\exp$ is bijective, on which we have $\log = \exp^{-1}$. ●

Thus, the exponential map returns the result of starting at the identity and moving with a given body velocity for unit time. Shortly, we will give another characterization of $\exp$ for a broad class of Lie groups.

2.3.3   Matrix Lie Groups

It is often useful to consider groups that are contained inside another group in the following sense.

Definition 2.20. A *Lie subgroup* is a immersed submanifold $H \subseteq G$ that is closed under the group operation of G (*i.e.*, if $h_1, h_2 \in H$, then $h_1 \cdot h_2 \in H$). On the other hand, a *Lie subalgebra* is a subspace $\mathfrak{h} \subseteq \mathfrak{g}$ that is closed under the Lie bracket of $\mathfrak{g}$ (*i.e.*, if $\xi_1, \xi_2 \in \mathfrak{h}$, then $[\xi_1, \xi_2] \in \mathfrak{h}$). ●

An extremely important class of Lie groups in robotics is the following.

Definition 2.21. A *matrix Lie group* is any Lie subgroup of $\mathrm{GL}(n)$. ●

In view of (2.42), it is unsurprising that the Lie algebra of any matrix group is a subalgebra of $\mathfrak{gl}(n) \subset \mathbb{R}^{n \times n}$, the Lie algebra of $\mathrm{GL}(n)$. A convenient property of matrix Lie groups is that most important quantities in such groups can be computed using only matrix multiplication, since the elements of the Lie group, the tangent space, and the Lie algebra can all be represented by square matrices. This makes it easy to work in any matrix Lie group in a unified manner. We state the following facts without further justification, where all operations on the right-hand side should be understood as matrix multiplication.

Fact 2.3. *The Lie bracket of a matrix Lie algebra $\mathfrak{g} \subseteq \mathfrak{gl}(n)$ is given by the matrix commutator:*

$$[\,\cdot\,,\,\cdot\,] : \mathfrak{g} \times \mathfrak{g} \to \mathfrak{g},\ (\xi, \eta) \mapsto \xi\eta - \eta\xi. \tag{2.47}$$

Similarly, the adjoint action of a matrix Lie group G on its Lie algebra $\mathfrak{g}$ is given by conjugation:

$$\mathrm{Ad}_g : \mathfrak{g} \to \mathfrak{g},\ \xi \mapsto g\,\xi\,g^{-1}, \tag{2.48}$$

and its exponential map is given by the matrix exponential:

$$\exp : \mathfrak{g} \to G,\ \xi \mapsto \sum_{k=0}^{\infty} \frac{1}{k!} \xi^k. \tag{2.49}$$

For many matrix Lie groups of interest, a closed-form expression for the exponential map is well-known (*e.g.*, Rodrigues' formula for SO(3)). Given the ubiquity of matrix Lie groups in robotics, it's worth reminding the reader that Lie groups can also be defined intrinsically without reference to $\mathrm{GL}(n)$ (even if the result is isomorphic to an "explicitly" matrix Lie group), and in fact there exist Lie groups which are not matrix at all. However, it will often be practically convenient to work with groups in this manner, and those Lie groups of particular interest in robotics (broadly speaking) can be expressed as matrix Lie groups. A prime example is the following well-known group of so-called "rotation matrices".

Example 2.4. The *special orthogonal group* of order n is the matrix Lie group given by

$$\mathrm{SO}(n) = \left\{ R \in \mathbb{R}^{n \times n} : R^{\mathsf{T}} R = RR^{\mathsf{T}} = I_{n \times n},\ \det R = 1 \right\}, \tag{2.50}$$

while its Lie algebra is

$$\mathfrak{so}(n) = \left\{ \omega \in \mathbb{R}^{n \times n} : \omega + \omega^{\mathsf{T}} = 0 \right\}, \tag{2.51}$$

namely the set of $n \times n$ skew-symmetric matrices. The inverse map is given by $\cdot^{-1} : R \mapsto R^{\mathsf{T}}$. $\bullet$

The elements of the special orthogonal group can be thought of as describing rotations of an n-dimensional space about the origin. As a result, they furnish a natural means to describe the orientation of a rigid body in 2D or 3D. Similarly, the following group of "transformation matrices" can be used to describe the full pose of a rigid body in n-dimensional space, comprising both its orientation and position.

Example 2.5. The *special Euclidean group* of order n is the matrix Lie group given by

$$\mathrm{SE}(n) = \left\{ \begin{bmatrix} R & x \\ 0 & 1 \end{bmatrix} \in \mathbb{R}^{n+1 \times n+1} : R \in \mathrm{SO}(n),\ x \in \mathbb{R}^n \right\}, \tag{2.52}$$

while its Lie algebra is given by

$$\mathfrak{se}(n) = \left\{ \begin{bmatrix} \omega & \xi \\ 0 & 0 \end{bmatrix} \in \mathbb{R}^{n+1 \times n+1} : \omega \in \mathfrak{so}(n), \xi \in \mathbb{R}^n \right\}. \tag{2.53}$$

Finally, it is easily verified that

$$(\cdot)^{-1} : \begin{bmatrix} R & x \\ 0 & 1 \end{bmatrix} \mapsto \begin{bmatrix} R^{\mathrm{T}} & -R^{\mathrm{T}}x \\ 0 & 1 \end{bmatrix}. \tag{2.54}$$

is the explicit form of the inverse map. ●

2.4   Group Actions

In this section, we describe a manner in which Lie groups interact with other manifolds. This interaction provides an explicit means of describing the symmetry of various data defined on the manifold. A more thorough exploration can also be found in [8] and [9].

Definition 2.22. A (*left*) *action* of a Lie group G on a manifold Q is a smooth map

$$\Phi : G \times Q \to Q \tag{2.55}$$

such that for all $q \in Q$ and $g, h \in G$:

1. $\Phi(e, q) = q$, and

2. $\Phi(g, \Phi(h, q)) = \Phi(gh, q)$. ●

The choice to work with *left* actions is historically motivated (see, *e.g.*, [13]) and a matter of preference. Moreover, *right* actions can be defined analogously, in which case the second property becomes

$$\Psi\big(g, \Psi(h, q)\big) = \Psi(hg, q), \tag{2.56}$$

since we multiply "on the right" in the group. It's easy to verify that for any left action Φ, the map $\Psi : (x, g) \mapsto \Phi(g^{-1}, x)$ is in fact a right action. Except when explicitly specified otherwise, all group actions considered in this thesis will be left actions.

Most of the time, we will write the action of each $g \in G$ as a map $\Phi_g : Q \to Q$ to emphasize its nature as a family of diffeomorphisms, parametrized by the elements of the group. This perspective highlights the viewpoint that a group action is nothing but a group homomorphism $\Phi : G \to \mathrm{Diff}(Q)$, where $\mathrm{Diff}(Q)$ is the diffeomorphism group of the manifold Q (but we do not explore this further here). We can also

21

illustrate the required properties of a group action via the following commutative diagram:

$$\Phi_e \circlearrowleft Q \xrightarrow{\Phi_h} Q$$
$$\Phi_{gh} \searrow \quad \downarrow \Phi_g$$
$$Q \tag{2.57}$$

It is also straightforward to see that the left and inner automorphisms of G given in Def. 2.14 are in fact left actions of G on itself, while the right automorphisms constitute a right action of G on itself, and the adjoint representation given in Def. 2.18 is a left action of G on $\mathfrak{g}$.

Example 2.6 (*Body-Fixed Rotation*). Consider the Lie group $G = (\mathbb{S}^1, +)$, where we represent elements of the group by angles, and addition operates modulo 2π. Let $\mathbb{S}^1$ act on the manifold $Q = \mathrm{SO}(3)$ via

$$\Phi : \mathbb{S}^1 \times \mathrm{SO}(3) \to \mathrm{SO}(3), \ (\theta, R) \mapsto R \cdot \begin{bmatrix} \cos\theta & -\sin\theta & 0 \\ \sin\theta & \cos\theta & 0 \\ 0 & 0 & 1 \end{bmatrix}. \tag{2.58}$$

If $R \in \mathrm{SO}(3)$ represents the orientation of a rigid body, this action can be understood as a rotation by an angle θ around the third body-fixed axis. It is easily verified that this is a valid group action, since:

1. $\Phi_0(R) = R$ (*i.e.*, a rotation by an angle of zero (the identity element of $\mathbb{S}^1$) does not change the orientation of the body), and

2. $\Phi_\alpha \circ \Phi_\beta(R) = \Phi_{\alpha+\beta}(R)$, (*i.e.*, a rotation by an angle α followed by a rotation by an angle β yields the same result as a rotation by an angle $\alpha + \beta$). ●

2.4.1 Properties and Orbits

The following are some useful properties that a group action may perhaps enjoy.

Definition 2.23. A group action Φ is said to be:

1. *free*, if the map Φ_g has no fixed points for all non-identity $g \in G$ (*i.e.*, $\Phi_g(q) = q \iff g = e$),

2. *proper*, if the map $(g, x) \mapsto (\Phi_g(x), x)$ is proper (*i.e.*, the preimage of any compact set is compact)

3. *transitive*, if for each pair $q_1, q_2 \in Q$, there exists some $g \in G$ such that $\Phi_g(q_1) = q_2$, and

4. *effective*, if only the identity element acts trivially on all elements (*i.e.*, $\Phi_g = \mathrm{id} \iff g = e$). ●

Clearly, all free actions are effective, but not all effective actions are free. Also, properness is a relatively mild property (*e.g.*, any compact group must act properly) enjoyed by most "garden variety" group actions.

Group actions establish a relationship between certain pairs of points, in the following manner.

Definition 2.24. The Φ-*orbit* (or simply *orbit*) of any point $q \in Q$, denoted $\Phi_G(q)$, consists of all points to which q is sent by the action as we vary the group element (*i.e.*, $\Phi_G(q) = \{\Phi_g(q) : g \in G\}$).　　　●

Clearly, a group action naturally partitions the manifold into equivalence classes, each of which is a single orbit of the action. In particular, a transitive action has a single orbit, while every orbit of the trivial action (*i.e.*, the action given by $\Phi_g = \mathrm{id}$ for all $g \in G$) contains a single point. It is also natural to ask to which orbit a given point in the manifold belongs, as follows.

Definition 2.25. The *quotient space*, denoted Q/G when the group action is understood, is the space whose elements are the orbits of the group action. The *projection* $\pi : Q \to Q/G$ sends each element of the manifold to its orbit in the quotient space.　　　●

Clearly, the following diagram must commute:

$$
\begin{array}{ccc}
Q & \xrightarrow{\ \Phi_g\ } & Q \\
 & {\scriptstyle \pi}\searrow & \downarrow{\scriptstyle \pi} \\
 & & Q/G
\end{array}
\tag{2.59}
$$

Quotient spaces can be quite messy, but under some additional assumptions, they are quite well-behaved.

Fact 2.4. *The quotient space $S = Q/G$ of a free and proper action inherits a unique smooth manifold structure.*

Example 2.6 (*Body-Fixed Rotation, continued*)**.** The same $\mathbb{S}^1$-action on $\mathrm{SO}(3)$ is:

1. free, since rotation by a nonzero angle always changes a body's orientation, and

2. proper, since $\mathbb{S}^1$ is compact.

Hence, the quotient space is a smooth manifold (and in particular, $\mathrm{SO}(3)\,/\,\mathbb{S}^1 \cong \mathbb{S}^2$), where the projection map can be given by

$$
\pi : \mathrm{SO}(3) \to \mathbb{S}^2, \ R \mapsto R\, e_3.
\tag{2.60}
$$

This projection maps the body's orientation to the world frame coordinates of its third body axis, the axis of the rotation performed by the group action. This is intuitive, since a rotation leaves unchanged exactly those points which lie on its axis.　　　●

2.4.2　Invariance and Equivariance

Group actions are helpful in describing the symmetry of other data defined on the manifold on which the group acts. Such symmetries come in two primary flavors: *invariance* and *equivariance*. In the most basic

sense, the two properties can be easily distinguished by asking whether the corresponding commutative diagram is a triangle or a square. However, many notions of equivariance can be reformulated as a notion of invariance from an alternative perspective (and vice-versa), as we will see.

Definition 2.26. A map $f : M \to N$ is *invariant* with respect to a group action $\Phi_g : M \to M$ if the following diagram commutes:

$$
\begin{array}{ccc}
M & & \\
\Phi_g \downarrow & \searrow f & \\
M & \xrightarrow{\quad f \quad} & N
\end{array}
\tag{2.61}
$$

Moreover, a map $f : M \to N$ is *equivariant* with respect to group actions $\Phi_g : M \to M$ and $\Psi_g : N \to N$ if the following diagram commutes:

$$
\begin{array}{ccc}
M & \xrightarrow{\quad f \quad} & N \\
\Phi_g \downarrow & & \downarrow \Psi_g \\
M & \xrightarrow{\quad f \quad} & N
\end{array}
\tag{2.62}
$$

Thus, invariance involves transforming only the input of the function, while equivariance involves also transforming the output in a corresponding manner. ●

The second action in the above diagram could, for example, be the left action of the group on itself (*e.g.*, $L_g : h \mapsto gh$), the *lifted action* induced by the differential of a given group action (*i.e.*, $d\Phi_g : TQ \to TQ$), or a completely separate action altogether. Also, invariance is clearly a special case of equivariance, wherein the group acts trivially on the codomain (*i.e.*, $\Psi_g = \mathrm{id}$ for all $g \in G$).

Example 2.7 (*Invariance of the Norm Under Rotation*). Let $G = \mathrm{SO}(n)$ act on $Q = \mathbb{R}^n$ via

$$
\Phi : \mathrm{SO}(n) \times \mathbb{R}^n \to \mathbb{R}^n, \ (R, x) \mapsto R\,x,
\tag{2.63}
$$

corresponding to rotation about the origin. The Euclidean norm given by

$$
|| \cdot || : \mathbb{R}^n \to \mathbb{R}, x \mapsto \sqrt{x^{\mathrm{T}} x}
\tag{2.64}
$$

is invariant under this action, since

$$
||\Phi_R\, x|| = \sqrt{(R\,x)^{\mathrm{T}}(R\,x)} = \sqrt{x^{\mathrm{T}}(R^{\mathrm{T}} R)\,x} = \sqrt{x^{\mathrm{T}} x} = ||x||.
\tag{2.65}
$$

We may also note that this action is not free, since $\Phi_R(0) = 0$ for any $R \in \mathrm{SO}(n)$, nor is it transitive, since vectors with different norms lie within different orbits. ●

The following map is also a nice example of equivariance.

Definition 2.27. For a free action $\Phi : G \times Q \to Q$, the *phase offset* map $\phi_q : \Phi_G(q) \to G$ of any point $q \in Q$ is the unique map such that for all $p \in \Phi_G(q)$, $\phi_q(p) = g$ if and only if $\Phi_g(q) = p$ •

Proposition 2.1. ϕ_q *is equivariant,* i.e., *the following diagram commutes:*

$$
\begin{array}{ccc}
\Phi_G(q) & \xrightarrow{\phi_q} & G \\
\Phi_g \downarrow & & \downarrow L_g \\
\Phi_G(q) & \xrightarrow{\phi_q} & G
\end{array}
\tag{2.66}
$$

Proof. We want to show that $L_g \circ \phi_q(p) = \phi_q \circ \Phi_g(p)$ for all $p \in \Phi_G(q)$. Since p and q lie on the same orbit, there exists some $h \in G$ such that $p = \Phi_h(q)$. Thus, the left-hand side can be written as $L_g \circ \phi_q \circ \Phi_h(q)$, which equals gh from the definition of ϕ_q. Likewise, the right-hand side can be written $\phi_q \circ \Phi_g \circ \Phi_h(q) = \phi_q \circ \Phi_{gh}(q) = gh$, so we are done. ∎

Definition 2.28. Consider a group action $\Phi : G \times Q \to Q$. We define notions of Φ-*invariance* for the following data defined on Q, where each condition below must hold for all $g \in G$:

- a subset $A \subseteq Q$ is Φ-invariant if $A = \Phi_g(A)$,

- a Riemannian metric κ on Q is Φ-invariant if $\kappa = \kappa\big(\mathrm{d}\Phi_g(\cdot), \mathrm{d}\Phi_g(\cdot)\big)$,

- a vector field $V \in \mathfrak{X}(Q)$ is Φ-invariant if $V = \mathrm{d}\Phi_g \circ V \circ \Phi_{g^{-1}}$,

- a covector field $\omega \in \mathfrak{X}^*(Q)$ is Φ-invariant if $\omega = \mathrm{d}\Phi_{g^{-1}}^* \circ \omega \circ \Phi_{g^{-1}}$,

- a distribution $D \subseteq TQ$ is Φ-invariant if $D = \mathrm{d}\Phi_g(D)$, and

- a codistribution $F \subseteq T^*Q$ is Φ-invariant if $F = \mathrm{d}\Phi_g^*(F)$. •

Although the definitions of Φ-invariance for distributions and codistributions above look very similar, it should be noted that for a Φ-invariant distribution D, a Φ-invariant codistribution F, and any $g \in G$,

$$
D_q = \mathrm{d}\Phi_g\big(D_{\Phi_g^{-1}(q)}\big), \quad \text{whereas} \quad F_q = \mathrm{d}\Phi_{g^{-1}}^*\big(F_{\Phi_g^{-1}(q)}\big).
\tag{2.67}
$$

The conditions on vector and covector fields can also be expressed via the following commutative diagrams:

$$
\begin{array}{ccc}
Q & \xrightarrow{V} & TQ \\
\Phi_g \downarrow & & \downarrow \mathrm{d}\Phi_g \\
Q & \xrightarrow{V} & TQ
\end{array}
\qquad
\begin{array}{ccc}
Q & \xrightarrow{\omega} & T^*Q \\
\Phi_g \downarrow & & \downarrow \mathrm{d}\Phi_{g^{-1}}^* \\
Q & \xrightarrow{\omega} & T^*Q
\end{array}
\tag{2.68}
$$

It's fair to say that the previous diagrams look a lot more like the notion of an *equivariant* (*vs.* invariant) map from Definition 2.26. For that reason, some authors choose to call such a vector or covector field "equivariant". Conversely, the perspective of Definition 2.28 can be rephrased as V being a fixed (*i.e.*, invariant) point of the action

$$\Psi : G \times \mathfrak{X}(Q) \to \mathfrak{X}(Q), \ V \mapsto \mathrm{d}\Phi_g \circ V \circ \Phi_{g^{-1}}, \tag{2.69}$$

and ω being a fixed point of the action

$$\Theta : G \times \mathfrak{X}^*(Q) \to \mathfrak{X}^*(Q), \ \omega \mapsto \mathrm{d}\Phi^*_{g^{-1}} \circ \omega \circ \Phi_{g^{-1}}, \tag{2.70}$$

where the action Ψ (resp. Θ) acts upon the function space $\mathfrak{X}(Q)$ (resp. $\mathfrak{X}^*(Q)$) to which V (resp. ω) belongs. While these perspectives are mathematically equivalent, clarifying the relationship between them can help minimize confusion in regards to the nomenclature.

Next, we prove a helpful lemma which characterizes how the musical isomorphisms of an invariant Riemannian metric behave. This result can also be helpful for performing calculations with $\mathrm{d}\Phi^*_g$, the dual of the lifted action, using the perhaps more familiar properties of $\mathrm{d}\Phi_g$, the lifted action itself.

Lemma 2.2. *For a Φ-invariant Riemannian metric κ on Q and any $g \in G$, the following diagram commutes:*

$$\tag{2.71}$$

Proof. Letting $p = \Phi_g(q)$ for some $p, q \in Q$, then for any $v_p \in T_pQ$ and $f_q \in T^*_qQ$, we compute

$$\langle \kappa^\flat \circ \mathrm{d}\Phi_g \circ \kappa^\sharp(f_q); v_p \rangle = \kappa \big(\mathrm{d}\Phi_g \circ \kappa^\sharp(f_q), v_p \big) \tag{2.72}$$

$$= \kappa \big(\kappa^\sharp(f_q), \mathrm{d}\Phi_{g^{-1}}(v_p) \big) \tag{2.73}$$

$$= \langle f_q; \mathrm{d}\Phi_{g^{-1}}(v_p) \rangle \tag{2.74}$$

$$= \langle \mathrm{d}\Phi^*_{g^{-1}}(f_q); v_p \rangle. \tag{2.75}$$

To complete the proof, it suffices to note that $(\kappa^\sharp)^{-1} = \kappa^\flat$, $(\mathrm{d}\Phi_g)^{-1} = \mathrm{d}\Phi_{g^{-1}}$, and $(\mathrm{d}\Phi^*_g)^{-1} = \mathrm{d}\Phi^*_{g^{-1}}$. ∎

2.5 Principal Bundles

In this section, we explore in greater detail the geometric structure induced on a manifold by a free and proper action, creating a setting known as a "principal bundle". The structure induced by such a group action has played a major role in the study of a diverse range of locomotory phenomena, and thus merits a tidier package in which to collect terminology and further analyze the geometric picture. [13] provides a relatively accessible introduction to many of these ideas, while a very thorough exploration is found in [6].

Definition 2.29. A (left) *principal bundle* is a manifold Q equipped with:

1. $\Phi : G \times Q \to Q$, the free and proper (left) action of a Lie group G on Q, and

2. $\pi : Q \to S$, the smooth projection to the quotient space induced by the action.

We call Q the *total space*, $S = Q/G$ the *shape space*, and G the *symmetry group*. We may also summarize this data by saying that $\pi : Q \to S$ *is a principal G-bundle*. The *fiber above* $s \in S$ is given by $\pi^{-1}(s)$. ●

Of course, *right* principal bundles can be defined analogously. It should be clear that each fiber is diffeomorphic to G, since it is in smooth, one-to-one correspondence with the orbit $\Phi_G(q)$ for any $q \in \pi^{-1}(s)$. This motivates the description of Q as a "bundle" of fibers, since (as a set) it is just the union of the fibers over each point in the shape space S.

Definition 2.30. A *section* of a principal bundle $\pi : Q \to S$ over a region $U \subseteq S$ is a smooth map of the form $\sigma : U \to Q$ such that the following diagram commutes:

$$
\begin{array}{ccc}
 & & Q \\
 & \sigma \nearrow & \downarrow \pi \\
U & \xrightarrow{\text{id}} & U
\end{array}
\tag{2.76}
$$

When $U = S$, we say that the section is *global*; otherwise, it is *local*. When π is clear from context, we denote by $\Gamma(Q)$ the family of all global sections of $\pi : Q \to S$. ●

In other words, a section smoothly selects one element of total space from the fiber above each point within a local region of shape space, just as a cross-sectional view of a three-dimensional object depicts one point along each line normal to the cutting plane. A section can also be understood as a "right inverse" of the projection, or a "lift of id through π".

Example 2.8 (*Translation of a Rigid Body*)**.** Consider the action of the Lie group $G = (\mathbb{R}^3, +)$ on the man-

ifold $Q = \mathrm{SE}(3)$ given by

$$\Phi_d : \mathrm{SE}(3) \to \mathrm{SE}(3), \quad \begin{bmatrix} R & x \\ 0 & 1 \end{bmatrix} \mapsto \begin{bmatrix} R & x+d \\ 0 & 1 \end{bmatrix}. \tag{2.77}$$

This action can easily be verified to be free and proper, hence we can say that $\mathrm{SE}(3)$ is a principal $\mathbb{R}^3$-bundle. Unsurprisingly, $\mathrm{SE}(3) \,/\, \mathbb{R}^3 = \mathrm{SO}(3)$, and the projection operator is given by

$$\pi : \mathrm{SE}(3) \to \mathrm{SO}(3), \quad \begin{bmatrix} R & x \\ 0 & 1 \end{bmatrix} \mapsto R, \tag{2.78}$$

while the fiber over any $R \in \mathrm{SO}(3)$ is given (by definition) as

$$\pi^{-1}(R) = \left\{ \begin{bmatrix} R & x \\ 0 & 1 \end{bmatrix} : x \in \mathbb{R}^3 \right\}, \tag{2.79}$$

namely the set of all poses with a given orientation. Thus, any section $\sigma \in \Gamma\big(\mathrm{SE}(3)\big)$ must take the form

$$\sigma : \mathrm{SO}(3) \to \mathrm{SE}(3), \quad R \mapsto \begin{bmatrix} R & \tau(R) \\ 0 & 1 \end{bmatrix}, \tag{2.80}$$

for some smooth map $\tau : \mathrm{SO}(3) \to \mathbb{R}^3$. For example, if some body-fixed point has coordinates $a \in \mathbb{R}^3$ in the body-fixed frame, then choosing $\tau : R \mapsto -R\,a$ results in a section σ which keeps the world coordinates of this point constant as we vary the body's orientation (*i.e.*, the body rotates "about" that point). •

2.5.1 Trivializations

The interpretation of Q as a bundle of fibers, where each fiber is diffeomorphic to G and associated with a single point in S, seems to suggest that Q has something in common with the Cartesian product $S \times G$. In fact, it is guaranteed that Q is *locally trivial*, meaning that for each point $s \in S$, there is some neighborhood U of s such that $\pi^{-1}(U)$ is diffeomorphic to $U \times G$. However, in general, this factorization into group and shape components can only be done locally. Also, such a factorization is not unique, and without additional structure, no choice is canonically designated. We explore these aspects in detail below.

Definition 2.31. A *product bundle* is a principal bundle for which:

1. the total space is the product of the shape space and symmetry group (*i.e.*, $Q = S \times G$),

2. the group acts directly on the second factor (*i.e.*, $\Phi_g = \mathrm{id} \times \mathrm{L}_g$, so that $\Phi_g(s,h) = (s, gh)$), and

3. the projection is the canonical projection onto the first factor (*i.e.*, $\mathrm{pr}_1 : (s,g) \mapsto s$). •

28

We now examine a very important class of mappings that makes an arbitrary principal bundle "look like" a product bundle, at least locally. Metaphorically speaking, such maps are a means of "combing out" the fibers of the bundle (like so many strands of tangled hair).

Definition 2.32. A *trivialization* of a principal bundle $\pi : Q \to S$ over a region $U \subseteq S$ is a diffeomorphism

$$\psi : U \times G \to \pi^{-1}(U) \tag{2.81}$$

that is equivariant and fiber-preserving, in the sense that the following diagram commutes:

$$
\begin{array}{ccc}
U \times G & \xrightarrow{\ \ \psi\ \ } & \pi^{-1}(U) \\
{\scriptstyle \mathrm{id} \times \mathrm{L}_g} \downarrow & & \downarrow {\scriptstyle \Phi_g} \\
U \times G & \xrightarrow{\ \ \psi\ \ } & \pi^{-1}(U) \\
\end{array}
\tag{2.82}
$$
$$\mathrm{pr}_1 \searrow \qquad \swarrow \pi$$
$$U$$

When $U = S$, we say that the trivialization is *global*; otherwise, it is *local*. ●

It should be clear that a trivialization can be understood as a special kind of diffeomorphism between a (local) region of the original bundle $\pi : Q \to S$ and the product bundle $\mathrm{pr}_1 : U \times G \to U$. In particular, the local structure of the original bundle is preserved, because the action of the group on the total space drops to the action of the group on itself, in an equivariant manner. It's worth noting that some authors would call ψ^{-1} the trivialization (instead of ψ), but this is equivalent to our definition, since ψ is a diffeomorphism.

Although local trivializations must exist, global trivializations do not always exist (and smoothness is the notable obstruction). We say that a principal bundle $\pi : Q \to S$ is *trivial* if a global trivialization $\psi : S \times G \to Q$ exists; otherwise, it is *nontrivial*. Any product bundle is trivial by construction, since the identity map is a valid trivialization (but it is not the only choice—one can easily check that for any smooth map $\phi : S \to G$, the map $(s, g) \mapsto \big(s, \mathrm{L}_g \circ \phi(s)\big)$ is also a global trivialization of the product bundle $\mathrm{pr}_1 : S \times G \to S$). On the contrary, the $\mathbb{S}^1$ bundle over $\mathbb{S}^2$ of Example 2.6 (corresponding to rotation about a body-fixed axis) is an example of a nontrivial bundle of great practical significance, as we will see later.

Example 2.9 (*Articulated Body System*). Consider a product bundle with symmetry group $G = \mathrm{SE}(3)$, shape space $S = \mathbb{T}^n$, and total space $Q = \mathbb{T}^n \times \mathrm{SE}(3)$. This can be recognized as the configuration manifold of a system of coupled rigid bodies (*e.g.*, a free-flying multibody robot with revolute joints). The most obvious trivialization for this (and any) product bundle is the identity map:

$$\psi : \mathbb{T}^n \times \mathrm{SE}(3) \mapsto \mathbb{T}^n \times \mathrm{SE}(3), \ (s, g) \mapsto (s, g).$$

One way of interpreting this trivialization is that we have chosen to use the body-fixed coordinate frame of some previously-designated "root body" to describe the pose of the system in $\mathrm{SE}(3)$. However, a coordinate frame fixed to any *other* body in the system would also furnish a valid trivialization. In particular, if $h_i : \mathbb{T}^n \to \mathrm{SE}(3)$ is a smooth map describing the pose of the ith body in the system relative to the root body, as a function of the configuration of the internal joints of the mechanism, then

$$\psi_i : \mathbb{T}^n \times \mathrm{SE}(3) \mapsto \mathbb{T}^n \times \mathrm{SE}(3), \ (s, g) \mapsto \big(s, \mathrm{L}_g \circ h_i(s)\big) \tag{2.83}$$

is another valid trivialization, because it is a diffeomorphism and the second component is easily seen to be equivariant, since the group action in a product bundle simply acts on the second factor on the left. These considerations highlight the fact that the designation of the "root body" is arbitrary; to factor the configuration of an articulated body system into its bulk pose in $\mathrm{SE}(3)$ and the configuration of its internal joints in $\mathbb{T}^n$, it is equally natural to use any body-fixed coordinate frame. More generally, a trivialization can be obtained from any smooth shape-dependent pose offset from an existing body-fixed frame.   ●

In the case of a principal bundle which is not a product bundle (and perhaps nontrivial), it may be unclear how to construct the "first" local trivialization from scratch, given the equivariance requirements imposed. However, we can do this directly from a section, in the following manner.

Proposition 2.2. *Sections and trivializations of a principal bundle are in one-to-one correspondence.*

Proof. It will suffice to construct a bijection between the sections and trivializations of a principal G-bundle $\pi : Q \to S$. Given a section $\sigma : U \to Q$ over some region $U \subseteq S$, we claim that the map

$$\psi : U \times G \to \pi^{-1}(U), \ (s, g) \mapsto \Phi_g \circ \sigma(s) \tag{2.84}$$

is a trivialization, which we call the *canonical trivialization* induced by σ. In particular,

$$\pi \circ \psi(s, g) = \pi \circ \Phi_g \circ \sigma(s) = \pi \circ \sigma(s) = s = \mathrm{pr}_1(s, g), \tag{2.85}$$

since Φ_g preserves the orbits by definition. Moreover, we compute

$$\Phi_h \circ \psi(s, g) = \Phi_h \circ \Phi_g \circ \sigma(s) = \Phi_{hg} \circ \sigma(s) = \psi(hg, s) = \psi \circ (\mathrm{id} \times \mathrm{L_h})(s, g). \tag{2.86}$$

Thus, (2.82) commutes, so ψ is a trivialization of $\pi : Q \to S$ over the region U. Moreover, given a trivialization $\psi : U \times G \to \pi^{-1}(U)$ over some region $U \subseteq S$, we claim that

$$\sigma : U \mapsto \pi^{-1}(U), \ s \mapsto \psi(s, e) \tag{2.87}$$

is a section, which we call the *canonical section* induced by ψ. From (2.82), it's easy to see that

$$\pi \circ \psi(s, e) = \mathrm{pr}_1(s, e) = s, \tag{2.88}$$

and thus (2.76) commutes, so σ is a section of $\pi : Q \to S$ over the region U. Finally, it's clear that for a given trivialization ψ, using its canonical section as defined in (2.87) to construct the canonical trivialization defined in (2.84) yields exactly the trivialization we started with, since $\Phi_g \circ \psi(s, e) = \psi(s, g)$. Thus we have a bijection, completing the argument. ∎

In view of this correspondence, the following corollary is obvious.

Corollary 2.1. *A principal bundle is trivial if and only if there exists a global section.*

Finally, we give a concrete example of constructing a trivialization directly from a section.

Example 2.6 (*Body-Fixed Rotation, continued*). We once again revisit the principal bundle $\pi : \mathrm{SO}(3) \to \mathbb{S}^2$, $R \mapsto R \, \mathrm{e}_3$ with symmetry group $\mathbb{S}^1$, arising from the rotation of a rigid body in $\mathrm{SO}(3)$ around the third body-fixed axis. This bundle happens to be nontrivial (*i.e.*, global trivializations do not exist, hence neither do global sections). However, we may define two maps

$$\sigma_N : \mathbb{S}^2 \setminus \{ -\mathrm{e}_3 \} \to \mathrm{SO}(3), \quad \begin{bmatrix} s_1 \\ s_2 \\ s_3 \end{bmatrix} \mapsto \begin{bmatrix} 1 - \frac{s_1{}^2}{s_3+1} & \frac{-s_1 s_2}{s_3+1} & s_1 \\ \frac{-s_1 s_2}{s_3+1} & 1 - \frac{s_2{}^2}{s_3+1} & s_2 \\ -s_1 & -s_2 & s_3 \end{bmatrix}, \tag{2.89}$$

$$\sigma_S : \mathbb{S}^2 \setminus \{ +\mathrm{e}_3 \} \to \mathrm{SO}(3), \quad \begin{bmatrix} s_1 \\ s_2 \\ s_3 \end{bmatrix} \mapsto \begin{bmatrix} 1 + \frac{s_1{}^2}{s_3-1} & \frac{-s_1 s_2}{s_3-1} & s_1 \\ \frac{s_1 s_2}{s_3-1} & -1 - \frac{s_2{}^2}{s_3-1} & s_2 \\ s_1 & -s_2 & s_3 \end{bmatrix}, \tag{2.90}$$

which can be verified to be sections, since they are smooth and $\pi \circ \sigma = \mathrm{id}$. Each section is defined over the entire shape space except for a single point (the "south pole" for σ_N and the "north pole" for σ_S), so these sections are *almost-global* (*i.e.*, they are defined over an open dense set in the shape space). The canonical trivialization for each of these sections then arises directly as a result of Proposition 2.2. ●

2.5.2 Principal Connections

The rich geometric structure of a principal bundle lifts to the tangent bundle as well. Our first step in this direction is to analyze the infinitesimal behavior of the group action.

Definition 2.33. The *infinitesimal generator* of any $\xi \in \mathfrak{g}$ is the map

$$\xi_Q : Q \to TQ, q \mapsto \left. \tfrac{\mathrm{d}}{\mathrm{d}t} \right|_{t=0} \Phi(\exp t\xi, q), \tag{2.91}$$

which is in fact a vector field $\xi_Q \in \mathfrak{X}(Q)$. ●

In the previous definition, the configuration is acted upon by a curve $t \mapsto \exp t\xi$ in the group, which is an integral curve of the left-invariant vector field $\xi_G : G \mapsto TG,\ g \mapsto \mathrm{dL}_g(\xi)$. In this regard, the infinitesimal generator can be thought of as lifting elements from the Lie algebra to the tangent bundle of the total space, in accordance with the group action. In a product bundle (or in a trivialization), the infinitesimal generators are simply the elements of the Lie algebra pushed forward by the group's *right* action on itself:

$$\xi_Q : Q \to TQ, (s, g) \mapsto \big(0, \mathrm{dR}_g(\xi)\big). \tag{2.92}$$

In view of this local description, it should be clear that the infinitesimal generators are *not* Φ-invariant vector fields, since the group acts on the left of the second factor in a product bundle. It can also be easily verified that for all $\xi \in \mathfrak{g}$, we have $\xi_Q(q) = \mathrm{d}\Phi^q(\xi)$.

The group action also designates a particular subspace of each tangent space (*i.e.*, a distribution) as follows.

Definition 2.34. The *vertical distribution* $VQ \subseteq TQ$ is given by $VQ = \ker \mathrm{d}\pi$. ●

The vertical distribution therefore consists of all vectors in TQ which are tangent to the group orbits, thus having no component pointing "across" fibers. It can also be shown that

$$V_q Q = \big\{\xi_Q(q) : \xi \in \mathfrak{g}\big\} \tag{2.93}$$

and therefore the vertical subspace at every point on the manifold is isomorphic to the Lie algebra of the symmetry group. It is natural to wonder how we might describe another subspace at each point on Q which, together with VQ, would split all of TQ into two complementary distributions, in a manner which respects the symmetry described by the group action. These considerations are formalized as follows.

Definition 2.35. A *principal connection* is a *horizontal distribution*, denoted $HQ \subseteq TQ$, such that:

1. HQ and VQ are complementary (*i.e.*, $TQ = VQ \oplus HQ$),

2. HQ is Φ-invariant (*i.e.*, $\mathrm{d}\Phi_g(HQ) = HQ$), and

3. the assignment of $H_q Q$ to each point $q \in Q$ is smooth. ●

Since VQ and HQ are complementary by definition, we can split any given tangent vector into its vertical and horizontal components (with respect to a particular choice of HQ).

Definition 2.36. The *vertical* and *horizontal projections* are the unique idempotent maps $\mathrm{ver} : TQ \to VQ$ and $\mathrm{hor} : TQ \to HQ$ such that $v_q = \mathrm{ver}\, v_q + \mathrm{hor}\, v_q$ for all $v_q \in TQ$. ●

As stated above, principal connections are not unique, and much like trivializations, no admissible choice is intrinsically more natural than any other. However, given some additional structure, a particular choice of principal connection can simplify the analysis of a particular problem. We now discuss several examples that are relevant to practical engineering problems, to build some intuition as to their role.

Example 2.10 *(Mechanical Connection).* Suppose that in addition to being a principal bundle, (Q, κ) is also a Riemannian manifold, where κ is Φ-invariant. Then, a natural choice for the horizontal distribution is the orthogonal complement of the vertical distribution with respect to the metric, namely,

$$HQ = VQ^\perp = \left\{ h_q \in TQ : \langle\langle h_q, v_q \rangle\rangle = 0 \text{ for all } v_q \in V_q Q \right\}. \tag{2.94}$$

In mechanics, this is called the *mechanical connection* derived from the kinetic energy metric of a mechanical system with symmetry. Concretely, the horizontal distribution then contains all those velocities which do not contribute to the system's net momentum. This connection plays a key role in understanding the conservation laws which arise due to symmetry, as characterized by Noether's Theorem. •

In the previous example, a particular choice of principal connection was especially salient due to the presence of additional structure, namely the metric. Similarly, the designation of a global trivialization of particular signifigance suggests another choice of principal connection.

Definition 2.37. For any global trivialization $\psi : S \times G \to Q$, the principal connection given by

$$HQ = \ker \mathrm{d}\left(\mathrm{pr}_2 \circ \psi^{-1}\right) \tag{2.95}$$

is called the *canonical flat connection* induced by ψ. •

We emphasize the parallelism between this definition and that of VQ, since $\pi = \mathrm{pr}_1 \circ \psi^{-1}$. Strictly speaking, ψ must be global for the canonical flat connection to be well-defined on the entire bundle, but we will sometimes abuse this terminology in a nontrivial bundle when it is clear that we are working only over a local trivialization. The following aims to build some intuition about the canonical flat connection.

Example 2.11 *(Self-Motion Connection).* Consider an orbital manipulator (*i.e.*, a space vehicle equipped with a serial manipulator arm with revolute joints). This system is an example of the free-flying articulated body system considered in Example 2.9, whose configuration manifold is the product bundle $Q = \mathbb{T}^n \times \mathrm{SE}(3)$. To perform manipulation tasks, it is necessary to control the pose of the end effector, and thus the trivialization constructed using the end effector pose is particularly natural.

In fact, the canonical flat connection of this trivialization contains all those velocities which do not move the end effector. This is analogous to the nullspace of the *manipulator Jacobian*, describing the tangent space of the so-called *self-motion manifold* at that configuration (*i.e.*, the submanifold of the configura-

tion manifold along which the configuration may evolve without affecting the end effector pose). This connection therefore captures the system's redundancy, describing all those directions along which the configuration may be adjusted (by altering both the vehicle pose and the arm's joint angles) without altering the end effector pose. The invariance of this principal connection (*i.e.*, of the horizontal distribution) reflects the fact that such directions can be described in a manner that is independent of the absolute pose of the system (*e.g.*, using the end effector frame).   •

There are many other examples of principal connections which characterize the essential features of other robotic or biological systems, especially *locomotion systems*, which achieve bulk motion through space (*i.e.*, the symmetry group) via undulatory motion in the shape space. In this setting, the connection characterizes the effect of "internal" motions in the shape space on the "external" motion in the group. Examples include the *kinematic connection* arising from Chaplygin nonholonomic constraints, the *mechanical connection* mentioned above which describes the reorientation of a falling cat, and the *nonholonomic connection* arising from a combination of momentum conservation and nonholonomic constraints [13]. This perspective also extends to more exotic forms of locomotion, such as microorganisms swimming at low Reynolds numbers, which are described by the *viscous connection* [14]. Our use of principal connections does not fit precisely within this formalism, so we will not explore the details fully, but only mention the rich and beautiful existing body of work relying on principal connections in both robotic and biological locomotion.

2.5.3 Connection Forms

Principal connections also admit an equivalent description in terms of differential forms. Although we will usually work with principal connections as distributions in this dissertation, it will occasionally be convenient to employ this alternative perspective.

Definition 2.38. A *principal connection one-form* is a one-form $\mathcal{A} : TQ \to \mathfrak{g}$ for which:

1. $\mathcal{A}$ is equivariant, in the sense that the following diagram commutes:

$$
\begin{array}{ccc}
TQ & \xrightarrow{\ \mathcal{A}\ } & \mathfrak{g} \\
{\scriptstyle T\Phi_g}\downarrow & & \downarrow{\scriptstyle \mathrm{Ad}_g} \\
TQ & \xrightarrow[\ \mathcal{A}\ ]{} & \mathfrak{g}
\end{array}
\tag{2.96}
$$

2. and vertical vectors are mapped to their generators (*i.e.*, $\mathcal{A}(\xi_Q) = \xi$).   •

This alternative description is related to the distribution perspective on principal connections as follows.

Fact 2.5. *Principal connections and principal connection one-forms are in one-to-one correspondence. In particular, they are identified by the relationship* $\ker \mathcal{A} = HQ$.

The differential forms perspective on principal connections makes it convenient to explicitly define the vertical and horizontal projections. Using the previous identification and the fact that connection forms map vertical vectors to their generators, it is straightforward to show that these maps are given by

$$\text{ver}: TQ \to VQ, \; v_q \mapsto \big(\mathcal{A}(v_q)\big)_Q(q), \qquad \text{hor}: TQ \to HQ, \; v_q \mapsto v_q - \text{ver}\, v_q. \tag{2.97}$$

We can also describe a principal connection one-form via a trivialization and a one-form on Q/G.

Fact 2.6 (Local Form of Connection). *In a trivialization $\psi^{-1}(q) = \big(s(q), g(q)\big)$, any principal connection one-form $\mathcal{A}$ can be written*

$$\mathcal{A} = \mathrm{dR}_{g^{-1}}(\mathrm{d}g) + \mathrm{Ad}_g \circ \mathbb{A}(\mathrm{d}s) \tag{2.98}$$

where the one-form $\mathbb{A}: TS \to \mathfrak{g}$ is called the local form *of $\mathcal{A}$.*

Example 2.12 *(Canonical Flat Connection One-Form)*. The kernel of any connection form is its horizontal distribution, and the canonical flat connection is the kernel of the trivialization's group component. Thus, the connection form of the canonical flat connection is $\mathcal{A} = \mathrm{dR}_{g^{-1}}(\mathrm{d}g)$, so its local form is $\mathbb{A} = 0$.   ●

Example 2.13 *(Mechanical Connection One-Form)*. Consider a principal bundle $\pi: Q \to S$ with an invariant Riemannian metric κ. Following [13], let the *momentum map* $\mathcal{J}: TQ \to \mathfrak{g}^*$ and the *locked inertia tensor* $\mathcal{I}(q): \mathfrak{g} \to \mathfrak{g}^*$ be defined such that for all $v_q \in TQ$ and all $\xi, \eta \in \mathfrak{g}$,

$$\langle \mathcal{J}(v_q); \xi \rangle = \langle\!\langle v_q, \xi_Q \rangle\!\rangle \text{ and } \langle \mathcal{I}(q)\, \eta; \xi \rangle = \langle\!\langle \eta_Q, \xi_Q \rangle\!\rangle. \tag{2.99}$$

Then, the principal connection one-form of the mechanical connection $HQ = VQ^\perp$ is given by

$$\mathcal{A}_{\text{mech}}: TQ \to \mathfrak{g}, \; v_q \mapsto \mathcal{I}(q)^{-1}\mathcal{J}(v_q), \tag{2.100}$$

and it is easily verified that $\ker \mathcal{A}_{\text{mech}} = VQ^\perp$. Moreover, the locked inertia tensor satisfies

$$\langle \mathcal{I}\big(\Phi_g(q)\big)\, \xi; \eta \rangle = \langle \mathcal{I}(q)\mathrm{Ad}_{g^{-1}}\xi; \mathrm{Ad}_{g^{-1}}\eta \rangle. \tag{2.101}$$

for all $g \in G$, $q \in Q$, and $\xi, \eta \in \mathfrak{g}$. Finally, we may define the *local locked inertia tensor* $\mathbb{I}(s): \mathfrak{g} \to \mathfrak{g}^*$ in a given trivialization $\psi: S \times G \to Q$ as $\mathbb{I}(s) = \mathcal{I} \circ \psi(s, e)$.   ●

2.5.4 Horizontal Lifts

Perhaps the main role of a principal connection is that it can be used to identify data defined on the shape space with horizontal data on the total space, as follows.

Definition 2.39. Consider a principal bundle $\pi: Q \to S$ with a designated principal connection HQ. We

define the following notions of *horizontal lifts* for data defined on S:

- the horizontal lift at $q \in \pi^{-1}(s)$ of a tangent vector $v_s \in TS$, denoted $(v_s)_q^{HQ}$, is the unique vector $h_q \in H_q Q$ such that $\mathrm{d}\pi(h_q) = v_s$,

- the horizontal lift of a vector field $X \in \mathfrak{X}(S)$ on the shape space, denoted $X^{HQ} \in \Gamma(HQ) \subseteq \mathfrak{X}(Q)$, is the vector field given by the pointwise horizontal lifts of the "downstairs" vectors, *i.e.*,

$$X^{HQ} : Q \to HQ, \; q \mapsto \left(X \circ \pi(q)\right)_q^{HQ}, \tag{2.102}$$

- and the horizontal lift at $q \in \pi^{-1}\big(\gamma(0)\big)$ of a smooth curve $\gamma : [0, 1] \to S$, denoted $\gamma_q^{HQ} : [0, 1] \to Q$, is the unique smooth curve such that

  1. $\gamma_q^{HQ}(0) = q$,

  2. $\pi \circ \gamma_q^{HQ} = \gamma$, and

  3. $\dot{\gamma}_q^{HQ}(t) \in HQ$ for all $t \in [0, 1]$. $\bullet$

CHAPTER 3

GEOMETRIC FLAT OUTPUTS OF MECHANICAL SYSTEMS WITH SYMMETRY

The material in this chapter is based on the publication [15], co-authored with Matthew D. Kvalheim and Vijay Kumar, as well as the non-archival report [16], co-authored with Vijay Kumar. The author of this thesis led the development of the theoretical contributions, developed the computational tools, and drafted the original manuscripts (in collaboration with his co-authors).

3.1 Introduction

An efficient, effective approach to the control of mechanical systems is to synthesize the overall controller via the composition of a low-rate "open-loop" planner (to select a reference trajectory) with a high-rate "closed-loop" tracking controller (to drive the system towards the reference trajectory) [17]. Such layered control architectures, often called "two degree of freedom" (2-DoF) designs, are found across an extremely diverse array of engineered and biological systems, demonstrating the effectiveness of the paradigm [18]. Such a decomposition allows the lower-frequency planner to consider, or at least approximate, more complex costs (*e.g.*, energy efficiency) and constraints (*e.g.*, obstacle avoidance, actuator saturation) than can be accomodated in the higher-frequency control layer. These methods are thus especially suitable for aerial and space robots, given the computational limitations imposed by their stringent size, weight, and power ("SWaP") constraints. Indeed, although such a decomposition is traditionally imposed *a priori* as a design choice, this layered architecture can also emerge naturally as a result of applying augmented Lagrangian methods to optimal control problems [19].

In order for the resulting closed-loop control architecture to achieve satisfactory tracking performance, it is desirable to ensure that the trajectory selected by the planning layer is "dynamically feasible", meaning that the system's dynamics do not prohibit it from following the prescribed motion. Such concerns are particularly relevant for "underactuated" systems (*i.e.*, those having less actuators than degrees of freedom)— because an underactuated system cannot accelerate in arbitrary directions, not all smooth trajectories through the configuration manifold are dynamically feasible. For example, a quadrotor's translational and rotational dynamics are coupled, because the direction of thrust is fixed in the body frame, requiring the vehicle to roll and pitch to achieve some desired translational motion. A wide range of algorithms for trajectory planning are available to solve such problems (*e.g.*, direct collocation [20], augmented Lagrangian methods [19], etc.); however, many such approaches require substantial computational resources due to the use of iterative numerical optimization to enforce the constraints imposed by the dynamics, which can become intractable for mobile systems with limited payload.

However, some control systems (including many common robotic systems) enjoy a powerful property known as "differential flatness", first introduced in [21], which can make dynamically feasible motion planning much easier. A flat system enjoys a locally bijective correspondence between dynamically feasible trajectories in the state space and arbitrary smooth curves in a so-called "flat space". Thus, planning and control problems can be solved efficiently in the flat space (where smoothness, and perhaps curvature bounds, are sufficient for dynamic feasibility), at which point the solution can be brought back to the physical space for execution [22]. In fact, planning for a flat system "looks" a lot like planning for a fully-actuated system, since arbitrary smooth curves are dynamically feasible, at least in the absence of actuator constraints. Moreover, flat systems are controllable, and all controllable linear systems are flat [23], although the same is not true of nonlinear systems.

3.1.1 Discovery of Flat Outputs

A central challenge in the broad application of flatness-based methods is the required knowledge of a so-called "flat output" (*i.e.*, the mapping to the flat space). Indeed, not all systems admit a flat output, nor are flat outputs unique, and finding a flat output for a given system (or even determining whether one exists) is a challenging task [24], which is usually achieved by manual trial and error on a case-by-case basis [25–27]. While necessary and sufficient conditions for flatness of underdetermined systems are known [28], they are broadly speaking too general to be tractably applied to multibody robotic systems, whose equations of motion grow rapidly in complexity as the number of bodies in the system increases, necessitating the use of numerical algorithms to perform dynamics computations efficiently [29].

In view of these analytical challenges, a number of computational methods have been developed with the goal of identifying flat outputs from sampled data about the system. For example, the approach of [30] involves generating a dataset of state and input trajectories and representing the candidate flat output and the inverse flatness diffeomorphism as weighted sums of basis functions. However, the resulting numerical flat output is only valid locally around the sampled trajectories, the basis functions chosen seem to reflect knowledge of an analytical flat output, and the approach becomes intractible for large bases. The identification of flat outputs from data in the complete absence of an analytical system model was considered in [31], but similar locality limitations remained. Moreover, since flat outputs are not unique, even with knowledge of a particular flat output (or a numerical approximation thereof), it is not necessarily clear whether there exists a "better" choice (*e.g.*, one for the system's true actuation constraints can be more closely approximated via tractable constraints in the flat space).

3.1.2 Flatness of Mechanical Systems

Despite these challenges, numerous mechanical systems are known to be differentially flat [32], and this property has been exploited for effective planning and control of highly dynamic maneuvers for under-actuated robots with limited computational budgets [25, 33, 34]. For example, a flatness-based controller

Table 3.1: Partial Catalog of Mechanical Systems with Geometric Flat Outputs

System	Q	G	S	Bundle	Ref.
Planar Rocket (*Fig. 3.2*)	$\mathrm{SE}(2)$	$\mathbb{R}^2$	$\mathbb{S}^1$	Trivial	[37]
Planar Aerial Manip. (*Fig. 3.3*)	$\mathrm{SE}(2) \times \mathbb{S}^1$	$\mathrm{SE}(2)$	$\mathbb{S}^1$	Trivial	[39]
Spatial Aerial Manipulator	$\mathrm{SE}(3) \times \mathbb{T}^2$	$\mathrm{SE}(3)$	$\mathbb{T}^2$	Trivial	[40]
Quadrotor (*Fig. 3.4*)	$\mathrm{SE}(3)$	$\mathbb{R}^3 \times \mathbb{S}^1$	$\mathbb{S}^2$	Nontrivial	[41]
Quadrotor with Slung Load	$\mathrm{SE}(3) \times \mathbb{S}^2$	$\mathbb{R}^3 \times \mathbb{S}^1$	$\mathbb{S}^2 \times \mathbb{S}^2$	Nontrivial	[26]
Chain of n Spring-Mass Systems	$\mathbb{R}^n$	$\mathbb{R}$	$\mathbb{R}^{n-1}$	Trivial	[42]

for a racing drone executing aggressive trajectories at the edge of the flight envelope showed only a small reduction in tracking performance as compared to a nonlinear model predictive controller; nonetheless, it required roughly two orders of magnitude less computational power [35]. Similarly, adapting residual dynamics learning to be compatible with differential flatness has reduced computational costs by orders of magnitude while still achieving similar control performance to that of optimization-based methods [36].

Towards the goal of a more comprehensive understanding of flatness in mechanical systems, previous work has employed the Riemannian structure of the equations of motion of certain classes of mechanical systems to obtain tractable conditions for flatness. For unconstrained systems with no more than one unactuated degree of freedom, [37] gave a constructive necessary and sufficient condition to obtain a *configuration flat output* (*i.e.*, a function of the configuration alone and not the velocities, inputs, or higher derivatives). Similar results were obtained in [38] for systems with more unactuated degrees of freedom, but a candidate output was assumed to be given. However, the flat outputs obtained in both these methods relied on local coordinates and thus are valid only in the neighborhood of some nominal operating point.

3.1.3 The Role of Symmetry

Mechanical systems often exhibit symmetry, meaning that the dynamics are (roughly speaking) equivalent at all those states related by a certain element of a transformation group. Indeed, the classical result of Noether's Theorem [43] demonstrates that such symmetries explain the existence of conserved quantities like linear momentum, angular momentum, and energy. Modern analyses show that when the transformation group's action on the state space lacks fixed points, a principal bundle structure emerges on the configuration manifold [7, 8], ultimately providing a formalism for analysis of a diverse range of locomotory phenomena, including swimming at low Reynolds numbers [14], the "falling cat problem" [44], and the locomotion of nonholonomic robots [13, 45], all of which can be described using a principal connection.

It has long been conjectured that such symmetries also have a role to play in differential flatness [32]. Indeed, in [46], the authors remark that for many mechanical systems,

> *"... the differentially flat output is not an arbitrary combination of the configuration variables and velocities of the system, but rather consists of a set of points and angles,"*

a phenomenon that the authors believed to be related to symmetry, although a clear connection was not established. In [37], it was shown that any flat output of a very special class of symmetric systems must have a related symmetry (*i.e.*, its level sets must be invariant); however, symmetry was not leveraged to construct the outputs, nor were such symmetries guaranteed for more general systems. Moreover, although the symmetry properties of the mapping from the physical space to the flat space were explored, the symmetry properties of the mapping from the flat space back to the physical space was not (which need not enjoy the same properties in general). On the other hand, in [24], the notion of a symmetry-preserving flat output was proposed, roughly requiring that the symmetry transformation be compatible with the round-trip transformation between the physical and flat spaces, imposing equivariance conditions involving both the mapping to the flat space and the inverse mapping back to physical space. While the authors gave a flat output of an example system that enjoys such a property, the existence of a symmetry-preserving flat output in general for a flat system with symmetry remained an open question.

In our own analysis of the literature on flatness, it has become clear that in fact, many known flat outputs of mechanical systems can be seen to be the group variables of a trivialization of the principal bundle arising from a symmetry of the system. This observation suggests that even many flat outputs obtained via ad hoc analysis were somehow informed or influenced by symmetry, despite lacking a formal understanding of this interplay. In Table 3.1, we give a partial catalog of such systems, along with their configuration manifold Q, symmetry group G, and shape space S. In a similar vein, [47] examined several locomotion systems with group and shape spaces of equal dimension, showing "partial differential flatness" (a more general yet significantly weaker property) with respect to the group variables of a trivialization, although none were found to be fully differentially flat. In fact, the potential relevance of principal bundle geometry to flatness first occurred to us after considering how [41] used trivializations of the Hopf fibration (an $\mathbb{S}^1$-bundle over $\mathbb{S}^2$) to parametrize a quadrotor's attitude quaternion in $\mathbb{S}^3$.

3.1.4   Overview and Contributions

The above discussion suggests a rich interplay between flatness and symmetry in mechanical systems. In view of these observations, this chapter is guided by two related (but distinct) overarching questions:

> *Can we exploit symmetry to develop a more systematic method*
> *for the construction of a flat output of a given mechanical system?*

> *When can we ensure that any flat output ultimately obtained by*
> *such a procedure is, in an appropriate sense, symmetry-preserving?*

While both questions pertain to the role of symmetry, the former seeks to develop systematic tools that

obviate ad hoc or bespoke approaches, while the latter concerns the construction of particularly "good" flat outputs (*i.e.*, those that respect the symmetry), since in general, flat outputs are not unique.

Towards these broader goals and informed by Table 3.1, we explore, in particular, when a mechanical system with an appropriate symmetry admits a trivialization of its principal bundle in which the group variables are a flat output of the system. We call this a *geometric flat output*, underscoring the connection with geometric mechanics [7]. In particular, such geometric flat outputs have several favorable properties:

1. They are *configuration* flat outputs [37], making it convenient to write constraints on positions, velocities and inputs in terms of flat output derivatives [34].

2. They are *equivariant* maps from the configuration manifold to the flat space, reflecting a consistency with the symmetry of the physical system.

3. They are often *global or almost global*, meaning they are well-defined over all or almost all of the configuration manifold, capturing more completely the system's performance envelope.

Our work in this chapter will consist of formal mathematical results and analytical worked examples, as well as somewhat less formal computational methods, which demonstrate preliminary progress towards operationalizing the more formal insights.

In what follows, we begin with some mathematical preliminaries that will make the particular theoretical goals of the chapter more precise. After setting the stage by considering the symmetries of the set of dynamically feasible trajectories, we analyze the dynamic feasibility constraints of a mechanical system in a trivialization of the principal bundle arising from its symmetry. Using this structure, we ultimately present a sufficient condition for the construction of a geometric flat output of a mechanical system with "broken" symmetry (wherein the kinetic energy, but perhaps not the potential energy, is invariant, a setting similar to that of [37]). Moreover, we show that this flat output will in fact be symmetry-preserving when the symmetry of the system is slightly stronger (*i.e.*, when the potential forces are also invariant). This condition amounts to a mild regularity criterion as well as the existence of a section of the bundle that is orthogonal to a certain computable distribution, from which we immediately construct the geometric flat output. Analytical worked examples demonstrate the approach for several concrete robotic systems.

Given the centrality of this so-called "orthogonal section" in our condition for flat output construction, the focus of the latter half of the chapter is the development of an approach for the discovery of the same, which we achieve through a mixture of geometric and computational methods. Applying our computational tools to two of the analytical worked examples from earlier in the chapter ultimately shows precise numerical agreement with the known closed-form solutions, providing evidence that the method can correctly recover numerical approximations of the true flat outputs. We also discuss the implications of a nontrivial bundle structure in regards to prohibiting the existence of truly global geometric flat outputs. Ultimately, the results in this chapter have broad applications in the control of an important class of multibody robotic

systems, including many vehicles and manipulators operating in air or space environments.

3.2   Mathematical Preliminaries

We now establish a mathematical context in which we can state the goals of this chapter more formally in regards to the relationship between flatness and symmetry in mechanical systems.

3.2.1   Mechanical Systems

In this chapter (and beyond), we will be concerned with the following class of systems. Note that in this thesis, we do not explicitly consider mechanical systems subject to nonholonomic constraints or intermittent contact with the environment.

Definition 3.1. A *mechanical system* $\Sigma = (Q, \kappa, P, F)$ consists of:

1. a smooth manifold Q (called the *configuration manifold*),

2. a Riemannian metric κ on Q (called the *kinetic energy metric*),

3. a smooth function $P : Q \to \mathbb{R}$ (called the *potential energy*), and

4. a smooth codistribution $F \subseteq T^*Q$ (called the *control codistribution*).

The system is *fully actuated* if $F = T^*Q$; otherwise, it is *underactuated.* Moreover, the *equations of motion* (or *dynamics*) are given by the forced Euler-Lagrange equations:

$$\nabla_{\dot{q}}\dot{q} + \mathrm{grad}_\kappa P(q) = \kappa^\sharp(f_q), \quad f_q \in F_q, \tag{3.1}$$

where $f_q \in F_q$ is the *control input*, $q \in Q$ is the *configuration*, and $(q, \dot{q}) \in TQ$ is the *state*.   ●

Remark 3.1. We present the equations of motion in this geometric form because it will allow us to more conveniently exploit their Riemannian structure. However, (3.1) is analogous to other representations that may be more familiar to some readers. For example, a mechanical system described by the so-called "manipulator equations"

$$M(q)\,\dot{v} + C(q, v)\,v + g(q) = B(q)\,u \tag{3.2}$$

can also be expressed in the form (3.1), where the kinetic energy metric is given by $\kappa(v, w) = v^\mathrm{T} M(q)w$, the Coriolis forces $C(q, v)\,v$ arise directly from the kinetic energy, the gravity term $g(q)$ corresponds to the differential $\mathrm{d}P(q)$ of the potential energy, and the control codistribution F_q at each point $q \in Q$ corresponds to the column space of $B(q)$. Moreover, in local coordinates $(q^1, \ldots, q^n)$, the dynamics (3.1) can be expressed as

$$\ddot{q}^i + \Gamma^i_{jk}\dot{q}^j\dot{q}^k + \kappa^{ij}\frac{\partial P}{\partial q^j} = \kappa^{ij} f_j, \tag{3.3}$$

42

where $\kappa^{ij}\kappa_{ij} = \delta_{ij}$, and Γ^i_{jk} are the Christoffel symbols. A thorough and informative exploration of the connections between the Riemannian perspective (3.1) seen more commonly in geometric control, the manipulator equations (3.2) seen more commonly in robotics, and the local form (3.3) can be found in [48].

It is clear that for an underactuated mechanical system, not all forces f_q are available at each configuration q. Thus, not all smooth curves in the configuration manifold lift to solutions of (3.1), introducing constraints that must be considered when planning trajectories. We formalize this consideration as follows.

Definition 3.2. The set of dynamically feasible smooth curves in the configuration manifold is given by

$$\mathsf{DF}(\Sigma) = \left\{ q \in \mathsf{C}^\infty(\mathbb{R}, Q) : \kappa^\flat\big(\nabla_{\dot{q}}\dot{q} + \mathrm{grad}_\kappa P(q)\big) \in F_q \right\}. \tag{3.4}$$

A curve $t \mapsto q(t)$ is said to be *dynamically feasible* if $q \in \mathsf{DF}(\Sigma)$. ●

3.2.2 Differential Flatness

We now briefly formalize the notion of differentially flat control systems. For more detailed, general, and formal presentations of differential flatness, we refer the reader to [49] and [50].

Definition 3.3. A control system $\dot{x} = f(x, u)$ with state $x \in X$ and input $u \in U$ is said to be *differentially flat* (or simply *flat*) if there exists a (perhaps non-unique) *flat output*

$$y = \Lambda(x, u, \dot{u}, \ddot{u}, \dots, u^{(\alpha)}) \tag{3.5}$$

such that the state and inputs are can be (locally) recovered via finitely many derivatives of the output:

$$(x, u) = \Lambda^{-1}(y, \dot{y}, \ddot{y}, \dots, y^{(\beta)}), \tag{3.6}$$

morally speaking inverting this mapping. ●

The abuse of notation Λ^{-1} is motivated by the fact that flat systems enjoy a one-to-one correspondence (at least locally) between smooth state-input trajectories of the system and arbitrary smooth curves in the flat output space, as illustrated by the following diagram:

$$\begin{array}{ccc} & \Lambda & \\ & \overset{\frown}{} & \\ \big\{\dot{x} = f(x, u)\big\} & & \mathsf{C}^\infty(\mathbb{R}, Y) \\ & \underset{\smile}{} & \\ & \Lambda^{-1} & \end{array} \tag{3.7}$$

where the left-hand set is understood as a subset of $\mathsf{C}^\infty(\mathbb{R}, X) \times \mathsf{C}^\infty(\mathbb{R}, U)$, and by abuse of notation, we

define overloads of Λ and Λ^{-1} for curves $x \in \mathsf{C}^\infty(\mathbb{R}, X)$, $u \in \mathsf{C}^\infty(\mathbb{R}, U)$, and $y \in \mathsf{C}^\infty(\mathbb{R}, Y)$ given by

$$\Lambda(x, u) = \Big(t \mapsto \Lambda\big(x(t), u(t), \dot{u}(t), \ldots, u^{(\alpha)}(t)\big) \Big), \tag{3.8}$$

$$\Lambda^{-1}(y) = \Big(t \mapsto \Lambda^{-1}\big(y(t), \dot{y}(t), \ldots, y^{(\beta)}(t)\big) \Big). \tag{3.9}$$

Boundary conditions for the original system can be mapped via the flat output to the flat space. Thus, given knowledge of a flat output, the dynamically feasible trajectory planning problem can be solved in the flat space, at which point the solution can be mapped to the state-input space.

Remark 3.2. Every fully-actuated system is differentially flat with respect to a flat output given by the system's configuration, namely,

$$\Lambda : (q, \dot{q}) \mapsto q, \tag{3.10}$$

since for any smooth curve q in Q, we may reconstruct the state $x = (q, \dot{q})$ in TQ and input f_q in F_q via

$$\Lambda^{-1} : (q, \dot{q}, \ddot{q}) \mapsto \Big(q, \dot{q}, \kappa^\flat \big(\nabla_{\dot{q}} \dot{q} + \operatorname{grad}_\kappa P(q) \big) \Big). \tag{3.11}$$

This observation motivates the definition of a *configuration flat output* [37], namely a flat output of a mechanical system (fully-actuated or not) that depends solely on the system's configuration, $y = \Lambda(q)$.

3.2.3 Symmetry and Dynamic Feasibility

Since we seek to explore connections between flatness and symmetry in mechanical systems, we must formalize the notion of symmetry in mechanical systems. In fact, we are interested in several different flavors of symmetry of increasing strength, since it is common for the symmetry of physical systems to be "broken" by ambient forces (*e.g.*, gravity).

Definition 3.4. Consider a mechanical system $\Sigma = (Q, \kappa, P, F)$. An action $\Phi : G \times Q \to Q$ is called:

1. a *symmetry* of Σ if κ, P, and F are Φ-invariant,

2. a *dynamic symmetry* of Σ if κ, dP, and F are Φ-invariant (but perhaps P is not), and

3. a *broken symmetry* of Σ if κ and F are Φ-invariant (but perhaps P and dP are not).   •

Since the Φ-invariance of P is a sufficient (but not necessary) condition for the Φ-invariance of dP, it should be clear that any symmetry is, in particular, a dynamic symmetry, and any dynamic symmetry is, in particular, a broken symmetry. While the strongest form of symmetry above is required to obtain conserved quantities (in the absence of external forcing) via Noether's Theorem, the two more general cases are common for robotic systems operating under the effects of gravity. Furthermore, a given action Φ of G on Q induces an action on $\mathsf{C}^\infty(\mathbb{R}, Q)$ that maps any curve $t \mapsto q(t)$ to the curve $t \mapsto \big(\Phi_g \circ q \big)(t)$.

Thus, we may examine the symmetry of $\mathsf{DF}(\Sigma)$, motivating the weaker notion of dynamic symmetry.

Proposition 3.1. *Suppose Φ is a dynamic symmetry of a mechanical system Σ. Then, $\mathsf{DF}(\Sigma)$ is Φ-invariant.*

Proof. It will suffice to show that for any curve $\gamma \in \mathsf{DF}(\Sigma)$, we have $\Phi_g \circ \gamma \in \mathsf{DF}(\Sigma)$. By [9, Thm. 5.70], the Φ-invariance of κ implies that for all $X, Y \in \mathfrak{X}(Q)$ and $g \in G$, we have

$$\nabla_{(\mathrm{d}\Phi_{g^{-1}} \circ X \circ \Phi_g)}(\mathrm{d}\Phi_{g^{-1}} \circ Y \circ \Phi_g) = \mathrm{d}\Phi_{g^{-1}} \circ \left(\nabla_X Y\right) \circ \Phi_g. \tag{3.12}$$

A consequence of the previous fact is that for any admissible path $\gamma \in \mathsf{A}(q)$ and any $Z \in \mathfrak{X}(\gamma)$, we have

$$\nabla_{(\Phi_g \circ \gamma)'}(\mathrm{d}\Phi_g \circ Z) = \mathrm{d}\Phi_g \circ \left(\nabla_{\dot{\gamma}} Z\right) \tag{3.13}$$

where we note that $\Phi_g \circ \gamma \in \mathsf{A}(Q)$ and $\mathrm{d}\Phi_g \circ Z \in \mathfrak{X}(\Phi_g \circ \gamma)$, while $\nabla_{(\Phi_g \circ \gamma)'} : \mathfrak{X}(\Phi_g \circ \gamma) \to \mathfrak{X}(\Phi_g \circ \gamma)$ is simply covariant differentiation along the given curve. With this in mind, we compute:

$$\kappa^\flat\left(\nabla_{(\Phi_g \circ q)'}(\Phi_g \circ q)' + \mathrm{grad}_\kappa P(\Phi_g \circ q)\right) = \kappa^\flat \circ \mathrm{d}\Phi_g\left(\nabla_{\dot{q}}\dot{q}\right) + \mathrm{d}P \circ \Phi_g \circ q \tag{3.14}$$

$$= \mathrm{d}\Phi^*_{g^{-1}} \circ \kappa^\flat\left(\nabla_{\dot{q}}\dot{q} + \mathrm{grad}_\kappa P(q)\right). \tag{3.15}$$

Thus, the claim follows directly from the Φ-invariance of F. $\blacksquare$

It is readily seen that for any mechanical system Σ, every smooth state-input trajectory satisfying (3.1) projects to exactly one smooth curve in the configuration manifold. Thus, a flat output establishes the following one-to-one correspondence (at least locally):

$$\begin{array}{c} \mathsf{DF}(\Sigma) \\ \Lambda\Big(\ \Big\uparrow\ \Big)\Lambda^{-1} \\ \mathsf{C}^\infty(\mathbb{R}, Y) \end{array} \tag{3.16}$$

where by mild abuse of notation we let Λ act directly on dynamically feasible curves in the configuration manifold (and not the state-input space), so that any curve $q \in \mathsf{DF}(\Sigma)$ has a corresponding flat space representative $\Lambda(q)$.

Suppose also that Φ is a dynamic symmetry of Σ. Then, by Prop. 3.1, the dynamically feasible curve $\Phi_g \circ q$ has as its flat space representative the curve $\Lambda(\Phi_g \circ q)$. A natural question thus asks whether these flat space curves are also related by a group action. Although [24] formulated a more general notion of symmetry preservation and flatness, we give a more specific definition suitable for the present setting.

Definition 3.5. Consider a mechanical system Σ with a dynamic symmetry $\Phi : G \times Q \to Q$ and a flat output Λ with flat space Y. We say that Λ is *symmetry-preserving* if, for some action on the flat space

$\Psi : G \times Y \to Y$ and all $g \in G$, the following diagram commutes:

$$
\begin{array}{ccc}
\mathsf{DF}(\Sigma) & \xrightarrow{\quad \Phi_g \quad} & \mathsf{DF}(\Sigma) \\[2pt]
\Lambda \Big\updownarrow \Lambda^{-1} & & \Lambda \Big\updownarrow \Lambda^{-1} \\[2pt]
\mathsf{C}^\infty(\mathbb{R}, Y) & \xrightarrow[\quad \Psi_g \quad]{} & \mathsf{C}^\infty(\mathbb{R}, Y)
\end{array}
\tag{3.17}
$$

In other words, the maps to and from the flat space (from and to the physical space) are *both* equivariant. $\quad \bullet$

3.3 Constructing Symmetry-Preserving Flat Outputs

In this section, we present the main formal results of this chapter, giving a sufficient condition for the construction of a flat output of a mechanical system with broken symmetry. In the case that the symmetry is, in particular, a dynamic symmetry, the flat output we obtain will also be symmetry-preserving.

3.3.1 Dynamic Feasibility in a Local Trivialization

We begin by expressing the dynamic feasibility constraints of a mechanical system Σ with respect to a local trivialization of its configuration manifold. Consider a principal bundle $\pi : Q \to (S := Q/G)$ induced by a free and proper action $\Phi : G \times Q \to Q$ (*e.g.*, a broken symmetry of Σ), and fix any arbitrary choice of:

1. a local trivialization $\psi : U \times G \to \pi^{-1}(U)$, where $\psi^{-1}(q) = \big(\pi(q), \varphi(q)\big)$,

2. a basis of vector fields $\{Z_\alpha : \alpha = 1, \ldots, \dim S\}$ for TU, and

3. a basis $\{\mathrm{e}_a : a = 1, \ldots, \dim G\}$ for $\mathfrak{g}$.

Consider expressing the velocities of smooth curves $t \mapsto s(t)$ in U and $t \mapsto g(t)$ in G as[3]

$$
\dot{s}(t) = v^\alpha(t)\, Z_\alpha\big(s(t)\big), \quad \dot{g}(t) = \mathrm{dL}_{g(t)}\big(\xi^a(t)\, \mathrm{e}_a\big),
\tag{3.18}
$$

where v^α and ξ^a are smooth scalar functions depending only on time. Then, we may express the velocity of the corresponding curve $q : t \mapsto \psi\big(s(t), g(t)\big)$ in $\pi^{-1}(U)$ as

$$
\dot{q} = \mathrm{d}\psi(\dot{s}, \dot{g}) = \mathrm{d}\psi\big(v^\alpha Z_\alpha(s), \mathrm{dL}_g(\xi^a \mathrm{e}_a)\big)
\tag{3.19}
$$

$$
= v^\alpha\, \mathrm{d}\psi^g \circ Z_\alpha(s) + \xi^a\, \mathrm{d}\psi_s \circ \mathrm{dL}_g(\mathrm{e}_a)
\tag{3.20}
$$

$$
= v^\alpha \big(\underbrace{\mathrm{d}\psi^{\varphi(q)} \circ Z_\alpha \circ \pi(q)}_{=:\, H_\alpha(q)} \big) + \xi^a \big(\underbrace{\mathrm{d}\psi_{\pi(q)} \circ \mathrm{dL}_{\varphi(q)}(\mathrm{e}_a)}_{=:\, V_a(q)} \big).
\tag{3.21}
$$

---

[3]We use index notation and the Einstein summation convention. For clarity, we use indices a, b, c for G and α, β, γ for S.

Thus, the previous calculations motivate us to define a *standard basis* of vector fields for $TQ\big|_U$ (relative to the three choices fixed above) given by $\{H_\alpha\} \cup \{V_a\}$. In particular, $\{V_a\}$ can be seen to be a basis of vector fields for the vertical subbundle $VQ\big|_U$, while $\{H_\alpha\}$ is a basis of vector fields for the "canonical flat connection"[4] induced by the trivialization ψ, given by $HQ\big|_U := \mathrm{d}\psi^G(TU)$. Moreover, it is easily verified that each H_α and V_a is a Φ-invariant vector field (*i.e.,* $H_\alpha = \mathrm{d}\Phi_g \circ H_\alpha \circ \Phi_{g^{-1}}$ and $V_a = \mathrm{d}\Phi_g \circ V_a \circ \Phi_{g^{-1}}$).

Using such a basis, we prove the following technical lemma, which will ultimately prove very convenient.

Lemma 3.1 (Implicit Dynamics in a Local Trivialization). *Let the free and proper action $\Phi : G \times Q \to Q$ be a broken symmetry of a mechanical system $\Sigma = (Q, \kappa, P, F)$, where $\dim G = \operatorname{rank} F$. For the principal bundle $\pi : Q \to (S = Q/G)$, let $\psi : U \times G \to \pi^{-1}(U)$ be a local trivialization, let $\{X_\delta\}$ be a local basis of vector fields for $\operatorname{coann} F$ defined over $\pi^{-1}(U)$, and let $\{V_a\} \cup \{H_\alpha\}$ be a standard basis. Define the map*

$$E : \big(s, g, \upsilon, \xi, \dot{\upsilon}, \dot{\xi}\big) \mapsto \tag{3.22}$$
$$\big\langle\!\big\langle X_\delta, \big(\dot{\xi}^a V_a + \dot{\upsilon}^\alpha H_\alpha + \xi^a \xi^b \nabla_{V_a} V_b + \xi^a \upsilon^\beta (\nabla_{V_a} H_\beta + \nabla_{H_\beta} V_a) + \upsilon^\alpha \upsilon^\beta \nabla_{H_\alpha} H_\beta + \operatorname{grad}_\kappa P\big)\big\rangle\!\big\rangle \circ \psi(s, g).$$

Then, a curve $q : t \mapsto \psi\big(s(t), g(t)\big)$ belongs to $\mathsf{DF}(\Sigma)$ if and only if $t \mapsto E\big(s(t), g(t), \upsilon(t), \xi(t), \dot{\upsilon}(t), \dot{\xi}(t)\big)$ vanishes identically, where the curves $t \mapsto \upsilon^\alpha(t)$ and $t \mapsto \xi^a(t)$ are defined such that $\dot{q} = \upsilon^\alpha H_\alpha + \xi^a V_a$.

Proof. Relying on the basic properties of affine connections and covariant differentiation described in Definitions 2.7 and 2.10, and following reasoning similar to that of [51], we may express the geometric acceleration of any such curve as

$$\nabla_{\dot{q}} \dot{q} = \dot{\xi}^a V_a + \dot{\upsilon}^\alpha H_\alpha + \xi^a \xi^b \nabla_{V_a} V_b + \xi^a \upsilon^\beta (\nabla_{V_a} H_\beta + \nabla_{H_\beta} V_a) + \upsilon^\alpha \upsilon^\beta \nabla_{H_\alpha} H_\beta. \tag{3.23}$$

Furthermore, a given curve $q : \mathbb{R} \to Q$ is dynamically feasible if and only if

$$\big\langle\!\big\langle X(q), \nabla_{\dot{q}} \dot{q} + \operatorname{grad} P(q)\big\rangle\!\big\rangle = 0 \text{ for all } X \in \Gamma(\operatorname{coann} F), \tag{3.24}$$

since the previous amounts to a projection of the forced Euler-Lagrange equations onto the unactuated subbundle, which eliminates the external control forces since $\big\langle\!\big\langle X, \kappa^\sharp(f_q)\big\rangle\!\big\rangle = \langle f_q ; X\rangle = 0$. Furthermore, due to the bilinearity of the metric, (3.24) holds if and only if it holds for each X_δ in the basis. Thus, we may locally express the dynamic feasibility constraint (3.24) in the form

$$\big\langle\!\big\langle X_\delta, \dot{\xi}^a V_a + \dot{\upsilon}^\alpha H_\alpha + \xi^a \xi^b \nabla_{V_a} V_b + \xi^a \upsilon^\beta (\nabla_{V_a} H_\beta + \nabla_{H_\beta} V_a) + \upsilon^\alpha \upsilon^\beta \nabla_{H_\alpha} H_\beta + \operatorname{grad}_\kappa P\big\rangle\!\big\rangle = 0. \tag{3.25}$$

Combining the previous equation with the given local trivialization completes the argument. ∎

---

[4]The canonical flat connection is only well-defined over the trivialization itself. Thus, on a nontrivial bundle, it cannot be extended to a globally-defined principal connection. Since we will work only within a trivialization, this suffices.

3.3.2 The Underactuation Distribution

The following distribution, analogous to those studied in [37] and [38], will feature prominently in our sufficient condition for flatness. In fact, it can be easily computed directly from the system model.

Definition 3.6. The *underactuation distribution* of a mechanical system $\Sigma = (Q, \kappa, P, F)$ is given by

$$\Delta(\Sigma) = \operatorname{span} \left\{ X, \nabla_Y X : X \in \Gamma(\operatorname{coann} F), \ Y \in \Gamma(TQ) \right\}, \tag{3.26}$$

where $\Gamma(\operatorname{coann} F)$ is the set of all vector fields annihilated by the control codistribution F. ●

It's worth noting that for any mechanical system $\Sigma = (Q, \kappa, P, F)$, we have

$$\dim Q - \operatorname{rank} F \ \leq \ \operatorname{rank} \Delta(\Sigma) \ \leq \ \dim Q, \tag{3.27}$$

since $\operatorname{coann} F \subseteq \Delta(\Sigma)$. Within this range, the particular value of $\operatorname{rank} \Delta(\Sigma)$ is determined by how the distribution of "unactuated velocities" (*i.e.*, $\operatorname{coann} F$) interacts with the kinetic energy metric κ (*i.e.*, via the Riemannian connection ∇) in (3.26). Also, when a distribution analogous to $\Delta(\Sigma)$ was defined in [37], the authors also made an observation analogous to the following (cf. [37, Lemma 4.1]).

Proposition 3.2. *Let Φ be a broken symmetry of a mechanical system Σ. Then, $\Delta(\Sigma)$ is Φ-invariant.*

Proof. Following the same line of reasoning as [37], the claim follows from the invariance of F and thus of its coannihilator, as well as the fact that ∇ corresponds to a Φ-invariant metric (and thus covariant derivatives of invariant vector fields are invariant). ∎

We will often simply write Δ when the system Σ is clear from context. It is also worth mentioning how to compute Δ in practice. Thanks to the linearity properties of the covariant derivative, it is readily shown that for any bases of vector fields $\operatorname{coann} F = \operatorname{span}\{U_i\}$ and $TQ = \operatorname{span}\{X_j\}$,

$$\Delta = \operatorname{span} \left\{ U_i, \nabla_{X_j} U_i : i = 1, \ldots, (\dim Q - \operatorname{rank} F), \ j = 1, \ldots, \dim Q \right\}. \tag{3.28}$$

Thus, we need only compute finitely many covariant derivatives to obtain a basis of vector fields for Δ, which can be done explicitly directly from the data provided to define any mechanical system Σ. Later, we will compute Δ for several concrete systems (see Examples 3.1-3.3).

3.3.3 Main Result

We are now ready to state this chapter's main result on flatness and symmetry.

Theorem 3.1 (Main Result). *Let the free and proper action $\Phi : G \times Q \to Q$ be a broken symmetry of a mechanical system $\Sigma = (Q, \kappa, P, F)$, where $\dim G = \operatorname{rank} F$. Let $\sigma : U \to Q$ be a section of the principal*

bundle $\pi : Q \to (S := Q/G)$, and define the map E as in Lemma 3.1 for the trivialization $\psi_\sigma : (s, g) \mapsto \Phi_g \circ \sigma(s)$ and a Φ-invariant basis $\{X_\delta\}$ for $\operatorname{coann} F$. Suppose the following conditions hold:

1. Orthogonality: Δ *is orthogonal to the image of σ as submanifold of Q.*

2. Regularity: *The partial differential $\partial_s E$ is full rank at generic points in $E^{-1}(0)$.*

Then, the group component of the trivialization ψ_σ is a configuration flat output of Σ, given by

$$\Lambda : T\big(\pi^{-1}(U)\big) \to G, \ v_q \mapsto \operatorname{pr}_2 \circ \psi_\sigma^{-1}(q). \tag{3.29}$$

Moreover, if Φ is a dynamic symmetry of Σ, then Λ is symmetry-preserving.

Remark 3.3. Theorem 3.1 is depicted visually in Fig. 3.1, with particular emphasis on the orthogonality condition. In fact, the regularity condition is relatively mild, and in practice the orthogonality condition is the harder one to satisfy. Moreover, singularities are permitted; we only forbid their occurence at *generic* points (*e.g.*, singularities are allowed over a closed set of measure zero, which happens often in examples), since flatness pertains to generic trajectories. Note that such singularities do not correspond to points $q \in Q$ but rather tuples $(q, \dot{q}, \ddot{q})$, or more formally, points in a second-order jet space [37].

Remark 3.4. The previous result does not require us to assume dynamic (*vs.* broken) symmetry to obtain a geometric flat output; however, this stronger assumption will ensure that the flat output obtained is symmetry-preserving. In fact, for the weaker result, the assumption of broken symmetry can be relaxed to the weaker requirement that $\kappa^\flat(\Delta) \subseteq T^*Q$ is a Φ-invariant codistribution, but we do not pursue the details here. Moreover, although this result bears similarities to the results of [37], a key distinction (besides the less-local formulation) is the exploration of symmetry preservation in regards to both Λ and Λ^{-1}, whereas [37] considered only the invariance of the level sets of the configuration flat output.

Proof of Theorem 3.1. As mentioned above, $HQ\big|_U := \mathrm{d}\psi^G(TU)$ defines a horizontal subbundle (*i.e.*, a principal connection) over the trivialization, spanned by $\{H_\alpha\}$. Moreover, HQ is Φ-invariant and, in particular, lies tangent to the image of σ. Thus, it follows from Proposition 3.2 that $HQ \perp \Delta$ everywhere throughout $\pi^{-1}(U) \subseteq Q$ (and not merely along the image of σ). We will use this observation to express the dynamic feasibility condition obtained in Lemma 3.1 in a simplified form.

In particular, from the fact that $HQ \perp \Delta$ and the definition of Δ, it is clear that for all $Y \in \mathfrak{X}(Q)$, we have

$$\langle\langle X_\delta, H_\alpha \rangle\rangle = 0, \quad \langle\langle \nabla_Y X_\delta, H_\alpha \rangle\rangle = 0. \tag{3.30}$$

Moreover, since ∇ is the Riemannian connection (and hence is compatible with the metric), we also have

$$\langle\langle X_\delta, \nabla_Y H_\alpha \rangle\rangle = \nabla_Y \langle\langle X_\delta, H_\alpha \rangle\rangle - \langle\langle \nabla_Y X_\delta, H_\alpha \rangle\rangle = 0. \tag{3.31}$$

$\uparrow \ \Delta \subseteq TQ$
underactuation distribution

$\sigma : S \to Q$
section of the bundle

$\uparrow \ HQ \subseteq TQ$
principal connection

$\Phi_g : Q \to Q$
group action

$\pi : Q \to S$
bundle projection

$y : Q \to G$
geometric flat output
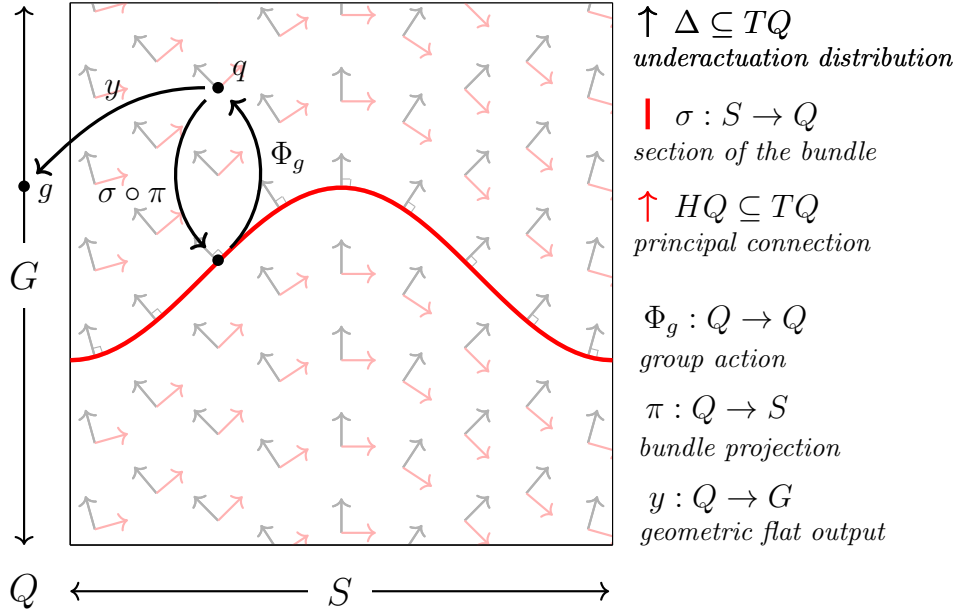
Figure 3.1: An illustration of Theorem 3.1, in which the section σ, depicted via a thick red line, is orthogonal to the distribution Δ, depicted via black arrows. Under additional (relatively mild) assumptions, the group variables of the corresponding trivialization will be a geometric flat output of the system. Moreover, if the symmetry in question is a dynamic symmetry, the flat outputs obtained will be symmetry-preserving.

Next, expanding the output of the dynamic feasibility constraint (3.22) using the bilinearity of the metric will show that all terms depending on υ and $\dot{\upsilon}$ are linear in one of the quantities shown to be zero in (3.30) and (3.31). Eliminating these vanishing terms, we obtain the simplified dynamic feasibility constraint

$$\langle\langle X_\delta, \dot{\xi}^a V_a + \xi^a \xi^b \nabla_{V_a} V_b + \mathrm{grad}_\kappa P \rangle\rangle \circ \psi(s,g) = 0, \tag{3.32}$$

that is, a constraint of the form

$$C\big(s, (g, \xi, \dot{\xi})\big) = 0, \tag{3.33}$$

where $C : S \times (G \times \mathfrak{g} \times \mathfrak{g}) \to \mathbb{R}^{\dim S}$ and $\xi = \xi^a \mathrm{e}_a$. Thanks to the regularity assumption on $\partial_s E$, the implicit function theorem applies at generic points in $C^{-1}(0)$, and it follows from continuity that we may locally solve for s in terms of g, ξ, and $\dot{\xi}$. Moreover, $\xi = \mathrm{dL}_{g^{-1}}(\dot{g})$, and differentiating this relationship to obtain $\dot{\xi}$ thus allows us to express the shape in terms of g, $\dot{g}$, and $\ddot{g}$, and thus reconstruct the configuration q using the trivialization ψ_σ. Differentiating again to obtain the velocity $\dot{q}$ and then also computing the geometric acceleration $\nabla_{\dot{q}} \dot{q}$ will ultimately yield the inputs f_q via the equations of motion. Thus, in the canonical trivialization ψ_σ, the group variables constitute a geometric flat output of the system.

Since the group component of any local trivialization is an equivariant map, it is clear that Λ is equivariant.

Assuming now that Φ is (in particular) a dynamic symmetry of Σ (so that $\mathrm{d}P$ is an invariant covector field), it remains to show that the map Λ^{-1} is equivariant.

Since $(\psi_\sigma)_s : g \mapsto \psi_\sigma(s, g)$ is equivariant with respect to L_g and Φ_g and the flatness diffeomorphism was constructed from solutions of (3.33), or more explicitly (3.32), for s, it will suffice to show that the quantity on the left-hand side of (3.32) is invariant to transformations of the flat output trajectory. Namely, for any curve $t \mapsto g(t)$, let $\Psi_h(g)$ be the curve $t \mapsto \mathrm{L}_g\big(h(t)\big)$. Then, for any $h \in G$, we define the transformed curve $g' = (\Psi_h g) : t \mapsto \mathrm{L}_h\big(g(t)\big)$ and compute

$$\xi' = \mathrm{dL}_{(hg)^{-1}}\big(\mathrm{dL}_h(\dot{g})\big) = \mathrm{dL}_{g^{-1}} \circ \mathrm{dL}_{h^{-1}} \circ \mathrm{dL}_h(\dot{g}) = \mathrm{dL}_{g^{-1}}(\dot{g}) = \xi, \tag{3.34}$$

thus also, $\dot{\xi}' = \dot{\xi}$. Moreover, since X_δ, V_a, and V_b are all Φ-invariant vector fields, it will suffice to note that $\mathrm{grad}_\kappa P$ is also Φ-invariant (since κ and $\mathrm{d}P$ are Φ-invariant). In particular, we may compute

$$\langle\langle X_\delta, \dot{\xi}^a V_a + \xi^a \xi^b \nabla_{V_a} V_b + \mathrm{grad}_\kappa P \rangle\rangle \circ \psi_\sigma\big(s, \mathrm{L}_h(g)\big)$$

$$= \langle\langle X_\delta \circ \Phi_h, \dot{\xi}^a V_a \circ \Phi_h + \xi^a \xi^b (\nabla_{V_a} V_b) \circ \Phi_h + \mathrm{grad}_\kappa P \circ \Phi_h \rangle\rangle \circ \psi_\sigma(s, g) \tag{3.35}$$

$$= \langle\langle \mathrm{d}\Phi_h \circ X_\delta, \dot{\xi}^a \mathrm{d}\Phi_h \circ V_a + \xi^a \xi^b \mathrm{d}\Phi_h \circ (\nabla_{V_a} V_b) + \mathrm{d}\Phi_h \circ \mathrm{grad}_\kappa P \rangle\rangle \circ \psi_\sigma(s, g) \tag{3.36}$$

$$= \langle\langle X_\delta, \dot{\xi}^a V_a + \xi^a \xi^b \nabla_{V_a} V_b + \mathrm{grad}_\kappa P \rangle\rangle \circ \psi_\sigma(s, g), \tag{3.37}$$

completing the argument. ∎

3.4 Analytical Examples

In this section, we apply the main result to several illustrative examples (see Figs. 3.2-3.4), demonstrating the abstract results on concrete systems. In some cases, we systematically obtain flat outputs already reported in the literature after discovery via ad hoc methods; in other cases, we discover new flat outputs.

3.4.1 The Planar Rocket

Example 3.1 *(Planar Rocket, Fig. 3.2)*. Also known as the ducted fan [32], this classic example of a flat system has configuration manifold $Q = \mathrm{SE}(2)$, to which we assign coordinates (x_1, x_2, θ) corresponding to the center of mass position and the angle of body rotation, so that

$$q = \begin{bmatrix} \cos\theta & -\sin\theta & x_1 \\ \sin\theta & \cos\theta & x_2 \\ 0 & 0 & 1 \end{bmatrix}. \tag{3.38}$$

The corresponding bases of vector and covector fields induced by this coordinate system are denoted

$$TQ = \mathrm{span}\{ \partial_{x_1}, \partial_{x_2}, \partial_\theta \}, \quad T^*Q = \mathrm{span}\{ \mathrm{d}x_1, \mathrm{d}x_2, \mathrm{d}\theta \}. \tag{3.39}$$
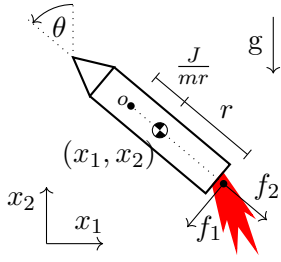
Figure 3.2: Planar Rocket
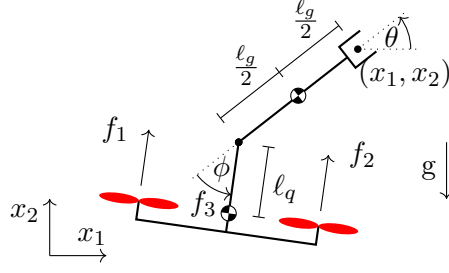
Figure 3.3: Planar Aerial Manipulator
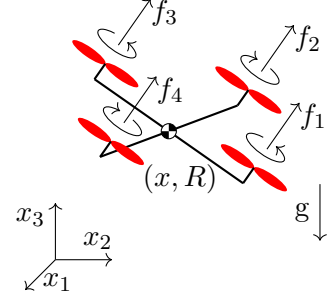
Figure 3.4: Quadrotor

The kinetic energy metric is given by

$$\kappa = m\left(\mathrm{d}x_1 \otimes \mathrm{d}x_1 + \mathrm{d}x_2 \otimes \mathrm{d}x_2\right) + J\left(\mathrm{d}\theta \otimes \mathrm{d}\theta\right), \tag{3.40}$$

a basis of vector fields for the control codistribution is given by

$$F = \mathrm{span}\left\{ \cos\theta\,\mathrm{d}x_1 + \sin\theta\,\mathrm{d}x_2 + r\,\mathrm{d}\theta,\ -\sin\theta\,\mathrm{d}x_1 + \cos\theta\,\mathrm{d}x_2 \right\}, \tag{3.41}$$

and the potential energy is given by $P : (x_1, x_2, \theta) \mapsto mgx_2$. Thus, $\mathrm{d}P = mg\,\mathrm{d}x_2$.

It's easily verified that the action of $(g_1, g_2) \in \mathbb{R}^2$ given (in local coordinates) by

$$\Phi : \mathbb{R}^2 \times \mathrm{SE}(2) \to \mathrm{SE}(2),\ \left((g_1, g_2), (x_1, x_2, \theta)\right) \mapsto (x_1 + g_1, x_2 + g_2, \theta). \tag{3.42}$$

is a dynamic symmetry of the system. This action induces a principal bundle structure over $\mathbb{S}^1$, where the projection map is given (again in coordinates) by

$$\pi : \mathrm{SE}(2) \to \mathbb{S}^1,\ (x_1, x_2, \theta) \mapsto \theta. \tag{3.43}$$

We may compute

$$\mathrm{coann}\,F = \mathrm{span}\left\{ -r\cos\theta\,\partial_{x_1} - r\sin\theta\,\partial_{x_2} + \partial_\theta \right\}, \tag{3.44}$$

and a local coordinate calculation will show that

$$\Delta = \mathrm{span}\left\{ -r\cos\theta\,\partial_{x_1} - r\sin\theta\,\partial_{x_2} + \partial_\theta,\ r\sin\partial_{x_1} - r\cos\partial_{x_2} \right\}, \tag{3.45}$$

whose orthogonal complement with respect to κ is given by

$$\Delta^\perp = \mathrm{span}\left\{ J\cos\theta\,\partial_{x_1} + J\sin\theta\,\partial_{x_2} + mr\,\partial_\theta \right\}. \tag{3.46}$$

Because we have $\mathrm{rank}\,\Delta^\perp = \dim S = 1$ and G is Abelian, by integration it is relatively straightforward

to obtain the global section

$$
\sigma \,:\, \mathbb{S}^1 \to \mathrm{SE}(2), \ \theta \mapsto
\begin{bmatrix}
\cos\theta & -\sin\theta & \frac{J}{m\,r}\sin\theta \\
\sin\theta & \cos\theta & -\frac{J}{m\,r}\cos\theta \\
0 & 0 & 1
\end{bmatrix},
\tag{3.47}
$$

whose image can easily be verified to be orthogonal to Δ using the metric. Moreover, a local coordinate calculation (whose details we omit) can be used to show that the regularity condition holds as well. Thus, by Theorem 3.1, the group variables in the canonical trivialization identified with σ, given by

$$
y : \mathrm{SE}(2) \to \mathbb{R}^2, \ q \mapsto (x_1 - \tfrac{J}{m\,r}\sin\theta, x_2 + \tfrac{J}{m\,r}\cos\theta),
\tag{3.48}
$$

are a flat output of the system, namely the coordinates of the point o shown in Fig. 3.2, known as the *center of oscillation*, in agreement with [37].

Moreover, since Φ was a dynamic symmetry, the flat output obtained is symmetry-preserving. Thus, for any generic smooth curve in the flat space $\mathbb{R}^2$, finding the corresponding curve in the configuration manifold and then transforming the result using Φ would yield the same result as translating the original curve in the flat space and then finding the corresponding curve in the configuration manifold.   ●

3.4.2 The Planar Aerial Manipulator

Example 3.2 *(Planar Aerial Manipulator, Fig. 3.3)*. This system consists of two planar rigid bodies connected by a revolute joint. The configuration manifold is $Q = \mathrm{SE}(2) \times \mathbb{S}^1$, to which we assign coordinates $q = (x_1, x_2, \theta, \phi)$ such that (x_1, x_2, θ) describe the end effector pose in $\mathrm{SE}(2)$ (in the same manner as in the previous example) while $\phi \in \mathbb{S}^1$ is the joint angle. In the given coordinates, the kinetic energy metric can be expressed in matrix form as

$$
\begin{bmatrix} \kappa_{ij} \end{bmatrix} =
\begin{bmatrix}
0 & 0 & 0 & 0 \\
0 & 0 & 0 & 0 \\
0 & 0 & J_g + J_q & J_q \\
0 & 0 & J_q & 0
\end{bmatrix}
+ m_g
\begin{bmatrix}
1 & 0 & \frac{\ell_g}{2}\sin\theta & 0 \\
0 & 1 & -\frac{\ell_g}{2}\cos\theta & 0 \\
\frac{\ell_g}{2}\sin\theta & -\frac{\ell_g}{2}\cos\theta & \frac{\ell_g{}^2}{4} & 0 \\
0 & 0 & 0 & 0
\end{bmatrix}
+
\tag{3.49}
$$
$$
m_q
\begin{bmatrix}
1 & 0 & \ell_q\sin(\phi+\theta)+\ell_g\sin\theta & \ell_q\sin(\phi+\theta) \\
0 & 1 & -\ell_g\cos\theta-l_q\cos(\phi+\theta) & -\ell_q\cos(\phi+\theta) \\
\ell_q\sin(\phi+\theta)+\ell_g\sin\theta & -l_q\cos(\phi+\theta)-\ell_g\cos\theta & 2\,\ell_g\ell_q\cos\phi+\ell_q{}^2+\ell_g{}^2 & \ell_q{}^2+\ell_g\ell_q\cos\phi \\
\ell_q\sin(\phi+\theta) & -\ell_q\cos(\phi+\theta) & \ell_q{}^2+\ell_g\ell_q\cos\phi & \ell_q{}^2
\end{bmatrix},
$$

while the potential energy is given (in coordinates) by

$$
P : \mathrm{SE}(2) \times \mathbb{S}^1 \to \mathbb{R}, \ (x_1, x_2, \theta, \phi) \mapsto m_g\mathrm{g}\big(x_2 - \tfrac{\ell_g}{2}\sin\theta\big) + m_q\mathrm{g}\big(x_2 - \ell_g\sin\theta - \ell_q\sin(\phi+\theta)\big). \tag{3.50}
$$

Relative to the basis of covector fields $\{\,\mathrm{d}x_1,\ \mathrm{d}x_2,\ \mathrm{d}\theta,\ \mathrm{d}\phi\,\}$, the control codistribution is given by

$$
F = \operatorname{span}\left\{
\begin{bmatrix} \cos(\phi+\theta) \\ \sin(\phi+\theta) \\ -\ell_g \sin\phi \\ 0 \end{bmatrix},
\begin{bmatrix} 0 \\ 0 \\ 1 \\ 1 \end{bmatrix},
\begin{bmatrix} 0 \\ 0 \\ 0 \\ 1 \end{bmatrix}
\right\},
\tag{3.51}
$$

so that relative to the basis of vector fields $\{\,\partial_{x_1},\ \partial_{x_2},\ \partial_\theta,\ \partial_\phi\,\}$, we have

$$
\operatorname{coann} F = \operatorname{span}\left\{
\begin{bmatrix} -\sin(\phi+\theta) \\ \cos(\phi+\theta) \\ 0 \\ 0 \end{bmatrix}
\right\}.
\tag{3.52}
$$

The system exhibits broken symmetry with respect to displacements in the plane described (in coordinates) as the action of $(g_1, g_2, g_3) \in \mathrm{SE}(2)$ on Q given by

$$
\Phi : \left(\begin{pmatrix} g_1 \\ g_2 \\ g_3 \end{pmatrix}, \begin{pmatrix} x_1 \\ x_2 \\ \theta \\ \phi \end{pmatrix}\right) \mapsto \begin{pmatrix} x_1 \cos g_3 - x_2 \sin g_3 + g_1 \\ x_1 \sin g_3 + x_2 \cos g_3 + g_2 \\ \theta + g_3 \\ \phi \end{pmatrix},
\tag{3.53}
$$

inducing a principal bundle structure over $\mathbb{S}^1$, for which the projection map is given (in coordinates) by

$$
\pi : \mathrm{SE}(2) \times \mathbb{S}^1 \to \mathbb{S}^1, \ (x_1, x_2, \theta, \phi) \mapsto \phi.
\tag{3.54}
$$

A straightforward but slightly tedious local coordinate calculation (best performed with the aid of a symbolic manipulation toolbox) will reveal that

$$
\Delta = \operatorname{span}\left\{
\begin{bmatrix} -\sin(\phi+\theta) \\ \cos(\phi+\theta) \\ 0 \\ 0 \end{bmatrix},
\begin{bmatrix} -\cos(\phi+\theta) \\ -\sin(\phi+\theta) \\ 0 \\ 0 \end{bmatrix}
\right\} = \operatorname{span}\left\{\partial_{x_1}, \partial_{x_2}\right\},
\tag{3.55}
$$

whose orthogonal complement with respect to the metric κ can be computed as

$$
\Delta^\perp = \operatorname{span}\left\{
\begin{bmatrix} -\ell_g\,(m_g + 2\,m_q)\sin\theta - 2\,\ell_q\,m_q\sin(\phi+\theta) \\ \ell_g\,(m_g + 2\,m_q)\cos\theta + 2\,\ell_q\,m_q\cos(\phi+\theta) \\ 2\,m_g + m_q \\ 0 \end{bmatrix},
\begin{bmatrix} -\ell_q\,m_q\sin(\phi+\theta) \\ \ell_q\,m_q\cos(\phi+\theta) \\ 0 \\ m_g + m_q \end{bmatrix}
\right\}.
\tag{3.56}
$$

54

Considering the second entry in the previous basis, Δ is clearly orthogonal to the image of a global section that can be expressed in local coordinates as

$$\sigma \,:\, \mathbb{S}^1 \to \mathrm{SE}(2) \times \mathbb{S}^1, \ \phi \mapsto \left(\left(\tfrac{\ell_q m_q}{m_g+m_q}\right) \cos \phi, \ \left(\tfrac{\ell_q m_q}{m_g+m_q}\right) \sin \phi, \ 0, \ \phi \right), \tag{3.57}$$

since $\mathrm{d}\sigma$ clearly takes values in $\Delta^\perp$, and the regularity condition can also be verified via local coordinate calculations. Thus, the group variables of the canonical trivialization are a global geometric flat output:

$$y : \mathrm{SE}(2) \times \mathbb{S}^1 \to \mathrm{SE}(2),$$
$$(x_1, x_2, \theta, \phi) \mapsto \left(x_1 - \left(\tfrac{\ell_q m_q}{m_g+m_q}\right) \cos(\phi + \theta), x_2 - \left(\tfrac{\ell_q m_q}{m_g+m_q}\right) \sin(\phi + \theta), \theta \right). \tag{3.58}$$

In harmony with the results presented in [40], this output amounts to the pose of the end effector if $\ell_q = 0$; otherwise, it is the pose of a frame parallel to the end effector frame, translated by an offset due to the eccentricity of the vehicle center of mass. However, Φ was only a broken (*vs.* dynamic) symmetry. While the map from the configuration manifold to the flat space is equivariant, the mapping from the flat space back to the state-input space is not. This corresponds to the fact that the gravity direction in the end effector frame is altered by Φ, and thus thrust must be generated in a different direction (requiring a different joint angle ϕ) to follow the same end effector trajectory. $\quad\bullet$

3.4.3   The Quadrotor

Example 3.3 *(Quadrotor, Fig. 3.4).* The configuration manifold is $Q = \mathrm{SE}(3)$, which can be expressed in so-called "homogeneous coordinates" as

$$q = \begin{bmatrix} R & x \\ 0_{1\times 3} & 1 \end{bmatrix} \tag{3.59}$$

where $R \in \mathrm{SO}(3)$ is the rotation from the body frame to the world frame and $x \in \mathbb{R}^3$ is the position of the center of mass. Relative to the usual basis of vector fields for $T\mathrm{SE}(3)$, corresponding to the components of the linear and angular velocities along body-fixed axes, the system is given by[5]

$$\kappa = \mathrm{diag}(m, m, m, J_{xx}, J_{xx}, J_{zz}), \tag{3.60a}$$
$$P : (x, R) \mapsto mg(\mathrm{e}_3^{\mathsf{T}} x), \tag{3.60b}$$

---

[5]Assuming the rotational inertia is symmetric about the thrust axis gives the system broken symmetry for the Abelian group action given, as opposed to considering a non-Abelian subgroup of $\mathrm{SE}(3)$. However, the flat outputs obtained are valid even without this assumption due to Remark 3.4.

$$F = \operatorname{span}\left\{ \begin{bmatrix} 0 \\ 0 \\ k_f \\ k_f \ell_a \\ 0 \\ k_m \end{bmatrix}, \begin{bmatrix} 0 \\ 0 \\ k_f \\ 0 \\ k_f \ell_a \\ -k_m \end{bmatrix}, \begin{bmatrix} 0 \\ 0 \\ k_f \\ -k_f \ell_a \\ 0 \\ k_m \end{bmatrix}, \begin{bmatrix} 0 \\ 0 \\ k_f \\ 0 \\ -k_f \ell_a \\ -k_m \end{bmatrix} \right\} \tag{3.60c}$$

where k_f and k_m are the thrust and moment coefficients of the propellers and ℓ_a is the arm length.

The system exhibits dynamic symmetry with respect to the action of $\mathbb{R}^3 \times \mathbb{S}^1$ described by

$$\Phi : \big((g_{123}, g_4), (x, R)\big) \mapsto \left(x + g_{123}, R \begin{bmatrix} \cos g_4 & -\sin g_4 & 0 \\ \sin g_4 & \cos g_4 & 0 \\ 0 & 0 & 1 \end{bmatrix} \right), \tag{3.61}$$

comprised of a translation in all three world-fixed axes and a rotation around the body-fixed thrust axis. This induces a nontrivial principal bundle over $\mathbb{S}^2$, where the projection map is given by

$$\pi : \mathrm{SE}(3) \to \mathbb{S}^2, \ (x, R) \mapsto R\,e_3. \tag{3.62}$$

Moreover, it is easily verified that

$$\operatorname{coann} F = \operatorname{span}\left\{ \begin{bmatrix} 1 \\ 0 \\ 0 \\ 0 \\ 0 \\ 0 \end{bmatrix}, \begin{bmatrix} 0 \\ 1 \\ 0 \\ 0 \\ 0 \\ 0 \end{bmatrix} \right\}, \tag{3.63}$$

corresponding to the body-frame directions perpendicular to the direction of the propellers. Also, a straightforward calculation will reveal that

$$\Delta = \operatorname{span}\left\{ \begin{bmatrix} 1 \\ 0 \\ 0 \\ 0 \\ 0 \\ 0 \end{bmatrix}, \begin{bmatrix} 0 \\ 1 \\ 0 \\ 0 \\ 0 \\ 0 \end{bmatrix}, \begin{bmatrix} 0 \\ 0 \\ 1 \\ 0 \\ 0 \\ 0 \end{bmatrix} \right\}, \quad \text{and thus} \quad \Delta^\perp = \operatorname{span}\left\{ \begin{bmatrix} 0 \\ 0 \\ 0 \\ 1 \\ 0 \\ 0 \end{bmatrix}, \begin{bmatrix} 0 \\ 0 \\ 0 \\ 0 \\ 1 \\ 0 \end{bmatrix}, \begin{bmatrix} 0 \\ 0 \\ 0 \\ 0 \\ 0 \\ 1 \end{bmatrix} \right\}, \tag{3.64}$$

since the inertia tensor is diagonal.

This principal bundle is nontrivial, so global sections do not exist. However, removing even a single fiber $\pi^{-1}(s_0)$ for any $s_0 \in \mathbb{S}^2$ yields a trivial bundle. Thus, we define two almost global sections: one defined on the "north" portion of the sphere (removing only the "south pole"), given by

$$\sigma_N : \mathbb{S}^2 \setminus \{-\mathrm{e}_3\} \to \mathrm{SE}(3), \quad \begin{bmatrix} s_1 \\ s_2 \\ s_3 \end{bmatrix} \mapsto \begin{bmatrix} 1 - \frac{s_1^2}{s_3+1} & \frac{-s_1 s_2}{s_3+1} & s_1 & 0 \\ \frac{-s_1 s_2}{s_3+1} & 1 - \frac{s_2^2}{s_3+1} & s_2 & 0 \\ -s_1 & -s_2 & s_3 & 0 \\ 0 & 0 & 0 & 1 \end{bmatrix}, \tag{3.65}$$

and another defined on the "south" portion of the sphere (removing only the "north pole"), given by

$$\sigma_S : \mathbb{S}^2 \setminus \{\mathrm{e}_3\} \to \mathrm{SE}(3), \quad \begin{bmatrix} s_1 \\ s_2 \\ s_3 \end{bmatrix} \mapsto \begin{bmatrix} 1 + \frac{s_1^2}{s_3-1} & \frac{-s_1 s_2}{s_3-1} & s_1 & 0 \\ \frac{s_1 s_2}{s_3-1} & -1 - \frac{s_2^2}{s_3-1} & s_2 & 0 \\ s_1 & -s_2 & s_3 & 0 \\ 0 & 0 & 0 & 1 \end{bmatrix}. \tag{3.66}$$

While these sections were derived from the quaternion calculations in [41], the expression (3.65) also appears in [52]. Moreover, Δ is orthogonal to the image of each section, since Δ spans the linear velocities, while only the rotational degrees of freedom vary along the sections, and the inertia matrix is block diagonal. The regularity condition can also be shown to hold using various local coordinate calculations, and thus the group variables of the canonical local trivialization for each local section are almost global geometric flat outputs, corresponding to the center of mass position and a so-called "body-fixed yaw angle" around the thrust axis, equivalent to the flat outputs proposed in [41]. Moreover, since Φ was a dynamic symmetry, these flat outputs are symmetry-preserving. $\bullet$

3.5 Flat Output Construction via Optimization

In Theorem 3.1, we formulated a relatively general sufficient condition for the construction of a geometric flat output; with an additional assumption, we also guaranteed that this output would be symmetry-preserving. While this theorem made several stipulations (most being relatively mild), it is undeniable that the greatest hurdle in applying this result is the assumed knowledge of a section that is orthogonal to Δ. The examples analyzed in Sec. 3.4 show that we may often discover such a section in closed form (and indeed, many known flat outputs in the literature actually correspond directly to this situation), but a systematic means of discovering such a section (if one exists) is not known in the general case. Moreover, when $\mathrm{rank}\,\Delta < \dim G$, such orthogonal sections are not necessarily unique, raising questions of optimality. Thus, towards the goal of applying this chapter's main result broadly, it is urgent to develop a systematic method for obtaining such "orthogonal sections", and we now pursue this objective.

For notational convenience, in the remainder of this section we assume that we work in a trivial bundle

$Q \cong S \times G$ (*i.e.*, $U = S$), since of course, one can always restrict a given system on a nontrivial bundle to this local domain. Assuming all other conditions of Theorem 3.1 hold, we are essentially left with the constraint satisfaction problem

$$\text{find} \quad \sigma \in \Gamma(Q) \tag{3.67a}$$

$$\text{s.\,t.} \quad \Delta \perp \sigma(S) \tag{3.67b}$$

where $\Gamma(Q)$ is the set of all sections $\sigma : S \to Q$ of $\pi : Q \to S$ and (3.67b) enforces that Δ is orthogonal to the image of σ (as a submanifold of Q).

Remark 3.5. It is clear that if $\text{rank}\,\Delta > \dim G$, the problem (3.67a)-(3.67b) is infeasible, since satisfying (3.67b) requires that $\dim S + \text{rank}\,\Delta \leq \dim Q$. Moreover, if $\text{rank}\,\Delta = \dim G$, a necessary (but not sufficient) condition for the feasibility of (3.67a)-(3.67b) is that $\text{coann}\,F$ be involutive (*i.e.*, for all $X, Y \in \Gamma(\text{coann}\,F)$, we have $[X, Y] \in \text{coann}\,F$). The previous claim is a direct consequence of the Frobenius theorem, while the sufficiency gap pertains partly to the global topological structure of S, since even a "flat" principal connection may have nontrivial "holonomy" (see [7, Fig. 3.14.2]) when S is not simply connected. It is less clear to us what precisely can be said about the feasibility of (3.67a)-(3.67b) in the case that $\text{rank}\,\Delta < \dim G$.

To obtain (at least approximate) solutions to this problem, we take inspiration from [53], which considered the problem of identifying the trivialization in which approximate, linear algorithms for planning connection-driven locomotion are most accurate (referred to as "optimal coordinates", or more pedantically, an optimal trivialization). Since trivializations and sections are in one-to-one correspondence, this problem bears significant similarity to the task at hand. In what follows, we use the tools of Riemannian geometry and differential forms to cast the constraint satisfaction problem (3.67a)-(3.67b) as a continuum optimization problem over the space of sections. Next, inspired by [53], we re-express the problem to optimize the "transition map" from an "initial guess" trivialization to a trivialization that minimizes the cost functional. Finally, using finite element methods similar to those employed in [53] and other approximations, we will ultimately obtain an approximate transcription of this continuum problem to a quadratic program (QP). Solving this QP numerically for two example systems obtains a solution in very close agreement with the closed-form flat outputs obtained above.

3.5.1 The Continuum Problem

We begin by formulating a continuum optimization problem, whose solution is also a solution to the constraint satisfaction problem (3.67a)-(3.67b), which will be expressed as follows:

$$\min_{\sigma \in \Gamma(Q)} \quad J(\sigma) \tag{3.68a}$$

$$\text{s.\,t.} \quad C(\sigma) = 0 \tag{3.68b}$$

where the cost and constraint functionals $J, C : \Gamma(Q) \to \mathbb{R}$ will be constructed below, and the constraint functional will simply enforce (3.67b). Since in general we may have $\operatorname{rank} \Delta < \dim G$, solutions to (3.67a)-(3.67b) may not be unique, even up to the group action. We therefore propose an additional cost $J(\sigma)$, which penalizes the deviation of the final flat output from the "minimum perturbation coordinates" of the system [54], a trivialization which approximates, *e.g.*, an "angular center of mass" when $G = SO(3)$ [55]. This cost will thus encourage the selection of a geometric flat output whose variation most completely captures the entire system's combined momentum, which seems convenient for motion planning.

Formulating the Cost Functional

We first recall (from Example 2.13) that since Q is equipped with a G-invariant metric κ, we may define a mechanical connection one-form $\mathcal{A}_{\mathrm{mech}} : TQ \to \mathfrak{g}$, such that $VQ^\perp = \ker \mathcal{A}_{\mathrm{mech}}$. Using this and the locked inertia tensor $\mathcal{I}(q) : \mathfrak{g} \to \mathfrak{g}^*$, we define an $\mathbb{R}$-valued bilinear form on Q given by

$$\rho_{\mathcal{A}} : (u_q, v_q) \mapsto \langle \mathcal{I}(q) \, \mathcal{A}_{\mathrm{mech}}(u_q) ; \mathcal{A}_{\mathrm{mech}}(v_q) \rangle, \tag{3.69}$$

which is clearly symmetric and positive semidefinite. Examining the pullback of $\rho_{\mathcal{A}}$ by σ, given by

$$\sigma^\star \rho_{\mathcal{A}} : (u_s, v_s) \mapsto \langle \mathcal{I}(q) \, \mathcal{A}_{\mathrm{mech}} \circ \mathrm{d}\sigma(u_s) ; \mathcal{A}_{\mathrm{mech}} \circ \mathrm{d}\sigma(v_s) \rangle, \tag{3.70}$$

we see that $\sigma^\star \rho_{\mathcal{A}}$ is also a positive semidefinite symmetric bilinear form, but this time on S. Moreover, $\sigma^\star \rho_{\mathcal{A}}$ will be identically zero over S if and only if $\ker \mathcal{A}_{\mathrm{mech}}$ is tangent to the image of σ. Such a situation can occur only if the mechanical connection is *flat* (*i.e.*, integrable in the Frobenius sense) [56] and can be completely integrated to yield a trivialization that amounts to "coordinates" with no "perturbation" whatsoever. Moreover, nontrivial principal bundles over a simply connected shape space do not admit flat principal connections, and thus the existence of flat connections is intimately linked to the topological structure of the principal bundle induced by the symmetry.

We also note that a G-invariant metric κ on Q induces a natural metric on $S = Q/G$ given by

$$\check{\kappa} : (u_s, v_s) \mapsto \langle\langle (u_s)_q^{VQ^\perp}, (v_s)_q^{VQ^\perp} \rangle\rangle \Big|_{q \,\in\, \pi^{-1}(s)}, \tag{3.71}$$

independent of the particular choice of q, where $(\cdot)_q^{VQ^\perp} : T_s S \to T_q Q$ is the horizontal lift via the mechanical connection (*i.e.*, the orthogonal complement of the vertical subbundle). Recall that the trace of a symmetric bilinear form ω on S is given by

$$\left(\operatorname{tr} \omega \right)(s) = \sum_k \omega(v_s{}^k, v_s{}^k) \tag{3.72}$$

for any orthonormal basis $T_s S = \operatorname{span}\{v_s{}^1, \ldots, v_s{}^n\}$. Thus, the trace of a positive semidefinite form is a

non-negative function which vanishes exactly at those points where the form itself vanishes, and so ω will vanish identically over S if and only if the integral of $\operatorname{tr}\omega$ over S vanishes.

Therefore, we define the cost functional

$$J : \Gamma(Q) \to \mathbb{R}, \; \sigma \mapsto \int_S \operatorname{tr}(\sigma^\star \rho_{\mathcal{A}}) \; \operatorname{vol}_{\tilde{\kappa}}, \tag{3.73}$$

where $\operatorname{vol}_{\tilde{\kappa}}$ is the Riemannian volume form (see [6, Prop. 6.4]), which provides an intrinsic notion of the integral of a real-valued function on a Riemannian manifold.

Finally, although here we consider minimum perturbation coordinates for the mechanical connection, the foregoing analysis is valid for any other principal connection, including the canonical flat connection induced by another trivialization. Such a choice could penalize (in a differential sense) the deviation of any geometric flat output obtained relative to, *e.g.*, some particular body-fixed frame.

Formulating the Constraint Functional

In the original constraint satisfaction problem, the orthogonality constraint (3.67b) must be enforced pointwise over all of $\sigma(S) \subset Q$. The problem will be much more amenable to practical solution if we re-express this constraint using a real-valued constraint functional that vanishes exactly when the constraint holds.

To this end, we define a bilinear form

$$\rho_\Delta : (u_q, v_q) \mapsto \langle\langle \operatorname{proj}_\Delta(u_q), \operatorname{proj}_\Delta(v_q) \rangle\rangle, \tag{3.74}$$

where $\operatorname{proj}_\Delta : TQ \to TQ$ is the orthogonal projection onto Δ. ρ_Δ is clearly symmetric and positive semidefinite, and

$$\Delta \perp \sigma(S) \;\; \text{if and only if} \;\; \sigma^\star \rho_\Delta = 0. \tag{3.75}$$

Thus, following a line of reasoning similar to that employed in formulating the cost functional, we enforce the orthogonality constraint using the constraint functional

$$C : \Gamma(Q) \to \mathbb{R}, \; \sigma \mapsto \int_S \operatorname{tr}(\sigma^\star \rho_\Delta) \; \operatorname{vol}_{\tilde{\kappa}}, \tag{3.76}$$

such that (3.67b) holds if and only if $C(\sigma) = 0$ i.e. (3.77b) holds.

Resulting Continuum Problem

In summary, we obtain the continuum optimization problem

$$\min_{\sigma \in \Gamma(Q)} \int_S \operatorname{tr}(\sigma^\star \rho_{\mathcal{A}}) \; \operatorname{vol}_{\tilde{\kappa}} \tag{3.77a}$$

$$\text{s. t.} \qquad \int_S \operatorname{tr}(\sigma^\star \rho_\Delta) \, \operatorname{vol}_{\check{\kappa}} = 0 \tag{3.77b}$$

where the cost functional (3.77a) penalizes "momentum perturbation" in the sense described above, while the constraint functional (3.77b) enforces that $\Delta \perp \sigma(S)$.

3.5.2 Local Form of the Continuum Problem

For an optimization problem over the space of sections, there is no intrinsic "origin" designated for the decision variables. However, relative to a fixed trivialization $\psi : S \times G \to Q$, *any* section can be written

$$\sigma : S \to Q, \ s \mapsto \psi\big(s, \phi(s)\big), \tag{3.78}$$

were $\phi : S \to G$ is called the *transition map* from ψ to the trivialization $\psi_\sigma : (s, g) \mapsto \Phi_g \circ \sigma(s)$. It will ultimately be more convenient to optimize ϕ, thereby working relative to an "initial guess" section $s \mapsto \psi(s, e)$. Thus, without loss of generality, we reformulate the cost and constraint functionals accordingly.

Reformulating the Cost Functional

In view of the previous, the integrand in the cost function (3.73) can also be given more explicitly by

$$\operatorname{tr}(\sigma^\star \rho_{\mathcal{A}})(s) = \sum_k \langle \, \mathbb{I}(s) \big(\mathrm{dL}_{\phi(s)}^{-1}(\mathrm{d}\phi) + \mathbb{A}_{\text{mech}} \big)(v_s{}^k) \, ; \, \big(\mathrm{dL}_{\phi(s)}^{-1}(\mathrm{d}\phi) + \mathbb{A}_{\text{mech}} \big)(v_s{}^k) \, \rangle, \tag{3.79}$$

which follows directly from (3.78), as well as (2.101) describing the symmetry properties of the locked inertia tensor and Fact 2.98 relating the connection form $\mathcal{A}_{\text{mech}}$ and the local form $\mathbb{A}_{\text{mech}}$.

Reformulating the Orthogonality Constraint

We now consider the local computation of the integrand in the constraint functional (3.76). Let $\Delta = \operatorname{span}\{\Delta_1, \ldots, \Delta_k\}$ define a local basis of vector fields for Δ that is both orthonormal (*i.e.,* $\langle\langle \Delta_i, \Delta_j \rangle\rangle = \delta_{ij}$) and Φ-invariant. We then have

$$\operatorname{proj}_\Delta(v_q) = \sum_i \langle\langle \Delta_i(q), v_q \rangle\rangle \, \Delta_i(q), \tag{3.80}$$

and moreover,

$$\rho_\Delta(u_q, v_q) = \sum_i \langle\langle u_q, \Delta_i(q) \rangle\rangle \, \langle\langle \Delta_i(q), v_q \rangle\rangle. \tag{3.81}$$

Since Δ_i is Φ-invariant, there exist maps $\eta_i : S \to \mathfrak{g}$ and vector fields $Z_i : S \to TS$ such that

$$\Delta_i \circ \psi(s, g) = \mathrm{d}\psi\big(Z_i(s), \mathrm{dL}_g \circ \eta_i(s)\big). \tag{3.82}$$

61

Using this symmetry, following [46] we may also express the metric product in the form

$$\langle\langle u_q, v_q \rangle\rangle = \langle\langle \, \mathrm{d}\psi(u_s, u_g), \mathrm{d}\psi(v_s, v_g) \rangle\rangle \tag{3.83}$$

$$= \begin{bmatrix} u_s \\ \mathrm{dL}_g^{-1}(u_g) \end{bmatrix}^{\mathrm{T}} \begin{bmatrix} m(s) & \mathbb{A}_{\mathrm{mech}}(s)^{\mathrm{T}}\mathbb{I}(s) \\ \mathbb{I}(s)\mathbb{A}_{\mathrm{mech}}(s) & \mathbb{I}(s) \end{bmatrix} \begin{bmatrix} v_s \\ \mathrm{dL}_g^{-1}(v_g) \end{bmatrix}, \tag{3.84}$$

With this fact in mind, a straightforward computation will show that

$$\mathrm{tr}(\sigma^\star \rho_\Delta)(s) = \sum_k \sum_i \begin{bmatrix} v_s{}^k \\ \mathrm{dL}_{\phi(s)}^{-1} \circ \mathrm{d}\phi(v_s{}^k) \end{bmatrix}^{\mathrm{T}} \mathbb{P}_i(s)^{\mathrm{T}}\, \mathbb{P}_i(s) \begin{bmatrix} v_s{}^k \\ \mathrm{dL}_{\phi(s)}^{-1} \circ \mathrm{d}\phi(v_s{}^k) \end{bmatrix}, \tag{3.85}$$

where we define

$$\mathbb{P}_i(s) = \begin{bmatrix} Z_i(s) \\ \eta_i(s) \end{bmatrix}^{\mathrm{T}} \begin{bmatrix} m(s) & \mathbb{A}_{\mathrm{mech}}(s)^{\mathrm{T}}\mathbb{I}(s) \\ \mathbb{I}(s)\mathbb{A}_{\mathrm{mech}}(s) & \mathbb{I}(s) \end{bmatrix}. \tag{3.86}$$

3.5.3 Gauge Freedom

Finally, to study the symmetry of the proposed cost and constraint functionals, consider transforming a given section σ by letting $\sigma' : s \mapsto \Phi_g \circ \sigma(s)$ for some $g \in G$. From (3.78), we have

$$\sigma'(s) = \Phi_g \circ \psi\big(s, \phi(s)\big) = \psi\big(s, \underbrace{\mathrm{L}_g \circ \phi(s)}_{=:\phi'}\big). \tag{3.87}$$

Noting that the cost functional as expressed in (3.79) and the constraint functional as expressed in (3.85) depend on ϕ (and indirectly, σ) only via the map $\mathrm{dL}_{\phi(s)} \circ \mathrm{d}\phi$. Thus, we compute

$$\mathrm{dL}_{\phi'(s)} \circ \mathrm{d}\phi' = \mathrm{dL}_{\mathrm{L}_g \circ \phi(s)}^{-1} \circ \mathrm{d}\big(\mathrm{L}_g \circ \phi\big) = \mathrm{dL}_{\phi(s)}^{-1} \circ \mathrm{dL}_g^{-1} \circ \mathrm{dL}_g \circ \mathrm{d}\phi = \mathrm{dL}_{\phi(s)} \circ \mathrm{d}\phi. \tag{3.88}$$

Therefore, J and C are invariant, showing that if σ is a solution to the problem (3.77a)-(3.67b), so is $\Phi_g \circ \sigma$ for all $g \in G$. Thus, either the addition of a symmetry-breaking cost or constraint can resolve this ambiguity, or this gauge freedom can be freely adjusted after solving the problem once, without re-solving.

3.6 Finite Element Methods

We have already formulated the problem in the continuum and re-expressed it relative to an initial guess. However, to solve the problem using numerical methods, it is necessary to transcribe our abstract optimization problem to a finite dimension. Inspired by [53], we parameterize the candidate section via (3.78)

using a transition map of the form

$$\phi : s \mapsto \exp\left(\sum_i w^i \zeta_i(s)\right), \tag{3.89}$$

where each $w^i \in \mathbb{R}$ is a weight to be optimized and $\zeta_i : S \to \mathfrak{g}$ is a basis function corresponding to a multivariate polynomial spline over a hypercube mesh (see [53] for a similar formulation with piecewise linear elements and a simplex mesh). Basis functions with high-order continuity are desirable (*e.g.*, two derivatives are necessary to express the group component of the system's acceleration). We note that Hermite polynomial basis functions with C^2 smoothness have been given in up to at least three dimensions [57], but may be available in higher dimensions as well. Since $\dim S = \dim Q - \operatorname{rank} F$ (and $\operatorname{rank} F$ is usually only slightly less than $\dim Q$), we are concerned with low-dimensional cases, an advantage of approximating the section $\sigma : S \to Q$ instead of the flat output $y : Q \to G$ directly.

3.6.1 Numerical Approximations

We now introduce several approximations made in the transcription of the continuum problem.

First Order Approximation of the Exponential Map

For $\mathfrak{g} \subseteq \mathfrak{gl}(n)$, we make the approximation $\exp \xi \approx e + \xi$ for small $\xi \in \mathfrak{g}$ (which is exact precisely when G is Abelian), so that $\phi(s) \approx e + w^i \zeta_i(s)$ where the sum is implied, and moreover,

$$\mathrm{dL}_{\phi(s)}^{-1} \circ \mathrm{d}\phi_s(v_s) \approx \left(e - w^i \zeta_i(s)\right)\left(w^i \, \mathrm{d}\zeta_i(v_s)\right) \approx w^i \, \mathrm{d}\zeta_i(v_s). \tag{3.90}$$

The cost functional integrand (3.79) is thus approximated by

$$\operatorname{tr}(\sigma^\star \rho_{\mathcal{A}})(s) \approx \sum_k \langle \mathbb{I}(s)\left(w^h \, \mathrm{d}\zeta_h + \mathbb{A}_{\mathrm{mech}}\right)(v_s{}^k) ; \left(w^j \, \mathrm{d}\zeta_j + \mathbb{A}_{\mathrm{mech}}\right)(v_s{}^k)\rangle, \tag{3.91}$$

and similarly for the constraint functional integrand (3.85),

$$\operatorname{tr}(\sigma^\star \rho_\Delta)(s) \approx \sum_k \sum_i \begin{bmatrix} v_s{}^k \\ w^h \, \mathrm{d}\zeta_h(v_s{}^k) \end{bmatrix}^{\mathrm{T}} \mathbb{P}_i(s)^{\mathrm{T}} \, \mathbb{P}_i(s) \begin{bmatrix} v_s{}^k \\ w^j \, \mathrm{d}\zeta_j(v_s{}^k) \end{bmatrix}. \tag{3.92}$$

Gaussian Quadrature Approximation of the Integrals

We employ Gaussian quadrature [58] to approximate the integrals in the functionals. Considering coordinates $(s^1, \ldots, s^n)$ on each element of $S = \bigcup_{j=1}^m E_j$ where E_j are finitely many disjoint elements,

$$\int_S f(s) \, \mathrm{vol}_{\check{\kappa}} = \sum_{j=1}^m \int_{E_j} \left(f(s)\sqrt{\det \check{\kappa}(s)}\right) ds^1 \ldots ds^n \approx \sum_{j=1}^m \sum_{i=1}^p c_{ij}\left(f(s_{ij})\sqrt{\det \check{\kappa}(s_{ij})}\right), \tag{3.93}$$

where each $c_{ij} \in \mathbb{R}$ and $s_{ij} \in S$ is a predetermined optimal weight and sampling point respectively, and $\check{\kappa}(s)$ is the induced Riemannian metric $\check{\kappa}$ in the coordinates s^i. Since Gaussian quadrature with p samples is exact when the integrand is a polynomial of degree $2p - 1$ or less, we expect this to be a good approximation if our mesh is sufficiently fine and ζ_i is a polynomial of degree p or less in s^i.

Approximate Transcription to a Quadratic Program

It is clear that pointwise over S, both (3.91) and (3.92) are quadratic forms in the weights w^i. Since quadrature approximates integrals via a weighted sum, our final approximations of (3.73) and (3.76) can be expressed in the form

$$J(\sigma) \approx \tfrac{1}{2} w^i A_{ij} w^j + b_i w^i + c, \tag{3.94}$$

$$C(\sigma) \approx \tfrac{1}{2} w^i D_{ij} w^j + e_i w^i + f = 0, \tag{3.95}$$

where A_{ij} and D_{ij} are positive semidefinite. Due to transcription, (3.95) may be infeasible even if a geometric flat output exists in the continuum. However, because (3.95) is nonnegative in view of (3.92), we relax the orthogonality constraint to simply enforce minimization of $C(\sigma)$ instead via the constraint $D_{ij} w^j + e_i = 0$, where minimization to zero (when feasible) corresponds to exact constraint satisfaction.

Thus, we obtain an approximate transcription of the continuum problem (3.77a)-(3.77b) to a QP:

$$\min_{w \in \mathbb{R}^N} \quad \tfrac{1}{2} w^i A_{ij} w^j + b_i w^i + c \qquad (\textit{momentum perturbation cost}) \tag{3.96a}$$

$$\text{s.t.} \quad D_{ij} w^j + e_i = 0 \qquad (\textit{orthogonality constraint}) \tag{3.96b}$$

$$w^i \zeta_i(s_0) = \log(g_0) \qquad (\textit{breaks symmetry}) \tag{3.96c}$$

where (3.96c) is added to resolve the gauge freedom. The QP is sparse due to the choice of basis functions with local support, permitting efficient solution even for very fine meshes.

3.6.2 Numerical Results

We implement the proposed method to identify geometric flat outputs on two example systems, namely the Planar Rocket (see Example 3.1) on $SE(2)$ (an $\mathbb{R}^2$ bundle over $\mathbb{S}^1$) and the Planar Aerial Manipulator(see Example 3.2) on $SE(2) \times \mathbb{S}^1$ (an $SE(2)$ bundle over $\mathbb{S}^1$). In both examples, we employ C^2 basis functions corresponding to quintic Hermite splines over an evenly divided mesh on $\mathbb{S}^1$ with $m = 8$ elements, and perform Gaussian quadrature with $p = 6$ sample points per element. The orthogonal section obtained for the Planar Rocket is visualized in Fig. 3.5, meanwhile the geometric flat output ultimately obtained is visualized in Fig. 3.6 for the Planar Aerial Manipulator. With suitable (and easily chosen) gauge freedom constraints, the numerical geometric flat outputs identified for both systems show precise numerical agreement with the closed form geometric flat outputs previously given in Section 3.4.
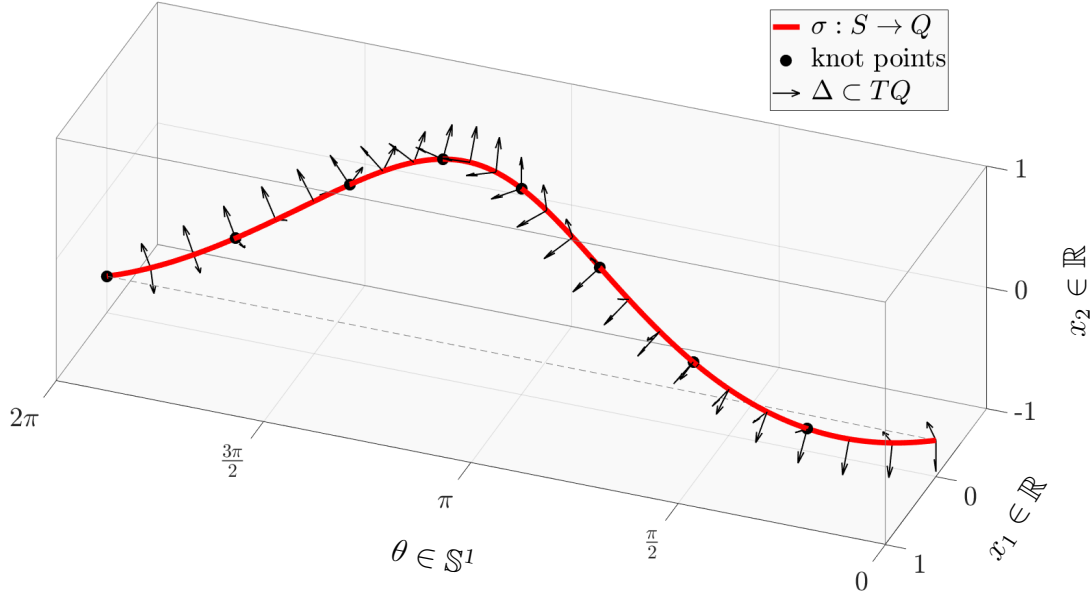
Figure 3.5: For the Planar Rocket in Example 3.2, we depict the finite element boundaries (*i.e.*, the knot points of the quintic spline) and the restriction of Δ to $\sigma(\mathbb{S}^1) \subset SE(2)$, which can be seen to be orthogonal to the solution $\sigma : \mathbb{S}^1 \to SE(2)$ to (3.96a)-(3.96c). To speak more precisely, we actually plot $\kappa^\flat(\Delta) \subset T^*Q$, and vectors and covectors appearing at right angles corresponds to orthogonality.
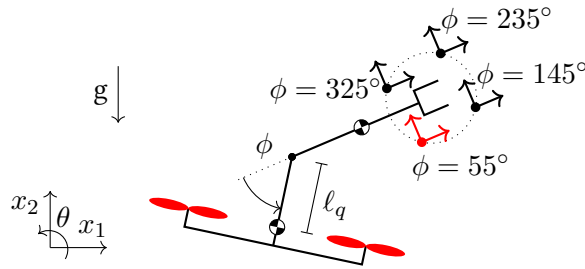
Figure 3.6: Visualization of the numerical geometric flat output obtained for the Planar Aerial Manipulator in Example 3.2. The flat output amounts to a frame parallel to the end effector with a ϕ-dependent offset. When $\ell_q = 0$, the offset goes to zero. Physical parameters have been chosen to exaggerate the offset for clarity. The frame in red corresponds to the angle ϕ visualized above.

3.7 Discussion

The existence of flat outputs that are the group variables of a particular trivialization echoes the thematic conclusions of [53], namely that although the dynamics of a mechanical system with symmetry can be represented equivalently in any trivialization, certain trivializations can be particularly favorable for analysis and efficient control design. Furthermore, viewing flat outputs through the geometric lens of trivializations suggests at least a partial answer to the open question as to why flat outputs often consist of a simple "set of points and angles" [32], as opposed to arbitrarily messy functions.

Moreover, as mentioned above, it is common to approximate sensor and actuator saturation constraints via convex constraints on the flat output derivatives [25] or via nonlinear constraints composed with the mapping from the flat space to the state-input space [34]. We believe that the computational effectiveness and convenience of such methods can, at least in part, be attributed to the use of a symmetry-preserving flat output, since constraint approximations can thus be chosen to be equally accurate at every point along each orbit with respect to a dynamic symmetry.

3.7.1 Generality and Extensions

Because our approach considers flat outputs taking values in an arbitrary Lie group (instead of limiting ourselves to $\mathbb{R}^n$), we are able to obtain globally-defined flat outputs when a global section is used. This is highly advantageous for agile systems like aerial robots, which stray far from a nominal operating point on the configuration manifold. When the bundle is nontrivial, global sections do not exist, providing an upper bound on the domain of geometric flat outputs. However, as explored in Example 3.3, the approach provides a principled means of generating a global atlas of overlapping local flat outputs generated from local sections, yielding a *differentially flat hybrid system* [26] and (in principle) enabling planning and control over the entire configuration manifold. While [41] leveraged such ideas to design a tracking controller for quadrotors performing aggressive inverted flight, in [59] we explored the application of the geometric flat outputs corresponding to (3.65)-(3.66) for global planning of dynamically feasible trajectories for quadrotors capable of reversing their propellers to exert bidirectional thrust.

The condition of Theorem 3.1 is only a sufficient condition (but not, in fact, necessary); in the future, we hope to close this gap, which we believe to be occupied by systems whose state and inputs depend on flat output derivatives of higher order [26], such as the last two entries of Table 3.1. Perhaps a recursive approach, in which the shape space is regarded as yet another bundle, could encompass those systems as well. Moreover, the dynamics of nonholonomic systems can also be described using an affine connection [60], suggesting the possibility of extension to systems with velocity constraints. Additionally, although our theoretical results concerned only mechanical systems without dissipation, recent work [36] has shown that knowledge of a flat output of a nominal model can sometimes be "bootstrapped" to construct the flatness mappings for a perturbed system (*e.g.*, a quadrotor subject to aerodynamic disturbances, as in [61]).

Finally, much remains unknown about the existence of symmetry-preserving flat outputs of mechanical systems in general, since we considered only the case where $\dim G = \operatorname{rank} F$ (although we note that any subgroup of a given symmetry induces a symmetry of lower dimension).

3.7.2 Maturation of the Numerical Methods

Overall, the implementation of the numerical methods in this chapter can rightfully be considered preliminary, and more general and robust tools should be developed to operationalize the method. For example, the linearization of the exponential map is almost surely the most egregious approximation in Section 3.6.1. It would thus be beneficial to develop an iterative approach, similar to Sequential Quadratic Programming (SQP) methods, where at each iteration, the exponential map is linearized about the current guess until convergence. Since this process happens offline, the computational requirements should not be an obstacle. Moreover, our numerical methods did not explore actually computing the mappings from the flat space back to the state-input space (as in, *e.g.*, [30] and [36]), and instead merely focused on finding (a numerical approximation of) a flat output, suggesting a clear direction for additional exploration.

In order to apply the approach to more complex systems, it would also be beneficial to explore computing the relevant quantities (*e.g.*, the underactuation distribution Δ and the mechanical connection $\mathcal{A}_{\mathrm{mech}}$) numerically from a standard modeling format for robotic systems (*e.g.*, a URDF [62]). Moreover, adapting efficient multibody dynamics solvers (*e.g.*, Pinocchio [63]) to use a suitable factorization of the Coriolis forces [64] would enable the efficient computation of covariant derivatives [48]. Such methods would permit the application of flatness-based planning and control techniques to complex multibody systems for which symbolic analysis is tedious or intractable.

More broadly, we are also interested in exploring the extent to which the relaxed orthogonality constraint that simply minimizes $C(\sigma)$ may yield an "approximate flat output" when a truly orthogonal section does not exist (even in the continuum setting), but our current theory cannot accomodate such notions. Lastly, it should be noted that our approach amounts to a continuous deformation of an existing section; thus, a potential pitfall is that in general, all sections of a principal bundle need not be homotopic, although over a contractible shape space (*e.g.*, a local region), all sections are homotopic.

3.8 Conclusion

In this work, we formally define and explore the concept of geometric flat outputs for robotic systems evolving on principal bundles. Under mild regularity assumptions, we use the (perhaps broken) symmetry of the system to construct a flat output from any section of the system's principal bundle that is orthogonal to an easily-computed distribution. These configuration flat outputs are equivariant (as maps from Q to G) and often global or almost global, and when the symmetry is sufficiently strong, the flat output is also symmetry-preserving, meaning the mapping from the flat space back to the physical space is also

equivariant. Similar to classic results in locomotion on principal bundles, a principal connection plays a key role; however, our connection is flat[6], whereas other locomotory phenomena result from curvature.

A central challenge of leveraging the previous results is the need to discover a so-called "orthogonal section". To tackle this challenge, we used the tools of Riemannian geometry and differential forms to cast the search for such a section as an optimization problem. An approximate transcription of this continuum formulation to a quadratic program was performed, and its solutions for two example systems showed precise agreement with the known closed-form flat outputs, providing evidence in favor of the method's feasibility for accurate identification of geometric flat outputs for more complex systems, for which closed form solutions are not known.

Overall, the results offer new fundamental insights into the dynamics of the broad class of mechanical systems without external constraints, including such free-flying systems as aerial and space robots. Most importantly, our approach enables the application of flatness-based planning and control approaches to new robotic systems by facilitating the discovery of flat outputs with strong, useful properties. The results combine geometric methods and numerical tools to ultimately point towards a systematic, automated approach to numerically identify geometric flat outputs directly from the system model, particularly useful when complexity renders pen and paper analysis intractable.

---

[6]It's worth commenting on the coincidence of nomenclature between a "flat" distribution (integrable in the Frobenius sense), and a "flat" system (integrable in the sense of equivalence to a "trivial" system [65]). This nomenclative correspondence is thematically fitting but indirect, since we refer to two different notions of integrability.

DYNAMICALLY FEASIBLE TASK SPACE PLANNING FOR UNDERACTUATED AERIAL MANIPULATORS

The material in this chapter is based on the publication [40], co-authored with James Paulos and Vijay Kumar, as well as the publication [27], co-authored with Vijay Kumar. The author of this thesis developed the theory and simulations and drafted the original manuscript (in collaboration with his co-authors).

4.1 Introduction

In Chapter 3, we developed methods for constructing flat outputs of mechanical systems by exploiting symmetry in the kinetic energy metric, while also ensuring that the flatness transformations preserved this symmetry when the potential forces were also invariant. Such symmetry-aware flat outputs can be leveraged within a trajectory planning scheme to plan trajectories that respect the underactuated dynamics of the system, as in [25,66]. However, while we gave some illustrative examples and an incomplete catalog of systems which enjoy such geometric flat outputs, certain robotics systems may not fit neatly within the setting of the previous results. Two main limitations are clear:

1. Our formal results considered those systems whose configuration manifold is acted upon by symmetry group of dimension equal to the number of control inputs. Thus, for robotic systems in 3D space, these results will primarily be applicable to systems with six or less actuators, where the symmetry group will usually be a subgroup of $SE(3)$, although extensions could be achieved by preconditioning the system with a feedback transformation that induces a larger symmetry group.

2. Flatness-based schemes for dynamically feasible trajectory planning typically specify (or optimize) the desired trajectory in the flat space. For many problems, this is a convenient representation, especially when the flat outputs have physical meaning (*e.g.*, the position of the system center of mass), as is common in the symmetry-aware setting. However, the flat outputs may not always correspond to the task of interest (see [67] for some discussion). In such settings, other tools are needed to synthesize trajectories which achieve the desired task while retaining dynamic feasibility.

In this chapter, we consider a class of systems that faces both these difficulties: the class of *underactuated aerial manipulators*, consisting of an underactuated vehicle (*i.e.*, a quadrotor), equipped with a manipulator arm with an arbitrary number of revolute joints. An obvious task for such a system is to achieve some desired motion of its end effector, in order to interact physically with its surroundings. Despite the special aerial manipulator geometries considered in Example 3.2 as well as [68], and [27], in general, the end effector's pose cannot be expressed as a function of the flat outputs alone (*i.e.*, without derivatives), necessitating other methods for planning trajectories which both kinematically achieve a desired end effector

motion and satisfy the system's underactuated dynamics.

The investigation in this chapter is less mathematically rigorous (lacking theorems or formal proofs) than the rest of this thesis. Rather, the aim of this chapter is for the reader to gain familiarity with a domain in robotics where planning algorithms can be aided by the more abstract contributions of the prior chapter, while also better understanding the limitations of those methods, and how they can be extended to tackle other kinds of problems.

4.1.1 Trends in Aerial Manipulation

Aerial manipulation seeks to combine the dexterity, precision, and robustness of manipulator arms with the unbounded workspace and terrain independence of aerial vehicles. Over the last decade, there have been many exciting advances in both theory and experimental practice [69]. Teams of robots with body-fixed grippers have performed cooperative assembly tasks [70], and a quadrotor with a planar 2-DOF arm has been shown to transport small objects [71]. Many early examples of aerial manipulators leveraged underactuated vehicles such as quadrotors and had arms of only a few joints, but did not fully account for the dynamic coupling of the arm and the vehicle, limiting performance and precision. Recently, there has been a greater prevalence of systems employing:

- fully-actuated vehicle platforms, enabling independent translation and rotation of the vehicle thanks to its ability to exert arbitrary forces and torques [72–74], or

- highly redundant manipulator arms, able to correct error as the slow, imprecise vehicle tracks a (perhaps dynamically infeasible) reference trajectory [75–77], in the spirit of a "macro-micro" manipulator [78].

However, such capabilities come at a price. Due to the physical limits of aerial vehicles, thrust is precious; to spend it supporting the weight of additional components makes it unavailable for dynamic maneuvers and reduces the endurance of the platform. The result is sluggish systems that strain to carry heavy actuators they may not need to complete the task.

4.1.2 Minimalist Aerial Manipulator Morphologies

In view of these characteristics, it is clear that lightweight underactuated vehicles with minimally jointed arms will outperform their redundant counterparts in terms of cost, endurance, and agility; the question is whether they can remain competitive in terms of dexterity and precision. We argue that the apparent shortcomings of underactuated aerial manipulators, in particular the tradeoff between precision and dynamic capabilities, can be largely resolved by planning trajectories which kinematically achieve the desired end effector motion while also satisfying the system's underactuated dynamics. This is especially vital when engaging in aggressive maneuvers or high-precision tasks, where dynamic feasibility is crucial

to ensure accurate tracking. For example, in [79], an aerial manipulator spray painting line art could only perform the task with acceptable quality under quasi-static conditions.

Methods to plan dynamically feasible manipulation trajectories for simplified special cases have been demonstrated. A quadrotor with a body-fixed gripper was shown to grasp moving objects in simulation using manually-designed dynamically feasible trajectories, but only for constant velocity targets [80]. A planar aerial manipulator with one joint moving at high speeds was shown to grasp stationary objects [39], and a theoretical extension to planar systems with more joints has also been developed [68]. However, in addition to the planar restriction, both of these works required that the system have specific geometry that can be difficult to realize in hardware, namely that the arm be attached at the vehicle center of mass. Likewise, our prior work demonstrated dynamically feasible planning of the end effector pose trajectory in SE(3) for a quadrotor with a 2-joint arm, but again only for manipulators with special geometry for which the system center of mass is static as viewed in the end effector reference frame [27].

4.1.3 Overview and Contributions

In this work, we show that all aerial manipulators consisting of an underactuated vehicle and an articulated arm are differentially flat systems, such that we may minimally describe the space of permissible trajectories in terms of sufficiently smooth trajectories for the flat outputs. We then formulate and solve the dynamically feasible inverse kinematics problem, determining which flat output trajectories will exactly produce a desired trajectory for the end effector, despite the system's underactuation and kinematic redundancy. Using these results, we present two classes of aerial manipulators possessing key properties beneficial for trajectory planning. Finally, in simulation, we show the applicability of the method to a broad domain of problems requiring precision and dynamic performance.

4.2 Mathematical Preliminaries

The class of systems in question is shown in Fig. 4.1, meant to represent a quadrotor equipped with a manipulator arm of arbitrary number of joints and geometry, including those with $n = 0$ or $n = 1$ joints.

4.2.1 System Definition

We model the vehicle and each link of the arm as a rigid body, specifying the configuration and velocities of the system as

$$q = (x, R, \theta) \in \mathbb{R}^3 \times \mathrm{SO}(3) \times \mathbb{T}^n, \qquad v = (\dot{x}, \Omega, \dot{\theta}) \in \mathbb{R}^{6+n}. \tag{4.1}$$

The chosen configuration variables are the global position $x \in \mathbb{R}^3$ of the center of mass of the entire system (including the arm), the rotation $R \in \mathrm{SO}(3)$ from the vehicle frame to the world frame, and the tuple of joint angles $\theta = (\theta_1, \ldots, \theta_n) \in \mathbb{T}^n$, where $\theta_i \in \mathbb{S}^1$. For the velocities, $\dot{x} \in \mathbb{R}^3$ is the center of mass velocity, $\Omega \in \mathbb{R}^3$ is the body-frame angular velocity of the vehicle, and $\dot{\theta} \in \mathbb{R}^n$ is the vector of joint velocities. The
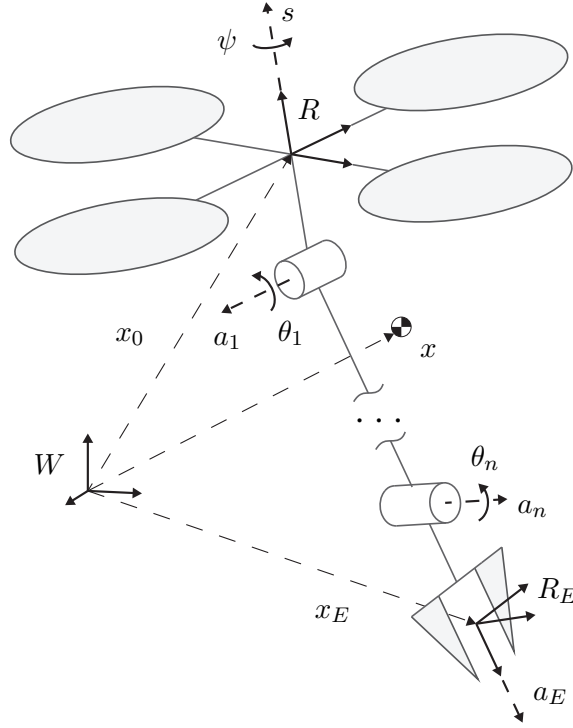
Figure 4.1: Schematic of a generic underactuated aerial manipulator, consisting of an underactuated aerial vehicle (*i.e.*, a quadrotor) equipped with an arbitrary n-joint articulated arm and an end effector.

system has inputs $u = (\mathrm{f}, \mathrm{m}, \mathrm{t}) \in \mathbb{R}^{4+n}$, where $\mathrm{f} \in \mathbb{R}$ is the magnitude of net rotor thrust, fixed in the e_3 direction in the vehicle frame, $\mathrm{m} \in \mathbb{R}^3$ is the net moment vector on the vehicle due to the rotors (in the body frame), and $\mathrm{t} \in \mathbb{R}^n$ is the tuple of applied joint torques. Appealing to the Lie group structure of the configuration manifold, we write the kinematics of the system as $\dot{q} = q\hat{v}$, or in expanded explicit form as

$$\tfrac{\mathrm{d}}{\mathrm{d}t}x = \dot{x}, \quad \tfrac{\mathrm{d}}{\mathrm{d}t}R = R\,\hat{\Omega}, \quad \tfrac{\mathrm{d}}{\mathrm{d}t}\theta = \dot{\theta}. \tag{4.2}$$

where the notation $\hat{\cdot}$ is the overloaded *hat map* from Euclidean coordinates to the appropriate Lie algebra.

4.2.2 Dynamic Modeling

Consider the position x_i and orientation R_i of each rigid body in the system relative to the world frame W, where $i \in \{0, \dots, n\}$ and R_0 is simply R. We remark that each body's global position and orientation may be expressed as

$$x_i(q) = x + Rp_i(\theta), \quad R_i(q) = RQ_i(\theta), \tag{4.3}$$

where x is the system center of mass position, $p_i(\theta)$ is the displacement vector from the center of mass to body i expressed in the vehicle frame, and $Q_i(\theta)$ gives the rotation from body i to the vehicle frame.

ROTATIONAL SUBSYSTEM

$\Omega, \dot\theta \in \mathbb{R}^{3+n}$

$u_{\text{rot}} \in \mathbb{R}^{3+n}$

$R, \theta \in SO(3) \times \mathbb{T}^n$

$$M_{\text{rot}} \begin{bmatrix} \dot\Omega \\ \ddot\theta \end{bmatrix} + C_{\text{rot}} \begin{bmatrix} \Omega \\ \dot\theta \end{bmatrix} = u_{\text{rot}}$$

$R\,\mathrm{e}_3 \in \mathbb{S}^2$
thrust direction

TRANSLATIONAL SUBSYSTEM

$\dot{x} \in \mathbb{R}^3$

$\mathrm{f} \in \mathbb{R}$

$x \in \mathbb{R}^3$

$$m\ddot{x} + mg e_3 = \mathrm{f}\, R\, \mathrm{e}_3$$
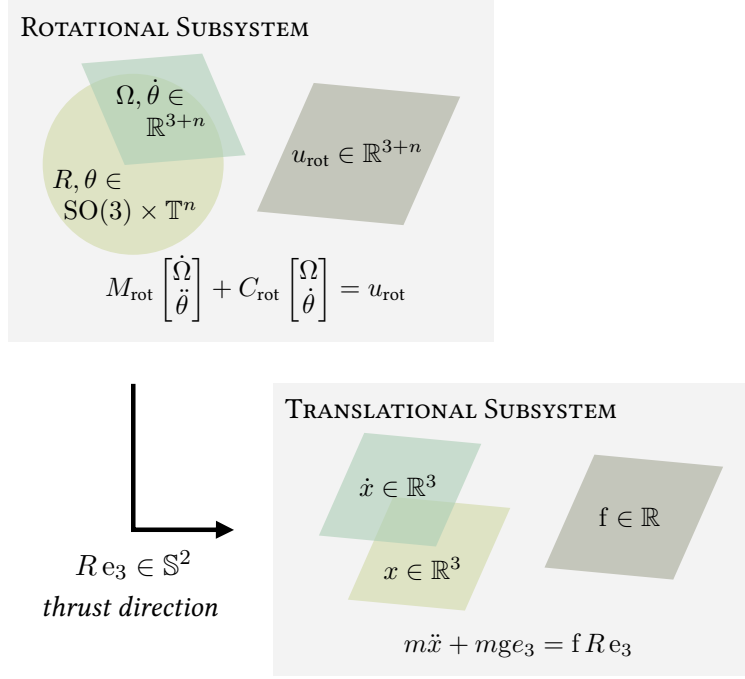
Figure 4.2: Using the system center of mass instead of the vehicle position in the configuration variables puts the equations of motion into an explicitly cascaded form, familiar from the dynamics of a quadrotor.

Forward kinematics in this form may be derived by first following standard recursive methods using the vehicle position x_0, then expressing the system center of mass as the weighted sum

$$x = \tfrac{1}{m}(m_0 x_0 + m_1 x_1 + \ldots + m_n x_n), \tag{4.4}$$

from which we may isolate x_0 in terms of our chosen chosen configuration variables, substituting that result back into our expressions for x_i and R_i to reveal the form of (4.3).

We use the generalized Lagrangian method presented in [81] to derive globally valid, singularity-free equations of motion. A more detailed overview of how to apply such methods to aerial manipulators can be found in [27]. Ultimately, we obtain the dynamics in terms of the standard "manipulator equations",

$$M(q)\dot{v} + C(q, v)v + g(q) = B(q)u. \tag{4.5}$$

4.2.3 Sparsity of the Manipulator Equations

The choice of the system center of mass in the configuration (*vs.* the more obvious choice of the vehicle position) is deliberate. It has been shown [75] that the dynamics of floating-base robots like aerial manipulators can be expressed in a decoupled form by transforming equations of motion derived in some

naive representation into a sparse form where the center of mass position and velocity appear explicitly. Informed by these results, we have chosen a state representation which effectively resolves this transformation at the kinematic level. The sparsity resulting from this choice will provide insight into the system structure and simplify implementation. In particular, the equations of motion (4.5) can be expanded as

$$\begin{bmatrix} m\mathrm{I}_{3\times3} & 0 \\ 0 & M_{\mathrm{rot}} \end{bmatrix} \dot{v} + \begin{bmatrix} 0 & 0 \\ 0 & C_{\mathrm{rot}} \end{bmatrix} v + \begin{bmatrix} mg\,\mathrm{e}_3 \\ 0 \end{bmatrix} = \begin{bmatrix} R\,\mathrm{e}_3 & 0 \\ B_{\mathrm{rot}} & \mathrm{I}_{(3+n)\times(3+n)} \end{bmatrix} u, \tag{4.6}$$

where the submatrices have the sparse state dependencies

$$M_{\mathrm{rot}} = M_{\mathrm{rot}}(\theta), \ B_{\mathrm{rot}} = B_{\mathrm{rot}}(\theta), \ C_{\mathrm{rot}} = C_{\mathrm{rot}}(\theta, \dot{\theta}, \Omega). \tag{4.7}$$

The effect of the thrust input on the rotational subsystem can easily be eliminated by a state-dependent change of input variables. Therefore, as seen in Fig. 4.2, the dynamics take the form of two cascaded subsystems—a fully actuated rotational subsystem evolves independently, feeding the direction of the thrust vector into the underactuated translational subsystem, resembling the observations of [82].

4.3   Differential Flatness

As discussed in Chapter 3 and widely leveraged in the aerial robotics literature, *differential flatness* is a system property that allows us to describe the dynamically feasible trajectories of an underactuated system in a representation not subject to differential constraints [25]. Briefly, we recall that a system is differentially flat if there exists some (non-unique) *flat output* $y \in Y$ such that the state and inputs (q, v, u) can be expressed as a function of finitely many derivatives of the flat output $(y, \dot{y}, \ldots, y^{(\alpha)})$, while the flat output y must be given in terms of the state and finitely many derivatives of the inputs, *i.e.*, $(q, v, u, \dot{u}, \ldots, u^{(\beta)})$. Moreover, the flat space and input space are of the same dimension.

The flat outputs must be differentially independent, meaning that there will be no dynamic feasibility requirements on trajectories in the flat space, other than that the chosen curve be C^α. Therefore, each sufficiently smooth trajectory in the flat space can be mapped to a dynamically feasible trajectory in the state-input space, enabling efficient trajectory planning and, in some sense, describing the structure of the family of dynamically feasible trajectories for the system.

4.3.1   The Configuration Manifold as a Fiber Bundle

To begin, we analyze the structure of the configuration manifold. To begin, we recall the Hopf fibration, leveraged in [41] for the control of a standard quadrotor. Briefly, the Hopf fibration is the nontrivial fiber bundle

$$\mathbb{S}^1 \hookrightarrow \mathbb{S}^3 \xrightarrow{h} \mathbb{S}^2, \tag{4.8}$$

where h is a smooth surjective map projecting $\mathbb{S}^3$ onto $\mathbb{S}^2$. The idea is that the *total space* $\mathbb{S}^3$ is locally indistinguishable from the product of the *base space* $\mathbb{S}^2$ and the *fiber space* $\mathbb{S}^1$ (even though this is not the case globally), and $h^{-1}(s)$ (the fiber of total space "above" $s \in \mathbb{S}^2$) is diffeomorphic to $\mathbb{S}^1$.

A double cover $\mathbb{S}^3 \to \mathrm{SO}(3)$ will reveal a related bundle

$$\mathbb{S}^1 \hookrightarrow \mathrm{SO}(3) \xrightarrow{p} \mathbb{S}^2, \tag{4.9}$$

where p is the map $R \mapsto R\,\mathrm{e}_3$. We may also construct a *local section* (in other words, a local right inverse of the bundle projection p) on some open set $U \subset \mathbb{S}^2$ in the form $\sigma : U \to \mathrm{SO}(3)$ which assigns to each element of U an element in the fiber above it, such that $p \circ \sigma(s) = s$. Let us establish a smooth family of such sections (in other words, a *local trivialization*) parametrized by $\psi \in \mathbb{S}^1$, on the open set $U :=$ $\mathbb{S}^2 \setminus \{-\mathrm{e}_3\}$, constructed using maps derived from [41] given by

$$H_1 : \mathbb{S}^1 \to \mathrm{SO}(3),\ \psi \mapsto \begin{bmatrix} \cos\psi & -\sin\psi & 0 \\ \sin\psi & \cos\psi & 0 \\ 0 & 0 & 1 \end{bmatrix}, \tag{4.10}$$

$$H_2 : \mathbb{S}^2 \to \mathrm{SO}(3),\ s \mapsto \begin{bmatrix} 1 - \frac{s_1^2}{1+s_3} & -\frac{s_1 s_2}{1+s_3} & s_1 \\ -\frac{s_1 s_2}{1+s_3} & 1 - \frac{s_2^2}{1+s_3} & s_2 \\ -s_1 & -s_2 & s_3 \end{bmatrix}. \tag{4.11}$$

Composing these rotations as

$$R = \sigma_p(s,\psi) := H_2(s)\,H_1(\psi) \tag{4.12}$$

yields a local trivialization $\sigma_p : U \times \mathbb{S}^1 \to \mathrm{SO}(3)$, describing any element $R \in \mathrm{SO}(3)$ with $p(R) \neq -\mathrm{e}_3$ in terms of two specifications:

1. a direction $s \in \mathbb{S}^2$ to point the vector $\mathrm{e}_3 \in \mathbb{S}^2$, and

2. a rotation around that vector by the angle $\psi \in \mathbb{S}^1$.

The quadrotor's actuation geometry manifests this structure. If we point the thrust in some direction, we are left with a remaining degree of freedom rotating around that vector, together constructing the full orientation. Due to the product structure of the configuration manifold, it is straightforward to use the map $\pi(q) = p \circ \mathrm{pr}_2(q) = p(R)$ to express the entire configuration manifold as the fiber bundle

$$\underbrace{\mathbb{R}^3 \times \mathbb{T}^{n+1}}_{Y} \hookrightarrow \underbrace{\mathbb{R}^3 \times \mathrm{SO}(3) \times \mathbb{T}^n}_{Q} \xrightarrow{\pi} \underbrace{\mathbb{S}^2}_{S} \tag{4.13}$$

where Q is the configuration manifold, S is the *shape space*, and it will be shown that Y is the flat space.

Thus, in particular, this system has the special property of *configuration flatness*, where the flat outputs depend only on the configuration and not the velocities or inputs. In particular, the flat outputs will be

$$y = (x, \theta^+) \in Y \tag{4.14}$$

where as before, $x \in \mathbb{R}^3$ is the system's center of mass, while $\theta^+ = (\psi, \theta) \in \mathbb{T}^{n+1}$ is the tuple of physical joint angles augmented by the *virtual joint* around the thrust vector. We may also construct a corresponding local trivialization given by

$$\sigma_\pi : S \times Y \to Q, \ (s, y) \mapsto (x, \sigma_p(s, \psi), \theta) \tag{4.15}$$

and the local flat output map $y = \varphi(q)$ can be given explicitly by extracting ψ in terms of R from (4.12), while the rest of the flat outputs are given by identity mappings. In particular, the local trivialization highlights the local product structure of the configuration manifold.

4.3.2 Deriving the Flatness Diffeomorphism

We must now give the state and inputs as functions of the flat outputs and their derivatives. In view of (4.15), if we can determine the shape s in terms of derivatives of the known flat outputs y, we can immediately reconstruct the entire configuration in terms of the flat output derivatives. Likewise, by differentiating (4.15) and invoking the kinematics we can also determine the velocities and accelerations, from which the inputs can be found with the equations of motion. Thus, we seek to express the system's dynamic feasibility constraints in a form which we can solve to give the shape in terms of flat output derivatives.

A trajectory is dynamically feasible if and only if the necessary generalized forces lie in the *actuated subspace*, namely the column space of B. This is evident in (4.5), since only when the left-hand side lies within the range of B can u be chosen to satisfy the equality. Equivalently, the required forces must be orthogonal to the *unactuated subspace*, such that the projection of the equations of motion onto this subspace takes the form

$$B_\perp(q)^{\mathrm{T}} \big(M(q)\,\dot{v} + C(q, v)\,v + g(q) \big) = 0, \tag{4.16}$$

where $B_\perp(q)$ is a matrix whose columns span the left nullspace of B in any configuration $q \in Q$. Because the rotational subsystem is fully actuated, it is easily verified that the choice

$$B_\perp(q) = \begin{bmatrix} \widehat{(R\,\mathrm{e}_3)} \\ 0_{3+n \times 3} \end{bmatrix} \tag{4.17}$$

suffices, where we use the hat map to encode the cross product in the form of matrix multiplication (*i.e.*, $\hat{a}b = a \times b$ for all $a, b \in \mathbb{R}^3$). Note that for all $q \in Q$, we have rank $B_\perp(q) = 2$, the degree of underactua-

tion. Using the local trivialization and its derivatives to express the state and accelerations in terms of the shape and flat output derivatives, (4.16) will simplify to

$$s \times (\ddot{x} + g\,e_3) = 0 \tag{4.18}$$

which indicates that the thrust must point along the prescribed center of mass acceleration plus the effect of gravity, a familiar requirement from the case of the standard quadrotor [25]. The constraint (4.18) has two solutions for s, antipodal on $\mathbb{S}^2$, and customarily we select the solution with strictly positive thrust[7],

$$s = \frac{\ddot{x} + g\,e_3}{\left|\left| \ddot{x} + g\,e_3 \right|\right|}. \tag{4.19}$$

from which we reconstruct the entire configuration using (4.15). We may then differentiate (4.18) twice, solving to give us the shape velocity and acceleration as

$$\dot{s} = \frac{\left(I_{3\times 3} - ss^{\mathrm{T}}\right) x^{(3)}}{\left|\left| \ddot{x} + g\,e_3 \right|\right|}, \tag{4.20}$$

$$\ddot{s} = \frac{\left(I_{3\times 3} - ss^{\mathrm{T}}\right) x^{(4)} - \left(2\dot{s}s^{\mathrm{T}} + s\dot{s}^{\mathrm{T}}\right) x^{(3)}}{\left|\left| \ddot{x} + g\,e_3 \right|\right|}. \tag{4.21}$$

From these solutions, we may reconstruct v and $\dot{v}$ via derivatives of the local trivialization (4.15). Finally, since we have already prescribed that the required generalized forces lie in the actuated subspace, we can find the inputs using the pseudoinverse of $B(q)$ as

$$u = B(q)^{\dagger}\big(M(q)\,\dot{v} + C(q,v)\,v + g(q)\big), \tag{4.22}$$

where we have

$$B(q)^{\dagger} = \left(B(q)^{\mathrm{T}}B(q)\right)^{-1}B(q)^{\mathrm{T}}, \tag{4.23}$$

since $B(q)$ has full column rank for all $q \in Q$.

Thus, we have shown that this class of systems is always differentially flat, regardless of the particular geometry. Because we require $\ddot{\theta}^{+}$ and $x^{(4)}$ to determine the inputs, it must hold that θ^{+} is C^2 and x is C^4 for there to exist a corresponding dynamically feasible trajectory for the physical system.

4.4   Task Space Planning

A natural means of specifying a task for a manipulator is to describe the desired motion of its end effector via some suitable task outputs $t \in T$. Then, given a desired trajectory for t, we must find the trajectories

---

[7]We could also choose the solution for which s and $\ddot{x} + g\,e_3$ are antiparallel (corresponding to negative thrust), thereby obtaining another flatness diffeomorphism. See [59] for further discussion.

$$T = \mathbb{R}^3 \times \mathbb{S}^1 \qquad T = \mathbb{R}^3 \times \mathbb{S}^2 \qquad T = \mathrm{SE}(3)$$

$$t = \{x_E, \psi\} \qquad t = \{x_E, a_E\} \qquad t = \{x_E, R_E\}$$
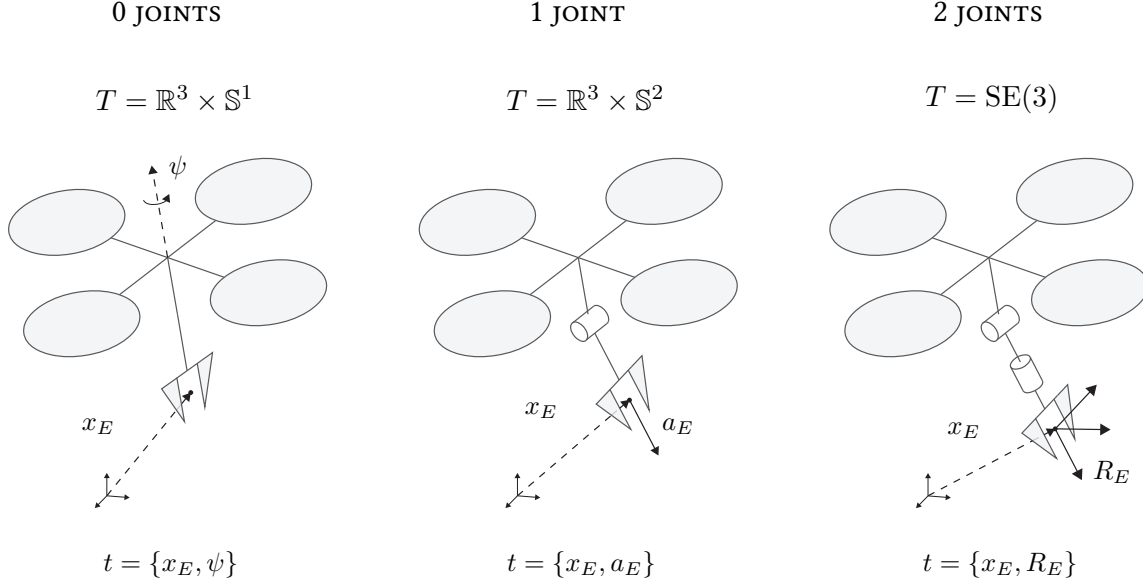
Figure 4.3: The structure of the task space T depends on n, the number of joints in the arm. In the degenerate case where adjacent axes are parallel, a different definition should be adopted. Appropriate definitions for $n > 2$ will be determined by the application and thus are not considered here.

for the configuration q which all throughout satisfy the kinematic constraint

$$\tau(q) = t \qquad\qquad (4.24)$$

where $\tau : Q \to T$ is the forward kinematic map. For fully-actuated manipulators (either minimal or re-dundant), this problem deals only with the manipulator geometry, since any configuration trajectory is feasible. However, for underactuated systems, many trajectories for q which *kinematically* satisfy (4.24) may not be dynamically feasible, so cannot be executed.

We argue that the generalization of this problem to differentially flat (and perhaps underactuated) systems is to determine trajectories for the flat outputs $y \in Y$ that produce the specified task motion for $t \in T$, since any such trajectory will be dynamically feasible. The appropriate task space will be of the same dimension as the flat outputs, and in Fig. 4.3 we show the natural choice for aerial manipulators of $n \in \{0, 1, 2\}$ joints, where for each case the task outputs consist of the position of the end effector x_E and some rotational information of varying dimension. Unfortunately, there will not in general exist a direct mapping between the flat outputs and the task outputs, because the task outputs will also depend on the shape $s \in S$.

4.4.1 Self-Motion Manifold

Due to the difference in dimension between the task space and configuration manifold, the kinematic structure of this problem resembles that of redundant, fully-actuated manipulators, wherein the subspace

of the configuration manifold consistent with a prescribed task output is known as the *self-motion manifold*, on which the configuration may evolve without affecting the task output [83]. For fully-actuated systems, the evolution on the self-motion manifold may be arbitrary, but for underactuated systems, even self-motion is subject to dynamic constraints.

To characterize the self-motion manifold, let us first divide the configuration manifold Q into open regular regions Q_i, bounded by the critical value surfaces of the forward kinematic map, i.e. the physical manipulation singularities. In particular, the singularity for $n = 0$ is due to the singularity in the local trivialization at $s = -\mathrm{e}_3$, while the other cases are of the same sort as the familiar *wrist singularity* occurring when axes align in a common plane. It can be shown that for each region, $\tau(Q_i) = T$, that is, each regular region has the entire task space as its image under the forward kinematic map. This can be seen by freezing the joints (since in the jointed case the critical value surfaces are given by critical values of the joint angles) and varying only the vehicle pose to cover all of T.

We therefore remark that each regular region Q_i is a trivial fiber bundle over T, with the forward kinematic map serving as the bundle projection [83]. Then, for the self-motion manifold of any $t \in T$, its component lying in Q_i is simply the fiber above t. We also remark that over each Q_i, the constraints

$$\tau(q) = t, \ \pi(q) = s \tag{4.25}$$

are independent (*i.e.*, for any prescribed task output, we may still choose the thrust direction). We will use this observation to construct a new local trivialization $\sigma_\tau^i : T \times U_i \to Q_i$ in the form

$$q = \sigma_\tau^i(t,s), \tag{4.26}$$

which, by varying the shape s, describes the fiber above $t \in T$.

To derive these local trivializations for each n, first consider the pose of the end effector in terms of the configuration a form directly analogous to (4.3), namely

$$x_E = x + Rp_E(\theta), \ \ R_E = RQ_E(\theta) \tag{4.27}$$

and substitute $R = H_2(s) H_1(\psi)$ from the family of sections (4.12). Clearly if we can determine ψ, we may reconstruct R, and if we can determine θ, we may also find x as

$$x = x_E - Rp_E(\theta) \tag{4.28}$$

combining these results to construct the full task preimage.

Thus we consider the subproblem of determining the virtual joint ψ and physical joint angles θ, separately for each number of joints $n \in \{0, 1, 2\}$:

$n = 2$: Beginning with the orientation constraint from (4.27), we move $H_2(s)$ to the left side, yielding

$$H_2(s)^{\mathrm{T}} R_E = H_1(\psi) Q_E(\theta) \tag{4.29}$$

This subproblem is equivalent to the inverse kinematics of a 3-joint wrist, which we may solve for ψ, θ_1, and θ_2 in terms of the prescribed R_E and s.

$n = 1$: Only the end effector axis $a_E = R_E \tilde{a}_E$ is prescribed instead of the full orientation, so similarly:

$$H_2(s)^{\mathrm{T}} a_E = H_1(\psi) Q_E(\theta) \tilde{a}_E \tag{4.30}$$

This subproblem is equivalent to the inverse kinematics of a 2-joint wrist, which we may likewise solve for ψ and θ_1.

$n = 0$: ψ is given explicitly and there are no physical joints to solve for.

Using the other trivialization (4.12) to derive these solutions seems to introduce a singularity at $s = -e_3$. However, precisely the same singularity appears in the flatness diffeomorphism (and such a singularity must always exist, since (4.13) is a nontrivial fiber bundle), therefore it is already present and will have no further deleterious effects on the final flat output trajectories. Also, a second diffeomorphism with a singularity elsewhere could be used to operate in this regime, as done in [41] and [59].

4.4.2 Simultaneous Consideration of Kinematics and Dynamics

To formulate the problem, we begin with the forward kinematic map (4.24) and substitute in the family of sections of the flatness bundle, expressing the kinematic constraint in terms of the flat outputs and the shape. By the definition of differential flatness, there are no feasibility constraints on the flat outputs other than smoothness, but the shape evolution is subject to the unactuated subspace constraint (4.18). Thus the combined planning problem is described by the differential algebraic equation (DAE)

$$\tau \circ \sigma_\pi(s,y) = t, \tag{4.31a}$$
$$s \times (\ddot{x} + \mathrm{g}\, e_3) = 0, \tag{4.31b}$$

where the first equation captures the algebraic (kinematic) constraints and the second equation captures the differential (dynamic) constraints. (Note that in a DAE, "algebraic" refers to the absence of derivatives, not a polynomial equation.)

Let us consider solutions over any particular Q_i. Then, applying the trivialization of the task bundle to the kinematic constraint (4.31a), followed by the flat output map, will yield a flat output trajectory in terms of the task outputs and the shape as

$$y = \varphi \circ \sigma_\tau^i(t,s), \tag{4.32}$$

so all that remains is to find a shape profile which also satisfies the feasibility constraint (4.31b). However, the dynamic constraint on s depends itself on some flat output derivatives, namely $\ddot{x}$. Let us therefore define the function

$$x = \chi(t,s) := \mathrm{pr}_1 \circ \varphi \circ \sigma_\tau^i(t,s) \tag{4.33}$$

expressing the subset of flat outputs whose derivatives appear in the unactuated subspace constraint (namely, x) in terms of the task outputs and the shape. Substituting this into (4.31b) gives us a second-order time-varying differential equation in s,

$$s \times \left(g\,e_3 + \frac{\mathrm{d}^2}{\mathrm{d}t^2}\,\chi(t,s) \right) = 0, \tag{4.34}$$

subject to the simple geometric constraint $s \in \mathbb{S}^2$, or more explicitly,

$$s^\mathsf{T}s = 1. \tag{4.35}$$

Thus, any joint solution of the two previous equations describes a dynamically feasible configuration space trajectory via (4.32) in the minimal form of a flat output trajectory. For sufficiently well-behaved systems (to be made precise in Sec. 4.5), the solution to the initial value problem for initial conditions $(s_0, \dot{s}_0) \in T\mathbb{S}^2$ is unique and exists on an arbitrary interval. Because the differential equation is nonlinear, we find approximate solutions numerically; to do so we expand the differential operator using the second-order chain rule and solve for the acceleration by also differentiating the geometric constraint. Integration in minimal coordinates using two antipodal stereographic projections dramatically improves solution accuracy.

The dimension of the initial conditions space is 2 rank $B_\perp = 4$, where the factor of 2 arises due to the second derivative in the unactuated subspace constraint. In view of (4.32), these initial conditions parametrize the continuous finite-dimensional function space of solutions to the overall problem[8], as seen in Fig. 4.4. We also remark that the flatness of the system ensures controllability, such that the system is capable of driving itself to the initial conditions required to execute a chosen solution.

4.4.3 Trajectory Optimization

Given the infinite space of solutions, we may consider a cost function to aid in the selection of a single solution, such as a running cost meant to minimize energy expenditure. The full state and inputs could be reconstructed to evaluate a more complex running cost, however this may be unnecessary. Letting $s^\star(t)$ be the solution to the initial value problem for $(s_0, \dot{s}_0)$, we pose the minimization problem

$$\min_{(s_0, \dot{s}_0)\, \in\, T\mathbb{S}^2} \int_0^T J\big(s^\star(t),\, \dot{s}^\star(t),\, \ddot{s}^\star(t)\big)\, dt \tag{4.36}$$

---

[8]The choice of some particular regular region Q_i also adds discrete multiplicity, as in classical inverse kinematics.
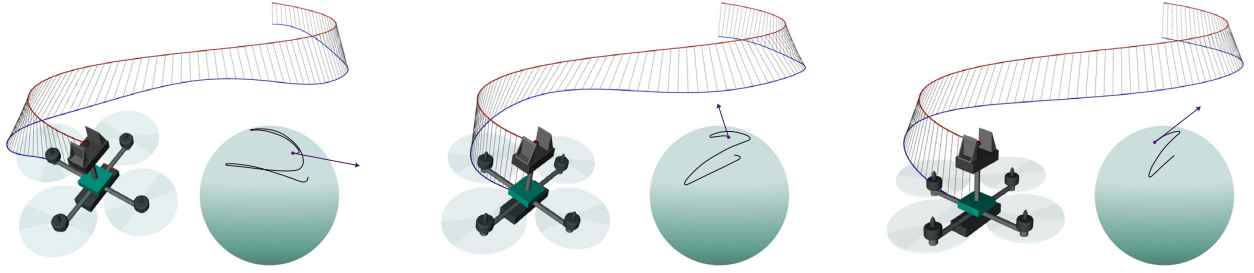
Figure 4.4: The family of trajectories in the flat space which will exactly produce a desired task trajectory can be parametrized by the initial conditions of the shape dynamics *(in purple)*. Above are several different solutions *(in blue)* for the same task trajectory *(in red)* for a zero-joint system, along with the corresponding evolution in shape space *(in black)*. Solutions decrease in cost from left to right according to (4.37). Animations are shown in the video attachment.

with a task-appropriate running cost; for example, choosing

$$J\big(s, \dot{s}, \ddot{s}\big) = \Big|\Big|\ddot{s}\Big|\Big|^2 \tag{4.37}$$

is very similar to the "minimum snap" cost used ubiquitously for quadrotors [25], since typically $\ddot{s}$ is dominated by $x^{(4)}$ as seen in (4.21). Because the dimension of the decision variables is very small, we can quickly find solutions to this shooting problem by numerical integration and gradient descent with a reasonable initial guess (*e.g.*, the hover condition). On a standard laptop, convergence occurs within seconds. Furthermore, the proposed formulation is an *anytime algorithm*, ideal for real-time planning: even if the optimization must be terminated early, the current best approximation specifies a (suboptimal) trajectory that is both dynamically feasible and guaranteed to achieve the desired task motion.

4.5   Internal Dynamics

The result of the previous section is that the dynamic feasibility constraint has been expressed in a minimal and convenient form which does not restrict the motion in the task space; the task outputs may evolve arbitrarily, while the shape dynamics arising from (4.34) govern the evolution of the system on the self-motion manifold, as excited by the task motion. We refer to this as the *internal dynamics* due to resemblance to the method of input-output linearization [84].

This view highlights the risk that by exciting the internal dynamics, even some modest task motions might require very aggressive or even unbounded self-motions which will not be physically realizable, making even some mundane task motions impossible to perform. In [85], a zero-joint underactuated aerial manipulator was treated as a redundant mechanism by regulating only the position of the tool and not the

yaw angle, leaving this last degree of freedom available to stabilize the internal dynamics, which otherwise may exhibit finite time escape.

We adopt a different approach, which is to determine geometric criteria on the manipulator design which will prohibit the finite time escape of the internal dynamics, without sacrificing a dimension of manipulability. The stability of the internal dynamics (and naturally the avoidance of the physical manipulation singularities) is then the previously mentioned condition that the differential equation (4.34) be sufficiently well-behaved to guarantee existence and uniqueness of solutions to the initial value problem.

4.5.1 Internal Stability

Consider the problem of maintaining the task output at a constant value, a capability that any manipulator should have. We refer to the internal dynamics under such a condition as the *zero dynamics*, borrowing language again from input-output linearization. We note that expanding the second order derivative in (4.34) via chain rule will in general produce terms that are quadratic in $\dot{s}$, such that the ODE expressed in state space form will not be globally Lipschitz. Thus finite time escape may occur even when keeping the task output constant, which is clearly unacceptable. However, recalling the function χ giving the center of mass in terms of the task outputs and shape defined in (4.33), it can be shown that if

$$\frac{\partial \chi}{\partial s}(t,s) = -\lambda \mathrm{I}_{3\times 3} \tag{4.38}$$

for some constant $\lambda \neq 0$, then the quadratic terms will vanish from the zero dynamics, yielding the differential equation

$$s \times \left(\mathrm{g}\,\mathrm{e}_3 - \lambda \ddot{s} \right) = 0. \tag{4.39}$$

By invoking the geometric constraint (4.35) on s, we can solve for the zero dynamics in the form

$$\ddot{s} = -\frac{\mathrm{g}}{\lambda}\hat{s}^2 \mathrm{e}_3 - \left|\left|\dot{s}\right|\right|^2 s, \tag{4.40}$$

which resembles the dynamics of an undamped spherical pendulum. We therefore consider the energy-inspired function

$$H(s, \dot{s}) = -\frac{\mathrm{g}}{\lambda}\mathrm{e}_3^{\mathrm{T}} s + \frac{1}{2}\dot{s}^{\mathrm{T}}\dot{s}, \tag{4.41}$$

which can be shown to be the Hamiltonian of the system (and thus, $\dot{H} = 0$), so the zero dynamics do not exhibit finite time escape since H is radially unbounded.[9] The system has equilibria at $(s, \dot{s}) = (\pm \mathrm{e}_3, 0)$, and it is easily verified using the Hamiltonian that the zero dynamics are globally stable in the sense of

---

[9]Using the Hamiltonian of the zero dynamics, we may also demonstrate that even the internal dynamics excited by an arbitrary task trajectory cannot escape in finite time. It can be shown that, for large shape velocities, the generalized power $\dot{H}$ injected into the internal subsystem is bounded by H as long as the task output derivatives are bounded. Then the comparison principle will show that finite time escape may not occur, and thus for any finite duration task output trajectory with any shape initial conditions, the internal state will remain bounded. We omit a full derivation here for brevity.

(a) *Stable Internal Dynamics*   (b) *Task Flatness*
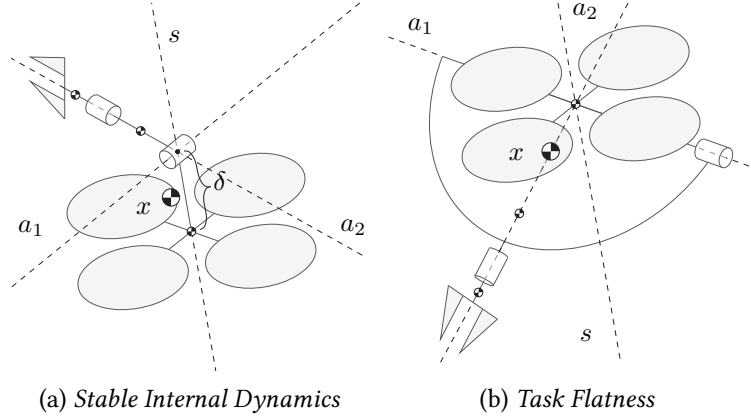
Figure 4.5: Systems satisfying certain geometric criteria will enjoy favorable properties that ensure the internal state remains bounded.

Lyapunov around the equilibrium with $s = \text{sgn}(\lambda)\, \text{e}_3$, while the other equilibrium is unstable, similar to the stability result given in [85] for aerial manipulators of $n = 0$ joints.

Underactuated aerial manipulators whose physical and virtual joint axes all intersect at a common point, in the spirit of a *spherical wrist*, will have the property (4.38), so long as both this intersection point and the center of mass of each arm link can be expressed directly in terms of the task outputs. Such a system is shown in Fig. 4.5a, and in general $\lambda = \frac{m_0}{m}\delta$, where δ is the signed distance along the thrust vector from the vehicle position to the intersection point. The systems shown in Figs. 4.3 and 4.4 also have this property. Choosing geometry with $\lambda > 0$ (where the intersection is above the vehicle body's center of mass) is preferred due to the singularities in the local trivialization and in the flatness diffeomorphism (occurring when the thrust vanishes). We want to remain local to the hover equilibrium, avoiding inversion of the vehicle, so that for typical trajectories, thrust remains positive.

4.5.2 Task Flatness

Now, consider systems with the special property

$$\frac{\partial \chi}{\partial s}(t,s) = 0, \tag{4.42}$$

namely the case where the center of mass can be expressed exclusively in terms of the task outputs with no dependence on the shape. Then, the internal dynamics vanish as (4.34) collapses into an algebraic constraint, which we solve for s in terms of derivatives of t and then explicitly reconstruct the flat output trajectory. The existence of such a mapping means that unlike in the general case, the solution family will be finite and discrete. Therefore, the task outputs of such a system constitute another valid choice of local flat outputs for the system, with the valid region bounded by the manipulation singularities. It can be
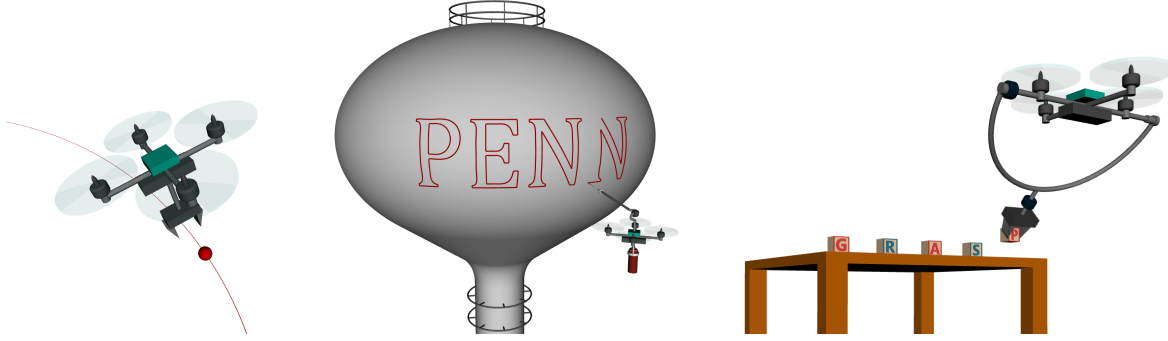
Figure 4.6: We plan dynamically feasible trajectories to perform several aerial manipulation tasks: the dynamic grasping of a moving object, precision spray painting, and 6-DOF pick and place. More details are given in the simulation video, available at `https://youtu.be/GOc6Begdb2s`.

verified that C^4 smoothness of t will be sufficient, as it was for the flat outputs. Because such manipulators are locally differentially flat with respect to the task outputs, we call this property *task flatness*.

For the task flatness condition (4.42) to hold for systems with $n \in \{0, 1, 2\}$ joints, the center of mass x must be fixed in the end effector frame.[10] For $n = 1$ it must also hold that x lies along the end effector axis a_E, while for $n = 0$, x must be at the end effector frame origin such that $x = x_E$. Then in each case, fixing the task outputs will fully determine the global position of the center of mass. To ensure that the system center of mass will be static in the end effector frame, all bodies inboard of any given joint must have their combined center of mass located along that joint's axis. One example of such an aerial manipulator is shown in Fig. 4.5b. We also remark that the geometric requirements imposed in previous work [39] [68] [27] to show differential flatness of special classes of aerial manipulators with respect to practically convenient flat outputs are essentially task flatness criteria from our perspective.

Task flatness is a useful property, and these requirements may be seen as design criteria for particularly nice aerial manipulators. Task flatness precludes the existence of poorly behaved internal dynamics, while also affording all the standard benefits of planning in the flat space; constraints in the state-input space can be mapped to constraints on flat output derivatives, efficiently encoding actuator saturation limits, obstacle avoidance, and physical manipulation singularities without integration. Task flatness also guarantees that periodic trajectories in the task space will always map to periodic trajectories in configuration space.

4.6 Simulations

The entire approach was implemented in simulation for a variety of aerial manipulator platforms and tasks. The flatness diffeomorphism was verified by simulating the open-loop dynamics under inputs corre-

---

[10]It's worth noting that a system enjoying this property will *still* enjoy this property after rigidly attaching additional mass to the end effector (since the added mass is *also* fixed in the end effector frame). Thus, picking up an object would not break task flatness, but it could alter the flatness diffeomorphism. For relatively lightweight objects, this discrepancy can likely be neglected.

sponding to aggressive flat output trajectories, showing precise agreement with the nominal trajectory. To demonstrate the usefulness of agile manipulation, we plan a dynamically feasible trajectory for a quadrotor with a body-fixed gripper to grasp a small object moving quickly along a curved path. We also simulate spray painting a pattern on the curved surface of an elevated structure using a system with one joint, motivating the importance of dynamic feasibility when error tolerance is small. Finally, we demonstrate the benefits of leveraging the vehicle agility to maximize manipulability by planning 6-DOF pick and place trajectories for a two-joint system. These simulations are shown in detail in the simulation video available at `https://youtu.be/GOc6Begdb2s`, as well as briefly in Fig. 4.6. In these simulations, we do not consider the exchange of wrenches between the system and objects in the environment, leaving them to ultimately be rejected by closed loop tracking control. This assumption is reasonable when performing pick and place tasks with small objects or when performing tasks that do not require physical contact.

4.7   Conclusion

In summary, we have demonstrated that all underactuated aerial vehicles equipped with articulated manipulators are differentially flat systems regardless of their geometry. We have developed a new method for determining the family of dynamically feasible trajectories which will produce a desired end effector trajectory, allowing lightweight underactuated systems to perform dynamic maneuvers accurately. We have also determined criteria for a class of aerial manipulators whose internal dynamics are guaranteed to be well behaved, and another class for which the task outputs are themselves alternate flat outputs of the system, each providing design specifications for hardware platforms. These specifications largely pertain to the attachment geometry between the manipulator and the vehicle, an aspect which has been explored in other mobile manipulation contexts as well [86, 87]. Our future work will address integration with closed loop control and implementation on hardware, as well as the consideration of changing modes of environmental contact and exerting non-negligible external wrenches while retaining dynamic feasibility.

ALMOST GLOBAL ASYMPTOTIC TRACKING ON HOMOGENEOUS RIEMANNIAN MANIFOLDS

The material in this chapter is based on the publication [88], co-authored with Vijay Kumar.
The author of this thesis developed the theoretical contributions and simulations
and drafted the original manuscript (in collaboration with his co-author).

5.1 Introduction

In Chapters 3 and 4, we focused on dynamically feasible trajectory planning for underactuated robotic systems, wherein the major focus was the identification and exploitation of the property of differential flatness. In the remainder of this thesis, we will consider the other half of the 2-DoF control architecture—the design of tracking controllers that drive the system asymptotically toward a planned reference trajectory.

A wide range of methods have been proposed for tracking control in robotic systems, including those based on model predictive control [35, 89, 90] or learning-based approaches [91–93]. However, explicit control policies that can be written in closed form are particularly attractive approach for aerial and space vehicles that must adhere to stringent computational budgets. Such methods typically require orders of magnitude less computational power than their optimization-based counterparts [35]. Moreover, they sometimes achieve performance similar to their learning-based counterparts [94] but typically do not suffer from the brittleness of many learned control policies or necessitate computationally burdensome offline training.

5.1.1 Tracking in Fully-Actuated and Underactuated Systems

While local, linear methods have been applied to tracking control for decades, the design of explicit tracking control laws with global or almost global convergence for general classes of mechanical systems has traditionally been limited to fully-actuated systems [95]. Intuitively, the control design problem is made drastically easier by the availability of all possible control forces. However, tracking laws for particular underactuated systems have also been designed via the hierarchical composition of tracking controllers for subsystems that "look" fully actuated (in a sense), such as in [96], which popularized a now-ubiquitous geometric control design for quadrotor trajectory tracking. This approach first prescribes a desired thrust force applied to the vehicle center of mass (treating it, temporarily, as a fully-actuated point mass) to track the desired position trajectory. Because the vehicle's net thrust direction is body-fixed, this determines two degrees of freedom of the vehicle's desired attitude; the third is determined by a desired yaw angle, and the resulting desired orientation is ultimately tracked via an attitude controller, which prescribes the desired moment generated by the propellers (since the attitude subsystem is a truly a fully-actuated subsystem).

More broadly, the results of Chapter 3 suggest that such a hierarchical control design might be applicable to a wider class of underactuated systems, where the desired shape is determined by the current state and desired acceleration in the group component of a trivialization corresponding to a geometric flat output. Tracking control laws designed for fully-actuated systems on both the shape space and symmetry group could then (in principle) be composed hierarchically to generate a tracking controller for the system as a whole (although, absent arguments of time-scale separation as in [26], the interaction between the subsystems would need to be carefully analyzed). Overall, these observations suggest that tracking controllers for fully-actuated systems (while also interesting and important in their own right) may have a significant role to play in the control of underactuated systems.

5.1.2 Tracking Control via Error Regulation

For some mechanical systems, it is possible to reduce the *"tracking problem"* (*i.e.*, rendering an arbitrary system trajectory attractive) to the easier *"regulation problem"* (*i.e.*, asymptotically stabilizing an equilibrium) for the same system, using a state-valued "tracking error" between the reference and actual states that "vanishes" only when the two are equal (*e.g.*, $(q - q_{\mathrm{d}}, \dot{q} - \dot{q}_{\mathrm{d}})$ for a mechanical system on $\mathbb{R}^n$). Then, feedback is designed to drive the error towards the origin, *i.e.*, a *constant* (equilibrium) trajectory. Such a reduction is substantially easier for fully-actuated (*vs.* underactuated) systems, since arbitrary forces can be exerted, both to compensate for time variation in the reference and to inject suitable artificial potential and dissipation terms to almost globally asymptotically stabilize the error [97].

Clearly, a smooth tracking controller suitable for operation on the entire state space (in general, the tangent bundle of a non-Euclidean manifold) *cannot* rely on a local, coordinate-based tracking error. When the configuration manifold is a Lie group, [95] shows that the group structure furnishes an intrinsic, globally-defined tracking error on the state space, via the action of the group on itself. Thanks to this global notion of error, the authors of [95] remark that:

> *"...the tracking problem on a Lie group is more closely related to tracking on $\mathbb{R}^n$*
> *than it is to the general Riemannian case, for which the group operation is lacking."*

Tracking via error regulation on manifolds that may *not* be Lie groups is proposed in [98]. The authors present a theorem ensuring almost global tracking for fully-actuated systems on compact Riemannian manifolds, assuming the control inputs can be chosen to solve a "rank one" overdetermined linear system at each state and time. Solutions exist in some special cases (*e.g.*, on $\mathbb{S}^2$ with carefully chosen potential, dissipation, and kinetic energy), although they are non-unique. In other cases, *no* solutions exist, and the question of *when* solutions exist in general is left open. Also, the inputs may not depend continuously on state and time, a desirable property that justifies seeking only *almost* global asymptotic stability [99]. Other approaches applicable to general smooth manifolds such as [100] are global in the sense that the trajectory is not restricted to a particular subset of the state space, but only local in the sense that only

those initial conditions sufficiently close to the reference will converge.

5.1.3 Overview and Contributions

In view of these observations, and in pursuit of a systematic approach to tracking control for fully-actuated mechanical systems in yet a broader setting, a question emerges:

> *For fully-actuated mechanical systems, on which class of manifolds*
> *can the tracking problem be reduced to the regulation problem?*

We pose this question in a global or almost global sense; if purely *local* convergence suffices, the answer is trivial (*i.e.*, "all of them"), since smooth manifolds are locally Euclidean. In particular, in this chapter, we consider the design of tracking controllers for mechanical systems evolving on *homogeneous spaces*, a class of manifolds that includes all Lie groups but is in fact more general.

Another more practical motivation for considering mechanical systems evolving on this class of manifolds is as follows. Recent work on trajectory tracking for quadrotors has designed controllers which construct a hierarchical controller out of tracking controllers for *three* (*vs.* two) fully-actuated subsystems [101–103]: a translational subsystem evolving on $\mathbb{R}^3$, a "tilt" subsystem (concerning the thrust direction) evolving on $\mathbb{S}^2$, and a yaw subsystem evolving on $\mathbb{S}^1$. Such an approach has several motivations:

1. the difference in control authority between yaw and tilt (which is roughly an order of magnitude),

2. the invariance of the translational dynamics to rotations around the thrust vector (making yaw tracking of lower priority than tilt tracking), and

3. the singularities inherent in constructing a desired orientation out of a desired tilt and yaw angle.

The third point above amounts to the observation that $SO(3)$ is *not* diffeomorphic to $\mathbb{S}^2 \times \mathbb{S}^1$, a fact closely related to the nontriviality of the fiber bundle described in (4.9) in the previous chapter. Moreover, while $\mathbb{R}^3$ and $\mathbb{S}^1$ clearly admit a Lie group structure, $\mathbb{S}^2$ does *not* (although it is a homogeneous space). Thus, tracking on $\mathbb{S}^2$ serves as a prototypical motivating example, while the general setting is also of interest.

In what follows, we consider fully-actuated mechanical systems evolving on homogeneous manifolds. We obtain globally valid "error dynamics" by extending an intrinsic error used in tracking for *kinematic* systems in [104] to the mechanical setting, exploiting the transitive action of a Lie group on the configuration manifold, even when the configuration manifold lacks a group structure of its own. Using this error, we design a tracking controller for fully-actuated mechanical systems evolving on yet a broader class of spaces, and obtain explicit expressions for the control law in the special cases of Lie groups and spheres of arbitrary dimension. These tracking control laws are applied to example mechanical systems evolving on $\mathbb{R}^3 \times SO(3)$ and $\mathbb{S}^2$. Overall, we contribute a systematic paradigm for synthesizing tracking controllers with guarantees for a broad class of systems, including many space, aerial, and underwater robots.

5.2 Mathematical Preliminaries

We begin by reviewing some mathematical background that will be essential for this chapter. In this chapter, we will also assume all given curves are smooth.

5.2.1 Homogeneous Riemannian Manifolds

In this chapter, we will work within the following class of manifolds.

Definition 5.1 *(see [10, Ch. 3]).* A *homogeneous Riemannian manifold* (Q, Φ, κ) consists of:

1. a smooth manifold Q,

2. a transitive left action $\Phi : G \times Q \to Q$, and

3. a Φ-invariant Riemannian metric κ.

The *stabilizer* of any point $q \in Q$ is the subgroup of G given by $G_q = \{g \in G : \Phi(g, q) = q\}$. $\qquad\bullet$

It bears repeating that because the action is transitive, then for any pair of points $q_1, q_2 \in Q$, there always exists some element $g \in G$ such that $\Phi(g, q_1) = q_2$. Moreover, because the Riemannian metric is Φ-invariant, for any pair of tangent vectors $v_q, w_q \in TQ$, we have $\kappa(v_q, w_q) = \kappa(\mathrm{d}\Phi_g(v_q), \mathrm{d}\Phi_g(\omega_q))$.

Example 5.1 *(A Lie Group with a Left-Invariant Metric).* Any Lie group G equipped with the left action of G on itself (*i.e.,* $\mathrm{L} : (h, g) \mapsto hg$) and any L-invariant metric $\kappa_{\mathbb{I}}$ is a homogeneous Riemannian manifold. In particular, by [9, Thm. 5.38], there exists an inner product $\mathbb{I}$ on $\mathfrak{g} = T_e G$ such that $\forall \, v_g, w_g \in TG$,

$$\kappa_{\mathbb{I}}(v_g, w_g) = \mathbb{I}\left(\mathrm{d}\mathrm{L}_{g^{-1}}(v_g), \mathrm{d}\mathrm{L}_{g^{-1}}(w_g)\right). \tag{5.1}$$

Moreover, L is a free action, *i.e.,* for $g \neq e$, the map L_g has no fixed points. Thus, for any $g \in G$, the stabilizer is just $G_g = \{e\}$. Moreover, it is clear that the musical isomorphisms of $\kappa_{\mathbb{I}}$ satisfy $\kappa_{\mathbb{I}}^\flat(\xi) = \mathbb{I}^\flat(\xi)$ and $\kappa_{\mathbb{I}}^\sharp(\tau) = \mathbb{I}^\sharp(\tau)$ for all $\xi \in \mathfrak{g}$ and $\tau \in \mathfrak{g}^*$ (see, *e.g.,* [9, Sec. 2.3.4]). $\qquad\bullet$

Example 5.2 *(The n-Sphere with the Induced Metric).* For any $n \in \mathbb{N}$, consider the sphere $\mathbb{S}^n$ and the rotation group $\mathrm{SO}(n+1)$. We recall that it is convenient to model these manifolds as embedded submanifolds of high-dimensional Euclidean spaces, *i.e.,* we let $\mathbb{S}^n = \{s \in \mathbb{R}^{n+1} : s^\mathsf{T} s = 1\}$ and

$$\mathrm{SO}(n+1) = \{R \in \mathbb{R}^{n+1 \times n+1} : R^\mathsf{T} R = R\, R^\mathsf{T} = I_{(n+1)\times(n+1)}, \ \det R = 1\}. \tag{5.2}$$

The Euclidean metric on $\mathbb{R}^{n+1}$ is given by $\langle\langle v_q, w_q \rangle\rangle = v_q^\mathsf{T} w_q$ for all $v_q, w_q \in T\mathbb{R}^{n+1}$. Let ρ be the restriction of this metric to $\mathbb{S}^n \subset \mathbb{R}^{n+1}$ (*i.e.,* let $\mathbb{S}^n$ be isometrically embedded in $\mathbb{R}^{n+1}$) and let Ψ be the

restriction of the usual action of $\mathrm{SO}(n{+}1)$ on $\mathbb{R}^{n+1}$ given by

$$\Psi : \mathrm{SO}(n{+}1) \times \mathbb{S}^n \to \mathbb{S}^n, \ (R, q) \mapsto R\,q. \tag{5.3}$$

Then, it is clear that $(\mathbb{S}^n, \Psi, \rho)$ is an $\mathrm{SO}(n{+}1)$-homogeneous Riemannian manifold. Moreover, since the dual of a tangent vector in $\mathbb{R}^{n+1}$ is just its transpose, ρ induces the canonical isomorphisms

$$\rho^\flat : T\mathbb{S}^n \to T^*\mathbb{S}^n, v_q \to v_q{}^\mathrm{T}, \qquad \rho^\sharp : T^*\mathbb{S}^n \to T\mathbb{S}^n, f_q \to f_q{}^\mathrm{T} \tag{5.4}$$

and it can be verified that $G_q \cong \mathrm{SO}(n)$ for all $q \in \mathbb{S}^n$. $\quad\bullet$

5.2.2 Fully-Actuated Mechanical Systems

In particular, we will consider the control of the following class systems on homogeneous spaces.

Definition 5.2. A *mechanical system on a homogeneous Riemannian manifold* is a mechanical system $\Sigma = (Q, \kappa, P, F)$ for which P and κ are invariant with respect to a transitive action $\Phi : G \times Q \to Q$. $\quad\bullet$

Since Φ is transitive, P is constant (hence $\mathrm{d}P = 0$). Thus, from (3.1), the dynamics are given by

$$\nabla_{\dot q} \dot q = \kappa^\sharp(f_q), \tag{5.5}$$

and for fully-actuated systems, the control input $f_q \in T^*Q$ may be chosen arbitrarily. We will consider only fully-actuated systems in the remainder of this chapter.

Remark 5.1 *(Generality).* Even if the system were governed by the Riemannian connection $\widetilde{\nabla}$ of a different metric $\widetilde{\kappa}$ that fails to be Φ-invariant, or it were subject to additional state-dependent forces $F : TQ \to T^*Q$, the system can be rendered in the form (5.5) by the static state feedback

$$f_q(\dot q) = \widetilde{\kappa}^\flat \Big(\big(\widetilde{\nabla} - \nabla\big)(\dot q, \dot q) - F(\dot q) + \tilde{\kappa}^\sharp(f_q') \Big), \tag{5.6}$$

where $\big(\widetilde{\nabla} - \nabla\big)$ is the "difference tensor" (see [10, Prop. 4.13]) between the Riemannian connection of $\tilde{\kappa}$ and of an invariant metric κ, while f_q' is a "virtual" input. Since any homogeneous space with compact stabilizer admits an invariant metric [10, Cor. 3.18], a tracking controller for a Φ-invariant unforced system will, in practice, often yield a tracking controller suitable for the more general system via (5.6). Also, the invariant case is common, and it simplifies the computations considerably.

5.2.3 Almost Global Asymptotic Tracking

In this chapter, our goal will be to design a controller that achieves the following control objective, where $\mathrm{dist}_{\hat\kappa}$ is the Riemannian distance in TQ corresponding to the Sasaki metric (the natural Riemannian metric

on TQ induced by κ, as described in [105]). We remind the reader that the notation $\dot{q} \in TQ$ encompasses *both* the position and velocity of the system simultaneously.

Definition 5.3. A control policy $(t, \dot{q}) \mapsto f_q(t, \dot{q})$ for the system (5.5) achieves *almost global asymptotic tracking* of a reference trajectory $q_{\mathrm{d}} : \mathbb{R} \to Q$ if, for each $t_0 \in \mathbb{R}$, there exists a residual set $S_{t_0} \subseteq TQ$ of full measure such that $\dot{q}(t_0) \in S_{t_0}$ implies that $\mathrm{dist}_{\hat{\kappa}} \left(\dot{q}(t), \dot{q}_{\mathrm{d}}(t) \right) \to 0$ as $t \to \infty$. $\qquad\qquad$ •

Remark 5.2. Like some prior definitions of asymptotic tracking [106], the previous definition contains no Lyapunov-like conditions, only an asymptotic condition. Thus, specializing the definition to a constant reference trajectory yields the notion of *attractiveness* (as opposed to *asymptotic stability*).

Remark 5.3. For each time t_0, some exceptional set of initial conditions $E_{t_0} = TQ \backslash S_{t_0}$ fails to converge to the reference. However, we require this set to be *measure zero* and *meager* (the countable union of nowhere dense sets). The latter notion is clearly topological (and thus independent of any explicit notion of "volume" in the state space), and in fact the former is as well [4, Ch. 6]. On the other hand, the measure-theoretic condition can be most easily interpreted as the requirement that for any smooth probability distribution over TQ and any time t_0, the probability of randomly sampling an initial state that fails to converge to the reference must be *exactly* zero. This is a stronger notion than the notion of "almost global" tracking employed in many other works (*e.g.*, [107, Sec. III] and [96]), which only required that $S_{t_0} \subseteq TQ$ (in the state space) project down to an almost global (*i.e.*, full measure) set in Q (in the configuration manifold).

5.2.4   Navigation Functions

The following functions were described in [97] (in the more general setting of manifolds with boundary). They are particularly useful in generating artificial potential forces for stabilization. We recall that a function $P : Q \to \mathbb{R}$ is a *Morse function* if all its critical points are nondegenerate (*i.e.*, the Hessian is non-singular at every critical point), and refer the reader to [9, Sec. 6.1.4] for details.

Definition 5.4. On a boundaryless manifold Q, a 0_Q-*navigation function* is a proper Morse function $P : Q \to \mathbb{R}$ that has the point $0_Q \in Q$ as its unique local minimizer. A navigation function is said to be *perfect* if its domain admits no other navigation function with fewer critical points. $\qquad$ •

For example, picking any point $0_{\mathbb{S}^n} \in \mathbb{S}^n$ and $k_P > 0$, the map

$$P_{\mathbb{S}^n} : \mathbb{S}^n \to \mathbb{R}, \ q \mapsto -k_P \left(0_{\mathbb{S}^n} \right)^{\mathrm{T}} q \tag{5.7}$$

is a $0_{\mathbb{S}^n}$-navigation function. Following [97], a perfect navigation function on SE(3) with its minimum at the identity can be given by

$$P_{\mathrm{SE}(3)} : \begin{bmatrix} R & x \\ 0_{1 \times 3} & 1 \end{bmatrix} \mapsto \mathrm{tr} \left(K_R(\mathrm{I} - R) \right) + x^{\mathrm{T}} K_x \, x, \tag{5.8}$$

where $x \in \mathbb{R}^3$, $R \in \mathrm{SO}(3)$, and K_x, K_R are 3×3 symmetric positive-definite matrices where K_R has distinct eigenvalues, and I is the 3×3 identity matrix. Navigation functions on $\mathbb{R}^3$, $\mathrm{SE}(2)$, $\mathrm{SO}(3)$, and $\mathrm{SO}(2)$ can be obtained from (5.8), and a navigation function on the product of boundaryless manifolds can be given by the sum of those on each factor [108]. Thus, we can easily obtain an explicit navigation function on any product space whose factors are all n-spheres or closed subgroups of $\mathrm{SE}(3)$, capturing a very broad class of homogeneous spaces of interest in robotics.

5.3   An Intrinsic, State-Valued Tracking Error

In this section, we take an approach similar to that of [104] (which dealt with *kinematic* systems evolving on homogeneous spaces) to describe an intrinsic state-valued tracking error suitable for *mechanical* systems evolving on homogeneous Riemannian manifolds.

5.3.1   Lifts of Curves

Definition 5.5. Consider a homogeneous Riemannian manifold (Q, Φ, κ). Given an *origin* $0_Q \in Q$ and a smooth curve $q_\mathrm{d} : \mathbb{R} \to Q$, a 0_Q-*lift of* q_d is any smooth curve $g_\mathrm{d} : \mathbb{R} \to G$ such that $\Phi\big(g_\mathrm{d}(t), 0_Q\big) = q_\mathrm{d}(t)$ for all $t \in \mathbb{R}$. ●

Lifts are (very) non-unique in general, but later we will discuss the existence and uniqueness of a certain kind of lift. The properties of a such a lift can also be illustrated via the following commutative diagram:

$$
\begin{array}{ccc}
 & & G \\
 & {\scriptstyle g_\mathrm{d}} \nearrow & \downarrow {\scriptstyle \Phi^{0_Q}} \\
\mathbb{R} & \xrightarrow[q_\mathrm{d}]{} & Q
\end{array}
\tag{5.9}
$$

where $\Phi^{0_Q} : g \mapsto \Phi(g, 0_Q)$.

Definition 5.6. For any actual and reference configuration trajectories $q, q_\mathrm{d} : \mathbb{R} \to Q$ and a given 0_Q-lift g_d of q_d, the *configuration error trajectory* is the smooth curve given by[11]

$$
q_\mathrm{e} : \mathbb{R} \to Q, \ t \mapsto \Phi\big(g_\mathrm{d}(t)^{-1}, q(t)\big),
\tag{5.10}
$$

while the *state error trajectory* is its time derivative, $\dot{q}_\mathrm{e} : \mathbb{R} \to TQ$. ●

In [104], the authors use a tracking error of the form (5.10) for kinematic (*i.e.*, first-order) systems to synthesize optimal tracking controllers with local convergence. (In fact, such an error state has its roots in observer design [109].) We lift this definition to the tangent bundle to obtain a state-valued tracking

---

[11]Note that the subscript in q_e indicates "error", and has nothing to do with the identity element $e \in G$.

error for mechanical (*i.e.*, second-order) systems. The following extends [104, Prop 4.1] to second-order systems.

Proposition 5.1. *Consider any actual and reference trajectories $q, q_\mathrm{d} : \mathbb{R} \to Q$. Let $g_\mathrm{d} : \mathbb{R} \to G$ be a 0_Q-lift of q_d, and let $0_{TQ} \in TQ$ be the zero tangent vector at 0_Q. Then, for any time $t \in \mathbb{R}$, it holds that $\dot{q}(t) = \dot{q}_\mathrm{d}(t)$ if and only if $\dot{q}_\mathrm{e}(t) = 0_{TQ}$.*

Proof. Suppressing explicit t-dependence, the actual and reference configuration can be expressed as

$$q = \Phi(g_\mathrm{d}, \Phi(g_\mathrm{d}^{-1}, q)) = \Phi(g_\mathrm{d}, q_\mathrm{e}), \quad q_\mathrm{d} = \Phi(g_\mathrm{d}, 0_Q), \tag{5.11}$$

since by assumption, g_d is a 0_Q-lift of q_d. Thus, we may express the actual and desired state trajectories as

$$\dot{q} = \mathrm{d}\Phi^{q_\mathrm{e}}(\dot{g}_\mathrm{d}) + \mathrm{d}\Phi_{g_\mathrm{d}}(\dot{q}_\mathrm{e}), \tag{5.12a}$$

$$\dot{q}_\mathrm{d} = \mathrm{d}\Phi^{0_Q}(\dot{g}_\mathrm{d}) + \mathrm{d}\Phi_{g_\mathrm{d}}(0_{TQ}). \tag{5.12b}$$

Assuming for sufficiency that $\dot{q}_\mathrm{e} = 0_{TQ}$ (and thus, in particular, $q_\mathrm{e} = 0_Q$), (5.12a)-(5.12b) immediately implies that $\dot{q} = \dot{q}_\mathrm{d}$. Assuming for necessity that $\dot{q} = \dot{q}_\mathrm{d}$ (and therefore, in particular, $q = q_\mathrm{d}$), we recall that for each $g \in G$, the maps Φ_g and $\mathrm{d}\Phi_g$ are automorphisms (*i.e.*, self-diffeomorphisms) of Q and TQ respectively. For this reason, (5.11) implies $q_\mathrm{e} = 0_Q$, while that conclusion and (5.12a)-(5.12b) imply that $\dot{q}_\mathrm{e} = 0_{TQ}$. ∎

In summary, the intrinsic tracking error smoothly transforms the state space (in a manner depending smoothly on time) in such a way that only the current reference state is mapped to the zero tangent vector over the origin of the lift. Also, for the (Φ-invariant) Riemannian distance dist_κ, (5.11) implies that $\mathrm{dist}_\kappa\big(q(t), q_\mathrm{d}(t)\big) = \mathrm{dist}_\kappa\big(q_\mathrm{e}(t), 0_Q\big)$. Thus, (5.10) encodes the distance from the reference "accurately".

5.3.2 Computing Horizontal Lifts

The following notions will aid in computing a lift of a given reference (and ultimately, the tracking error).

Definition 5.7 *(see [5, Sec. 23.4])*. Consider a homogeneous Riemannian manifold (Q, Φ, κ) with a designated origin $0_Q \in Q$. A *reductive decomposition* is a splitting $\mathfrak{g} = \mathfrak{f} \oplus \mathfrak{q}$ such that $\mathfrak{q} \subseteq \mathfrak{g}$ is an Ad_F-invariant subspace, where $F = \exp \mathfrak{f} = G_{0_Q}$ (the stabilizer at 0_Q). •

Note that $\mathfrak{q}$ is a subspace of $\mathfrak{g}$, but not necessarily a subalgebra, (*i.e.*, it need not be closed under $[\cdot, \cdot]$). Moreover, referring to [110, Prop. 1], we have the following convenient fact.

Fact 5.1. *Every homogeneous Riemannian manifold admits a (perhaps non-unique) reductive decomposition.*

Thus, we may use the notion of reductive decompositions to describe the following kind of lifts.

Proposition 5.2 (Horizontal Lifts in Reductive Homogeneous Spaces). *Consider a homogeneous Rieman-nian manifold (Q, Φ, κ) with origin $0_Q \in Q$ and reductive decomposition $\mathfrak{g} = \mathfrak{f} \oplus \mathfrak{q}$. For each smooth curve $q_{\mathrm{d}} : \mathbb{R} \to Q$ and any initial point $g_0 \in G$ such that $\Phi(g_0, 0_Q) = q_{\mathrm{d}}(0)$, there exists a unique smooth curve $g_{\mathrm{d}} : \mathbb{R} \to G$ (called the* horizontal lift of q_{d} through g_0*) with the following properties:*

1. *Lifting: g_{d} is a 0_Q-lift of q_{d},*

2. *Initial Condition: $g_{\mathrm{d}}(0) = g_0$, and*

3. *Horizontality: $\mathrm{dL}_{g_{\mathrm{d}}(t)}^{-1}\big(\dot{g}_{\mathrm{d}}(t)\big) \in \mathfrak{q}$ for all $t \in \mathbb{R}$.*

Proof. By [6, Prop 9.33], G is a (left) principal F-bundle over $Q = G/F$, where $F = \exp \mathfrak{f}$. In particular, the projection map is given by $\pi : G \to Q$, $g \mapsto \Phi(g, 0_Q)$, while the free and proper action is given by

$$\Upsilon : F \times G \to G, (f, g) \mapsto \mathrm{R}_{f^{-1}}(g). \tag{5.13}$$

Moreover, we claim that the distribution on G given by

$$HG = \big\{ \mathrm{dL}_g(\mathfrak{q}) : g \in G \big\} \tag{5.14}$$

is a well-defined principal connection on the principal F-bundle $\pi : G \to Q$. Since this is clearly a smooth distribution and $H_g G$ is complementary to $V_g G$ (the vertical distribution) for all $g \in G$, it suffices to show that HG is Υ-invariant. To do so, we compute

$$\mathrm{d}\Upsilon_f \big(H_{\Upsilon_f^{-1}(g)} G \big) = \mathrm{dR}_f^{-1}\big(\mathrm{dL}_{gf}(\mathfrak{q}) \big) = \mathrm{dL}_g \circ \mathrm{Ad}_f(\mathfrak{q}) = \mathrm{d}L_g(\mathfrak{q}) = H_g G, \tag{5.15}$$

where we have relied upon the Ad_F-invariance of $\mathfrak{q}$. Thus, the claim follows from the existence and uniqueness of horizontal lifts of curves in principal bundles (see [7, Sec. 2.9]). ∎

Remark 5.4 (*Sections, Lifts, and Nontrivial Bundles*). The proof of Proposition 5.2 describes a sense in which a lift projects "down" to the original curve via π. If the principal bundle $\pi : G \to Q$ is trivial (*i.e.,* $G \cong Q \times F$ *globally* and not merely *locally*), then there exist global sections $\sigma : Q \to G$, *i.e.,* smooth maps satisfying $\pi \circ \sigma = \mathrm{id}$. In fact, any such section furnishes a (perhaps non-horizontal) lift $g_{\mathrm{d}} : t \mapsto \sigma \circ q_{\mathrm{d}}(t)$. However, when $\pi : G \to Q$ is a *nontrivial* bundle (*e.g.,* the bundle corresponding to $(\mathbb{S}^2, \Psi, \rho)$, namely $\pi : \mathrm{SO}(3) \to \mathbb{S}^2$), the nonexistence of global sections makes it impossible to generate global lifts using a section. Nor can the initial value g_0 of a horizontal lift depend continuously on $q_{\mathrm{d}}(0)$ alone. Thus, continuous deformation of the reference trajectory can result in discontinuous changes in the tracking error. However, such a discontinuity is with respect to the *choice* of reference trajectory (*i.e.,* the planning layer); once a reference trajectory q_{d} has been selected, the configuration error will depend smoothly on both time and state. Note also that even for a *horizontal* lift g_{d} of some q_{d}, when $q_{\mathrm{d}}(t_1) = q_{\mathrm{d}}(t_2)$ it may

still be that $g_\mathrm{d}(t_1) \neq g_\mathrm{d}(t_2)$ due to nontrivial "holonomy" (see [7, Fig. 3.14.2]).

Remark 5.5 *(Computing Horizontal Lifts Numerically).* Let $(\pi \times \varphi^i) : \pi^{-1}(U_i) \subseteq G \to (U_i \subseteq Q) \times F$, $i \in \{1, \dots, k\}$ be a collection of local trivializations covering $\pi : G \to Q$. Let $\mathbb{A}^i : TU_i \to \mathfrak{f}$ be the local connection forms for HG (see [7, Prop. 2.9.12]). Suppose $q_\mathrm{d}(t) \in U_j$ for $t \in [t_1, t_2]$ and let $f^j : [t_1, t_2] \to F$ solve the initial value problem (IVP)

$$f^j(t_1) = \varphi^j\big(g(t_1)\big), \quad \dot{f}^j(t) = \mathrm{dL}_{f^j(t)} \circ \mathbb{A}^j\big(\dot{q}_\mathrm{d}(t)\big). \tag{5.16}$$

Then the horizontal lift g_d through g_0 of the curve q_d satisfies

$$g_\mathrm{d}(t) = (\pi \times \varphi^j)^{-1}\big(q_\mathrm{d}(t), f^j(t)\big) \text{ for all } t \in [t_1, t_2]. \tag{5.17}$$

Moreover, the restriction of the reference trajectory to any finite interval may be subdivided into finitely many segments, each contained within a single trivialization. We repeatedly solve the IVP (5.16) numerically for each segment, ultimately reconstructing a smooth lift in G via (5.17). Computationally, this is preferable to solving an IVP in G directly, since it ensures that integration error will accumulate only along the fibers (*vs.* horizontally). Hence, numerical integration accuracy is not paramount (reducing the computational burden), since the solution will be an *exact* lift, even if it is not perfectly horizontal. The lifted reference at time t can also be computed "just in time" to compute the tracking error.

With these tools in mind, we can now describe the computation of the tracking error for some examples.

Example 5.1 *(A Lie Group, continued).* Since the stabilizer of any point g on the homogeneous Riemannian manifold $(G, L, \kappa_\mathbb{I})$ is $G_g = \{e\}$, 0_G-lifts (of any kind, horizontal or otherwise) are unique for each $0_G \in G$. Making the usual choice $0_G = e$, the lift is the original curve itself, and the configuration error is

$$g_\mathrm{e} : \mathbb{R} \to G, \ t \mapsto g_\mathrm{d}(t)^{-1} g(t), \tag{5.18}$$

showing that in the special case of Lie groups, the configuration error reduces elegantly to a familiar, intuitive form, called the "right group error function" [9, p. 548]. In the additive group $G = (\mathbb{R}^n, +)$, *i.e.*, a vector space, the configuration error is (unsurprisingly) the map $t \mapsto g(t) - g_\mathrm{d}(t)$. ●

Example 5.2 *(The n-Sphere, continued).* On the homogeneous Riemannian manifold $(\mathbb{S}^n, \Psi, \rho)$, we choose the origin $0_{\mathbb{S}^n} = \mathrm{e}_n := (0, \dots, 1)$ and identify $\mathfrak{so}(n)$ with the $n \times n$ skew-symmetric matrices. Following [5, Sec. 23.5], we have the reductive decomposition $\mathfrak{so}(n+1) = \mathfrak{f} \oplus \mathfrak{q}$, where

$$\mathfrak{f} = \left\{ \begin{bmatrix} \xi & 0 \\ 0 & 0 \end{bmatrix} : \xi \in \mathfrak{so}(n) \right\}, \quad \mathfrak{q} = \left\{ \begin{bmatrix} 0 & v \\ -v^\mathrm{T} & 0 \end{bmatrix} : v \in \mathbb{R}^n \right\}. \tag{5.19}$$

We horizontally lift a given configuration reference trajectory $q_\mathrm{d} : \mathbb{R} \to \mathbb{S}^n$ in the sense of Proposition

5.2 to obtain the lifted reference $R_{\mathrm{d}} : \mathbb{R} \to \mathrm{SO}(n+1)$. Then, the configuration error in the form (5.10) is simply

$$q_{\mathrm{e}} : \mathbb{R} \to \mathbb{S}^n, \ t \mapsto R_{\mathrm{d}}(t)^{\mathrm{T}} q(t), \tag{5.20}$$

where the lifted reference R_{d} is computed numerically in the manner of Remark 5.5 for accuracy. ●

5.4 Almost Global Asymptotic Tracking

This section presents the main result of this chapter, namely, a controller guaranteeing almost global asymptotic tracking for fully-actuated mechanical systems on arbitrary homogeneous Riemannian manifolds. First, we prove a helpful lemma that will be used in the proof of the main result.

5.4.1 Families of Curves

Following [10, Ch. 6], we introduce the following notion, which will help us account for the contributions of both the reference and actual trajectories in the time variation of certain quantities.

Definition 5.8. A *family of curves* on a manifold Q is a smooth map $F : \mathbb{R}^2 \to Q$. Moreover, a family of curves F has a *diagonal curve* given by $f : t \mapsto F(t,t)$, as well as *transverse* and *main* curves at each s and r, given respectively by $F^s : r \mapsto F(r,s)$ and $F_r : s \mapsto F(r,s)$. In addition, let $\mathfrak{X}(F)$ denote the set of *vector fields over F*, defined as smooth maps $(r,s) \mapsto V(r,s)$ such that $V(r,s) \in T_{F(r,s)}Q$ for all $r, s \in \mathbb{R}$. Finally, the *transverse* and *main velocity* of F are defined respectively as

$$\partial_r F : (r,s) \mapsto \dot{F}^s(r), \quad \partial_s F : (r,s) \mapsto \dot{F}_r(s), \tag{5.21}$$

which are easily verified to be elements of $\mathfrak{X}(F)$. ●

For any $V \in \mathfrak{X}(F)$, we may also compute its partial covariant derivative along the transverse or main direction, operations denoted respectively by $\mathrm{D}_r, \mathrm{D}_s : \mathfrak{X}(F) \to \mathfrak{X}(F)$. This operation is defined by restricting the vector field over the family of curves to a vector field along each transverse (resp. main) curve and computing the usual covariant derivative along that curve, then combining the results. That is,

$$\big(\mathrm{D}_r V\big)(r,s) = \big(\nabla_{\dot{F}^s} V^s\big)(r,s), \quad \big(\mathrm{D}_s V\big)(r,s) = \big(\nabla_{\dot{F}_r} V_r\big)(r,s), \tag{5.22}$$

where $V^s : r \mapsto V(r,s)$ and $V_r : s \mapsto V(r,s)$.

We now prove the helpful lemma.

Lemma 5.1. *For a Riemmanian manifold (Q, κ) and a family of curves $F : \mathbb{R}^2 \to Q$, the "diagonal" curve*

given by $\gamma : t \mapsto F(t, t)$ *satisfies the identity*

$$(\nabla_{\dot\gamma}\dot\gamma)(t) = \big(\mathrm{D}_r\,\partial_r F + 2\,\mathrm{D}_r\,\partial_s F + \mathrm{D}_s\,\partial_s F\big)(t, t). \tag{5.23}$$

Proof. Since this is a purely local question, we are free to work in local coordinates (q^i) around any point $\gamma(t) = F(r, s) \in Q$. Expressing the coordinate form of F as $F(r, s) = \big(q^1(r, s), \dots, q^n(r, s)\big)$, the coordinate form of γ is given by $\gamma(t) = \big(q^1(t, t), \dots, q^n(t, t)\big)$, so that $\dot\gamma(t) = \big(\frac{\partial q^k}{\partial r} + \frac{\partial q^k}{\partial s}\big)\partial_k$, where the previous partial derivatives (and all subsequent ones) are evaluated at $(r, s) = (t, t)$. Then, by the coordinate formula for covariant derivatives along curves,

$$(\nabla_{\dot\gamma}\dot\gamma)(t) = \Big(\tfrac{\partial^2 q^k}{\partial r^2} + \tfrac{\partial^2 q^k}{\partial r \partial s} + \tfrac{\partial^2 q^k}{\partial s \partial r} + \tfrac{\partial^2 q^k}{\partial s^2} + \big(\tfrac{\partial q^i}{\partial r} + \tfrac{\partial q^i}{\partial s}\big)\big(\tfrac{\partial q^j}{\partial r} + \tfrac{\partial q^j}{\partial s}\big)\Gamma^k_{ij}\Big)\partial_k, \tag{5.24}$$

where Γ^k_{ij} are the "Christoffel symbols" for ∇. Meanwhile, $\partial_r F = \frac{\partial q^k}{\partial r}\partial_k$ and $\partial_s F = \frac{\partial q^k}{\partial s}\partial_k$, and using the same coordinate formula, we obtain

$$(\mathrm{D}_r\,\partial_r F)(t, t) = \Big(\tfrac{\partial^2 q^k}{\partial r^2} + \tfrac{\partial q^i}{\partial r}\tfrac{\partial q^j}{\partial r}\Gamma^k_{ij}\Big)\partial_k, \tag{5.25a}$$

$$(\mathrm{D}_r\,\partial_s F)(t, t) = \Big(\tfrac{\partial^2 q^k}{\partial s \partial r} + \tfrac{\partial q^i}{\partial s}\tfrac{\partial q^j}{\partial r}\Gamma^k_{ij}\Big)\partial_k, \tag{5.25b}$$

$$(\mathrm{D}_s\,\partial_s F)(t, t) = \Big(\tfrac{\partial^2 q^k}{\partial s^2} + \tfrac{\partial q^i}{\partial s}\tfrac{\partial q^j}{\partial s}\Gamma^k_{ij}\Big)\partial_k. \tag{5.25c}$$

To complete the argument, it suffices to substitute (5.25a)-(5.25c) into (5.23) and use the equality of mixed partials and the symmetry of the Christoffel symbols to obtain (5.24). ∎

5.4.2 Main Result

We now present the main result on trajectory tracking. First, we recall that the *body velocity* of any curve $g : \mathbb{R} \to G$ is the curve in $\mathfrak{g}$ given by $t \mapsto \mathrm{d}\mathrm{L}^{-1}_{g(t)}\big(\dot g(t)\big)$.

Theorem 5.1 (Almost Global Asymptotic Tracking on Homogeneous Riemannian Manifolds). *Consider a fully-actuated mechanical system on (Q, Φ, κ), a reference trajectory $q_{\mathrm{d}} : \mathbb{R} \to Q$, and any smooth 0_Q-lift $g_{\mathrm{d}} : \mathbb{R} \to G$ of q_{d} with bounded body velocity. Let P be a 0_Q-navigation function and ν be a Riemannian metric on Q. For each ("fixed") state $\dot q \in TQ$, define a curve in Q and a vector field along it given by*

$$\gamma^q : r \mapsto \Phi^{-1}_{g_{\mathrm{d}}(r)}(q), \quad X^{\dot q} : r \mapsto \mathrm{d}\Phi^{-1}_{g_{\mathrm{d}}(r)}(\dot q). \tag{5.26}$$

Then, the smooth time-and-state feedback control policy

$$f_q(t, \dot q) = -\,\mathrm{d}\Phi^*_{g_{\mathrm{d}}^{-1}}\Big(\mathrm{d}P(q_{\mathrm{e}}) + \nu^\flat(\dot q_{\mathrm{e}}) + \kappa^\flat \circ \big(\nabla_{\dot\gamma^q}\big(\dot\gamma^q + 2\,X^{\dot q}\big)\big)(t)\Big) \tag{5.27}$$

achieves almost global asymptotic tracking of the reference and local exponential convergence of the error.

Remark 5.6. We use the "dummy variable" r when defining e^q and $X^{\dot{q}}$ to emphasize that $\dot{q}$ (and, in particular, q) is held fixed as r varies (despite the dependence of $\dot{q}$ on t). This allows us to rigorously and intrinsically express (5.27) using only the standard formalism for covariant differentiation along curves. It follows from [10, Prop. 4.26] that (5.27) depends only on $t \in \mathbb{R}$ and $\dot{q} \in TQ$. Additionally, although the control policy (5.27) requires *choosing* (and computing) a certain lift g_{d}, we show that the qualitative closed-loop stability properties are ultimately independent of this choice. Later, we will also explore a case in which it is not necessary to actually compute the lift, as the control action can be computed directly from the state and derivatives of the reference (without any integration).

Proof of Theorem 5.1. Observe that the configuration error (5.10) is the diagonal curve of the family of curves

$$E : \mathbb{R}^2 \to Q, \ (r, s) \mapsto \Phi\big(g_{\mathrm{d}}(r)^{-1}, q(s)\big), \tag{5.28}$$

in the sense that $q_{\mathrm{e}}(t) = E(t, t)$. We will use this observation to express the covariant derivative $\nabla_{\dot{q}_{\mathrm{e}}} \dot{q}_{\mathrm{e}}$ in terms of the respective contributions of the reference and actual trajectories. From Lemma 5.1, we have

$$\big(\nabla_{\dot{q}_{\mathrm{e}}} \dot{q}_{\mathrm{e}}\big)(t) = \big(\mathrm{D}_r\, \partial_r E + 2\,\mathrm{D}_r\, \partial_s E + \mathrm{D}_s\, \partial_s E\big)(t, t), \tag{5.29}$$

where we have evaluated the right-hand side at $(r, s) = (t, t)$. We now aim to compute the terms on the right-hand side of (5.29). Observing that $E^s(r) = \gamma^{q(s)}(r)$ and also that

$$\partial_s E(r, s) = \mathrm{d}\Phi_{g_{\mathrm{d}}(r)^{-1}}\big(\dot{q}(s)\big) = X^{\dot{q}(s)}(r), \tag{5.30}$$

we may verify that

$$\big(\mathrm{D}_r\, \partial_r E\big)(t, t) = \big(\nabla_{\dot{E}^t} \dot{E}^t\big)(t) = \big(\nabla_{\dot{\gamma}^q} \dot{\gamma}^q\big)(t), \quad \big(\mathrm{D}_r\, \partial_s E\big)(t, t) = \big(\nabla_{\dot{\gamma}^q} X^{\dot{q}}\big)(t). \tag{5.31}$$

Recall (see [9, Thm. 5.70]) that the Φ-invariance of κ implies that for any $\gamma \in \mathsf{A}(q)$ and $Z \in \mathfrak{X}(\gamma)$,

$$\nabla_{(\Phi_g \circ \gamma)'}(\mathrm{d}\Phi_g \circ Z) = \mathrm{d}\Phi_g \circ \big(\nabla_{\dot{\gamma}} Z\big). \tag{5.32}$$

From this fact, (5.5), and (5.30), it follows that

$$(\mathrm{D}_s\, \partial_s E)(t, t) = \big(\nabla_{\dot{E}_t} \dot{E}_t\big)(t) = \mathrm{d}\Phi_{g_{\mathrm{d}}(t)}^{-1} \circ \kappa^{\sharp}\big(f_q(t)\big), \tag{5.33}$$

where $t \mapsto f_q(t)$ is the input force signal corresponding to $t \mapsto q(t)$. Substituting these results into (5.29),

$$\big(\nabla_{\dot{q}_{\mathrm{e}}} \dot{q}_{\mathrm{e}}\big)(t) = \nabla_{\dot{\gamma}^q}(\dot{\gamma}^q + 2\,X^{\dot{q}})(t) + \mathrm{d}\Phi_{g_{\mathrm{d}}(t)}^{-1} \circ \kappa^{\sharp}\big(f_q(t)\big), \tag{5.34}$$

yielding the desired covariant derivative.

99

We now apply the control policy given in (5.27). From Lemma 2.2, it follows that $(\mathrm{d}\Phi_g \circ \kappa^\sharp)^{-1} = \mathrm{d}\Phi_g^* \circ \kappa^\flat$ for any $g \in G$. Using this fact and substituting (5.27) into (5.34), we obtain the autonomous error dynamics

$$\nabla_{\dot{q}_\mathrm{e}} \dot{q}_\mathrm{e} = -\kappa^\sharp\big(\mathrm{d}P(q_\mathrm{e}) + \nu^\flat(\dot{q}_\mathrm{e})\big), \tag{5.35}$$

which is a mechanical system with strict dissipation and a navigation function potential. Thus, it follows from [97, Thm. 2] that there exists an open dense set $S \subseteq TQ$ of full measure, such that for any $t_0 \in \mathbb{R}$ (since (5.35) is autonomous), if $\dot{q}_\mathrm{e}(t_0) \in S$, then $\dot{q}_\mathrm{e}(t) \to 0_{TQ}$ as $t \to \infty$, and the local exponential stability of 0_{TQ} for (5.35) follows from [9, Thm. 6.45].

To complete the argument, it remains to formally show that

$$\lim_{t\to\infty} \dot{q}_\mathrm{e}(t) = 0_{TQ} \implies \lim_{t\to\infty} \mathrm{dist}_{\hat{\kappa}}\big(\dot{q}(t), \dot{q}_\mathrm{d}(t)\big) = 0. \tag{5.36}$$

Towards this end, we note that $\dot{q}_\mathrm{e}(t) \to 0_{TQ}$ implies in particular that $q_\mathrm{e}(t) \to 0_Q$, and thus we have $\mathrm{dist}_\kappa\big(q_\mathrm{e}(t), 0_Q\big) \to 0$. Since dist_κ is Φ-invariant, in view of (5.11) this implies that $\mathrm{dist}_\kappa\big(q(t), q_\mathrm{d}(t)\big) \to 0$. For sufficiently large t, it then follows from the analysis in [111, II.A.2] that we have

$$\mathrm{dist}_{\hat{\kappa}}\big(\dot{q}(t), \dot{q}_\mathrm{d}(t)\big) \leq \mathrm{dist}_\kappa\big(q(t), q_\mathrm{d}(t)\big) + \big|\big|\tau_{\gamma_t}\big(\dot{q}(t)\big) - \dot{q}_\mathrm{d}(t)\big|\big|_\kappa, \tag{5.37}$$

where $\gamma_t : [0,1] \to Q$ is the shortest geodesic from $q(t)$ to $q_\mathrm{d}(t)$ and $\tau_{\gamma_t} : T_{\gamma_t(0)}Q \to T_{\gamma_t(1)}Q$ is parallel transport along γ_t. Then, (5.37), (5.12a)-(5.12b), and the triangle inequality imply that

$$\begin{aligned}\lim_{t\to\infty} \mathrm{dist}_{\hat{\kappa}}\big(\dot{q}(t), \dot{q}_\mathrm{d}(t)\big) \leq \\ \lim_{t\to\infty} \mathrm{dist}\,\kappa\big(q_\mathrm{e}(t), 0_Q\big) + \lim_{t\to\infty} \big|\big|\tau_{\gamma_t} \circ \mathrm{d}\Phi_{g_\mathrm{d}}\big(\dot{q}_\mathrm{e}(t)\big)\big|\big|_\kappa + \lim_{t\to\infty} \big|\big|(\tau_{\gamma_t} \circ \mathrm{d}\Phi^{q_\mathrm{e}(t)} - \mathrm{d}\Phi^{0_Q})\big(\dot{g}_\mathrm{d}(t)\big)\big|\big|_\kappa.\end{aligned} \tag{5.38}$$

The first limit on the right-hand side has already been shown to be zero. Since parallel transport preserves Riemannian norms and κ is Φ-invariant, the second is zero as well.

Finally, we consider the third limit on the right-hand side of (5.38). From the basic properties of group actions (in particular, $\Phi_g \circ \Phi_h = \Phi_{gh}$), it can be verified that $\mathrm{d}\Phi^q : TG \to TQ$ is an equivariant map for each $q \in Q$ (i.e., $\mathrm{d}\Phi_g \circ \mathrm{d}\Phi^q = \mathrm{d}\Phi^q \circ \mathrm{d}L_g$). Moreover, since κ is Φ-invariant, the parallel transport map satisfies $\mathrm{d}\Phi_g \circ \tau_\gamma = \tau_{(\Phi_g \circ \gamma)} \circ \mathrm{d}\Phi_g$. Together, these facts enable us to reexpress the third limit, obtaining

$$\lim_{t\to\infty} \mathrm{dist}_{\hat{\kappa}}\big(\dot{q}(t), \dot{q}_\mathrm{d}(t)\big) \leq \lim_{t\to\infty} \big|\big|(\tau_{\alpha_t} \circ \mathrm{d}\Phi^{q_\mathrm{e}(t)} - \mathrm{d}\Phi^{0_Q})\big(\xi_\mathrm{d}(t)\big)\big|\big|_\kappa, \tag{5.39}$$

where ξ_d is the body velocity of g_d and $\alpha_t := \Phi_{g_\mathrm{d}(t)^{-1}} \circ \gamma_t$ can be recognized as the shortest geodesic from $q_\mathrm{e}(t)$ to 0_Q. Defining the linear map

$$A_t : \mathfrak{g} \to T_{0_Q}Q, \quad \xi \mapsto \big(\tau_{\alpha_t} \circ \mathrm{d}\Phi^{q_\mathrm{e}(t)} - \mathrm{d}\Phi^{0_Q}\big)(\xi) \tag{5.40}$$

100

and letting $||\cdot||_{\mathfrak{g}}$ be *any* norm on $\mathfrak{g}$, it is now clear that

$$\lim_{t \to \infty} \text{dist}_{\hat{\kappa}}\left(\dot{q}(t), \dot{q}_{\mathrm{d}}(t)\right) \leq \lim_{t \to \infty} \left|\left|A_t\right|\right|_{\mathrm{op}} \left|\left|\xi_{\mathrm{d}}(t)\right|\right|_{\mathfrak{g}}, \tag{5.41}$$

where $||\cdot||_{\mathrm{op}}$ is the operator norm induced on linear maps from $\mathfrak{g}$ to $T_{0_Q}Q$ by $||\cdot||_{\mathfrak{g}}$ and κ. Since ξ_{d} is bounded for all time, uniform equivalence of norms implies the existence of a constant $C > 0$ such that

$$\lim_{t \to \infty} \text{dist}_{\hat{\kappa}}\left(\dot{q}(t), \dot{q}_{\mathrm{d}}(t)\right) \leq C \lim_{t \to \infty} \left|\left|A_t\right|\right|_{\mathrm{op}}. \tag{5.42}$$

It then suffices to observe that $\tau_{\alpha_t} \to \text{id}$ as $q_{\mathrm{e}}(t) \to 0_Q$, and thus $\left|\left|A_t\right|\right|_{\mathrm{op}} \to 0$ as $t \to \infty$. Thus, we have shown that $\text{dist}_{\hat{\kappa}}\left(\dot{q}(t), \dot{q}_{\mathrm{d}}(t)\right) \to 0$ as $t \to \infty$, completing the argument. ∎

5.5 Explicit Control Policies for Particular Cases

In this section, we specialize the controller proposed in Theorem 5.1 to two familiar classes of homogeneous Riemannian manifolds, obtaining concise and explicit expressions for the control policy (5.27) in each case.

5.5.1 Tracking Control on Lie Groups

We first consider the special case most studied in prior work, namely that of the Lie group. Our primary goal in examining the Lie group setting in detail is to underscore that although our approach is strictly more general than prior work such as [95], we nonetheless recover a comparable result in this restricted setting—in the case of a Lie group, the only e-lift of the reference trajectory is the reference trajectory itself, so the approximation procedures of Sec. 5.3 are not needed. The tracking control policy we will now recover uses the same configuration error as in [9, Thm. 11.29], although our different feedforward terms lead to guaranteed almost global asymptotic tracking. In that sense, our result is qualitatively more similar to [95, Thm. 1], but they use a different configuration error (*i.e.*, $g_{\mathrm{e}} = g_{\mathrm{d}}\, g^{-1}$).

In what follows, we denote the body velocities of trajectories g, g_{d}, and g_{e} (*i.e.*, the actual, reference, and error configurations) by ξ, ξ_{d}, and ξ_{e} respectively. Also, for any smooth function $P : G \to \mathbb{R}$ on a Lie group G, we define the map

$$\zeta_P : G \to \mathfrak{g}^*, \ g \mapsto \mathrm{dL}_g^* \circ \mathrm{d}P(g). \tag{5.43}$$

Corollary 5.1 (Almost Global Asymptotic Tracking on a Lie Group). *For any Lie group G, consider a fully-actuated mechanical system on $(G, L, \kappa_{\mathbb{I}})$ and a smooth reference trajectory $g_{\mathrm{d}} : \mathbb{R} \to G$ with bounded body velocity. Let P be a e-navigation function on G and let $\mathbb{D}$ be an inner product on $\mathfrak{g}$. Then, for the virtual control $\tau = \mathrm{dL}_g^*(f_g)$, the control policy*

$$\tau\left((g, \xi), (g_{\mathrm{d}}, \xi_{\mathrm{d}}, \dot{\xi}_d)\right) = -\zeta_P(g_{\mathrm{e}}) - \mathbb{D}^\flat(\xi_{\mathrm{e}}) + \mathbb{I}^\flat\left(\mathrm{Ad}_{g_{\mathrm{e}}}^{-1}(\dot{\xi}_d) + [\xi, \xi_{\mathrm{e}}]\right) + \mathrm{ad}_{\xi_{\mathrm{e}}}^* \mathbb{I}^\flat(\xi_{\mathrm{e}}) - \mathrm{ad}_\xi^* \mathbb{I}^\flat(\xi) \tag{5.44}$$

achieves almost global asymptotic tracking of the reference and local exponential convergence of the error.

Proof. It will suffice to apply Theorem 5.1 with the configuration error (5.18), the given navigation function, and the metric $\nu = \nu_{\mathbb{D}}$, namely the left-invariant Riemannian metric on G induced by $\mathbb{D}$ as in (5.1). In particular, Since $\gamma^g(r) = \mathrm{L}_{g_{\mathrm{d}}(r)}^{-1}(g) = g_{\mathrm{d}}(r)^{-1}g = R_g\big(g_{\mathrm{d}}(r)^{-1}\big)$ and

$$\tfrac{\mathrm{d}}{\mathrm{d}r}\big(g_{\mathrm{d}}(r)^{-1}\big) = -\,\mathrm{d}\mathrm{L}_{g_{\mathrm{d}}(r)^{-1}} \circ \mathrm{d}R_{g_{\mathrm{d}}(r)^{-1}} \circ \dot{g}_{\mathrm{d}}(r), \tag{5.45}$$

we may use (5.45) to compute

$$\dot{\gamma}^g(r) = \mathrm{d}R_g\Big(-\,\mathrm{d}\mathrm{L}_{g_{\mathrm{d}}(r)^{-1}} \circ \mathrm{d}R_{g_{\mathrm{d}}(r)^{-1}} \circ \dot{g}_{\mathrm{d}}(r)\Big) = \mathrm{d}\mathrm{L}_{\gamma^g(r)}\big(-\,\mathrm{Ad}_{\gamma^g(r)}^{-1} \circ \xi_{\mathrm{d}}(r)\big). \tag{5.46}$$

It is also clear that

$$X^{\dot{g}}(r) = \mathrm{d}\mathrm{L}_{g_{\mathrm{d}}(r)}^{-1}(\dot{g}) = \mathrm{d}\mathrm{L}_{g_{\mathrm{d}}(r)^{-1}} \circ \mathrm{d}\mathrm{L}_g(\xi) = \mathrm{d}\mathrm{L}_{\gamma^g(r)}(\xi), \tag{5.47}$$

so that altogether, we have

$$(\dot{\gamma}^g + 2X^{\dot{g}})(r) = \mathrm{d}\mathrm{L}_{\gamma^g(r)}\big(2\,\xi - \mathrm{Ad}_{\gamma^g(r)}^{-1} \circ \xi_{\mathrm{d}}(r)\big). \tag{5.48}$$

The result [9, Thm. 5.40] implies that that for any smooth curve γ in G, any vector field $X \in \mathfrak{X}(\gamma)$, and curves υ, η in $\mathfrak{g}$ such that $\dot{\gamma}(r) = \mathrm{d}\mathrm{L}_{\gamma(r)}\big(\upsilon(r)\big)$ and $X(r) = \mathrm{d}\mathrm{L}_{\gamma(r)}\big(\eta(r)\big)$, we have

$$\big(\nabla_{\dot{\gamma}}X\big)(r) = \mathrm{d}\mathrm{L}_{\gamma(r)}\big(\dot{\eta}(r) + \nabla_{\mathbb{I}}(\upsilon(r), \eta(r))\big), \tag{5.49}$$

where $\nabla_{\mathbb{I}} : \mathfrak{g} \times \mathfrak{g} \to \mathfrak{g}$ is the bilinear map given by

$$(\upsilon, \eta) \mapsto \tfrac{1}{2}[\upsilon, \eta] - \tfrac{1}{2}\mathbb{I}^{\sharp}\big(\mathrm{ad}_{\upsilon}^* \, \mathbb{I}^{\flat}\, \eta + \mathrm{ad}_{\eta}^* \, \mathbb{I}^{\flat}\, \upsilon\big). \tag{5.50}$$

In preparation for applying the rule (5.49), with $\nu(r)$ given by the argument on the right-handside of (5.46) and $\eta(r)$ given by the argument on the right-hand side of (5.48), we verify by direct computation that

$$\tfrac{\mathrm{d}}{\mathrm{d}r}\big(2\,\xi - \mathrm{Ad}_{\gamma^g(r)}^{-1} \circ \xi_{\mathrm{d}}(r)\big) = -\mathrm{Ad}_{\gamma^g(r)}^{-1} \circ \dot{\xi_d}(r) \tag{5.51}$$

After verifying $\xi_{\mathrm{e}} = \xi - \mathrm{Ad}_{g_{\mathrm{e}}}^{-1}(\xi_{\mathrm{d}})$, we substitute the above calculations into (5.49) and simplify:

$$\nabla_{\dot{\gamma}^g}(\dot{\gamma}^g + 2X^{\dot{g}})(t) = \mathrm{d}\mathrm{L}_{g_{\mathrm{e}}}\Big(-\mathrm{Ad}_{g_{\mathrm{e}}}^{-1}(\dot{\xi}_d) + \nabla_{\mathbb{I}}\big(-\mathrm{Ad}_{g_{\mathrm{e}}}^{-1}(\xi_d), 2\xi - \mathrm{Ad}_{g_{\mathrm{e}}}^{-1}(\xi_d)\big)\Big) \tag{5.52}$$

$$= \mathrm{d}\mathrm{L}_{g_{\mathrm{e}}}\Big(-\mathrm{Ad}_{g_{\mathrm{e}}}^{-1}(\dot{\xi}_d) + \nabla_{\mathbb{I}}\big(-\xi + \underbrace{\xi - \mathrm{Ad}_{g_{\mathrm{e}}}^{-1}(\xi_d)}_{=\,\xi_{\mathrm{e}}}, \xi + \underbrace{\xi - \mathrm{Ad}_{g_{\mathrm{e}}}^{-1}(\xi_d)}_{=\,\xi_{\mathrm{e}}}\big)\Big) \tag{5.53}$$

$$= \mathrm{d}\mathrm{L}_{g_{\mathrm{e}}}\Big(-\mathrm{Ad}_{g_{\mathrm{e}}}^{-1}(\dot{\xi}_d) + \nabla_{\mathbb{I}}\big(\xi_{\mathrm{e}} - \xi, \xi_{\mathrm{e}} + \xi\big)\Big). \tag{5.54}$$
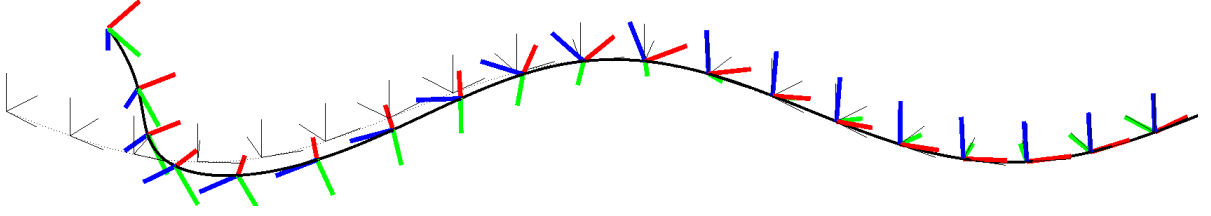
Figure 5.1: Almost global asymptotic tracking for a mechanical system on $\mathbb{R}^3 \times \mathrm{SO}(3)$ (*e.g.*, the Omnidirectional Aerial Robot), using the controller proposed in Corollary 5.1 (a special case of Theorem 5.1).

Since $\nabla_{\mathbb{I}}$ is bilinear, and its first term is antisymmetric while its second is symmetric, we have

$$\nabla_{\mathbb{I}}\big(\xi_{\mathrm{e}} - \xi, \xi_{\mathrm{e}} + \xi\big) = \nabla_{\mathbb{I}}(\xi_{\mathrm{e}}, \xi_{\mathrm{e}}) - \nabla_{\mathbb{I}}(\xi, \xi) + \nabla_{\mathbb{I}}(\xi_{\mathrm{e}}, \xi) - \nabla_{\mathbb{I}}(\xi, \xi_{\mathrm{e}}) \tag{5.55}$$

$$= -\mathbb{I}^{\sharp}\big(\mathrm{ad}^*_{\xi_{\mathrm{e}}} \mathbb{I}^{\flat} \xi_{\mathrm{e}}\big) + \mathbb{I}^{\sharp}\big(\mathrm{ad}^*_{\xi} \mathbb{I}^{\flat} \xi\big) + \tfrac{1}{2}[\xi_{\mathrm{e}}, \xi] - \tfrac{1}{2}[\xi, \xi_{\mathrm{e}}] \tag{5.56}$$

$$= [\xi_{\mathrm{e}}, \xi] + \mathbb{I}^{\sharp}\big(\mathrm{ad}^*_{\xi} \mathbb{I}^{\flat} \xi - \mathrm{ad}^*_{\xi_{\mathrm{e}}} \mathbb{I}^{\flat} \xi_{\mathrm{e}}\big). \tag{5.57}$$

Substituting this result into (5.54), we obtain the covariant derivative term in (5.27):

$$\nabla_{\dot{\gamma}^g}(\dot{\gamma}^g + 2X^{\dot{g}})(t) = \mathrm{dL}_{g_{\mathrm{e}}}\Big(-\mathrm{Ad}^{-1}_{g_{\mathrm{e}}}(\dot{\xi}_d) + [\xi_{\mathrm{e}}, \xi] + \mathbb{I}^{\sharp}\big(\mathrm{ad}^*_{\xi} \mathbb{I}^{\flat} \xi - \mathrm{ad}^*_{\xi_{\mathrm{e}}} \mathbb{I}^{\flat} \xi_{\mathrm{e}}\big)\Big). \tag{5.58}$$

Finally, using this result to compute $\tau = \mathrm{dL}^*_g(f_g)$ with f_g as defined in (5.27) yields

$$\tau = -\mathrm{d}L^*_{g_{\mathrm{e}}}\Big(\mathrm{d}P(g_{\mathrm{e}}) + \nu^{\flat}_{\mathbb{D}}(\dot{g}_{\mathrm{e}}) + \kappa^{\flat}_{\mathbb{I}} \circ \mathrm{dL}_{g_{\mathrm{e}}}\big(-\mathrm{Ad}^{-1}_{g_{\mathrm{e}}}(\dot{\xi}_d) + [\xi_{\mathrm{e}}, \xi] + \mathbb{I}^{\sharp}(\mathrm{ad}^*_{\xi} \mathbb{I}^{\flat} \xi - \mathrm{ad}^*_{\xi_{\mathrm{e}}} \mathbb{I}^{\flat} \xi_{\mathrm{e}})\big)\Big) \tag{5.59}$$

$$= -\underbrace{\mathrm{d}L^*_{g_{\mathrm{e}}} \circ \mathrm{d}P}_{=\zeta_P}(g_{\mathrm{e}}) - \underbrace{\mathrm{d}L^*_{g_{\mathrm{e}}} \circ \nu^{\flat}_{\mathbb{D}} \circ \mathrm{dL}_{g_{\mathrm{e}}}}_{=\nu^{\flat}_{\mathbb{D}}}(\xi_{\mathrm{e}})$$

$$\qquad - \underbrace{\mathrm{d}L^*_{g_{\mathrm{e}}} \circ \kappa^{\flat}_{\mathbb{I}} \circ \mathrm{dL}_{g_{\mathrm{e}}}}_{=\kappa^{\flat}_{\mathbb{I}}}\big(-\mathrm{Ad}^{-1}_{g_{\mathrm{e}}}(\dot{\xi}_d) + [\xi_{\mathrm{e}}, \xi] + \mathbb{I}^{\sharp}(\mathrm{ad}^*_{\xi} \mathbb{I}^{\flat} \xi - \mathrm{ad}^*_{\xi_{\mathrm{e}}} \mathbb{I}^{\flat} \xi_{\mathrm{e}})\big) \tag{5.60}$$

where the annotations are direct consequences of (5.43) and the application of Lemma 2.2, and we note that $\mathrm{dL}^*_g \circ \mathrm{dL}^*_{g_{\mathrm{d}}{}^{-1}} = \mathrm{dL}^*_{g_{\mathrm{e}}}$. Finally, noting that by construction, $\kappa^{\flat}_{\mathbb{I}}\big|_{T_eG} = \mathbb{I}^{\flat} : \mathfrak{g} \to \mathfrak{g}^*$ (and likewise for $\nu_{\mathbb{D}}$), we may simplify (5.60) to obtain exactly (5.44). Thus, the claim follows immediately by Theorem 5.1. ∎

Example 5.3 (*The Omnidirectional Aerial Robot [112]*). Consider an aerial robot consisting of a single rigid body and actuators capable of applying arbitrary wrenches. Compensating for the gravity forces in the manner described in Remark 5.1 yields a fully-actuated mechanical system on $(\mathbb{R}^3 \times \mathrm{SO}(3), L, \kappa_{\mathbb{I}})$, where $\mathbb{I} = \mathrm{diag}(m\mathbb{I}_{3\times3}, \mathbb{J}_{3\times3})$. We use Corollary 5.1 with (5.8) to design a controller for tracking pose trajectories. A rollout of the resulting control policy is shown in Fig. 5.1. ●

5.5.2 Tracking Control on Spheres

We now consider tracking control on spheres of arbitrary dimension. It should be understood that the calculations below are performed in the ambient space (*i.e.*, we explicitly consider that $q, q_\mathrm{d} \in \mathbb{S}^n \subseteq \mathbb{R}^{n+1}$ and $R_\mathrm{d} \in \mathrm{SO}(n+1) \subseteq \mathbb{R}^{(n+1)\times(n+1)}$, and follow the rules of matrix multiplication). We also denote the identity matrix of dimension $(n+1) \times (n+1)$ simply by I.

Corollary 5.2 (Almost Global Asymptotic Tracking on $\mathbb{S}^n$). *For any $n \in \mathbb{N}$, consider a fully-actuated mechanical system on $(\mathbb{S}^n, \Psi, \rho)$. Let $q_\mathrm{d} : \mathbb{R} \to \mathbb{S}^n$ be a smooth reference trajectory and $R_\mathrm{d} : \mathbb{R} \to \mathrm{SO}(n+1)$ be any $0_{\mathbb{S}^n}$-lift of q_d with bounded body velocity. Then, for any $k_P, k_D > 0$, the control policy*

$$f_q(t, \dot{q}) = -k_P\, q_\mathrm{d}{}^\mathrm{T}\big(q\, q^\mathrm{T} - \mathrm{I}\big) - k_D\big(\dot{q}^\mathrm{T} + q^\mathrm{T} \dot{R}_\mathrm{d}\, R_\mathrm{d}{}^\mathrm{T}\big) + \big(q^\mathrm{T}\ddot{R}_\mathrm{d} + 2\,\dot{q}^\mathrm{T}\dot{R}_\mathrm{d}\big)\, R_\mathrm{d}{}^\mathrm{T}\big(q\, q^\mathrm{T} - \mathrm{I}\big) \tag{5.61}$$

achieves almost global asymptotic tracking of the reference and local exponential convergence of the error.

Proof. It will suffice to apply Theorem 5.1 with the configuration error (5.20), the navigation function (5.7), and the dissipation metric $\nu = k_D\,\rho$. To show this, we begin by computing

$$\mathrm{d}P(q_\mathrm{e}) = (-k_P\, 0_{\mathbb{S}^n})^\mathrm{T}(\mathrm{I} - q_\mathrm{e}\, q_\mathrm{e}{}^\mathrm{T}) = -k_P\, q_\mathrm{d}{}^\mathrm{T}\big(\mathrm{I} - q\, q^\mathrm{T}\big)R_\mathrm{d}. \tag{5.62}$$

Recalling that $\rho^\flat(v_q) = (v_q)^\mathrm{T}$ for the usual metric on the sphere, we also have

$$\nu^\flat(\dot{q}_\mathrm{e}) = k_D\, \rho^\flat(\dot{q}_\mathrm{e}) = k_D(q^\mathrm{T}\, \dot{R}_\mathrm{d} + \dot{q}^\mathrm{T}\, R_\mathrm{d}). \tag{5.63}$$

Following [9, Ex. 4.99], the covariant derivative along a smooth curve γ of any $X \in \mathfrak{X}(\gamma)$ is given by

$$\big(\nabla_{\dot{\gamma}}X\big)(r) = \big(\mathrm{I} - \gamma(r)\, \gamma(r)^\mathrm{T}\big)\, \dot{X}(r), \tag{5.64}$$

where $X(r)$ is thought of as a vector in $\mathbb{R}^3$. Following (5.26), we compute directly $\gamma^q(r) = R_\mathrm{d}(r)^\mathrm{T}\, q$ (thus, $\dot{\gamma}^q(r) = \dot{R}_\mathrm{d}(r)^\mathrm{T}\, q$) and $X^{\dot{q}}(r) = R_\mathrm{d}(r)^\mathrm{T}\, \dot{q}$, so that we may compute the covariant derivative in (5.27) as

$$\nabla_{\dot{\gamma}^q}(\dot{\gamma}^q + 2\, X^{\dot{q}})(t) = \big(\mathrm{I} - q_\mathrm{e}q_\mathrm{e}{}^\mathrm{T}\big)\big(\ddot{R}_\mathrm{d}{}^\mathrm{T}\, q + 2\, \dot{R}_\mathrm{d}{}^\mathrm{T}\, \dot{q}\big). \tag{5.65}$$

For any $R \in \mathrm{SO}(n+1)$ and $\omega \in T^*\mathbb{S}^n$, by Lemma 2.2 we have

$$\mathrm{d}\Psi_R^*(\omega) = \rho^\flat \circ \mathrm{d}\Psi_R^{-1} \circ \rho^\sharp(\omega) = \rho^\flat \circ \mathrm{d}\Psi_{(R^\mathrm{T})}(\omega^\mathrm{T}) = \rho^\flat(R^\mathrm{T}\omega^\mathrm{T}) = \omega\, R. \tag{5.66}$$

Thus, we may compute (5.27) by substituting in (5.62), (5.63), and (5.65) and applying (5.66). Simplifying yields exactly (5.61), and thus, the claim follows immediately by Theorem 5.1. ∎

The control law (5.61) given in Corollary 5.2 is explicit; nonetheless, its direct implementation requires
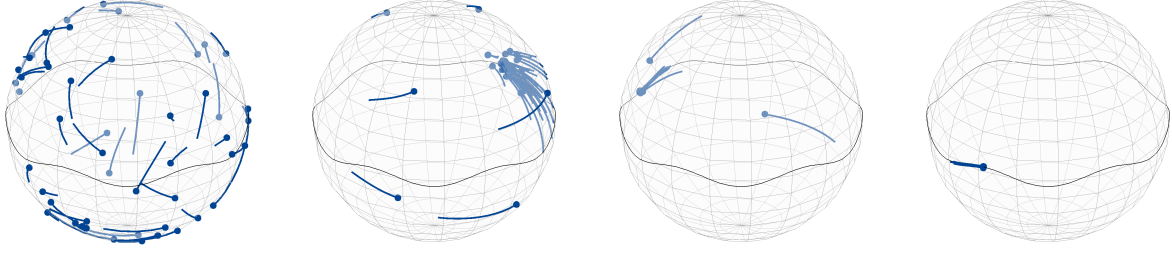
Figure 5.2: The controller proposed in Corollary 5.3 (a special case of Corollary 5.2 and Theorem 5.1), applied to a mechanical system on the homogeneous Riemannian manifold $\mathbb{S}^2$ (*e.g.*, the Axisymmetric Satellite). We show snapshots of parallel rollouts from a random sampling of initial states (configuration and velocity) in $T\mathbb{S}^2$. All sampled rollouts converge asymptotically to the reference. An animation of these simulations is available at `https://tinyurl.com/SphereTracking`.

the computation of a lift of the reference trajectory. While Sec. 5.3 outlined an effective and robust means of approximating lifts numerically, a tracking control law that depends not on the lift but rather on the reference trajectory directly would be even more advantageous—besides eliminating the need for online approximation of a lift when tracking dynamically updated references, such a result would also facilitate more easily differentiating the control policy (*e.g.*, for backstepping-style control or automatic gain tuning).

In the following corollary, we give such a control policy in the special case of a system evolving on $\mathbb{S}^2$. Below, $\hat{\cdot} : \mathbb{R}^3 \to \mathfrak{so}(3)$ is the usual "hat map", also written $(\cdot)_\times$, defined by $\hat{a}b := a \times b$ for all $a, b \in \mathbb{R}^3$.

Corollary 5.3 (Almost Global Asymptotic Tracking on $\mathbb{S}^2$ via Implicit Lift)**.** *Consider a fully-actuated mechanical system on $(\mathbb{S}^2, \Psi, \rho)$ and let $q_\mathrm{d} : \mathbb{R} \to \mathbb{S}^2 \subset \mathbb{R}^3$ be a smooth reference trajectory with bounded velocity $\dot{q}_\mathrm{d}$. Then, for any $k_P, k_D > 0$, the control policy*

$$
\begin{aligned}
f_q\big((q, \dot{q}), (q_\mathrm{d}, \dot{q}_\mathrm{d}, \ddot{q}_\mathrm{d})\big) = {}& - k_P\, q_\mathrm{d}{}^\mathrm{T}\big(q\,q^\mathrm{T} - \mathrm{I}\big) - k_D\big(\dot{q}^\mathrm{T} + q^\mathrm{T}\,(q_\mathrm{d} \times \dot{q}_\mathrm{d})_\times\big) \\
& + \big(q^\mathrm{T}\,(q_\mathrm{d} \times \dot{q}_\mathrm{d})_\times^2 + q^\mathrm{T}\,(q_\mathrm{d} \times \ddot{q}_\mathrm{d})_\times + 2\,\dot{q}^\mathrm{T}(q_\mathrm{d} \times \dot{q}_\mathrm{d})_\times\big)\big(q\,q^\mathrm{T} - \mathrm{I}\big)
\end{aligned}
\tag{5.67}
$$

achieves almost global asymptotic tracking of the reference and local exponential convergence of the error.

Proof. It will suffice to apply Corollary 5.2 for a horizontal lift $R_\mathrm{d} : \mathbb{R} \to \mathrm{SO}(3)$ corresponding to the reductive decomposition (5.19) and simplify. By the properties of horizontal lifts in Prop. 5.2 and the reductive decomposition (5.19), we have have two constraints on R_d and its derivative, namely,

$$
q_\mathrm{d} = \Psi(R_\mathrm{d}, \mathrm{e}_3) \quad \text{and} \quad \mathrm{d}\mathrm{L}_{R_\mathrm{d}}^{-1}\big(\dot{R}_\mathrm{d}\big) \in \mathrm{span}\{\hat{\mathrm{e}}_1, \hat{\mathrm{e}}_2\}.
\tag{5.68}
$$

Letting $\Omega_d : \mathbb{R} \to \mathbb{R}^3$ be the vector representative of the body velocity of R_d (*i.e.*, $\dot{R}_\mathrm{d} = R_\mathrm{d}\,\hat{\Omega}_d$), we differ-

entiate the first constraint and re-express both constraints explicitly in terms of Ω_d, yielding

$$(e_3)_\times \Omega_d = -R_d{}^\mathsf{T} \dot{q}_d, \quad e_3{}^\mathsf{T} \Omega_d = 0, \tag{5.69}$$

or in matrix form,

$$\begin{bmatrix} (e_3)_\times \\ e_3{}^\mathsf{T} \end{bmatrix} \Omega_d = \begin{bmatrix} -R_d{}^\mathsf{T} \dot{q}_d \\ 0 \end{bmatrix}. \tag{5.70}$$

Solving this linear system by multiplying both sides by the transpose of the coefficient matrix yields

$$\Omega_d = e_3 \times R_d{}^\mathsf{T} \dot{q}_d = R_d{}^\mathsf{T}\big((R_d{}^\mathsf{T} e_3) \times \dot{q}_d\big) = R_d{}^\mathsf{T}(q_d \times \dot{q}_d), \tag{5.71}$$

where we recall that $(R\,v)_\times = R\,(v)_\times R^\mathsf{T}$ for all $R \in SO(3)$ and $v \in \mathbb{R}^3$ (see [8, p. 311]). Thus, it is also clear that the body velocity of the lift R_d is bounded. Moreover, we may compute

$$\dot{R}_d = R_d \hat{\Omega}_d = R_d \left(R_d{}^\mathsf{T}(q_d \times \dot{q}_d)\right)_\times = R_d R_d{}^\mathsf{T}(q_d \times \dot{q}_d)_\times R_d = (q_d \times \dot{q}_d)_\times R_d, \tag{5.72}$$

and another derivative gives us

$$\ddot{R}_d = (q_d \times \dot{q}_d)_\times \dot{R}_d + (q_d \times \ddot{q}_d + \underbrace{\dot{q}_d \times \dot{q}_d}_{=0})_\times R_d = \big((q_d \times \dot{q}_d)^2_\times + (q_d \times \ddot{q}_d)_\times\big)R_d. \tag{5.73}$$

After substituting these results into the tracking control law (5.61) and simplifying, all instances of R_d and $R_d{}^\mathsf{T}$ cancel, yielding exactly (5.67). Thus, the claim follows immediately by Corollary 5.2. ∎

We now apply the controller obtained in the previous corollary to a classic example.

Example 5.4 *(The Axisymmetric Satellite).* Consider a free-floating satellite, modeled as an (underactuated) mechanical system on $(SO(3), L, \kappa_\mathbb{J})$ consisting of a rigid body with inertia tensor $\mathbb{J} = \mathrm{diag}(J_1, J_2, J_3)$ with $J_1 = J_2$ and control torques lying in a two-dimensional left-invariant codistribution corresponding to $\mathrm{span}\{\hat{e}_1, \hat{e}_2\} \subset \mathfrak{so}(3)^*$, where $\hat{\cdot} : \mathbb{R}^3 \to \mathfrak{so}(3)^* \cong \mathfrak{so}(3)$ is the usual isomorphism satisfying $\hat{a}b = a \times b$.

The satellite is equipped with a camera or antenna aligned with the e_3 axis, whose bearing is thus described by the output $y : \dot{R} \mapsto R\,e_3$. This system is invariant under the (left) action of $SO(2)$ on $SO(3)$ corresponding to a *body-fixed* rotation around e_3. By Noether's Theorem, the evolution around the symmetry axis is governed by conservation of momentum (*i.e.* $\frac{d}{dt}\big(J_3\,\Omega_3(t)\big) = 0$). When $\Omega_3(t_0) = 0$, reduction by this symmetry (see [9, Thm. 5.83]) will yield a fully-actuated mechanical system on $(\mathbb{S}^2 = SO(3)/SO(2), \Psi, J_1\,\rho)$.

It is clear that output tracking for the original (underactuated) system on $SO(3)$ amounts to asymptotically tracking a state trajectory for the reduced (fully-actuated) system on $\mathbb{S}^2$. We apply the explicit tracking control policy obtained in Corollary 5.3. Fig. 5.2 shows rollouts of the controller from 100 randomly sampled initial states for a particular reference trajectory, all of which converge to the reference. •

5.6 Discussion

Of the n-spheres, only $\mathbb{S}^1$ and $\mathbb{S}^3$ admit a Lie group structure, and thus methods like [95] are not applicable to tracking on, *e.g.*, $\mathbb{S}^2$. As pointed out in [98], methods which do not rely on reduction to regulation often fail to achieve or certify almost global convergence, in large part because they cannot benefit from results like [97, Thm. 2]. Other smooth tracking controllers on $\mathbb{S}^2$ (*e.g.* [100] or [107, Sec. III]) do *not* guarantee convergence from almost every initial state in TQ, rather ensuring convergence from a smaller region that, *e.g.*, may contain the *zero* tangent vector over almost every point in Q (not TQ), sometimes leading to an abuse of the term "almost global" in the literature in regards to asymptotic stability.

We also note that the differential properties of a state-valued tracking error are important, since it was the surjectivity of the partial derivative of the tracking error appearing in (5.34) that enabled the feedforward cancellation of other terms and the injection of arbitrary dissipation and potential, regardless of the system considered (a difficulty of the approach proposed in [98]). Also, Example 5.4 demonstrates applicability to output tracking for certain underactuated systems, and more broadly, the control policies obtained here could also serve as subsystem controllers in a larger hierarchical control scheme, a common approach for underactuated systems [26, 96].

Unfortunately, it is not yet clear to us whether an "implicit lift" control law like the one obtained in Corollary 5.3 can be generalized to $\mathbb{S}^n$ for arbitrary $n \in \mathbb{N}$ (or more broadly, to arbitrary homogeneous Riemmanian manifolds), since we made use of specific properties of the vector cross product in $\mathbb{R}^3$. In achieving this result for the special case of $\mathbb{S}^2$, several choices seem to have played an important role:

1. the chosen lift g_d was horizontal (and thus, its body velocity depended only on $\dot{q}_\mathrm{d}$ and g_d),

2. the chosen navigation function P was invariant to the action of the origin's stabilizer group G_{0_Q} (in fact, the level sets of the navigation function are exactly the orbits of the stabilizer group), and

3. the chosen damping metric ν was G-invariant (in fact, simply a scaling of the kinetic energy metric).

Although we leave the goal of generalizing this result to future work, we suspect that the choices listed above will play an essential role in any successful attempt.

5.7 Conclusion

In this chapter, we proposed a systematic, unified tracking controller for fully-actuated mechanical systems evolving on homogeneous Riemannian manifolds. Because the controller achieves almost global asymptotic tracking, we guarantee exactly zero probability of nonconvergence from an initial state randomly selected from a smooth probability distribution. After obtaining explicit control policies for two common cases, we apply the method to example systems on two different configuration manifolds. At a conceptual level, our results illustrate that it is the *transitivity* of a Lie group's action on the configuration manifold

(and *not* the absence of fixed points) that enables us to perform tracking control via error regulation in mechanical systems.

ALMOST GLOBAL ASYMPTOTIC STABILITY OF CASCADES

The material in this chapter is based on the publication [113], co-authored with Matthew D. Kvalheim and Vijay Kumar. The author of this thesis developed the theoretical contributions and drafted the original manuscript in very close collaboration with his co-authors (especially the second author).

6.1   Introduction

In Chapter 5, we considered the design of tracking controllers for fully-actuated systems evolving on a broad class of manifolds. A major motivation for considering the control of fully-actuated systems, despite our broader focus on *underactuated* systems, is the prominence of tracking controllers for underactuated systems that are designed via the hierarchical composition of tracking controllers for fully-actuated subsystems [26, 96, 102]. However, a major shortcoming of these existing approaches is the apparent need to design and certify these hierarchical controllers for particular systems on a case-by-case basis. Indeed, [96] carefully analyzes the stability of the overall cascade's dynamics, guessing and explicitly verifying a Lyapunov function for the overall system. On the other hand, the approach of [26] may perhaps be more immediately generalized, but its certificate of stability relies on assumptions of time scale separation between the subsystems that are hard to justify for realistic systems. Broadly speaking, to develop scalable and generalized approaches for the design and certification of hierarchical controllers for underactuated systems (along the lines discussed at the start of Chapter 5), it seems necessary to explicitly leverage the hierarchical structure of the control architecture, and to ultimately develop compositional certificates whose criteria depend only (or at least primarily) on properties of the subsystems in isolation.

Towards this end, in this chapter, we study cascade dynamical systems. Indeed, a long research tradition has studied the implications of cascade structure to simplify analysis and aid design [114]. This compositional approach is largely motivated by the observation that control design for a subsystem is typically easier (*e.g.*, due to lower dimensionality, lower relative degree, or full actuation). Cascades appear in many interesting and important physical systems, and many underactuated mechanical systems can be rendered as a cascade after a feedback transformation [115].

6.1.1   Cascades in Hierarchical Control

To better situate our interest in cascade stability within the context of control design, we consider the following situation, largely based on [116, Sec. VII]. For some smooth manifold X, consider a control system with state $(x, z) \in X \times \mathbb{R}^k$, and inputs $u \in \mathbb{R}^k$ given by

$$\dot{x} = h(x, z), \tag{6.1a}$$

$$\dot{z} = u, \tag{6.1b}$$

where h is smooth. A standard motivation for considering such a system is augmenting an existing plant model (6.1a) with actuator dynamics (modeled here in (6.1b) as a simple integrator), in which case the goal is to "bootstrap" a control policy for the original system into one suitable for controlling the system with actuator dynamics. Suppose that for some differentiable function $x \mapsto K(x)$, the system

$$\dot{x} = h\big(x, K(x)\big) \tag{6.2}$$

has an asymptotically stable equilibrium $0_X \in X$. In other words, if we temporarily regard z as a control input, the feedback $z = K(x)$ stabilizes (6.1a). Then, it is reasonable to design a control policy for u that will drive z asymptotically towards the "outer loop" control policy $K(x)$ (a simple approach which is closely related to a class of methods frequently called "backstepping" control [117]). In particular, proposing the "inner loop" control law

$$u = -z + K(x) + \mathrm{d}K\big(h(x, z)\big) \tag{6.3}$$

and defining an error state $y = z - K(x)$, we may compute

$$\dot{y} = \dot{z} - \mathrm{d}K(\dot{x}) = -z + K(x) + \mathrm{d}K\big(h(x, z)\big) - \mathrm{d}K\big(h(x, z)\big) = -y. \tag{6.4}$$

Expressing the system's closed-loop dynamics in these new variables, we have

$$\dot{x} = h\big(x, K(x) + y\big), \tag{6.5a}$$

$$\dot{y} = -y. \tag{6.5b}$$

It is natural to wonder what can be said about the stability[12] of the combined system (6.5a)-(6.5b), given our knowledge of the stability of (6.5b) with respect to $y = 0$ and the stability of (6.5a) when $y = 0$. Such a question is motivated by the observation that if we can formulate stability guarantees for the overall system based only on properties of the subsystems in isolation, the design problem for each subsystem can be decoupled, facilitating a compositional approach to control synthesis.

6.1.2 Local Asymptotic Stability of Cascades

In fact, at a minimum, we can always say the following.

Fact 6.1 (Local Asymptotic Stability of Cascades, see [118]). *Consider a cascade of the form*

$$\dot{x} = f(x, y), \tag{6.6a}$$

---

[12]While one can consider the stability of more general invariant sets, we will study only the stability of point attractors.

110

$$\dot{y} = g(y), \tag{6.6b}$$

where x and y evolve on smooth manifolds X and Y and f and g are smooth. Suppose that $0_Y \in Y$ is a locally asymptotically stable equilibrium of $\dot{y} = g(y)$ and $0_X \in X$ is a locally asymptotically stable equilibrium of $\dot{x} = f(x, 0_Y)$. Then, $(0_X, 0_Y)$ is a locally asymptotically stable equilibrium of the full cascade.

Thus, considering $f(x, y) := h\big(x, K(x) + y\big)$ and $g(y) := -y$, the proposed control design (6.3) for (6.1a)-(6.1b) renders the closed loop dynamics (6.5a)-(6.5b) at least *locally* asymptotically stable. However, the basin of attraction for the full cascade may be very small, making such a control design brittle.

6.1.3 Global Asymptotic Stability of Cascades

It is clear that if both subsystems of a cascade are asymptotically stable *linear* systems, then the full cascade is in fact *globally* asymptotically stable. However, in the *nonlinear* setting, even if the subsystems are *globally* asymptotically stable, the same cannot immediately be said for the full cascade. Nonetheless, it turns out that only one additional assumption is needed to ensure the global asymptotic stability of a cascade with globally asymptotically stable subsystems. The following is now a classic result.

Fact 6.2 (Global Asymptotic Stability of Cascades, see or [118] or [119])**.** *Consider a cascade of the form*

$$\dot{x} = f(x, y), \tag{6.7a}$$

$$\dot{y} = g(y), \tag{6.7b}$$

where x and y evolve on smooth manifolds[13] X and Y and f and g are smooth. Suppose that $0_Y \in Y$ is a globally asymptotically stable equilibrium of $\dot{y} = g(y)$ and $0_X \in X$ is a globally asymptotically stable equilibrium of $\dot{x} = f(x, 0_Y)$. Moreover, suppose that every trajectory of the full cascade (6.7a)-(6.7b) is bounded for all forward time. Then, $(0_X, 0_Y)$ is a globally asymptotically stable equilibrium of the full cascade.

A straightforward implication of the previous fact in regards to the hierarchical control design (6.3) is the following: if we also assume that (6.2) is globally asymptotically stable, and we can somehow guarantee that x remains within some arbitrary compact set for all trajectories of (6.5a)-(6.5b), then the closed-loop cascade (6.5a)-(6.5b) is globally asymptotically stable.

In fact, the long tradition of research on the global asymptotic stability of cascades has largely served to identify various conditions that ultimately imply the boundedness requirement of Fact 6.2. Many approaches rely on explicit disturbance robustness properties of the driven subsystem, leveraging properties such as "input to state stability", which roughly requires the asymptotic response of the system under a disturbance input to be bounded by the size of the input (and therefore also implies global asymptotic stability of the system in the absence of disturbances). A celebrated result then establishes the global asymptotic

---

[13]This result is usually stated on Euclidean spaces, but we are free to state it on smooth manifolds, noting that the basin of attraction of any equilibrium of a smooth vector field is diffeomorphic to $\mathbb{R}^n$ for some n [120], so X and Y are "secretly" Euclidean.

stability of a cascade for which the driven subsystem is input to state stable and the driving subsystem is globally asymptotically stable [119].

On the other hand, singular perturbation techniques assume a time scale separation between a "fast" inner loop and a "slow" outer loop, and show that a system's behavior tends toward that of a "reduced" system as the ratio between convergence rates tends to zero [121]. While these methods can be applied to analyze cascades, such an approach would necessitate an inner loop control design that achieves very rapid convergence, which can be quite challenging (or even impossible) for a control system with realistic input constraints. Methods avoiding explicit robustness or time scale assumptions have often relied on local exponential stability of the driving subsystem as well as growth restrictions on the "interconnection term" coupling the system and on a suitable Lyapunov function for the unforced dynamics [117].

6.1.4 Almost Global Asymptotic Stability of Cascades

The already-discussed global results have numerous important applications, but their utility in the analysis of geometric controllers is rather limited. Indeed, the smooth tracking controllers developed in Chapter 5 only guaranteed convergence from an *almost* global set of initial conditions—and in fact, continuous vector fields with a globally asymptotically stable equilibrium exist only on those manifolds that are diffeomorphic to $\mathbb{R}^n$ [122], whereas the state space of many robotic systems (*e.g.*, free-flying robots) is not [123]. It is reasonable to wonder whether one can avoid this obstruction by accepting the need for discontinuous control policies. However, the hierarchical control design proposed in (6.3) depends on the differential $\mathrm{d}K$, thus it is reasonable to require K to be continuously differentiable. Moreover, if K is continuously differentiable, the same is true of the vector field $x \mapsto h\big(x, K(x)\big)$ in (6.2). Since an equilibrium of a continuously differentiable vector field on a non-Euclidean manifold can be no better than *almost* globally asymptotically stable, standard results on the stability of cascades with *globally* asymptotically stable subsystems do not seem applicable in settings where the control action applied to a system evolving on a non-Euclidean manifold will ultimately be exerted by another subsystem (governed by its own dynamics).

Such obstructions motivated the development of an almost global notion of input to state stability [116], in which an asymptotic gain holds for all but a measure zero set of initial conditions; a cascade is then guaranteed to be almost globally asymptotically stable if its driven subsystem is almost globally input to state stable and its driving subsystem is almost globally asymptotically stable. While verifying almost global input to state stability can be challenging, this can be achieved under conditions on the exponential instability of other equilibria as well as the "ultimate boundedness" of trajectories of the system even when subjected to arbitrary disturbances [124].

However, not all almost globally asymptotically stable cascades have a driven subsystem enjoying this "almost input to state stability" property; indeed, it seems to be an inherently stricter property than necessary, since it characterizes the response of the system to arbitrary disturbances, while for our purposes, the driven subsystem is subjected to a converging disturbance for almost every initial condition of the driving
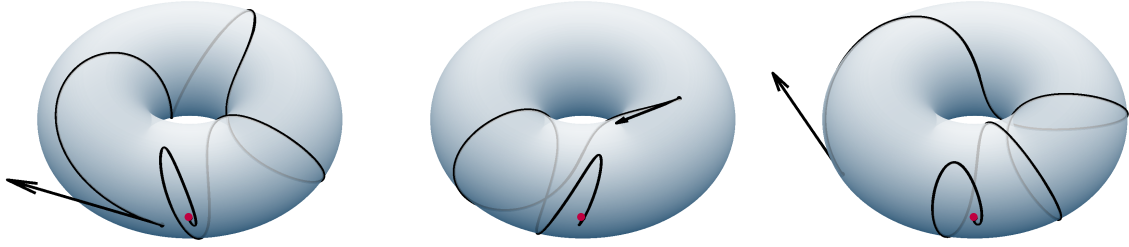
Figure 6.1: A sampling of initial conditions and resulting trajectories of the motivating example system (6.8a)-(6.8b), projected down to $\mathbb{T}^2$ from the full state space $T\mathbb{T}^2 = T\mathbb{S}^1 \times T\mathbb{S}^1$, where the "small" axis of the torus corresponds to θ and the "large" axis corresponds to ϕ. All sampled trajectories converge to $(0,0,0,0) \in T\mathbb{T}^2$, marked in red. Despite the highly non-local and topologically complex behavior of the trajectories, our results certify the almost global asymptotic stability of the system, without the need to guess an explicit Lyapunov function for the full cascade. An animation of parallel rollouts from randomly sampled initial conditions is available at https://tinyurl.com/TorusCascade.

subsystem. Yet, the lack of a comprehensive understanding of such systems has required unsubstantiated assumptions or bespoke stability certificates for hierarchical controllers with almost global asymptotic stability in practice, inhibiting generalization; for example, a Lyapunov function for the combined system may be handcrafted via human intuition, even though the cascaded structure inspired the control design [96], or it may be necessary to resort to time scale separation arguments that may not hold in reality [26].

6.1.5   Illustrative Example

To further motivate our investigation, we present a simple representative example. Consider a cascade evolving on $T\mathbb{T}^2$ (the tangent bundle of the torus), given by

$$\ddot{\theta} = -(\sin\theta + \dot{\theta})\cos 2\phi, \tag{6.8a}$$

$$\ddot{\phi} = -(\sin\phi + \dot{\phi}), \tag{6.8b}$$

where $x = (\theta, \dot{\theta}) \in T\mathbb{S}^1$, $y = (\phi, \dot{\phi}) \in T\mathbb{S}^1$, and we make the identification $T\mathbb{S}^1 \cong \mathbb{S}^1 \times \mathbb{R}$ for notational convenience. A sampling of system trajectories is shown in Fig. 6.1. In fact, (6.8b) describes a damped pendulum with total energy given by $W : (\phi, \dot{\phi}) \mapsto 1 - \cos\phi + \frac{1}{2}\dot{\phi}^2$. Using W as a LaSalle function, it can be shown that that $(\phi, \dot{\phi}) = (0,0)$ is almost globally asymptotically stable for the driving subsystem (6.8b). By the same reasoning, $(\theta, \dot{\theta}) = (0,0)$ is also almost globally asymptotically stable for the restriction of the driven subsystem (6.8a) to the stable equilibrium of the driving subsystem.

It turns out that the entire cascade (6.8a)-(6.8b) is almost globally asymptotically stable, but the system does not satisfy the hypotheses of any of the previously discussed results. In particular, the subsystems are not globally asymptotically stable, nor is there a time scale separation between the loops (since when

113
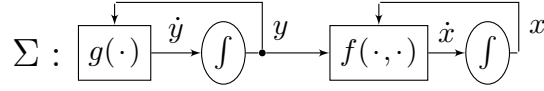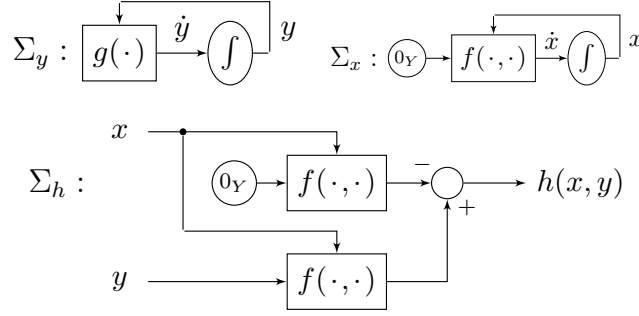
Figure 6.2: We give sufficient conditions for the almost global asymptotic stability of a cascade system Σ in terms of qualitative properties of the "driving subsystem" Σ_y and the "unforced subsystem" Σ_x, as well as growth rate criteria on the "interconnection term" Σ_h and a Lyapunov function for Σ_x. In the diagram above, 0_Y is the stable equilibrium of Σ_y.

decoupled, they are identical). Furthermore, viewing $(\phi, \dot{\phi})$ as a disturbance to (6.8a), it can be seen that the driven subsystem is *not* almost globally input to state stable (in the sense of [116, Def. 2.1]), since the response to the bounded disturbance $(\phi, \dot{\phi}) = (\pi/2, 0)$ grows unbounded from almost all initial conditions. Nonetheless, the results presented in this chapter will ultimately guarantee the almost global asymptotic stability of a class of systems that includes (6.8a)-(6.8b).

6.1.6 Overview and Contributions

In this chapter, we study the asymptotic stability of cascades of the form

$$\dot{x} = f(x, y), \tag{6.9a}$$

$$\dot{y} = g(y), \tag{6.9b}$$

where x and y evolve smooth, connected, complete Riemannian manifolds without boundary X and Y, and f and g are smooth (see Remark 6.2 for further explanation of the choice of setting). The cascade system is depicted graphically in in Fig. 6.2 as system Σ. In what follows, we use properties of the decomposed subsystems Σ_x, Σ_y, and Σ_h in Fig. 6.2 to certify the almost global asymptotic stability of Σ. In Sec. 6.3, we present the main results, which show that when Σ_x and Σ_y are almost globally asymptotically stable and locally exponentially stable and all chain recurrent points of Σ_x are hyperbolic equilibria, then the

cascade is almost globally asymptotically stable and locally exponentially stable as long as all trajectories are bounded in forward time. We extend this result inductively to upper triangular systems with arbitrarily many subsystems. In Sec. 6.4, we examine the hypotheses of the main results in greater detail, discussing some important classes of systems enjoying the stated chain recurrence property and also showing that forward boundedness can be verified via growth rate criteria on Σ_h and on a Lyapunov function for Σ_x. In Sec. 6.5, we apply our results to the motivating example, before discussing the results and concluding the chapter in Secs. 6.6 and 6.7.

6.2 Mathematical Preliminaries

We begin with a brief review of relevant concepts from dynamical systems theory. We adopt the definitions of [125], whose results on asymptotically autonomous semiflows are central to our approach.

6.2.1 Autonomous and Nonautonomous Semiflows

Definition 6.1. A *nonautonomous semiflow* on a smooth Riemannian manifold (M, μ) is a continuous map

$$\Phi : \{(t, s) : 0 \leq s \leq t < \infty\} \times M \to M \tag{6.10}$$

such that $\Phi(s, s, x) = x$ and $\Phi\big(t, s, \Phi(s, r, x)\big) = \Phi(t, r, x)$ for all $t \geq s \geq r > 0$. A semiflow is called *autonomous* when additionally, $\Phi(t + r, s + r, x) = \Phi(t, s, x)$ for all $r > 0$. ●

In the previous, the parameters s and t can be thought of as respective "start" and "end" times. Hereafter, we will use the shorthands $\Phi_{(t,s)} : x \mapsto \Phi(t, s, x)$ for nonautonomous semiflows and $\Phi_t : x \mapsto \Phi(t, 0, x)$ for autonomous semiflows.

Remark 6.1 (*Notation and Setting*). A *forward complete* vector field $V \in \mathfrak{X}(M)$ is one for which unique solutions to the initial value problem (IVP)

$$\dot{x}(t) = V\big(x(t)\big), \quad x(0) = x_0 \tag{6.11}$$

exist for all positive time and from all initial conditions $x_0 \in M$. A forward complete vector field generates an autonomous semiflow Φ, where for each for $x_0 \in M$, the curve $t \mapsto \Phi_t(x_0)$ is the solution to IVP for x_0. On the other hand, a "time-varying" vector field $V : \mathbb{R} \to \mathfrak{X}(M)$ whose initial value problems have unique solutions for all forward time can generate a non-autonomous semiflow. Moreover, a vector field that is both forward complete and backward complete (with unique solutions for all negative time as well) generates a *flow*, which is in fact a group action $\Phi : \mathbb{R} \times M \to M$, motivating the choice of notation. However, we consider only the forward evolution of the system, and thus work with semiflows.

The following class of nonautonomous semiflows defined in [125] will be of particular interest.

Definition 6.2. A nonautonomous semiflow Φ is *asymptotically autonomous with limit semiflow* Θ if

$$\Phi_{(t_j+s_j,s_j)}(x_j) \to \Theta_t(x) \text{ as } j \to \infty. \tag{6.12}$$

for all arbitrary sequences $t_j \to t$, $s_j \to \infty$, and $x_j \to x$. $\qquad\qquad\bullet$

6.2.2 Notions of Stability

In this chapter, we consider the stability of the simplest kind of invariant set (*i.e.*, a fixed point).

Definition 6.3. The *equilibrium set* of an autonomous semiflow Φ is given by

$$\mathcal{E}(\Phi) = \left\{ x \in M : \Phi_t(x) = x \text{ for all } t \geq 0 \right\}. \tag{6.13}$$

The *basin of attraction* of any equilbrium $0_M \in \mathcal{E}(\Phi)$ is given by

$$\mathcal{B}(0_M) = \left\{ x \in M : \Phi_t(x) \to 0_M \text{ as } t \to \infty \right\}, \tag{6.14}$$

and 0_M is *hyperbolic* if its linearization has no purely imaginary eigenvalues (see [126, p. 149]). $\qquad\bullet$

We define the following notions of stability for equilibria.

Definition 6.4 (*Notions of Stability*)**.** An equilibrium $0_M \in \mathcal{E}(\Phi)$ is said to be

- *Lyapunov stable* if for every open neighborhood $N_\varepsilon \subseteq M$ of 0_M, there exists an open neighborhood $N_\delta \subseteq M$ of 0_M such that $\Phi_t(N_\delta) \subseteq N_\varepsilon$ for all $t \geq 0$,

- *almost globally attractive* if $\mathcal{B}(0_M)$ is full measure and residual, *i.e.*, the complement of $\mathcal{B}(0_M)$ is measure zero (see [4, p.128]) and meager (a countable union of nowhere dense sets) in M,

- *almost globally asymptotically stable* if it is Lyapunov stable and almost globally attractive, and

- *locally exponentially stable* if there exists an open neighborhood $N \subseteq M$ of 0_M and constants $\alpha, \lambda > 0$ such that for all $x \in N$ and $t \geq 0$, we have $\mathrm{dist}_\mu\left(\Phi_t(x), 0_M\right) \leq \alpha \, \mathrm{dist}_\mu\left(x, 0_M\right) e^{-\lambda t}$. $\qquad\bullet$

We recall that because we define local exponential stability using the Riemannian distance, an equilibrium is locally exponentially stable if and only if it is hyperbolic.

6.2.3 The Chain Recurrent Set

The following points in state space, visualized in Fig. 6.3, are particularly notable.

Definition 6.5. For an autonomous semiflow Φ on (M, μ) and constants $\varepsilon, T > 0$, an (ε, T)-*chain* is a pair

$$\text{dist}_\mu\big(\Phi_{t_i}(x_{i-1}), x_i\big) < \varepsilon$$
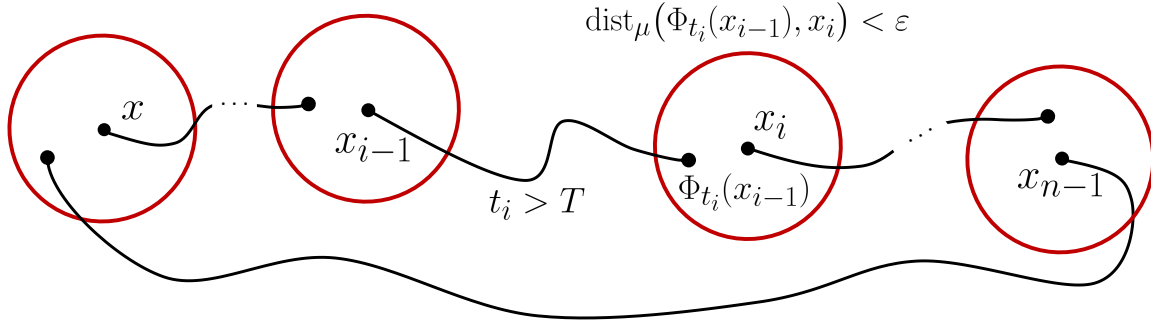
Figure 6.3: A point $x \in M$ is a chain recurrent point if there exists a closed (ε, T)-chain at x for every $\varepsilon, T > 0$. An (ε, T)-chain is a sequence of points in state space, where each adjacent pair is connected by a "long" trajectory segment (of duration greater than T) and a "short" jump (of distance less than ε).

of finite sequences $(x_0, x_1, \ldots, x_n)$ and $(t_1, t_2, \ldots, t_n)$ satisfying

$$\text{dist}_\mu\big(\Phi_{t_i}(x_{i-1}), x_i\big) < \varepsilon \text{ and } t_i > T, \quad i = 1, 2, \ldots, n, \tag{6.15}$$

where $\text{dist} : M \times M \to \mathbb{R}$ is the Riemannian distance induced by μ. The *chain recurrent set*, denoted $\mathcal{R}(\Phi)$, consists of all points $x \in M$ for which an (ε, T)-chain with $x = x_0 = x_n$ exists for every $\varepsilon, T > 0$. ●

The chain recurrent set plays a central role in describing the topological structure of a dynamical system [126]. Our present interest in chain recurrence will revolve around the following powerful result.

Fact 6.3 (Long-Term Behavior of Asymptotically Autonomous Semiflows, see [125])**.** *Precompact forward trajectories of an asymptotically autonomous semiflow converge to the chain recurrent set of the limit semiflow.*

Remark 6.2. We define chain recurrence using (ε, T)-chains with respect to a distance function and some $\varepsilon > 0$ because we rely on the results of [125], in which the same choice is made. In a complete Riemannian manifold (our chosen setting), a set is precompact (*i.e.*, has compact closure) if and only if it is bounded.

6.3 Main Results

We now present the main results of this chapter.

6.3.1 Almost Global Asymptotic Stability of Cascades

Theorem 6.1 (Almost Global Asymptotic Stability of Cascades)**.** *Consider a cascade on $X \times Y$ given by*

$$\dot{x} = f(x, y), \tag{6.16a}$$

$$\dot{y} = g(y). \tag{6.16b}$$

Suppose that (6.16b) *and the unforced subsystem*

$$\dot{x} = f(x, 0_Y) \tag{6.17}$$

are almost globally asymptotically stable with respect to $0_Y \in Y$ *and* $0_X \in X$ *respectively, while* 0_Y *and all chain recurrent points of* (6.17) *are hyperbolic equilibria. Moreover, suppose that every trajectory of the full cascade* (6.16a)-(6.16b) *starting in* $X \times \mathcal{B}(0_Y)$ *is bounded for all forward time. Then,* $(0_X, 0_Y)$ *is an almost globally asymptotically stable and locally exponentially stable equilibrium of* (6.16a)-(6.16b).

Proof. Since $X \times \mathcal{B}(0_Y)$ is invariant for (6.16a)-(6.16b) and all forward trajectories beginning in $X \times \mathcal{B}(0_Y)$ are bounded, the cascade induces an autonomous semiflow

$$\Psi_t : X \times \mathcal{B}(0_Y) \to X \times \mathcal{B}(0_Y). \tag{6.18}$$

Similarly, (6.17) and (6.16b) induce the autonomous semiflows

$$\Theta_t : X \to X, \ x_0 \mapsto \mathrm{pr}_1 \circ \Psi_t(x_0, 0_Y), \tag{6.19a}$$

$$\Upsilon_t : \mathcal{B}(0_Y) \to \mathcal{B}(0_Y), \ y_0 \mapsto \mathrm{pr}_2 \circ \Psi_t(0_X, y_0), \tag{6.19b}$$

where pr_1 and pr_2 are the natural projections onto X and Y, and we have carefully chosen the domains of the semiflows. We observe that for each initial condition $y_0 \in \mathcal{B}(0_Y)$, (6.16a) may be interpreted as time-varying dynamics on X given by

$$\dot{x} = f\big(x, \Upsilon_t(y_0)\big). \tag{6.20}$$

In this manner, each initial condition $y_0 \in \mathcal{B}(0_Y)$ induces a corresponding *nonautonomous* semiflow on X given by

$$\Phi_{(t,s)}^{y_0} : X \to X, \ x_0 \mapsto \mathrm{pr}_1 \circ \Psi_{t-s}\big(x_0, \Upsilon_s(y_0)\big), \tag{6.21}$$

such that we may also conclude

$$\Psi_t(x_0, y_0) = \big(\Phi_{(t,0)}^{y_0}(x_0), \Upsilon_t(y_0)\big). \tag{6.22}$$

Using these constructions, we prove the claim in five steps.

STEP 1. $\mathcal{E}(\Psi) = \mathcal{R}(\Theta) \times \{0_Y\}$, *and all equilibria of* Ψ *are hyperbolic, but only* $(0_X, 0_Y)$ *is stable.*

All equilibria $(x, y) \in X \times \mathcal{B}(0_Y)$ must have $y = 0_Y$ by the definition of $\mathcal{B}(0_Y)$ as a basin of attraction, and therefore $f(x, 0_Y) = 0$, *i.e.*, x is an equilibrium of (6.17). The equality then follows from the assumption that $\mathcal{R}(\Theta) \subseteq \mathcal{E}(\Theta)$, since equilibria are always chain recurrent, *i.e.*, $\mathcal{E}(\Theta) \subseteq \mathcal{R}(\Theta)$. Denoting the vector field on $X \times Y$ describing the full cascade (6.16a)-(6.16b) by $F : (x, y) \mapsto \big(f(x, y), g(y)\big)$, we may express

118

its linearization at any equilibrium $(x, 0_Y) \in X \times \mathcal{B}(0_Y)$ as

$$dF|_{(x,0_Y)} = \begin{bmatrix} \partial_x f \big|_{(x,0_Y)} & \partial_y f \big|_{(x,0_Y)} \\ 0 & \partial_y g \big|_{0_Y} \end{bmatrix}. \tag{6.23}$$

Since the eigenvalues of a triangular block matrix are simply the eigenvalues of the blocks on the diagonal, the hyperbolicity claim follows directly from the hyperbolicity of 0_Y for (6.16b) and the hyperbolicity of all equilibria of (6.17).

An almost globally asymptotically stable system has only one stable equilibrium (since all other equilibria lie on the boundary of its basin of attraction). Therefore, at $x = 0_X$ all eigenvalues of the top left block have negative real part, but one or more eigenvalues at all other equilibria of (6.17) have positive real part. Hence $(0_X, 0_Y)$ is locally exponentially stable and all other equilibria in $X \times \mathcal{B}(0_Y)$ are unstable. To complete the proof, it will thus suffice to show that the equilibrium $(0_X, 0_Y)$ is almost globally attractive. ▼

STEP 2. *For any $y_0 \in \mathcal{B}(0_Y)$, the nonautonomous semiflow Φ^{y_0} is asymptotically autonomous, and its limit semiflow is Θ.*

For any sequences $t_j \to t$, $s_j \to \infty$, and $x_j \to x$, we have

$$\lim_{j \to \infty} \Phi^{y_0}_{(t_j+s_j, s_j)}(x_j) = \lim_{j \to \infty} \mathrm{pr}_1 \circ \Psi_{t_j}\big(x_j, \Upsilon_{s_j}(y_0)\big) \tag{6.24}$$

$$= \mathrm{pr}_1 \circ \Psi_{\big(\lim_{j \to \infty} t_j\big)} \left(\lim_{j \to \infty} x_j, \lim_{j \to \infty} \Upsilon_{s_j}(y_0) \right) \tag{6.25}$$

$$= \mathrm{pr}_1 \circ \Psi_t(x, 0_Y) = \Theta_t(x), \tag{6.26}$$

where (6.24) follows immediately from (6.21), (6.25) is obtained by the continuity of pr_1 and Ψ, and (6.26) relies on the attractivity of 0_Y. Thus for any $y_0 \in \mathcal{B}(0_Y)$, by definition Φ^{y_0} is asymptotically autonomous with limit semiflow Θ. ▼

STEP 3. *Every trajectory of Ψ converges to a hyperbolic equilibrium.*

Together, Step 2, Fact 6.3, and the boundedness (hence, precompactness) of forward trajectories of Ψ imply that for each $y_0 \in \mathcal{B}(0_Y)$, every trajectory of Φ^{y_0} converges to $\mathcal{R}(\Theta)$, and asymptotic stability of (6.16b) ensures that every trajectory of Υ converges to 0_Y. Thus, in view of (6.22) it is clear that every trajectory of Ψ converges to $\mathcal{R}(\Theta) \times \{0_Y\}$, and all points in this set are hyperbolic equilibria by Step 1. Since hyperbolic equilibria are isolated, by continuity every trajectory converges to a particular hyperbolic equilibrium. ▼

STEP 4. *Almost no trajectories of (6.16a)-(6.16b) converge to an unstable equilibrium.*

All points converging to a hyperbolic equilibrium lie on its global stable manifold, which (for an unstable equilibrium) is the union of countably many embedded submanifolds of positive codimension (see [127, p. 73] or [128, Sec. 2.1]). Hence, this is a meager set of measure zero. Also, all unstable equilibria in $X \times \mathcal{B}(0_Y)$ are hyperbolic by Step 1, and there are countably many of these equilibria due to the isolation of hyperbolic equilibria and the second countability of $X \times \mathcal{B}(0_Y)$ (see [129, Thm 2.50 and Prop. 3.11]). Thus, the set of points in $X \times \mathcal{B}(0_Y)$ converging to an unstable equilibrium is a countable union of meager sets of measure zero and is thus meager (essentially by definition) and measure zero (see [4, p. 128]) in $X \times Y$. ▾

STEP 5. *Almost every trajectory of* (6.16a)-(6.16b) *converges to the stable equilibrium* $(0_X, 0_Y)$.

Since $\mathcal{B}(0_Y)$ is full measure and residual in Y by assumption, $X \times \mathcal{B}(0_Y)$ is full measure and residual in $X \times Y$. By Step 3, every initial condition in this set converges to a hyperbolic equilibrium, and by Step 4, the subset converging to an unstable equilibrium is meager and measure zero in $X \times Y$. Since the difference of a residual set of full measure by a meager set of measure zero is residual and full measure, the remainder constitutes a residual set of full measure in $X \times Y$ for which all initial conditions converge to the unique stable equilibrium $(0_X, 0_Y)$, completing the proof. ∎

Remark 6.3. The main potential pitfall of the driven subsystem being only *almost* globally asymptotically stable is the possibility of "funneling" a non-negligible (*i.e.*, non-meager or positive measure) set to a point $(x, 0_Y)$, where x is an unstable equilibrium of (6.17). However, such behavior is precluded by the hyperbolicity of all unstable equilibria of (6.17). This can be relaxed to the requirement that all unstable equilibria of (6.17) are isolated and have at least one eigenvalue with positive real part, similar to [124]. Then, the argument proceeds similarly, but relies on the center-stable manifold theorem instead of the stable manifold theorem. Similarly, the hyperbolicity assumption on 0_X can be relaxed at the cost of local exponential stability. We present the more succinct but less general result in detail for clarity and brevity.

6.3.2 Extension to Upper Triangular Systems

In fact, much like analogous results for global asymptotic stability of cascades, our conclusions extend immediately to upper triangular systems (*i.e.*, cascade interconnections of cascade systems).

Corollary 6.1 (Almost Global Asymptotic Stability of Upper Triangular Systems)**.** *Consider an upper triangular system evolving on* $X_1 \times X_2 \times \cdots \times X_n$, *given by*

$$\dot{x}_1 = f_1(x_1, x_2, \ldots, x_n), \tag{6.27a}$$

$$\dot{x}_2 = f_2(x_2, \ldots, x_n), \tag{6.27b}$$

$$\ddots$$

$$\dot{x}_n = f_n(x_n), \tag{6.27c}$$

where for all $i = 1, 2, \ldots, n$, the unforced system

$$\dot{x}_i = f_i(x_i, 0_{i+1}, 0_{i+2}, \ldots, 0_n) \tag{6.28}$$

is almost globally asymptotically stable with respect to $0_i \in X_i$ and the chain recurrent set of (6.28) *contains only hyperbolic equilibria. Moreover, suppose that every trajectory of* (6.27a)-(6.27c) *is bounded for all forward time. Then, $(0_1, 0_2, \ldots, 0_n)$ is an almost globally asymptotically stable and locally exponentially stable equilibrium of the upper triangular system* (6.27a)-(6.27c).

Proof. The claim follows directly via induction. In particular, the claim is trivial for $n = 1$, and assuming it holds for $n = k - 1$, the claim for $n = k$ follows by Theorem 6.1 with (6.27a) as the driving subsystem (6.16a) and (6.27b)-(6.27c) as the driven subsystem (6.16b), *i.e.*, $x = x_1$ and $y = (x_2, x_3, \ldots, x_n)$. ∎

6.4 Hypotheses of the Main Results

In this section, we explore the hypotheses of Theorem 6.1 and Corollary 6.1 further and in greater detail, also showing some ways in which they may be verified.

6.4.1 Gradient-Like Systems

A central assumption of Theorem 6.1 was that all chain recurrent points of (6.17) were equilibria. Such systems are usually referred to as follows.

Definition 6.6. An autonomous semiflow Φ is called *gradient-like* if $\mathcal{R}(\Phi) = \mathcal{E}(\Phi)$. ●

The following fact shows that such a property is often easily verified.

Fact 6.4 (Verifying Gradient-Like Systems). *If $\mathcal{E}(\Phi)$ consists of isolated points and there exists a proper, continuous function $V : M \to \mathbb{R}$ that is decreasing along nonequilibrium trajectories, then Φ is gradient-like.*

While we omit a proof of this fact, very similar notions have been discussed in slightly different settings in [124, Sec. IV], [130, Cor. 2.4], and [126, Sec. 7.12]. Above, we recall that a function $V : M \to \mathbb{R}$ is *proper* if it has compact sublevel sets, which is analogous to the notion of "radially unbounded" functions on $\mathbb{R}^n$. Additionally, a function $f : \mathbb{R} \to \mathbb{R}$ is *decreasing* if $f(t_2) < f(t_1)$ whenever $t_1 < t_2$ (but this does *not* imply $\dot{f}(t) < 0$ for all t, since $t \mapsto -t^3$ is a counterexample).

Remark 6.4. From Fact 6.4, it is clear that Theorem 1 also holds if the assumption that (6.17) is almost globally asymptotically stable and gradient-like is replaced by the existence of a Lyapunov function for (6.17) around 0_X which is decreasing along all nonequilibrium trajectories. Some authors [126,130] call this a *strict* Lyapunov function, but the control community tends to reserve this term for Lyapunov functions with strictly negative derivative along nonequilibrium trajectories [131].

We now examine two important classes of gradient-like systems of particular relevance to geometric control design, which are already widely known to be almost globally asymptotically stable. Using Fact 6.4, we verify the straightforward but less widely-known fact that such systems have a chain recurrent set consisting solely of hyperbolic equilibria. The following facts are not particularly novel (see, *e.g.*, the discussion in [124, Sec. IV] and [130]), but they add context to our main result, so we present them for completeness.

No doubt the most obvious gradient-like system is, in fact, a gradient system. We recall the notion of a *navigation function* (originally defined in [97]) from Definition 5.4.

Proposition 6.1 (Gradient Systems). *For a Riemannian manifold* (Q, κ), *an origin* $0_Q \in Q$, *a* 0_Q-*navigation function* V, *the dynamical system*

$$\dot{q} = -\mathrm{grad}_\kappa V(q) \tag{6.29}$$

is almost globally asymptotically stable and locally exponentially stable with respect to 0_Q, *and all chain recurrent points of* (6.29) *are hyperbolic equilibria.*

Proof. The almost global asymptotic stability of (6.29) with respect to 0_Q is proved in [97, Proposition 2.1] for compact Q. However, the extension to the noncompact case is immediate since the sublevel sets of V are compact and forward invariant, since by direct computation,

$$\dot{V} = dV(-\mathrm{grad}_\kappa V) = -\kappa\big(\mathrm{grad}_\kappa V, \mathrm{grad}_\kappa V\big) \leq 0. \tag{6.30}$$

Since the equilibria of (6.29) are simply the critical points of V, the nondegeneracy of the critical points of Morse functions ensures hyperbolicity and therefore the local exponential stability of 0_Q. Finally, since V is decreasing on nonequilibrium trajectories and hyperbolic equilibria are isolated, Fact 6.4 implies that the chain recurrent set of (6.29) is exactly the set of equilibria. ∎

We now turn our attention to the important class of dissipative mechanical systems. Consider a fully-actuated mechanical system Σ in the sense of Definition 3.1, and prescribe the feedback $f_q(\dot{q}) = -\nu^\flat(\dot{q})$ for some Riemannian metric ν (also called a "strict Rayleigh dissipation"). The resulting closed-loop dynamics are then given by

$$\nabla_{\dot{q}}\dot{q} + \mathrm{grad}_\kappa V(q) = -\kappa^\sharp \circ \nu^\flat(\dot{q}). \tag{6.31}$$

Such systems have been studied at length, since the introduction of artificial dissipation and potential shaping via feedback can result in closed-loop dynamics with desirable limit behavior. In fact, closed loop dynamics of this form have enabled trajectory tracking on arbitrary Lie groups [95] and have also been present in the unforced and driving subsystems of cascaded geometric controllers for underactuated robotic systems [96]—indeed, (6.31) is precisely the form of the error dynamics (5.35) in Theorem 5.1, the main result on almost global asymptotic tracking in the previous chapter.

Proposition 6.2 (Dissipative Mechanical Systems). *For a Riemannian manifold* (Q, κ), *an origin* $0_Q \in Q$,

a 0_Q-navigation function V, and any Riemannian metric ν, the dynamical system (6.31) is almost globally asymptotically stable and locally exponentially stable with respect to $0_{TQ} = (0_Q, 0) \in TQ$ (i.e., the zero tangent vector at 0_Q), and all chain recurrent points of (6.31) are hyperbolic equilibria.

Proof. It is clear that the equilibrium set of (6.31) is precisely the image of the critical points of V in the zero section of TQ, and moreover these equilibria can be verified to be hyperbolic since ν is a strict linear dissipation and the critical points of a Morse function are nondegenerate. Moreover, only 0_{TQ} is (locally exponentially) stable, while all other equilibria are unstable, since 0_Q is the unique minimum of V. Considering the total energy function given by

$$W : (q, \dot{q}) \mapsto V(q) + \tfrac{1}{2}\kappa(\dot{q}, \dot{q}), \tag{6.32}$$

we compute

$$\dot{W} = dV(q)\dot{q} + \kappa(\nabla_{\dot{q}}\dot{q}, \dot{q}) \tag{6.33}$$

$$= dV(q)\dot{q} + \kappa(-\mathrm{grad}_\kappa V(q) - \kappa^\sharp \circ \nu^\flat(\dot{q}), \, \dot{q}) \tag{6.34}$$

$$= dV(q)\dot{q} - dV(q)\dot{q} - \nu(\dot{q}, \dot{q}) = -\nu(\dot{q}, \dot{q}) \leq 0. \tag{6.35}$$

For any trajectory $t \mapsto q(t)$ of the Euler-Lagrange dynamics, (6.31) and strictness of ν imply that the quantity $\nu(\dot{q}(t), \dot{q}(t))$ is strictly positive for almost all t if and only if the trajectory is nonequilibrium, so W is decreasing along nonequilibrium trajectories. Thus, by Fact 6.4, the chain recurrent set of (6.31) is exactly the set of equilibria. Becuase W is proper (since V is proper and ν is positive definite) and nonincreasing along trajectories, all forward trajectories are precompact and therefore converge to the chain recurrent set [125]. Since hyperbolic equilibria are isolated, all trajectories converge to some equilibrium. Application of the global stable manifold theorem shows that almost no trajectories converge to an unstable hyperbolic equilibrium, so the unique stable equilibrium 0_{TQ} is almost globally asymptotically stable. ∎

For further discussion, we direct the reader to the seminal work [97] which studies the stability properties and global behavior of such systems (in the more general setting of manifolds with boundary), as well as the more recent reference [9, Chap. 6] which provides a comprehensive and detailed overview. Finally, we note that a primary contribution of [97] is the observation that the global limit behavior of a dissipative mechanical system is essentially determined by the global limit behavior of the associated gradient system, which is often called the "lifting property" of dissipative mechanical systems [9]. Here, we have verified that a similar lifting property holds for these systems in regards to the chain recurrent set.

6.4.2 Boundedness of Forward Trajectories

Another central assumption of Theorem 6.1 was that all forward trajectories of the cascade are bounded. While forward boundedness is guaranteed when the driven subsystem evolves on a compact manifold,

to use Theorem 6.1 to certify the stability of a cascade evolving on a noncompact manifold (e.g. $\mathbb{R}^n$ or any tangent bundle), we require compositional criteria for forward boundedness. In this section, we give growth rate criteria suitable for our geometric setting on the "interconnection term" Σ_h and a on Lyapunov function for the unforced subsystem Σ_x. The result is analogous to (and inspired by) [117, Thm. 4.7], which certifies forward boundedness in $\mathbb{R}^n$ using the standard Euclidean norm. In a Riemannian manifold (X, μ), we use instead the Riemannian distance and the dual norms on each tangent and cotangent space induced by the metric. We denote both norms by $||\cdot||_\mu$.

Theorem 6.2 (Forward Boundedness of Cascades). *Consider a cascade on $X \times Y$ given by*

$$\dot{x} = f(x, y), \tag{6.36a}$$

$$\dot{y} = g(y). \tag{6.36b}$$

Suppose the following conditions hold on the subsystems:

Σ_y: *For (6.36b), $0_Y \in Y$ is a stable hyperbolic equilibrium.*

Σ_x: *$W : X \to \mathbb{R}_{\geq 0}$ is a proper Lyapunov function for*

$$\dot{x} = f(x, 0_Y) \tag{6.37}$$

such that for some constants $\lambda \geq 0, d_0 \geq 1$,

$$||\mathrm{d}W_x||_\mu \operatorname{dist}(0_X, x) \leq \lambda W(x) \tag{6.38}$$

for all $(x, y) \in \{x \in M : \operatorname{dist}(0_X, x) \geq d_0\} \times \mathcal{B}(0_Y)$.

Σ_h: *For some continuous maps $\alpha, \beta : \mathcal{B}(0_Y) \to \mathbb{R}_{\geq 0}$ that are vanishing and differentiable at 0_Y, the interconnection term $h : (x, y) \mapsto f(x, y) - f(x, 0_Y)$ satisfies*

$$||h(x, y)||_\mu \leq \alpha(y) \operatorname{dist}(0_X, x) + \beta(y). \tag{6.39}$$

Then, the trajectory of (6.36a)-(6.36b) through any initial condition $(x_0, y_0) \in X \times \mathcal{B}(0_Y)$ is bounded for all forward time.

Proof. Since W is a proper Lyapunov function for (6.37), the forward trajectory through any initial condition of the form $(x_0, 0_Y)$ is bounded, so it suffices to consider initial conditions (x_0, y_0) with $y_0 \neq 0_Y$. Fix $(x_0, y_0) \in X \times \mathcal{B}(0_Y)$ with $y_0 \neq 0_Y$ and let $(x(t), y(t))$ denote its forward trajectory.

STEP 1. *There exist positive constants A and ω such that $\alpha(y(t)) + \beta(y(t)) \leq Ae^{-\omega t}$ for all $t \geq 0$.*

124

Let $d(t) := \operatorname{dist}(0_Y, y(t)) > 0$. Since 0_Y is hyperbolic, there exist $C_0, \omega > 0$ such that, for all $t \geq 0$,

$$d(t) \leq C_0 e^{-\omega t}. \tag{6.40}$$

Next, since α and β are vanishing and differentiable at 0_Y, a local coordinate calculation (using uniform equivalence of continuous Riemannian metrics over compact sets) shows

$$\limsup_{t \to \infty} \frac{\alpha\big(y(t)\big) + \beta\big(y(t)\big)}{d(t)} < \infty. \tag{6.41}$$

The quotient in the previous limit is a continuous function of t and thus is bounded for all $t \geq 0$ by some $C_1 > 0$. With (6.40), this yields the desired bound with $A := C_0 C_1$. ▼

STEP 2. $W\big(x(t)\big)$ is bounded for all $t \geq 0$.

Since W is a Lyapunov function for (6.37), we have

$$\dot{W} \leq \mathrm{d}W_x\big(h(x, y)\big) \leq ||\mathrm{d}W_x||_\mu \, ||h(x, y)||_\mu \tag{6.42}$$

$$\leq ||\mathrm{d}W_x||_\mu \, \big(\alpha(y) \operatorname{dist}(0_X, x) + \beta(y)\big), \tag{6.43}$$

from (6.39). Hence, whenever $\operatorname{dist}(0_X, x) \geq d_0 \geq 1$, we have

$$\dot{W} \leq ||\mathrm{d}W_x||_\mu \operatorname{dist}(0_X, x)\big(\alpha(y) + \beta(y)\big). \tag{6.44}$$

Define $W_0 = \sup_{\{x : \operatorname{dist}(0_X, x) \leq d_0\}} W(x)$ and consider any $t_2 \geq t_1 \geq 0$ where $W(x([t_1, t_2])) \subseteq [W_0, \infty)$. Then for all $t \in [t_1, t_2]$, (6.38), (6.44), and the conclusion of Step 1 imply

$$\tfrac{d}{dt} W\big(x(t)\big) \leq \lambda A e^{-\omega t} \, W\big(x(t)\big). \tag{6.45}$$

By Grönwall's inequality, we obtain the bound

$$W(x(t_2)) \leq e^{\int_{t_1}^{t_2} \lambda A e^{-\omega t} dt} W(x(t_1)) \leq e^{\frac{\lambda A}{\omega}} W(x(t_1)). \tag{6.46}$$

This implies that for all $t \geq 0$,

$$W(x(t)) \leq C := e^{\frac{\lambda A}{\omega}} \max\big\{W_0, W\big(x(0)\big)\big\}. \quad ▼$$

Thus, since W is proper and 0_Y is attractive, it follows that $\big(x(t), y(t)\big)$ is bounded for all $t \geq 0$. ∎

Such a method can be iterated (*cf.* Corollary 6.1) to check forward boundedness in upper triangular systems.

6.5 Application of the Results

We now revisit the motivating example (6.8a)-(6.8b). It is easily verified that (6.8b) takes the form of the Euler-Lagrange dynamics (6.31) for the kinetic energy metric and Rayleigh dissipation $\kappa = \nu = d\phi \otimes d\phi$ and the navigation function $V : \mathbb{S}^1 \to \mathbb{R}$, $\phi \mapsto 1 - \cos\phi$. Thus by Proposition 6.2, (6.8b) is almost globally asymptotically stable and locally exponentially stable with respect to $y = (\phi, \dot{\phi}) = (0,0)$, and moreover its chain recurrent set consists solely of hyperbolic equilibria. Clearly, the same is true for $x = (\theta, \dot{\theta}) = (0,0)$ with respect to the restriction of (6.8a) to $y = (\phi, \dot{\phi}) = (0,0)$.

By Theorem 6.1, for almost global asymptotic stability it will suffice to show forward boundedness, which we accomplish using the total energy (6.32). The natural choice of metric on the tangent bundle $X = T\mathbb{S}^1$ is the Sasaki metric [105], *i.e.*, $\tilde{\kappa} = \mathrm{d}\theta \otimes \mathrm{d}\theta + \mathrm{d}\dot{\theta} \otimes \mathrm{d}\dot{\theta}$. Then, considering (without loss of generality) the range of angles $\theta \in [-\pi, \pi)$, we have

$$||\mathrm{d}W_x||_{\tilde{\kappa}} \operatorname{dist}(0_X, x) = \sqrt{\sin^2\theta + \dot{\theta}^2}\sqrt{\theta^2 + \dot{\theta}^2} \leq \theta^2 + \dot{\theta}^2 \leq \underbrace{\tfrac{\pi^2}{2}}_{\lambda} \underbrace{(1 - \cos\theta + \tfrac{\dot{\theta}^2}{2})}_{W(x)},$$

since $|\sin\theta| \leq |\theta|$ and $\theta^2 \leq \frac{\pi^2}{2}(1 - \cos\theta)$ for $\theta \in [-\pi, \pi)$, verifying that (6.38) holds. Furthermore, we compute

$$||h(x,y)||_{\tilde{\kappa}} = (1 - \cos 2\phi)(\sin\theta + \dot{\theta}) \leq \underbrace{(1 - \cos 2\phi)\sqrt{2}}_{\alpha(y)} \underbrace{\sqrt{\theta^2 + \dot{\theta}^2}}_{\operatorname{dist}(0_X, x)}, \tag{6.47}$$

so (6.39) holds as well. Thus it follows by Theorem 6.2 that all forward trajectories of (6.8a)-(6.8b) with $y = (\phi, \dot{\phi})$ starting in the basin of attraction of (6.8b) are bounded, and so the system is almost globally asymptotically stable and locally exponentially stable with respect to $(0,0,0,0) \in T\mathbb{T}^2$.

6.6 Discussion

The disturbance robustness of systems with some similar properties, and the connection to gradient-like systems, was discussed in [124, Sec. IV]. However, those results (when combined with [116]) can only certify the stability of a cascade if the driven subsystem is almost globally input to state stable, requiring also "ultimate boundedness" with respect to *any* bounded disturbance, absent from our motivating example.

Our main results show that an upper triangular system consisting of almost globally asymptotically stable, gradient-like subsystems with no degenerate equilibria is itself almost globally asymptotically stable as long as all forward trajectories are bounded. Since *globally* asymptotically stable systems are gradient-like (with a single chain recurrent point at the stable equilibrium, a consequence of Fact 6.4 and the converse Lyapunov theorems), our almost global result is closely analogous to Fact 6.2, the classic result on the

global asymptotic stability cascades with bounded trajectories. Our second theorem generalizes a classic compositional method of verifying forward boundedness using growth rate criteria on the interconnection term and on a Lyapunov function for the unforced subsystem. Unfortunately, the Riemannian distance function used in our condition can be difficult to compute explicitly in complex examples, but even upper and lower bounds on this distance could potentially be used to verify the inequalities.

Gradient-like dynamics are common in the closed-loop subsystems of geometric controllers (*e.g.*, the controllers proposed in Chapter 5 as well as in [95] and [96]). Indeed, since cascades of mechanical systems with suitable dissipation and potential enjoy the required stability and chain recurrence properties, we see promising directions for the constructive synthesis of cascaded geometric controllers with almost global asymptotic stability for underactuated robotic systems, such as those possessing a geometric flat output (such as quadrotors and aerial manipulators). As explored in Chapter 3, such systems enjoy a hierarchical structure wherein the evolution of the system in the shape space is uniquely determined by the evolution in the symmetry group, which may perhaps enable a change of variables to a cascade form, in a manner similar to the hierarchical control example at the start of this chapter.

However, the stability certificates obtained in this chapter are not immediately applicable to the certification of hierarchical *tracking* controllers, because at a minimum, the interconnection term will in general be time-varying. Future work should explore how the ideas presented in this chapter might be extended to this more general setting in order to enable compositional certification of tracking controllers, whereas the current results are only directly applicable to hierarchical designs for regulation. Nonetheless, the observations above provide evidence that our results in this chapter may have notable implications for the systematic synthesis of controllers for complex underactuated systems.

6.7   Conclusion

In this work, we present sufficient conditions for the almost global asymptotic stability of a cascade in which the subsystems are only almost globally asymptotically stable. The result is extended inductively to upper triangular systems of arbitrary size. The approach relies on the forward boundedness of trajectories (which can be verified by growth rate criteria on the interconnection term and on a Lyapunov function for the unforced subsystem) and the absence of chain recurrent points other than hyperbolic equilibria in the unforced subsystem. The results are analogous to classic results for cascades of globally asymptotically stable systems. The compositional nature of the criteria facilitates stability verification for arbitrarily complex cascades, so long as the subsystems enjoy certain fundamental properties.

CHAPTER 7

SYMMETRY-ACCELERATED REINFORCEMENT LEARNING FOR TRAJECTORY TRACKING CONTROL

The material in this chapter is based on the publication [132], co-authored with Nishanth Rao, Pratik Kunapuli, Dinesh Jayaraman, and Vijay Kumar. The author of this thesis led the development of the theoretical contributions and drafted the bulk of the original manuscript. Overall, Nishanth Rao, Pratik Kunapuli, and the author of this thesis all contributed equally to the underlying publication [132].

7.1 Introduction

The last four chapters explored the synthesis of planning and control algorithms (or components thereof) and the prediction of the behavior of dynamical systems (*e.g.*, the closed-loop dynamics induced by a particular control design) using analytical techniques. However, the methods pursued so far relied heavily on assumptions on the structure of the system under consideration (*e.g.*, differential flatness, full actuation, or cascade structure). While many systems of both academic and practical interest enjoy such properties, many others do not, or we may be ignorant of the right point of view from which they can be identified.

In such circumstances, we may have no choice but to turn towards more flexible and generalized tools, such as optimization-based control or data-driven methods, even if guarantees of performance are far murkier or computational costs are far greater. We argue that in such settings, it is *especially* important to leverage what little structure we can, in order to gain traction on the problem. In this chapter, we explore how the symmetries enjoyed by free-flying robotic systems can be used to mitigate the computational burden of training tracking controllers via reinforcement learning, by sharing experience between "equivalent" states. Ultimately, our methods will improve sample efficiency and also empirically yield better-performing policies at convergence, likely due to the simpler structure of the control problem after reducing the symmetry group. The methods in this chapter can be very broadly applied to an extremely wide range of robotic systems, showing that even in very general settings (and for learning-based approaches), structured methods developed from a geometric perspective still have a role to play.

7.1.1 Learned Tracking Controllers

In contrast to analytically-designed control methodologies, controllers trained via reinforcement learning (RL) have relaxed structural assumptions while enabling real-time operation with moderate resources [133]. In [91], the authors train a single hovering policy for deployment across a range of quadrotors, generalizing satisfactorily to moving references. Meanwhile, massively parallel training of quadrupedal walking policies from high-dimensional observations enabled startling robustness to uneven terrain [134],

and learned controllers augmented with adaptive feedforward compensation have been shown to reject large disturbances [93]. Unfortunately, these benefits come at a price: RL tends to scale poorly with the size of the given Markov decision process (MDP), making it challenging to perform the exploration needed to discover high-performance policies.

7.1.2 Symmetry in Reinforcement Learning

To mitigate this burden, an RL agent should share experience across all those states that can be considered "equivalent" with respect to the reward and dynamics. Indeed, robotic systems enjoy substantial symmetry [46, 135, 136], which has been thoroughly exploited in analytical control design [15, 137, 138] and optimization [139]. In fact, many learned controllers have leveraged symmetry in an ad hoc or approximate manner (*e.g.*, penalizing the *error* between actual and reference states [91] or working in the body frame [93]). More formally, the optimal policy of an MDP with symmetry is equivariant (and its value function is invariant) [140], and neural architectures can be designed accordingly to improve sample efficiency and generalization [141].

Instead of incorporating symmetry into the network architecture, [142] proposed "MDP homomorphisms", which establish a mapping from the given MDP to one of lower dimension. There, a policy may be trained more easily (using standard tools) and then lifted back to the original setting. Such methods were originally restricted to discrete state and action spaces, necessitating coarse discretization of robotic tasks (which are naturally described on smooth manifolds). [143] explored related ideas in continuous state and action spaces, but assumed deterministic dynamics (whereas stochasticity is fundamental to many tasks). However, [144] recently extended the theory of homomorphisms of stochastic MDPs to the continuous setting, recovering analogous value equivalence and policy lifting results. They also learned approximate homomorphisms from data, but do not give a sufficient condition to construct a well-behaved homomorphism (*i.e.*, for which the new state and action spaces are also smooth manifolds) from a continuous symmetry known *a priori* (as is the case for free-flying robotic systems [135]).

7.1.3 Overview and Contributions

In this chapter, we explore the role of the continuous symmetries of free-flying robotic systems in learned tracking control. After reviewing mathematical preliminaries in Sec. 7.2, in Sec. 7.3 we cast a general tracking control problem as a continuous MDP, using a stochastic process to model the (*a priori* unknown) reference trajectory. We show that this MDP inherits the symmetry enjoyed by the underlying dynamics and running costs, and we prove that such symmetries can be used to construct an MDP homomorphism, reducing the dimensionality. In Sec. 7.4, we apply this method to three physical systems (including aerial and space robots), obtaining MDPs of reduced dimension that nonetheless capture the essential features of the tracking problem. We then apply standard reinforcement learning techniques to learn policies for these reduced MDPs, accelerating training, improving tracking accuracy, and generalizing zero-shot to new

trajectories. We discuss our results and contributions in Secs. 7.5-7.6. Ultimately, we believe these insights will facilitate the efficient development of accurate tracking controllers for various robotic systems.

7.2 Mathematical Preliminaries

We begin by briefly introducing some concepts of measure-theoretic probability. Throughout this chapter, we largely follow the treatment of [144], which (along with the authors' prior work [145]) extends [142] to study homomorphisms of Markov decision processes with continuous (*i.e.*, not discrete) state and action spaces. Thus, we refer to [144, Appx. B] for a more complete overview of the basic topological and measure-theoretic tools used in this chapter. However, we briefly mention the basics.

7.2.1 Measure Theory and Probability

For any given set X, the *power set*, denoted 2^X, is the set containing all subsets of X. The following class of subsets of the power set are suitable for working with probability.

Definition 7.1. A subset $F \subseteq 2^X$ is called a *σ-algebra* if:

1. $\varnothing \in F$,

2. $X \setminus B \in F$ for all $B \in F$, and

3. for all countable collections $B_1, B_2, \ldots \in F$, it holds that $\left(\bigcup_{i=1}^{\infty} B_i\right) \in F$. ●

In particular, $\mathsf{B}(X)$ denotes the *Borel σ-algebra* of a topological space X, which is defined as the smallest σ-algebra containing all open (or equivalently, closed) subsets of X. In probability theory, each element of a σ-algebra represents an event whose probability can be measured.

Definition 7.2. $\mathsf{P}(X)$ is the set of *Borel probability measures* on X, *i.e.*, maps $\mu : \mathsf{B}(X) \to [0, 1]$ such that:

1. $\mu(\varnothing) = 0$,

2. $\mu(X) = 1$,

3. for all countable, disjoint collections $B_1, B_2, \ldots \in \mathsf{B}(X)$, we have $\sum_{i=1}^{\infty} \mu(B_i) = \mu\left(\bigcup_{i=1}^{\infty} B_i\right)$. ●

For example, the *Dirac measure* $\delta_x \in \mathsf{P}(X)$ of any given element $x \in X$ is defined by

$$\delta_x(B) = \begin{cases} 1, & x \in B, \\ 0, & x \notin B. \end{cases} \tag{7.1}$$

Moreover, given $\mu_1 \in \mathsf{P}(X_1)$ and $\mu_2 \in \mathsf{P}(X_2)$, the *product measure* $\mu_1 \times \mu_2 \in \mathsf{P}(X_1 \times X_2)$ is the unique

measure defined such that for all $B_1 \in \mathsf{B}(X_1)$ and $B_2 \in \mathsf{B}(X_2)$, we have

$$(\mu_1 \times \mu_2)(B_1 \times B_2) = \mu_1(B_1)\,\mu_2(B_2). \tag{7.2}$$

For a function $f : X \to \mathbb{R}$ and a probability measure $\mu \in \mathsf{P}(X)$, the *expectation* of f over μ is given by

$$\mathbb{E}_{x \sim \mu}[\,f\,] = \int_X f \,\mathrm{d}\mu. \tag{7.3}$$

We direct the reader to [144, Appx. B] for further details on probability and measure theory.

7.2.2 Continuous Markov Decision Processes

Definition 7.3 *(see [144]).* A *continuous Markov decision process*[14] is a tuple $\mathcal{M} = (S, A, R, \tau, \gamma)$, where:

- the *state space* S is a smooth manifold,

- the *action space* A is a smooth manifold,

- the *instantaneous reward* is $R : S \times A \to \mathbb{R}$,

- the *transition dynamics* are $\tau : S \times A \to \mathsf{P}(S)$, and

- the *discount factor* γ is a value in the interval $[0, 1)$.   ●

Starting from state s_t and taking action a_t, the probability that the post-transition state s_{t+1} is contained in a set $B \in \mathsf{B}(S)$ is given by $\tau(B \mid s_t, a_t) \in [0, 1]$.

Definition 7.4. A *policy* for $\mathcal{M}$ is a map $\pi : S \to \mathsf{P}(A)$. The *action-value function* $Q^\pi : S \times A \to \mathbb{R}$ of a given policy π is defined by

$$Q^\pi(s, a) = \mathbb{E}_{\tau \sim \pi}\left[\sum_{t=0}^{\infty} \gamma^t R(s_t, a_t) \,\middle|\, s_0 = s, a_0 = a\right], \tag{7.4}$$

where $\tau \sim \pi$ denotes the expectation over both the transitions and the policy (*i.e.*, $s_{t+1} \sim \tau(\,\cdot\mid s_t, a_t)$ and $a_t \sim \pi(\,\cdot\mid s_t)$ for all $t \in \mathbb{N}$). If a policy π^* satisfies

$$\pi^* = \arg\max_\pi \mathbb{E}_{\tau \sim \pi}\left[\sum_{t=0}^{\infty} \gamma^t R(s_t, a_t) \,\middle|\, s_0 = s\right]. \tag{7.5}$$

for all $s \in S$, we say it is an *optimal policy*.   ●

---

[14]The more general definition in [144] does *not* assume S and A are smooth manifolds, nor that $\tau(\,\cdot\mid s, a)$ is a Borel measure. For our purposes, the present level of generality is all we will need.

7.2.3 Homomorphisms of Markov Decision Processes

The following describes a powerful link between two continuous MDPs (of perhaps different dimensions).

Definition 7.5 (*Continuous MDP Homomorphism, [144, Def. 11]*). Consider two continuous MDPs

$$\mathcal{M} = (S, A, R, T, \gamma), \quad \widetilde{\mathcal{M}} = \big(\widetilde{S}, \widetilde{A}, \widetilde{R}, \widetilde{\tau}, \gamma\big) \tag{7.6}$$

and a pair of maps $p : S \to \widetilde{S}$ and $h : S \times A \to \widetilde{A}$. We call $(p, h) : \mathcal{M} \to \widetilde{\mathcal{M}}$ a *continuous MDP homomorphism* if p and the maps $h_s : a \mapsto h(s, a)$ for each $s \in S$ are measurable, surjective maps, such that

$$R(s, a) = \widetilde{R}\big(p(s), h(s, a)\big), \tag{7.7a}$$

$$\tau\big(p^{-1}(\widetilde{B}) \,|\, s, a\big) = \widetilde{\tau}\big(\widetilde{B} \,|\, p(s), h(s, a)\big) \tag{7.7b}$$

for all $s \in S$, $a \in A$, and $\widetilde{B} \in \mathsf{B}(\widetilde{S})$.   ●

Furthermore, policies for two different continuous MDPs can be related in the following manner.

Definition 7.6 (*Policy Lifting, [144, Def. 14]*). Consider a continuous MDP homomorphism $(p, h) : \mathcal{M} \to \widetilde{\mathcal{M}}$ and a policy $\widetilde{\pi}$ for $\widetilde{\mathcal{M}}$. A policy π for $\mathcal{M}$ is called a *lift of $\widetilde{\pi}$* if

$$\pi\big(h_s^{-1}(\widetilde{A}) \,|\, s\big) = \widetilde{\pi}\big(\widetilde{A} \,|\, p(s)\big) \tag{7.8}$$

for all $s \in S$ and $A \in \mathsf{B}(A)$.   ●

MDP homomorphisms facilitate the synthesis and certification of an optimal policy for the "upstairs" MDP $\mathcal{M}$ from an optimal policy for the "downstairs" MDP $\widetilde{\mathcal{M}}$, via the following powerful theorem.

Theorem 7.1 (Value Equivalence [144, Thms. 12 and 16]). *Let $(p, h) : \mathcal{M} \to \widetilde{\mathcal{M}}$ be an MDP homomorphism and π be any lift of some policy $\widetilde{\pi}$ for $\widetilde{\mathcal{M}}$. Then,*

$$Q^{\pi}(s, a) = \widetilde{Q}^{\widetilde{\pi}}\big(p(s), h(s, a)\big). \tag{7.9}$$

Moreover, if $\widetilde{\pi}$ is optimal for $\widetilde{\mathcal{M}}$, then π is optimal for $\mathcal{M}$.

Subsequently, we often omit the word "continuous" for brevity, since we consider only this setting.

7.2.4 Lie Group Symmetries of Markov Decision Processes

A group action can describe a symmetry of some object defined on the manifold. We now formulate the following definition of a Lie group symmetry of a continuous MDP.

Definition 7.7. Consider an MDP $\mathcal{M} = (S, A, R, \tau, \gamma)$ and let the G act on S and A via Lie group actions Φ and Ψ respectively. We call (Φ, Ψ) a *Lie group symmetry* of $\mathcal{M}$ if, for all Φ-invariant sets $B \in \mathsf{B}(S)$,

$$R(s, a) = R(\Phi_g(s), \Psi_g(a)), \tag{7.10a}$$

$$\tau(B \mid s, a) = \tau(B \mid \Phi_g(s), \Psi_g(a)). \tag{7.10b}$$

for all $s \in S$, $a \in A$, and $g \in G$. $\qquad\qquad\qquad\qquad\qquad\qquad\qquad\qquad\bullet$

Remark 7.1. The qualifier "Φ-invariant" on B broadens the class of symmetries considered (and is more general than [140] and [141], as noted in [146, Def. 35]). The deterministic case (*i.e.*, when $\tau(\cdot \mid s_t, a_t)$ is the Dirac measure corresponding to $\{s_{t+1}\} \subseteq S$) gives the intuition, since then (7.10b) requires the image of any orbit in $S \times A$ to lie within some orbit in S, *without* enforcing equivariance *within* each orbit.

7.3 Tracking Control Problems with Symmetry

In this section, we formulate a general trajectory tracking problem as an MDP that models the evolution of both the physical and reference systems. We give a sufficient condition for this MDP to have a Lie group symmetry that will be used (in Sec. 7.3.3) to reduce the problem's dimensionality.

Definition 7.8. A *tracking control problem* is a tuple $\mathcal{T} = (X, U, f, J_X, J_U, \rho, \gamma)$, where:

- the *physical state space* X is a smooth manifold,

- the *physical action space* U is a smooth manifold,

- $f : X \times U \to \mathsf{P}(X)$ is the the *physical dynamics* (*i.e.*, $x_{t+1} \sim f(\cdot \mid x_t, u_t)$ describes the system's evolution),

- $J_X : X \times X \to \mathbb{R}$ is the *tracking cost*,

- $J_U : U \times U \to \mathbb{R}$ is the *effort cost*,

- $\rho \in \mathsf{P}(U)$ is the *reference action distribution*, and

- $\gamma \in [0, 1)$ is the *discount factor*. $\qquad\qquad\qquad\qquad\qquad\qquad\qquad\qquad\bullet$

The distribution ρ is not a traditional part of the notion of a tracking control problem, but it will play an essential role in our approach (see Remark 7.2).

Going forward, we will use the following system as a running example to illustrate the theoretical concepts and the impact of a symmetry-informed approach (even for a simple system).

Example 7.1 (`Particle`). Consider a particle in $\mathbb{R}^3$ with mass m subject to a controlled external force (sometimes used as a reduced-order model for a quadrotor or rocket [93]). The state

$$x = (r, v) \in X = T\mathbb{R}^3 \simeq \mathbb{R}^3 \times \mathbb{R}^3 \tag{7.11}$$

consists of the particle's position and velocity, and the control input is the applied force $u \in U = \mathbb{R}^3$. The (deterministic) equations of motion, when discretized with timestep dt, are given by

$$r_{t+1} = r_t + v_t\,\mathrm{dt}, \quad v_{t+1} = v_t + \tfrac{1}{m}u_t\,\mathrm{dt}, \tag{7.12}$$

so the transition probabilities $f : T\mathbb{R}^3 \times \mathbb{R}^3 \to \mathsf{P}(T\mathbb{R}^3)$ can be expressed using a Dirac measure as

$$f(B \mid x, u) := \begin{cases} 1, & (r + v\,\mathrm{dt}, v + \tfrac{1}{m}u\,\mathrm{dt}) \in B, \\ 0, & \text{otherwise.} \end{cases} \tag{7.13}$$

For some chosen constants $c_r, c_v, c_u \geq 0$, we define the running costs

$$J_{T\mathbb{R}^3}\big((r, v), (r^{\mathrm{d}}, v^{\mathrm{d}})\big) := \alpha(r - r^{\mathrm{d}}) + c_v\big||v - v^{\mathrm{d}}\big||, \tag{7.14a}$$

$$J_{\mathbb{R}^3}(u, u^{\mathrm{d}}) := c_u\big||u - u^{\mathrm{d}}\big||, \tag{7.14b}$$

where $\alpha(y) := c_r\big||y\big|| + \tanh(a_r\big||y\big||) - 1$. Selecting a covariance Σ and a discount factor $0 \leq \gamma < 1$, we define the tracking problem $\mathcal{T} = \big(T\mathbb{R}^3, \mathbb{R}^3, f, J_{T\mathbb{R}^3}, J_{\mathbb{R}^3}, \mathcal{N}(0, \Sigma), \gamma\big)$. ●

7.3.1 Modeling a Tracking Control Problem as a Markov Decision Process

Two essential considerations in the modeling of the tracking control problem are the following:

1. we assume the reference trajectory is unknown *a priori* and is thus unavailable at training time, and

2. we desire a time-invariant policy, so the tracking problem should not depend explicitly on time.

We accomodate these considerations by formulating the trajectory tracking task in the following manner. Our formulation is also illustrative in Fig. 7.1.

Definition 7.9. A given tracking control problem $\mathcal{T} = \big(X, U, f, J_X, J_U, \rho, \gamma\big)$ induces a *tracking control MDP* $\mathcal{M}_{\mathcal{T}} = (S = X \times X \times U, A = U, R, \tau, \gamma)$, where:

- the state is given by $(x, x^{\mathrm{d}}, u^{\mathrm{d}}) \in X \times X \times U$, where $x, x^{\mathrm{d}} \in X$ are the *actual* and *reference states* and $u^{\mathrm{d}} \in U$ is the *reference action*,

- the actions are $a = u \in U$ (*i.e.*, the *actual action*),

$$R\big((x, x^{\mathrm{d}}, u^{\mathrm{d}}), u\big) := -\underbrace{J_X(x, x^{\mathrm{d}})}_{\text{tracking cost}} - \underbrace{J_U(u, u^{\mathrm{d}})}_{\text{effort cost}}$$

physical system

$$x_{t+1} \sim f(\,\cdot\,|\,x_t, u_t)$$

reference trajectory

$$x_{t+1}^{\mathrm{d}} \sim f(\,\cdot\,|\,x_t^{\mathrm{d}}, u_t^{\mathrm{d}}), \quad u_{t+1}^{\mathrm{d}} \sim \rho$$

$$\underbrace{u_t}_{\text{actions}} \sim \pi(\,\cdot\,|\,\underbrace{x_t, x_t^{\mathrm{d}}, u_t^{\mathrm{d}}}_{\text{extended state}})$$
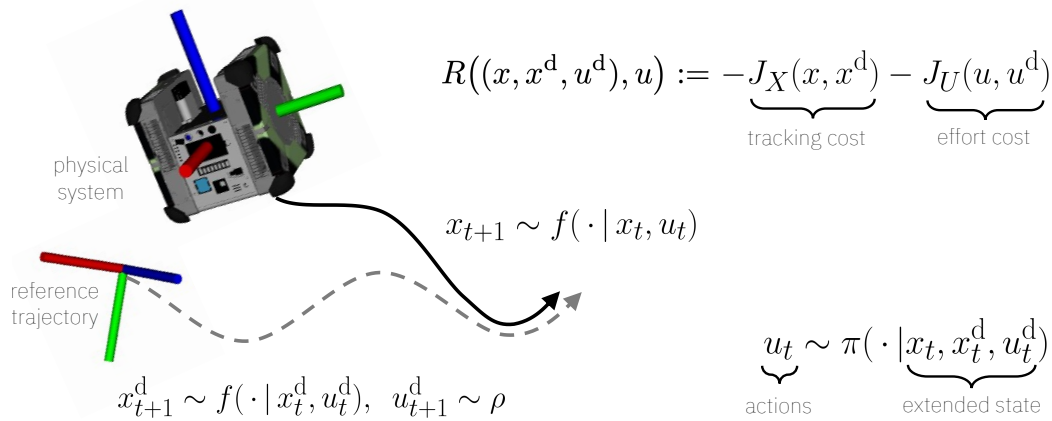
Figure 7.1: We model the tracking control problem using an MDP that governs the evolution of both the physical system (governed by the physical dynamics, subject to the chosen actions) *and* the reference trajectory (governed by the physical dynamics, subjected to *randomly* sampled actions). We seek a policy which selects the actual control actions, conditioned upon an extended state (composed of the actual and reference states and the reference actions), in order to minimize accumulated tracking and effort costs.

- the instantaneous reward $R : S \times A \to \mathbb{R}$ is given by

$$R\big((x, x^{\mathrm{d}}, u^{\mathrm{d}}), u\big) := -J_X(x, x^{\mathrm{d}}) - J_U(u, u^{\mathrm{d}}), \tag{7.15}$$

- and the transitions $\tau : S \times A \to \Delta(S)$ are defined by

$$x_{t+1} \sim f(\,\cdot\,|\,x_t, u_t), \quad x_{t+1}^{\mathrm{d}} \sim f(\,\cdot\,|\,x_t^{\mathrm{d}}, u_t^{\mathrm{d}}), \quad u_{t+1}^{\mathrm{d}} \sim \rho, \tag{7.16}$$

   i.e., the actual state, reference state, and reference inputs are sampled independently. ●

Remark 7.2. This formulation allows us to model a tracking control problem over a broad class of reference trajectories (*i.e.*, those generated by a certain stochastic process) as a single *stationary* MDP (*i.e.*, with time-invariant transitions and reward). While we could also formulate a (*non-stationary*) MDP corresponding to a *particular* reference trajectory by making the tracking cost a function of time t and the actual state x, an optimal policy for that MDP would be useless for tracking *other* references. In Sec. 7.4.2, we will show empirically that policies trained in the proposed manner also effectively track pre-planned reference trajectories, for which the sequence of reference actions $\{u_0^{\mathrm{d}}, u_1^{\mathrm{d}}, u_2^{\mathrm{d}}, \cdots\}$ is chosen to induce a pre-selected state trajectory $\{x_0^{\mathrm{d}}, x_1^{\mathrm{d}}, x_2^{\mathrm{d}}, \cdots\}$.

Example 7.1 (`Particle`, *continued*)**.** The state and inputs of $\mathcal{M}_{\mathcal{T}}$ for `Particle` are given by

$$\big((r, v), (r^{\mathrm{d}}, v^{\mathrm{d}}), u^{\mathrm{d}}\big) \in S = T\mathbb{R}^3 \times T\mathbb{R}^3 \times \mathbb{R}^3, \quad u \in A = \mathbb{R}^3. \tag{7.17}$$

Following (7.12) and (7.16), the transitions dynamics are given by

$$r_{t+1} = r_t + v_t \, \mathrm{dt}, \quad v_{t+1} = v_t + \tfrac{1}{m} u_t \, \mathrm{dt}, \tag{7.18a}$$

$$r_{t+1}^{\mathrm{d}} = r_t^{\mathrm{d}} + v_t^{\mathrm{d}} \, \mathrm{dt}, \quad v_{t+1}^{\mathrm{d}} = v_t^{\mathrm{d}} + \tfrac{1}{m} u_t^{\mathrm{d}} \, \mathrm{dt}, \quad u_{t+1}^{\mathrm{d}} \sim \mathcal{N}(0, \Sigma), \tag{7.18b}$$

while the reward is easily computed as

$$R(s, a) = -\alpha(r - r^{\mathrm{d}}) - c_v \lVert v - v^{\mathrm{d}} \rVert - c_u \lVert u - u^{\mathrm{d}} \rVert, \tag{7.19}$$

following (7.14) and (7.15). ●

7.3.2 Lie Group Symmetries of Tracking Control MDPs

In this section, we will show that the MDP induced by a tracking control problem with certain symmetries will inherit a related symmetry with certain convenient properties. Towards this end, we first prove the following helpful lemma on group actions built out of other group actions.

Lemma 7.1. *Suppose that the action of G on M via Υ is free and proper. Then, the* diagonal action *of G on $M \times M$ given by*

$$\Gamma : \big(g, (m_1, m_2)\big) \mapsto \big(\Upsilon_g(m_1), \Upsilon_g(m_2)\big) \tag{7.20}$$

is also free and proper. Suppose also that the action of H on N via Θ is free and proper. Then, the product action *of $G \times H$ on $M \times N$ given by*

$$\Pi : \big((g, h), (m, n)\big) \mapsto \big(\Upsilon_g(m), \Theta_h(n)\big) \tag{7.21}$$

is also free and proper.

Proof. It is easily verified that (7.20) and (7.21) satisfy the identity and compatibility conditions necessary to be a valid group action.

We first show that the actions are free. Suppose that $\Gamma_g(m_1, m_2) = (m_1, m_2)$. Then it is clear from (7.20) that $\Upsilon_g(m_1) = m_1$ (and hence $g = e_G$, since Υ is free). Likewise, suppose $\Pi_{(g,h)}(m, n) = (m, n)$. Then it is clear from (7.21) that $\Upsilon_g(m) = m$ and $\Theta_h(n) = n$ (and hence $(g, h) = (e_G, e_H) = e_{G \times H}$, since Υ and Θ are free). Thus, Π and Γ are free.

We now show that the actions are proper. By definition, a group action $\Phi : G \times X \to X$ is proper if

$$\hat{\Phi} : G \times X \to X \times X, \ (g, x) \mapsto \big(\Phi_g(x), x\big) \tag{7.22}$$

is a proper map (*i.e.*, the preimage of any compact set is compact). Since smooth manifolds are locally compact and Hausdorff, the product of continuous proper maps between them is also proper [147, §1.5]. Observing that

$$\hat{\Pi} : (g, h, m, n) \mapsto \big(\Upsilon_g(m), \Theta_h(n), m, n\big) \tag{7.23}$$

is (up to permutation of the components) the product map of $\hat{\Upsilon}$ and $\hat{\Theta}$, it follows that Π is proper. Additionally, since Υ is proper, for every compact $C \subseteq \mathcal{M}$, the set

$$G_C^{\Upsilon} = \{g \in G : C \cap \Upsilon_g(C) \neq \varnothing\} \tag{7.24}$$

is compact [4, Prop. 21.5]. Considering any compact subset $L \subseteq \mathcal{M} \times \mathcal{M} \times \mathcal{M} \times \mathcal{M}$, we define the set

$$K = \mathrm{pr}_1(L) \cup \mathrm{pr}_2(L) \cup \mathrm{pr}_3(L) \cup \mathrm{pr}_4(L). \tag{7.25}$$

We may then verify that

$$\hat{\Gamma}^{-1}(L) \subseteq \hat{\Gamma}^{-1}(K \times K \times K \times K) \tag{7.26}$$

$$= \{(g, m_1, m_2) : \Upsilon_g(m_1), \Upsilon_g(m_2), m_1, m_2 \in K\} \tag{7.27}$$

$$\subseteq G_K^{\Upsilon} \times K \times K. \tag{7.28}$$

To complete the argument, it suffices to note that the continuity of $\hat{\Gamma}$ implies that $\hat{\Gamma}^{-1}(L)$ is a closed subset of the compact set $G_K^{\Upsilon} \times K \times K$ and is thus compact. ∎

We now present this section's main result.

Theorem 7.2 (Lie Group Symmetries of Tracking Control MDPs). *Consider a tracking control problem $\mathcal{T} = (X, U, f, J_X, J_U, \rho, \gamma)$, and let $\Upsilon : K \times X \to X$ and $\Theta : H \times U \to U$ be Lie group actions on the physical state and input spaces. Suppose that:*

- *J_X is Υ-invariant and J_U is Θ-invariant, i.e., for all $x, x^{\mathrm{d}} \in X$, $u, u^{\mathrm{d}} \in U$, $k \in K$, and $h \in H$,*

$$J_X(x, x^{\mathrm{d}}) = J_X\big(\Upsilon_k(x), \Upsilon_k(x^{\mathrm{d}})\big), \quad J_U(u, u^{\mathrm{d}}) = J_U\big(\Theta_h(u), \Theta_h(u^{\mathrm{d}})\big), \tag{7.29}$$

- *and for each $(k, h) \in K \times H$, there exists $k' \in K$ such that for all $(x, u) \in X \times U$ and $B \in \mathsf{B}(X)$,*

$$f\big(\Upsilon_{k'}(B) \,|\, x, u\big) = f\big(B \,|\, \Upsilon_k(x), \Psi_h(u)\big). \tag{7.30}$$

Let the direct product group $G = K \times H$ act on $S = X \times X \times U$ and $A = U$ respectively via the actions

$$\Phi_{(k,h)}(x, x^{\mathrm{d}}, u^{\mathrm{d}}) := \big(\Upsilon_k(x), \Upsilon_k(x^{\mathrm{d}}), \Theta_h(u^{\mathrm{d}})\big), \tag{7.31a}$$

$$\Psi_{(k,h)}(u) := \Theta_h(u). \tag{7.31b}$$

Then, (Φ, Ψ) is a Lie group symmetry of $\mathcal{M}_{\mathcal{T}}$. Moreover, suppose additionally that Υ and Θ are free and proper. Then Φ is also a free and proper group action.

Remark 7.3. Because we do *not* assume that $k' = k$, (7.30) is a more general requirement than equivariance of the transitions. However, k' must depend only on k and h, and not on x and u.

Proof of Theorem 7.2. From (7.15), we compute the transformed reward as

$$R\big(\Phi_{(k,h)}(s), \Psi_{(k,h)}(a)\big) = -J_X\big(\Upsilon_k(x), \Upsilon_k(x^{\mathrm{d}})\big) - J_U\big(\Theta_h(u), \Theta_h(u^{\mathrm{d}})\big) \tag{7.32}$$

$$= -J_X(x, x^{\mathrm{d}}) - J_U(u, u^{\mathrm{d}}) = R(s, a), \tag{7.33}$$

where we have substituted in (7.31) and simplified using (7.29). Thus, (7.10a) holds. Considering now the transitions, we note that (7.16) can also be written using the product measure as

$$\tau\big(\,\cdot\,|\,(x, x^{\mathrm{d}}, u^{\mathrm{d}}), u\big) = f(\,\cdot\,|\,x, u) \times f(\,\cdot\,|\,x^{\mathrm{d}}, u^{\mathrm{d}}) \times \rho. \tag{7.34}$$

We then apply the group action (7.31) to the transition dynamics as written in (7.34) and compute

$$\tau\big(\,\cdot\,|\,\Phi_{(k,h)}(s), \Psi_{(k,h)}(a)\big) = f\big(\,\cdot\,|\,\Upsilon_k(x), \Theta_h(u)\big) \times f\big(\,\cdot\,|\,\Upsilon_k(x^{\mathrm{d}}), \Theta_h(u^{\mathrm{d}})\big) \times \rho \tag{7.35}$$

$$= f\big(\Upsilon_{k'}(\,\cdot\,)|\,x, u\big) \times f\big(\Upsilon_{k'}(\,\cdot\,)|\,x^{\mathrm{d}}, u^{\mathrm{d}}\big) \times \rho, \tag{7.36}$$

where (7.36) follows from (7.30). Thus, considering any Φ-invariant set $B \in \mathsf{B}(S)$, in view of (7.36) and the fact that $B = \Phi_g(B)$ for all $g \in K \times H$ by definition, we have

$$\tau\big(B\,|\,\Phi_{(k,h)}(s), \Psi_{(k,h)}(a)\big) = \Big(f\big(\Upsilon_{k'}(\,\cdot\,)|\,x, u\big) \times f\big(\Upsilon_{k'}(\,\cdot\,)|\,x^{\mathrm{d}}, u^{\mathrm{d}}\big) \times \rho\Big) \circ \Phi_{(k'^{-1}, e_H)}(B) \tag{7.37}$$

$$= \big(f(\,\cdot\,|\,x, u) \times f(\,\cdot\,|\,x^{\mathrm{d}}, u^{\mathrm{d}}) \times \rho\big)(B) = \tau\big(B\,|\,s, a\big), \tag{7.38}$$

where (7.38) follows directly from the definition of Φ in (7.31a). Thus, (7.10b) holds as well, and thus (Φ, Ψ) is a Lie group symmetry of $\mathcal{M}_{\mathcal{T}}$.

It remains to show that Φ is free and proper when Υ and Θ are free and proper. Let Γ be the diagonal action of Υ (*i.e.*, $\Gamma_k = \Upsilon_k \times \Upsilon_k$). Then Φ is the product action of Γ and Θ (*i.e.*, $\Phi_{(k,h)} = \Gamma_k \times \Theta_h$). It then suffices to apply Lemma 7.1 twice to show that Γ and ultimately Φ are free and proper actions. ∎

Example 7.1 (`Particle`, *continued*). Considering the Lie groups $K := T\mathbb{R}^3$ (with the obvious group

operation inherited from its identification with $\mathbb{R}^3 \times \mathbb{R}^3$) and $H := \mathbb{R}^3$, we let a K-action on $S = T\mathbb{R}^3$ and an H-action on $A = \mathbb{R}^3$ be given by the left action of the groups on themselves, *i.e.*,

$$\Upsilon_k(r,v) := L_{(k_1,k_2)}(r,v) = (r + k_1, v + k_2), \tag{7.39a}$$

$$\Theta_h(u) := L_h(u) = u + h, \tag{7.39b}$$

which are free and proper. It is clear that the tracking and effort costs (7.14) are invariant to these actions, *i.e.*, (7.29) holds. Moreover, for any $B \in \mathsf{B}(T\mathbb{R}^3)$, we have

$$f\big(B \,|\, \Upsilon_k(x), \Theta_h(u)\big) = f\big(B \,|\, (r + k_1, v + k_2), u + h\big) \tag{7.40}$$

$$= \begin{cases} 1, & \big(r + k_1 + (v + k_2)\,\mathrm{dt}, v + k_2 + \frac{1}{m}(f + h)\,\mathrm{dt}\big) \in B, \\ 0, & \text{otherwise.} \end{cases} \tag{7.41}$$

$$= \begin{cases} 1, & \big(r + v\,\mathrm{dt}, v + \frac{1}{m}f\,\mathrm{dt}\big) \in B - \big(k_1 + k_2\,\mathrm{dt}, k_2 + \frac{1}{m}h\,\mathrm{dt}\big), \\ 0, & \text{otherwise.} \end{cases} \tag{7.42}$$

$$= f\big(\Upsilon_{k'}(B) \,|\, x, u\big), \;\; k' = -(k_1, k_2) - (k_2, \tfrac{1}{m}h)\,\mathrm{dt}. \tag{7.43}$$

Thus, the transitions satisfy (7.30). In the manner of (7.31), the group actions (7.39) induce actions of $G = K \times H = T\mathbb{R}^3 \times \mathbb{R}^3$ on S and A, given respectively by

$$\Phi_{(k,h)}(s) := (r, v, r^{\mathrm{d}}, v^{\mathrm{d}}, u^{\mathrm{d}}) + (k_1, k_2, k_1, k_2, h), \tag{7.44a}$$

$$\Psi_{(k,h)}(a) := u^{\mathrm{d}} + h. \tag{7.44b}$$

Thus, by Theorem 7.2, (Φ, Ψ) is a Lie group symmetry of $\mathcal{M}_\mathcal{T}$ for `Particle`, and Φ is free and proper. $\quad\bullet$

7.3.3 MDP Homomorphisms Induced by Lie Group Symmetries

We will use the following theorem to show that symmetries of a tracking control MDP can be used to reduce its dimensionality via a homomorphism and also give an explicit formula for policy lifting. Although related results are known in the discrete [142] and deterministic [143] settings, we require a more general result due to our continuous state and action spaces and the random sampling of the reference actions (even when the underlying dynamics f are deterministic). The following theorem is illustrated in Fig. 7.2.

Theorem 7.3 (Reduction of Lie Group Symmetries in Continuous MDPs)**.** *Let (Φ, Ψ) be a Lie group symmetry of an MDP $\mathcal{M} = (S, A, R, \tau, \gamma)$. Suppose that Φ is free and proper and $\lambda : S \to G$ is any*[15] *equivariant*

---

[15]Since λ need not be continuous, it can be constructed from a collection of *local* trivializations of the principal G-bundle $p : S \to S/G$ [6, §9.9]. Note that S here is the total space of the bundle (not the quotient or "shape" space, as in earlier chapters).
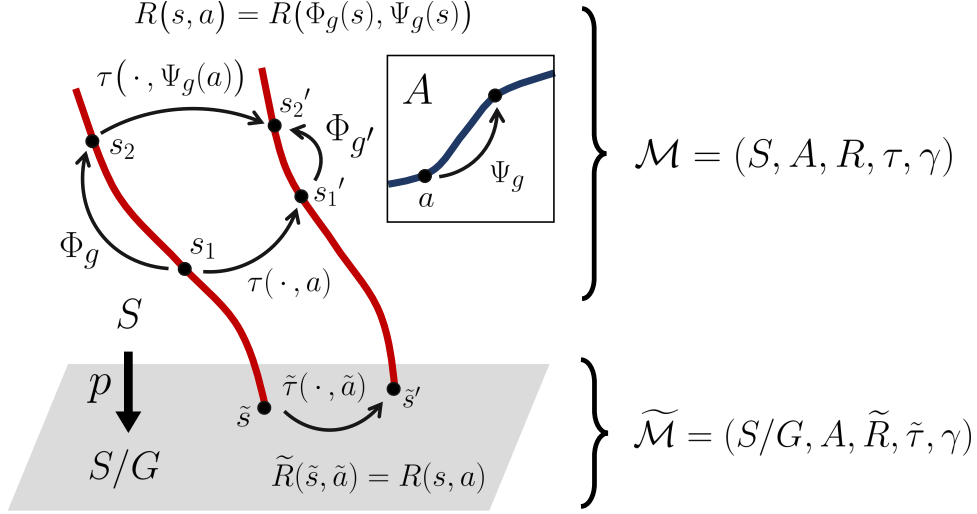
Figure 7.2: A visualization of Theorem 7.3 in the deterministic case, *i.e.*, $s_{t+1} = \tau(s_t, a_t)$. Using a Lie group symmetry (Φ, Ψ), we construct a continuous MDP homomorphism from the "upstairs" MDP $\mathcal{M}$ to a "downstairs" MDP $\widetilde{\mathcal{M}}$ that is a lower-dimensional, lossless abstraction. Theorem 7.1 from [144] guarantees that a (sub)optimal policy for $\widetilde{\mathcal{M}}$, when lifted to an "upstairs" policy for $\mathcal{M}$, is equally (sub)optimal.

map, and define the maps

$$p : S \to S/G, \ s \mapsto \Phi_G(s), \tag{7.45a}$$

$$h : S \times A \to A, \ (s, a) \mapsto \Psi_{\lambda(s)^{-1}}(a). \tag{7.45b}$$

Then, $(p, h) : \mathcal{M} \to \widetilde{\mathcal{M}}$ *is an MDP homomorphism with* $\widetilde{\mathcal{M}} = \big(\widetilde{S} = S/G, \widetilde{A} = A, \widetilde{R}, \widetilde{\tau}, \gamma\big)$, *where we define*

$$\widetilde{R}(\tilde{s}, \tilde{a}) := R\big(s, \Psi_{\lambda(s)}(\tilde{a})\big)\big|_{s \in p^{-1}(\tilde{s})}, \tag{7.46a}$$

$$\widetilde{\tau}(\widetilde{B} \,|\, \tilde{s}, \tilde{a}) := \tau\big(p^{-1}(\widetilde{B}) \,|\, s, \Psi_{\lambda(s)}(\tilde{a})\big)\big|_{s \in p^{-1}(\tilde{s})}, \tag{7.46b}$$

where the right-hand sides of (7.46a) and (7.46b) are independent of the particular choice of s. *Moreover, for any policy* $\widetilde{\pi}$ *for* $\widetilde{\mathcal{M}}$, *a policy for* $\mathcal{M}$ *that is a lift of* $\widetilde{\pi}$ *can be given by*

$$(\widetilde{\pi})^{\uparrow}(A \,|\, s) := \widetilde{\pi}\big(\Psi_{\lambda(s)^{-1}}(A) \,|\, p(s)\big). \tag{7.47}$$

Proof. Because Φ is free and proper, S/G is a smooth manifold of dimension $\dim S - \dim G$ [4, Thm. 21.10]. We first verify that $\widetilde{R}$ and $\widetilde{\tau}$ are well-defined (*i.e.*, their values do not depend on the particular choice of $s \in p^{-1}(\tilde{s})$). Since p maps states to Φ-orbits, for any $s_1, s_2 \in p^{-1}(\tilde{s})$, there exists some $g \in G$

such that $s_1 = \Phi_g(s_2)$. Thus, following (7.46a), we compute

$$R(\tilde{s}, \tilde{a}) = R\big(s_1, \Psi_{\lambda(s_1)}(\tilde{a})\big) \tag{7.48}$$

$$= R\big(\Phi_g(s_2), \Psi_{\lambda(s_2)} \circ \Psi_g(\tilde{a})\big) \tag{7.49}$$

$$= R\big(\Phi_g(s_2), \Psi_{g\lambda(s_2)}(\tilde{a})\big) \tag{7.50}$$

$$= R\big(s_2, \Psi_{\lambda(s_2)}(\tilde{a})\big) = R(\tilde{s}, \tilde{a}), \tag{7.51}$$

where (7.49) follows from the the invariance of the reward, (7.50) follows from the equivariance of λ, and (7.51) uses the invariance of the reward again. Similarly, from (7.46b), we compute

$$\widetilde{\tau}(\widetilde{B} \,|\, \tilde{s}, \tilde{a}) = \tau\big(p^{-1}(\widetilde{B}) \,|\, s_1, \Psi_{\lambda(s_1)}(\tilde{a})\big) \tag{7.52}$$

$$= \tau\big(p^{-1}(\widetilde{B}) \,|\, \Phi_g(s_2), \Psi_{g\lambda(s_2)}(\tilde{a})\big) \tag{7.53}$$

$$= \tau\big(p^{-1}(\widetilde{B}) \,|\, s_2, \Psi_{\lambda(s_2)}(\tilde{a})\big) = \widetilde{\tau}(\widetilde{B} \,|\, \tilde{s}, \tilde{a}), \tag{7.54}$$

where (7.54) follows from (7.10b), since for any $\widetilde{B} \in \mathsf{B}(\widetilde{S})$, $p^{-1}(\widetilde{B}) \in \mathsf{B}(S)$ is a Φ-invariant Borel set.

We now verify that (p, h) is an MDP homomorphism. Since for each $g \in G$, the map Ψ_g is a diffeomorphism, h_s is measurable and surjective for each $s \in S$. On the other hand, p is surjective by construction and measurable because orbits of proper actions are closed [4, Cor. 21.8]. Since clearly $s \in p^{-1}\big(p(s)\big)$, it follows directly from (7.45b) and (7.46a) that

$$\widetilde{R}\big(p(s), h(s, a)\big) = R\big(s, \Psi_{\lambda(s)} \circ \Psi_{\lambda(s)^{-1}}(a)\big) = R(s, a),$$

hence (7.7a) holds. We verify (7.7b) similarly, since by (7.45b) and (7.46b),

$$\widetilde{\tau}\big(\widetilde{B} \,|\, p(s), h(s, a)\big) = \tau\big(p^{-1}(\widetilde{B}) \,|\, s, \Psi_{\lambda(s)} \circ \Psi_{\lambda(s)^{-1}}(a)\big) = \tau\big(p^{-1}(\widetilde{B}) \,|\, s, a\big). \tag{7.55}$$

Thus, $(p, h) : \mathcal{M} \to \widetilde{\mathcal{M}}$ is an MDP homomorphism. Finally, to see that $(\widetilde{\pi})^{\uparrow}$ is a lift of $\widetilde{\pi}$, we compute

$$(\widetilde{\pi})^{\uparrow}\big(h_s^{-1}(\widetilde{A}) \,|\, s\big) = (\widetilde{\pi})^{\uparrow}\big(\Psi_{\lambda(s)}(\widetilde{A}) \,|\, s\big) \tag{7.56}$$

$$= \widetilde{\pi}\big(\Psi_{\lambda(s)^{-1}} \circ \Psi_{\lambda(s)}(\widetilde{A}) \,|\, p(s)\big) = \widetilde{\pi}\big(\widetilde{A} \,|\, p(s)\big), \tag{7.57}$$

where (7.56) follows directly from (7.45b) and the fact that Ψ_g is a diffeomorphism for all $g \in G$, and (7.57) follows directly from (7.47). ∎

Remark 7.4. In the case that Ψ is the trivial action, (p, h) will in fact be a special case of MDP homomorphism known as a "bisimulation relation" (see [144, Def. 4] and discussion therein). Moreover, the condition that Φ is free and proper is required in order to ensure that the state space of the "downstairs" MDP is also a smooth manifold. Notably, a corresponding assumption is absent from the hypothesis of

analogous results on symmetry reduction in discrete MDP's (see, *e.g.*, [141]). This is because the quotient space of a discrete space by an equivalence relation arising from a discrete group action is *always* another discrete space, even though the orbits of the group action may, for example, be of non-uniform cardinality.

7.4 Application to Free-Flying Robotic Systems

In this section, we apply the abstract results of the previous section to reduce the dimensionality of tracking control MDPs for several free-flying robotic systems, visualized on the left-hand side of Fig. 7.3.

7.4.1 Quotient MDPs for Tracking Control Problems

We now formulate the tracking control MDPs for three example tracking control problems, and apply our approach to obtain a reduction of dimensionality. In particular, we will apply Theorem 7.2 to identify a certain kind of Lie group symmetry of the tracking control MDP, Theorem 7.3 to parlay this symmetry into a continuous MDP homomorphism (thereby reducing the dimension of the MDP) and obtain a formula for policy lifting, and Theorem 7.1 (from [144]) to certify the value equivalence of the lifted policy.

Example 7.1 (`Particle`, *continued*). Using the symmetry (7.44) of $\mathcal{M}_{\mathcal{T}}$ for the `Particle`, we will construct an MDP homomorphism using Theorem 7.3. To do so, we first define the maps

$$\lambda\big((r, v), (r^{\mathrm{d}}, v^{\mathrm{d}}), u^{\mathrm{d}}\big) := \big((r^{\mathrm{d}}, v^{\mathrm{d}}), u^{\mathrm{d}}\big), \tag{7.58}$$

$$p\big((r, v), (r^{\mathrm{d}}, v^{\mathrm{d}}), u^{\mathrm{d}}\big) := (r - r^{\mathrm{d}}, v - v^{\mathrm{d}}). \tag{7.59}$$

It is easily verified that λ is equivariant and p maps each state s to its Φ-orbit. We now define a quotient MDP $\widetilde{\mathcal{M}}_{\mathcal{T}}$ as described in Theorem 7.3, where the state and actions of $\widetilde{\mathcal{M}}_{\mathcal{T}}$ are given by

$$\tilde{s} = (r^{\mathrm{e}}, v^{\mathrm{e}}) \in \widetilde{S} = S/G \simeq T\mathbb{R}^3, \quad \tilde{a} = u^{\mathrm{e}} \in \widetilde{A} = \mathbb{R}^3. \tag{7.60}$$

From (7.45b) and (7.58), we may derive

$$h(s, a) = \Psi_{(-r^{\mathrm{d}}, -v^{\mathrm{d}}, -u^{\mathrm{d}})}(u) = u - u^{\mathrm{d}}. \tag{7.61}$$

Since clearly $\big((r^{\mathrm{e}}, v^{\mathrm{e}}), (0,0), 0\big) \in p^{-1}(r^{\mathrm{e}}, v^{\mathrm{e}})$, from (7.46a), (7.44b), and (7.58) we may construct the reduced reward as

$$\widetilde{R}(\tilde{s}, \tilde{a}) = R\big(s, \Psi_{\lambda(s)}(\tilde{a})\big)\Big|_{s=\big((r^{\mathrm{e}}, v^{\mathrm{e}}), (0,0), 0\big)} = -\alpha(r^{\mathrm{e}}) - c_v \big|\big|v^{\mathrm{e}}\big|\big| - c_u \big|\big|u^{\mathrm{e}}\big|\big|. \tag{7.62}$$

Likewise, a straightforward calculation using (7.18), (7.44b), and (7.46b) will show that the reduced transi-

tions are given by

$$\widetilde{\tau}(\widetilde{B} \mid \tilde{s}, \tilde{a}) = \tau\big(p^{-1}(\widetilde{B}) \mid s, \Psi_{\lambda(s)}(\tilde{a})\big)\Big|_{s=\big((r^{\mathrm{e}},v^{\mathrm{e}}),(0,0),0\big)}$$

$$= \begin{cases} 1, & (r^{\mathrm{e}} + v^{\mathrm{e}}\,\mathrm{dt},\, v^{\mathrm{e}} + \frac{1}{m}u^{\mathrm{e}}\,\mathrm{dt}) \in \widetilde{B}, \\ 0, & \text{otherwise}, \end{cases} \tag{7.63}$$

which is nothing but the usual "error dynamics" [95] governing the state-valued error in Def. 5.6, *i.e.*,

$$r^{\mathrm{e}}_{t+1} = r^{\mathrm{e}}_t + v^{\mathrm{e}}_t\,\mathrm{dt}, \quad v^{\mathrm{e}}_{t+1} = v^{\mathrm{e}}_t + \tfrac{1}{m}u^{\mathrm{e}}_t\,\mathrm{dt}. \tag{7.64}$$

Finally, by Theorem 7.3, (p,h) is an MDP homomorphism from $\mathcal{M}_{\mathcal{T}}$ to $\widetilde{\mathcal{M}}_{\mathcal{T}} = \big(T\mathbb{R}^3, \mathbb{R}^3, \widetilde{R}, \widetilde{\tau}, \gamma\big)$, and moreover we may lift any policy $\widetilde{\pi}$ for $\widetilde{\mathcal{M}}_{\mathcal{T}}$ to $\widetilde{\mathcal{M}}$ using (7.47), obtaining

$$(\widetilde{\pi})^{\uparrow}(A \mid s) = \widetilde{\pi}(A - u^{\mathrm{d}} \mid r - r^{\mathrm{d}}, v - v^{\mathrm{d}}). \tag{7.65}$$

By Theorem 7.1, the action-value function for $(\widetilde{\pi})^{\uparrow}$ satisfies

$$Q^{(\widetilde{\pi})^{\uparrow}}(s, a) = \widetilde{Q}^{\widetilde{\pi}}\big((r - r^{\mathrm{d}}, v - v^{\mathrm{d}}), u - u^{\mathrm{d}}\big). \tag{7.66}$$

In summary, an optimal policy for the `Particle` can observe only the position and velocity error and augment the result with the reference force. For a deterministic "downstairs" policy $\tilde{\pi}$, this would result in a lifted policy of the form $u = (\widetilde{\pi})^{\uparrow}(s) = \tilde{\pi}(r - r^{\mathrm{d}}, v - v^{\mathrm{d}}) + u^{\mathrm{d}}$.   ●

While the `Particle` example was chosen to be deliberately simple for illustrative purposes, we now turn our attention to somewhat more realistic examples of free-flying robotic systems.

Example 7.2 (`Astrobee` *[148]*)**.** This space robot has state $x = (q, \xi)$ in $X = \mathrm{SE}(3) \times \mathbb{R}^6$, where q is the system's pose as a homogeneous transform and $\xi = (\omega, v)$ is the system's twist (*i.e.*, its angular and linear velocities). The action $u = (\mu, f)$ in $U = \mathbb{R}^6$ is the control wrench, where μ is the applied torque in the body frame and f is the applied force in the world frame. The dynamics are given by

$$q_{t+1} = q_t \exp(\hat{\xi}_t\,\mathrm{dt}), \tag{7.67a}$$

$$v_{t+1} = v_t + \tfrac{1}{m}f_t\,\mathrm{dt}, \quad \omega_{t+1} = \omega_t + \mathbb{J}^{-1}(\mu_t - \omega_t \times \mathbb{J}\,\omega_t)\,\mathrm{dt}, \tag{7.67b}$$

where $\hat{\cdot} : \mathbb{R}^6 \to \mathfrak{se}(3)$ is the "hat map" sending twists to the Lie algebra. The running costs are defined by

$$J_X(x, x^{\mathrm{d}}) := \alpha(r - r^{\mathrm{d}}) + c_R\big|\big|\log(R^{\mathrm{T}}R^{\mathrm{d}})\big|\big| + c_\xi\big|\big|\xi - \xi^{\mathrm{d}}\big|\big|, \tag{7.68a}$$

$$J_U(u, u^{\mathrm{d}}) := c_u\big|\big|u - u^{\mathrm{d}}\big|\big|, \tag{7.68b}$$

where r and R are the $\mathbb{R}^3$ and $\mathrm{SO}(3)$ components of q. Letting $\rho = \mathcal{N}(0, \Sigma)$ for some covariance Σ, we may construct $\mathcal{M}_{\mathcal{T}}$ as in Def. 7.9.

Next, let $K = \mathrm{SE}(3)$ and $H = \{e\}$ (the trivial group) act on X and U respectively via the group actions

$$\Psi_k(q, \xi) := (kq, \xi), \quad \Upsilon_h(w) := w. \tag{7.69}$$

It can easily be verified that these are free and proper actions for which (7.29) and (7.30) also hold. Using Theorem 7.2 to derive a symmetry of $\mathcal{M}_{\mathcal{T}}$ as in (7.31), we apply Theorem 7.3 with $\lambda : s \mapsto q$ to ultimately obtain an MDP homomorphism (p, h), where $h_s = \mathrm{id}$ for all $s = (q, \xi, q^{\mathrm{d}}, \xi^{\mathrm{d}}, u^{\mathrm{d}}) \in S$, and

$$p(s) := \left(q^{-1}q^{\mathrm{d}}, \xi, \xi^{\mathrm{d}}, u^{\mathrm{d}}\right). \tag{7.70}$$

Thus, an optimal policy (and its Q function) can be written

$$(\widetilde{\pi})^{\uparrow}(A \mid s) = \widetilde{\pi}\left(A \mid (q^{-1}q^{\mathrm{d}}, \xi, \xi^{\mathrm{d}}, u^{\mathrm{d}})\right), \tag{7.71}$$

$$Q^{(\widetilde{\pi})^{\uparrow}}(s, a) = \widetilde{Q}^{\widetilde{\pi}}\left((q^{-1}q^{\mathrm{d}}, \xi, \xi^{\mathrm{d}}, u^{\mathrm{d}}), u\right), \tag{7.72}$$

where $\widetilde{\pi}$ is an optimal policy for the reduced tracking control MDP $\widetilde{M_{\mathcal{T}}}$. In summary, an optimal policy for the `Astrobee` can be expressed using an observation that sees only the *error* between the actual and reference poses, instead of observing these poses separately. $\bullet$

Example 7.3 (`Quadrotor` *[25]*). Analogous to Example 3.3, this aerial robot has the same state space as the `Astrobee`, but the actions are the "single-rotor thrusts" $u \in U = \mathbb{R}^4$. The dynamics and running costs are as given in (7.67) and (7.68), but with the applied force and torque given by

$$f_t = \begin{bmatrix} 0 \\ 0 \\ u_t^1 + u_t^2 + u_t^3 + u_t^4 \end{bmatrix}, \quad \mu_t = \begin{bmatrix} \ell\left(u_t^1 - u_t^3\right) \\ \ell\left(u_t^2 - u_t^4\right) \\ c\left(u_t^1 - u_t^2 + u_t^3 - u_t^4\right) \end{bmatrix}, \tag{7.73}$$

while the translational dynamics in (7.67) are replaced by

$$v_{t+1} = v_t + \left(\tfrac{1}{m}f_t - R_t^{\mathrm{T}}(\mathrm{g}\,\mathrm{e}_3)\right)\mathrm{dt}, \tag{7.74}$$

where g is the magnitude of gravitational acceleration and $\mathrm{e}_3 = (0, 0, 1)$.

Gravity "breaks" the $\mathrm{SE}(3)$ symmetry of the system, but preserves the subgroup of $\mathrm{SE}(3)$ given by

$$K' = \left\{ \begin{bmatrix} \mathrm{rot}_z(\theta) & r \\ 0 & 1 \end{bmatrix} : (r, \theta) \in \mathbb{R}^3 \times \mathbb{S}^1 \right\} \tag{7.75}$$

144

which is isomorphic (as a Lie group) to the direct product $\mathrm{SE}(2) \times \mathbb{R}$. This subgroup inherits an action on $\mathrm{SE}(3) \times \mathbb{R}^6$ via the restriction of (7.69). Using Theorems 7.2 and 7.3, we may derive an MDP homomorphism (p, h) for which $h_s = \mathrm{id}$ for all $s = (q, \xi, q^\mathrm{d}, \xi^\mathrm{d}, u^\mathrm{d}) \in S$ and $p : S \to S/G$ is given by

$$p(s) := (q^{-1}q^\mathrm{d}, R^\mathrm{T}\mathrm{e}_3, \xi, \xi^\mathrm{d}, u^\mathrm{d}), \tag{7.76}$$

where we note that $R^\mathrm{T}\mathrm{e}_3$ is nothing but the gravity direction expressed in body coordinates. Thus, an optimal policy (and its Q function) can be written

$$(\widetilde{\pi})^\uparrow(A \mid s) = \widetilde{\pi}\big(A \mid (q^{-1}q^\mathrm{d}, R^\mathrm{T}\mathrm{e}_3, \xi, \xi^\mathrm{d}, u^\mathrm{d})\big), \tag{7.77}$$

$$Q^{(\widetilde{\pi})^\uparrow}(s, a) = \widetilde{Q}^{\widetilde{\pi}}\big((q^{-1}q^\mathrm{d}, R^\mathrm{T}\mathrm{e}_3, \xi, \xi^\mathrm{d}, u^\mathrm{d}), u\big). \tag{7.78}$$

where $\tilde{\pi}$ is an optimal policy for $\widetilde{M}_{\mathcal{T}}$. In summary, our theory demonstrates that for quadrotors, the state space of the tracking problem can be reduced by replacing the reference and actual poses with the pose error and the body-frame gravity vector, without degrading the best-case learned policy. Consider how this differs from heuristic approximations in prior work such as [91], whose state included the entire orientation R (incompletely reducing the symmetry) and replaced the actual and reference angular velocities with the velocity error, which corresponds to an *approximate* symmetry due to the "cross terms" in the Euler rotation equations in (7.67), which are small for small angular velocities. ●

7.4.2 Numerical Experiments

To explore the effects of our symmetry-informed approach on sample efficiency and the performance of trained policies, we perform numerical experiments in which we apply a standard reinforcement learning algorithms to the reduced tracking control MDPs for the three example systems.[16]

RL environments were implemented for each of the tracking control MDPs in Examples 7.1-7.3, written in `jax` [150] for performance. To implement environments for the quotient MDP arising from reduction by a symmetry group, we modify each environment's observation to the reduced state given in (7.59), (7.70), and (7.76), whereas the baseline sees the full-state observation $(x, x^\mathrm{d}, u^\mathrm{d})$. As indicated respectively by (7.65)-(7.66), (7.71)-(7.72), and (7.77)-(7.78), we also modify (*i.e*, lift) the actions generated by the learned policy and those passed to the action-value function (which was necessary only for the `Particle`, since the MDP homomorphisms for the other two systems were bisimulation relations). For the `Particle` environment, we further isolate the effects of reduction by different subgroups of the symmetry given in (7.44) by also implementing environments where the reduction is by translational symmetry alone (*i.e.*, $p(s) := (r - r^\mathrm{d}, v, v^\mathrm{d}, u^\mathrm{d})$) and by translational and velocity symmetry alone (*i.e.*, $p(s) := (r - r^\mathrm{d}, v - v^\mathrm{d}, u^\mathrm{d})$).

---

[16]The reinforcement learning environments described in this section were developed by Pratik Kunapuli and Nishanth Rao, who also performed the numerical experiments described in this section [149]. All code necessary to reproduce these experiments is open source, available at `https://pratikkunapuli.github.io/EQTrackingControl/`.

Table 7.1: Comparison of RMS Tracking Error on Planned Trajectories

Environment	G	r [cm]	v [cm/s]	R [rad]	ω [rad/s]
Particle	Baseline	298.3 ± 1.2	103.0 ± 1.1	-	-
	$\mathbb{R}^3$	10.0 ± 0.1	4.8 ± 0.1	-	-
	$T\mathbb{R}^3$	9.8 ± 0.2	4.3 ± 0.0	-	-
	$T\mathbb{R}^3 \times \mathbb{R}^3$	$\mathbf{8.3 \pm 0.1}$	$\mathbf{3.9 \pm 0.2}$	-	-
Astrobee	Baseline	10.4 ± 1.0	6.0 ± 1.0	0.75 ± 0.01	0.24 ± 0.02
	$\mathrm{SE}(3)$	$\mathbf{1.3 \pm 2.7}$	$\mathbf{3.3 \pm 3.1}$	$\mathbf{0.37 \pm 0.04}$	$\mathbf{0.16 \pm 0.06}$
Quadrotor	Baseline	66.3 ± 3.2	41.3 ± 2.5	0.48 ± 0.02	0.25 ± 0.02
	$\mathrm{SE}(2) \times \mathbb{R}$	$\mathbf{28.4 \pm 4.1}$	$\mathbf{19.6 \pm 3.1}$	$\mathbf{0.25 \pm 0.05}$	$\mathbf{0.12 \pm 0.01}$

We report the mean and standard deviation (over 10 training seeds) of the trained policy's RMS tracking error (for a dataset of 20 planned trajectories). The baseline policies correspond to reduction by the trivial group (*i.e.*, no reduction).

We use a custom implementation of Proximal Policy Optimization (PPO) [151] with the same hyperparameters across all variants of each environment. During training, the reference actions are sampled from a stationary distribution (as in Def. 7.9), while during evaluation, we measure the performance of the policy obtained on pre-planned dynamically feasible reference trajectories. Fig. 7.3 and Table 7.1 report total reward (during training) and average tracking error (during evaluation) when starting from a randomly sampled initial state. Rollouts of trained policies are visualized at `https://youtu.be/AosGBe2uzxM`.

7.5   Discussion

There is a clear pattern in the left-hand plots of Fig. 7.3: as we increase the dimension of the symmetry group by which we reduce the tracking control MDP, we see an improvement in sample efficiency. Moreover, the tracking error evaluation shown in Table 7.1 and the right-hand plots of Fig. 7.3 follow a similar trend, in which performance at (or near) convergence improves with greater symmetry exploitation. For the `Particle`, the vast majority of this benefit is achieved by reduction of the translational symmetry, although incorporating the velocity and force symmetries yields modest additional gains. This seems consistent with the large improvement we see for the `Astrobee` and `Quadrotor` after reduction by (a subgroup of) $\mathrm{SE}(3)$, although future work could also consider reducing a larger symmetry group that incorporates a linear velocity symmetry for these systems as well. It's worth noting that careful reward engineering or hyperparameter tuning might improve the performance of *all* trained policies (especially the baselines, which currently perform relatively poorly). However, we instead focus on analyzing the benefit of exploiting symmetry for a fixed reward. Nonetheless, any reward depending only on the reduced state $\tilde{s} = p(s)$ would preserve the symmetry.
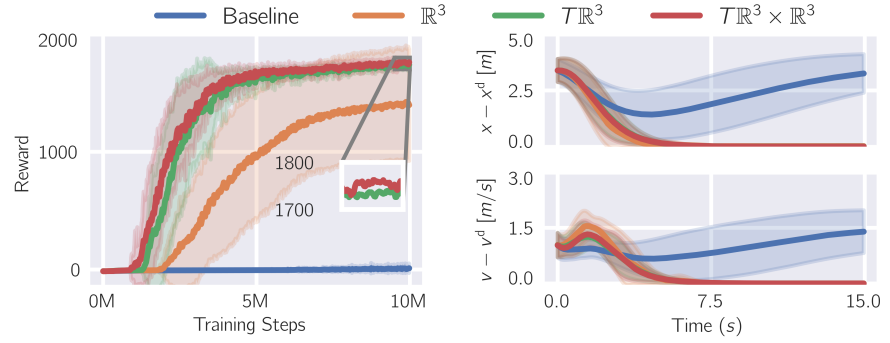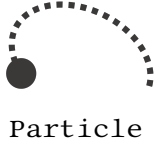
(a) Training curves (left) and evaluation results (right) for `Particle`.
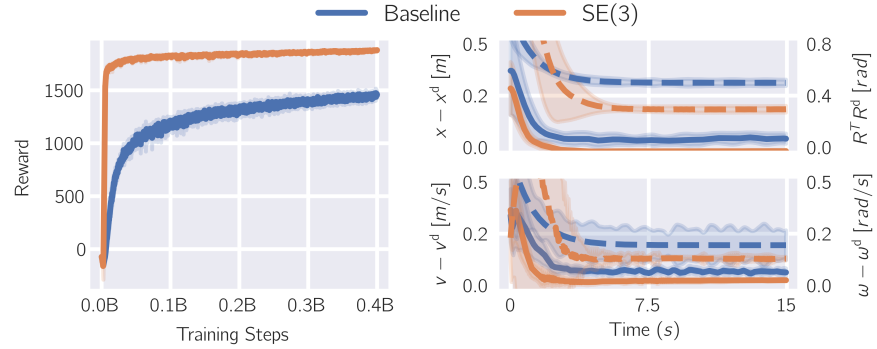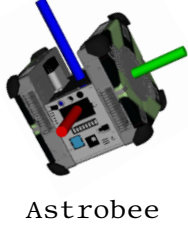
(b) Training curves (left) and evaluation results (right) for `Astrobee`.
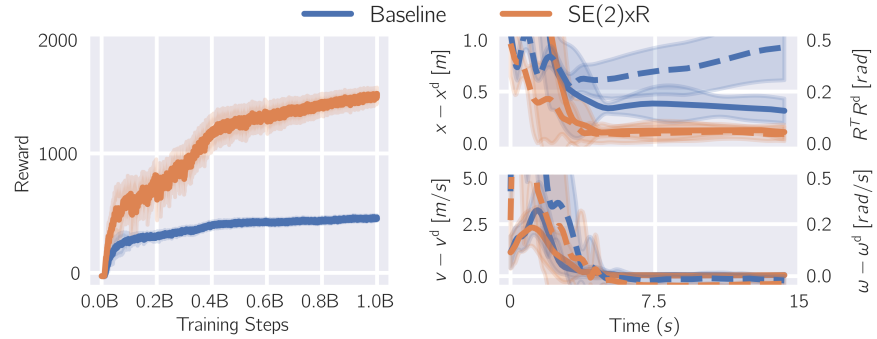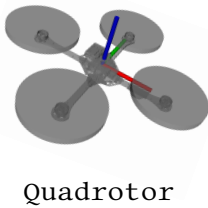
(c) Training curves (left) and evaluation results (right) for `Quadrotor`.

Figure 7.3: To evaluate our approach, we compare baseline policies (trained directly on the original tracking control MDP) with symmetry-informed policies (trained on the reduced tracking control MDP and lifted to the original setting). We report mean reward and standard deviation during training (over 10 training seeds) and, for the best-performing seed, mean tracking error during evaluation (for 20 trajectories), with translational errors as solid lines and rotational errors as dashed lines.

Our approach assumes that at deployment, an upstream planner provides dynamically feasible reference trajectories. For the (underactuated) `Quadrotor`, these trajectories are planned using differential flatness [25] from Lissajous curves in the flat space. However, in theory any other method (*e.g.*, direct collocation [20]) could be used to generate a suitable reference. We expect our policies to generalize well to a wide range of upstream planning methodologies, and future work should explore this hypothesis. Going forward, we also hope to apply these methods to new robot morphologies that are too complex for real-time numerical optimal control or for which no closed-form analytical controllers are known (whereas explicit geometric controllers have been shown to perform quite well, even comparably to learned controllers, for simple systems like quadrotors [94]). To enable such applications, a more unified treatment of the reduction of tracking control MDPs for multibody robotic systems would be beneficial, instead of applying our abstract results on symmetries of tracking control MDPs (Theorems 7.2 and 7.3) individually to each robot morphology (as we did in Sec. 7.4.1).

7.6   Conclusion

In this chapter, we have exploited the natural Lie group symmetries of free-flying robotic systems to mitigate the challenges of training trajectory tracking controllers via reinforcement learning. We formulate the tracking problem as a single stationary MDP, proving that the underlying symmetries of the dynamics and running costs permit the reduction of this MDP to a lower-dimensional problem. When learning tracking controllers for space and aerial robots, training is accelerated and tracking error is reduced after the same number of training steps. We believe our theoretical framework provides insight into the use of RL for systems with symmetry in robotics applications.

CHAPTER 8

CONCLUSION

In this dissertation, we have developed a range of methods enabling dynamically feasible trajectory planning and trajectory tracking controller synthesis for mechanical systems, which have significant bearing on the control of free-flying robotic systems, especially those that are underactuated. While a wide range of formal tools were brought to bear on these problems, a recurring theme was the use of differential geometry to develop abstractions in an explainable and structured manner, thereby capturing only the most essential features of the problem and ultimately leading to computationally efficient solutions.

8.1 The Recurring Theme of Abstraction

At this point, it's worth revisiting in more detail the theme of abstraction described in the introduction, and examining how it has played out within the body of this thesis. In the case of flatness-based methods, a flat output can be thought of (at least locally) as a minimal representation of the family of dynamically feasible trajectories. We developed methods of systematically constructing such abstractions (instead of guessing them individually for particular systems), and moreover of ensuring that the abstraction we obtain preserves symmetries found in the original system. Such abstractions also afforded a deeper insight into the role of robot morphology in enabling tractable solutions to control problems, as explored in the setting of trajectory planning for underactuated aerial manipulators, and the insights obtained in regards to the mechanical design of such systems for "task flatness" or stable internal dynamics.

In our work synthesizing explicit tracking controllers for fully-actuated systems, the central ingredient in the approach was finding a means of reducing the tracking control problem to the "easier" problem of regulation (*i.e.*, stabilizing an equilibrium). In particular, we showed that this can be done on a more general class of manifolds than previously understood (something of a "Goldilocks" setting, in which we have just enough structure, but no more than necessary), enabling the broader application of such methods while also affording a deeper conceptual understanding of existing approaches. Such a reduction from tracking to regulation is inherently lossy, since the chosen control action must be independent of the absolute state of the system, depending instead on the error alone. However, we demonstrate that the asymptotic behavior of the closed-loop system is still as desired, and the control policy can be written down explicitly.

Moreover, in our work analyzing (and exploiting) the symmetries of tracking control problems, we showed that for some systems, optimal tracking control policies indeed need only to observe the error between particular reference and actual states (and thus, in some cases, working with error states is in fact lossless). We also showed that compositional tools for stability certification in cascade systems can be reformulated in a more general "almost global" manner, the natural setting for systems evolving on manifolds. Our

conclusions were analogous to classical *global* results on cascade stability, identifying circumstances in which we can analyze a more complex system via properties of its constituent subsystems. We believe our results in this direction will ultimately have a role to play in certifying the stability of complex hierarchical controllers built out of simpler subsystem controllers.

8.2   Limitations and Future Work

The methods presented herin rely fundamentally on exploiting structural properties of the system under consideration. Thus, their limitations are most keenly apparent in regards to systems which do *not* enjoy these properties (or exhibit them only in an approximate sense). For example, our sufficient conditions for flatness are formulated for mechanical systems in the absence of dissipation (however, other methods [36] have been developed for working with flat systems perturbed by unmodeled disturbances, *e.g.*, air resistance). Moreover, essentially all of these methods require an accurate model of the system to be controlled—*including* the reinforcement learning approach of Chapter 7, since the poor sample efficiency of so-called "model-free" RL necessitates training in simulation (*i.e.*, using a model), introducing a host of well-known challenges for transferring policies to the real-world system.

The contributions of this thesis are primarily theoretical and computational in nature, and thus the most urgent direction for future work is to operationalize these insights and implement them on practical robotic systems, in order to determine the extent to which they are applicable in real-world scenarios. However, it must be noted that many of the methods proposed in this work generalize or systematize existing ad hoc approaches that have *already* been demonstrated on real robot hardware (and are, in some cases, ubiquitous). Thus, in addition to the mathematical and computational results presented herein, we have strong reasons to believe that our approaches will be suitable for practical applications, but this hypothesis must be tested empirically.

Towards such practical ends, the computational maturation of many of the methods developed herein is essential. For example, developing more robust software capable of applying our sufficient conditions for flat output construction from Chapter 3 to arbitrary robotic systems (described in a standard modeling format) would allow practitioners to leverage these tools, even without significant expertise in the geometric methods used in their development. Similarly, while the customized reinforcement learning environments developed for the numerical experiments of Chapter 7 were highly optimized for the particular systems considered, it would be beneficial (and relatively straightforward) to integrate the insights obtained into more generalized reinforcement learning environments that already integrate multibody dynamics engines (*e.g.*, Isaac Gym [152]), in order to apply them more broadly.

In a different vein, the mechanical design criteria for underactuated aerial manipulators discovered in Chapter 4 suggest that significant improvements in dynamic and dexterous manipulation tasks can be achieved not only via more sophisticated control algorithms, but also via control-informed system design.
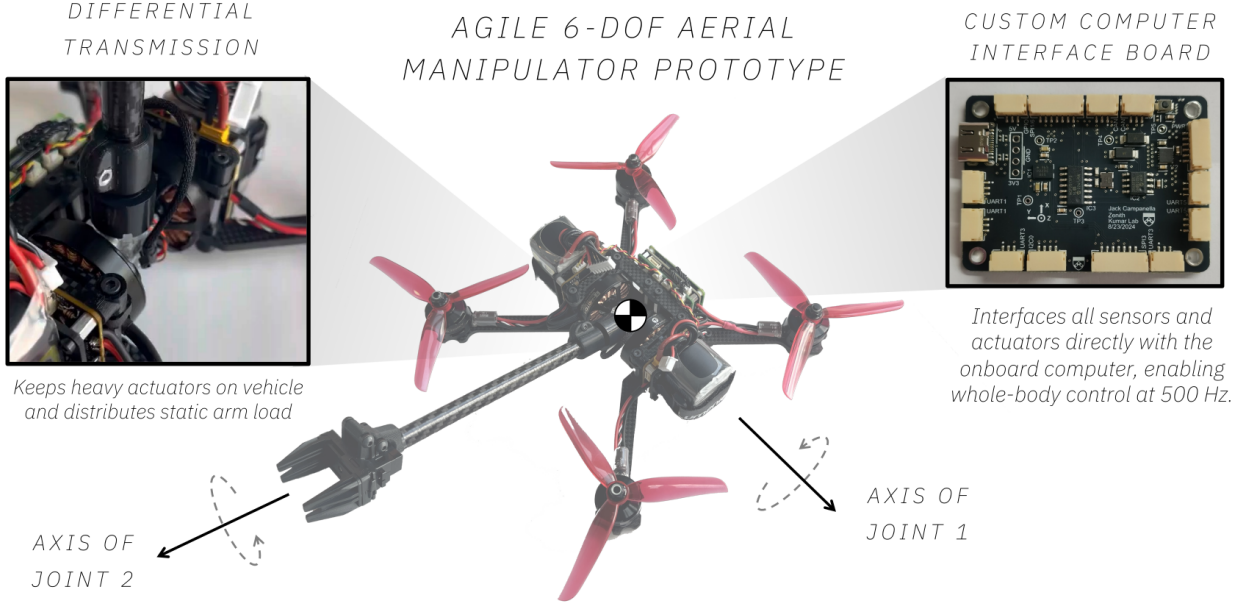
Figure 8.1: In-progress prototype of a 2-joint aerial manipulator, designed to meet the task flatness criteria of Chapter 4, towards the goal of agile 6-DoF aerial manipulation. In particular, the custom electronics were developed in collaboration with Jack Campanella, who designed the printed circuit board layout [153], and Saibernard Yogendran also contributed to the development of actuator communication firmware.

In our ongoing work, we have developed a hardware prototype of a quadrotor equipped with a 2-DoF manipulator arm (see Fig. 8.1), targeted towards highly dynamic manipulation tasks. This system has been designed with "task flatness" in mind (*i.e.*, ensuring that the end effector pose is a flat output of the system) by distributing the vehicle's mass symmetrically around the intersection of the two joints in the arm. This intersection occurs at the center of a differential gearbox, which transmits torques from two powerful brushless motors located on the vehicle body (and arranged symmetrically about the sagittal plane of the robot), keeping the arm lightweight. In order to tightly coordinate the control of both the vehicle and the arm degrees of freedom (jointly recruiting effort from both the propellers and the internal joint actuators), custom software and electronics have been developed to integrate all sensors and actuators directly with an onboard computer running real-time Linux. In our ongoing work, we pursue dynamic manipulation tasks with this platform, in hopes of operationalizing the design criteria of Chapter 4, the subsystem tracking controller designs of Chapter 5, and the cascade stability certificates of Chapter 6.

In a broader sense, the control algorithms developed in this thesis aim to achieve greater generality and computational efficiency by leveraging the structural properties of mechanical systems. In that sense, the physical characteristics of the system under consideration inform control design. Conversely, the mechanical design criteria obtained in Chapter 4 constitute feedback in the opposite direction, in which mathematically rigorous control insights inform physical morphology design, at least for a particular class of

systems (*i.e.*, aerial manipulators). However, this feedback is essentially parametric (helping us to choose the link lengths, center of mass position, *etc.*), and we lack a means of automatically synthesizing a completely new aerial robot morphology suited to a particular task. In the future, we hope to tighten (and also generalize) this feedback loop, achieving yet a stronger interplay between control design and morphology design for robotic systems. Indeed, in Nature, behavior and morphology evolve in tandem, and we aspire to the same for robotic systems—not only in terms of computational methods of co-design, but also in regards to a deeper conceptual understanding of the functional impact of design choices in both domains.

BIBLIOGRAPHY

[1] S. Mac Lane, *Categories for the Working Mathematician.* Springer, 1971.

[2] H. Poincaré, *Science et méthode.* E. Flammarion, Paris, 1908.

[3] L. Poinsot, *Théorie nouvelle de la rotation des corps.* Bachelier, Paris, 1851.

[4] J. M. Lee, *Introduction to Smooth Manifolds*, 2nd ed. Springer New York, 2013.

[5] J. Gallier and J. Quaintance, *Differential Geometry and Lie Groups: A Computational Perspective.* Springer, 2020.

[6] ——, *Differential Geometry and Lie Groups: A Second Course.* Springer, 2020.

[7] A. M. Bloch, *Nonholonomic Mechanics and Control.* Springer-Verlag, 2003.

[8] J. E. Marsden and T. S. Ratiu, *Introduction to Mechanics and Symmetry.* Springer-Verlag, 1999.

[9] F. Bullo and A. D. Lewis, *Geometric Control of Mechanical Systems.* Springer Verlag, 2004.

[10] J. M. Lee, *Introduction to Riemannian Manifolds.* Springer, 2018, vol. 176.

[11] J. Solà, J. Deray, and D. Atchuthan, "A micro Lie theory for state estimation in robotics," 2021, `arXiv:1812.01537 [cs.RO]`.

[12] A. Kirillov, Jr., *An Introduction to Lie groups and Lie Algebras.* Cambridge University Press, 2008.

[13] J. P. Ostrowski, "The Mechanics and Control of Undulatory Robotic Locomotion," Ph.D. dissertation, California Institute of Technology, 1996.

[14] A. Shapere and F. Wilczek, "Geometry of self-propulsion at low Reynolds number," *Journal of Fluid Mechanics*, vol. 198, p. 557–585, 1989.

[15] J. Welde, M. D. Kvalheim, and V. Kumar, "The Role of Symmetry in Constructing Geometric Flat Outputs for Free-Flying Robotic Systems," in *2023 IEEE International Conference on Robotics and Automation*, 2023, pp. 12 247–12 253.

[16] J. Welde and V. Kumar, "Towards Automatic Identification of Globally Valid Geometric Flat Outputs via Numerical Optimization," 2023, `arXiv:2305.09442 [cs.RO]`.

[17] K. J. Åström and R. M. Murray, *Feedback Systems: An Introduction for Scientists and Engineers.* Princeton University Press, 2021.

[18] N. Matni, A. D. Ames, and J. C. Doyle, "A Quantitative Framework for Layered Multirate Control: Toward a Theory of Control Architecture," *IEEE Control Systems Magazine*, vol. 44, no. 3, pp. 52–94, 2024.

[19] A. Srikanthan, V. Kumar, and N. Matni, "Augmented Lagrangian Methods as Layered Control Architectures," 2023, `arXiv:2311.06404 [math.OC]`.

[20] M. Kelly, "An Introduction to Trajectory Optimization: How to Do Your Own Direct Collocation," *SIAM Review*, vol. 59, no. 4, pp. 849–904, 2017.

[21] M. Fliess, J. Lévine, P. Martin, and P. Rouchon, "Sur les systèmes nonlinéaires différentiellement plats," *C.R. Acad. Sci. Paris*, p. 619, 1992.

[22] M. J. Van Nieuwstadt and R. M. Murray, "Real Time Trajectory Generation for Differentially Flat Systems," *International Journal of Robust and Nonlinear Control*, vol. 8, no. 11, pp. 995–1020, 1998.

[23] M. Fliess, J. Levine, P. Martin, F. Ollivier, and P. Rouchon, "Controlling Nonlinear Systems by Flatness," in *Systems and Control in the Twenty-First Century*. Birkhäuser Boston, 1997, pp. 137–154.

[24] P. Martin, R. M. Murray, and P. Rouchon, "Flat systems: open problems, infinite dimensional extension, symmetries and catalog," in *Advances in the Control of Nonlinear Systems*. Springer, 2001, pp. 33–57.

[25] D. Mellinger and V. Kumar, "Minimum snap trajectory generation and control for quadrotors," in *IEEE International Conference on Robotics and Automation*, 2011, pp. 2520–2525.

[26] K. Sreenath, T. Lee, and V. Kumar, "Geometric control and differential flatness of a quadrotor UAV with a cable-suspended load," in *IEEE Conference on Decision and Control*, 2013, pp. 2269–2274.

[27] J. Welde and V. Kumar, "Coordinate-Free Dynamics and Differential Flatness of a Class of 6DOF Aerial Manipulators," in *IEEE International Conference on Robotics and Automation*, 2020, pp. 4307–4313.

[28] J. Lévine, "On necessary and sufficient conditions for differential flatness," *Applicable Algebra in Engineering, Communications and Computing*, vol. 22, pp. 47–90, 2011.

[29] P. M. Wensing, M. Posa, Y. Hu, A. Escande, N. Mansard, and A. D. Prete, "Optimization-Based Control for Dynamic Legged Robots," *IEEE Transactions on Robotics*, vol. 40, pp. 43–63, 2024.

[30] C. Sferrazza, D. Pardo, and J. Buchli, "Numerical search for local (partial) differential flatness," *IEEE International Conference on Intelligent Robots and Systems*, pp. 3640–3646, 2016.

[31] S. F. Ma, G. Leylaz, and J.-Q. Sun, "Identification of Differentially Flat Output of Underactuated Dynamic Systems," *International Journal of Control*, vol. 0, pp. 1–27, 2020.

[32] R. M. Murray, M. Rathinam, and W. Sluis, "Differential flatness of mechanical control systems: A catalog of prototype systems," *ASME International Mechanical Engineering Congress and Exposition*, 1995.

[33] S. Tang, V. Wüest, and V. Kumar, "Aggressive Flight with Suspended Payloads Using Vision-Based Control," *IEEE Robotics and Automation Letters*, vol. 3, pp. 1152–1159, 2018.

[34] J. Thomas, J. Welde, G. Loianno, K. Daniilidis, and V. Kumar, "Autonomous Flight for Detection, Localization, and Tracking of Moving Targets with a Small Quadrotor," *IEEE Robotics and Automation Letters*, vol. 2, pp. 1762–1769, 2017.

[35] S. Sun, A. Romero, P. Foehn, E. Kaufmann, and D. Scaramuzza, "A Comparative Study of Nonlinear MPC and Differential-Flatness-Based Control for Quadrotor Agile Flight," *IEEE Transactions on Robotics*, vol. 38, no. 6, pp. 3357–3373, 2022.

[36] F. Yang, J. Welde, and N. Matni, "Learning Flatness-Preserving Residuals for Pure-Feedback Systems," in *IEEE Conference on Decision and Control (Accepted)*, 2025.

[37] M. Rathinam and R. M. Murray, "Configuration flatness of Lagrangian systems underactuated by one control," *SIAM Journal on Control and Optimization*, vol. 36, pp. 164–179, 1998.

[38] K. Sato and T. Iwai, "Configuration flatness of Lagrangian control systems with fewer controls than degrees of freedom," *Systems and Control Letters*, vol. 61, pp. 334–342, 2012.

[39] J. Thomas, G. Loianno, J. Polin, K. Sreenath, and V. Kumar, "Toward autonomous avian-inspired grasping for micro aerial vehicles," *Bioinspiration and Biomimetics*, vol. 9, 2014.

[40] J. Welde, J. Paulos, and V. Kumar, "Dynamically Feasible Task Space Planning for Underactuated Aerial Manipulators," *IEEE Robotics and Automation Letters*, vol. 6, pp. 3232–3239, 2021.

[41] M. Watterson and V. Kumar, "Control of Quadrotors using the Hopf Fibration on SO(3)," *International Symposium on Robotics Research*, 2017.

[42] R. Seifried and W. Blajer, "Analysis of servo-constraint problems for underactuated multibody systems," *Mechanical Sciences*, vol. 4, pp. 113–129, 2013.

[43] E. Noether, "Invariante variationsprobleme," *Nachrichten von der Gesellschaft der Wissenschaften zu Göttingen, Mathematisch-Physikalische Klasse*, vol. 1918, pp. 235–257, 1918.

[44] R. Montgomery, "Gauge Theory of the Falling Cat," *Fields Institute Communications*, 1993.

[45] A. M. Bloch, P. Krishnaprasad, J. E. Marsden, and R. M. Murray, "Nonholonomic mechanical systems with symmetry," *Archive for Rational Mechanics and Analysis*, vol. 136, no. 1, pp. 21–99, 1996.

[46] R. M. Murray, "Nonlinear Control of Mechanical Systems: A Lagrangian Perspective," *Annual Reviews in Control*, vol. 21, pp. 31–42, 1997.

[47] T. Dear, S. D. Kelly, M. Travers, and H. Choset, "Motion planning and differential flatness of mechanical systems on principal bundles," in *ASME Dynamic Systems and Control Conference*, 2015.

[48] P. M. Wensing, J. Englsberger, and J.-J. E. Slotine, "Coriolis Factorizations and their *Connections* to Riemannian Geometry," 2023, `arXiv:2312.14425 [eess.SY]`.

[49] P. Martin, P. Rouchon, and R. M. Murray, "Flat Systems, Equivalence and Trajectory Generation," *CDS Technical Report*, pp. 1–81, 2003.

[50] M. Rathinam, "Differentially Flat Nonlinear Control Systems," Ph.D. dissertation, California Institute of Technology, 1997.

[51] F. Bullo, "On Controllability and Symmetries in Simple Mechanical Systems," California Institute of Technology, Tech. Rep., 1996.

[52] M. Konz and J. Rudolph, "Quadrotor tracking control based on a moving frame," in *IFAC Symposium on Nonlinear Control Systems*, 2013, pp. 80–85.

[53] R. L. Hatton and H. Choset, "Geometric motion planning: The local connection, Stokes' theorem, and the importance of coordinate choice," *International Journal of Robotics Research*, vol. 30, pp. 988–1014, 2011.

[54] M. Travers, R. Hatton, and H. Choset, "Minimum perturbation coordinates on SO(3)," in *American Control Conference*, 2013, pp. 2006–2012.

[55] Y.-M. Chen, G. Nelson, R. Griffin, M. Posa, and J. Pratt, "Angular Center of Mass for Humanoid Robots," 2022, `arXiv:2210.08111 [cs.RO]`.

[56] A. Saccon, S. Traversaro, F. Nori, and H. Nijmeijer, "On Centroidal Dynamics and Integrability of Average Angular Velocity," *IEEE Robotics and Automation Letters*, vol. 2, pp. 943–950, 2017.

[57] H. A. Boateng and K. Bradach, "Triquintic interpolation in three dimensions," *Journal of Computational and Applied Mathematics*, 2023.

[58] S. Jayan and K. Nagaraja, "Numerical integration over n-dimensional cubes using generalized Gaussian quadrature," in *the Jangjeon Mathematical Society*, vol. 17, 2014, pp. 63–69.

[59] K. Mao, J. Welde, M. A. Hsieh, and V. Kumar, "Trajectory Planning for the Bidirectional Quadrotor as a Differentially Flat Hybrid System," in *IEEE International Conference on Robotics and Automation*, 2023, pp. 1242–1248.

[60] A. D. Lewis, "Affine Connection Control Systems," in *Lagrangian and Hamiltonian Methods for Non-linear Control*, 2000, pp. 123–128.

[61] M. Faessler, A. Franchi, and D. Scaramuzza, "Differential Flatness of Quadrotor Dynamics Subject to Rotor Drag for Accurate Tracking of High-Speed Trajectories," *IEEE Robotics and Automation Letters*, vol. 3, no. 2, pp. 620–626, 2018.

[62] Willow Garage, Inc., "Unified Robot Description Format," `http://wiki.ros.org/urdf/`, 2009.

[63] J. Carpentier, F. Valenza, N. Mansard, *et al.*, "Pinocchio: fast forward and inverse dynamics for poly-articulated systems," `https://stack-of-tasks.github.io/pinocchio`, 2015–2023.

[64] S. Echeandia and P. M. Wensing, "Numerical Methods to Compute the Coriolis Matrix and Christoffel Symbols for Rigid-Body Systems," *Journal of Computational and Nonlinear Dynamics*, vol. 16, no. 9, 07 2021.

[65] M. van Nieuwstadt, M. Rathinam, and R. Murray, "Differential flatness and absolute equivalence," in *1994 33rd IEEE Conference on Decision and Control*, vol. 1, 1994, pp. 326–332 vol.1.

[66] J. Thomas, "Grasping, Perching, and Visual Servoing for Micro Aerial Vehicles," Ph.D. dissertation, University of Pennsylvania, 2017.

[67] M. van Nieuwstadt and R. Murray, "Approximate Trajectory Generation for Differentially Flat Systems with Zero Dynamics," in *1995 34th IEEE Conference on Decision and Control*, vol. 4, 1995, pp. 4224–4230.

[68] B. Yüksel, G. Buondonno, and A. Franchi, "Differential Flatness and Control of Protocentric Aerial Manipulators with Any Number of Arms and Mixed Rigid/Elastic Joints," in *IEEE International Conference on Intelligent Robots and Systems*, 2016, pp. 561–566.

[69] X. Ding, P. Guo, K. Xu, and Y. Yu, "A review of aerial manipulation of small-scale rotorcraft unmanned robotic systems," *Chinese Journal of Aeronautics*, vol. 32, pp. 200–214, 2019.

[70] F. Augugliaro, S. Lupashin, M. Hamer, C. Male, M. Hehn, M. W. Mueller, J. S. Willmann, F. Gramazio, M. Kohler, and R. D'Andrea, "The Flight Assembled Architecture installation: Cooperative construction with flying machines," *IEEE Control Systems Magazine*, vol. 34, pp. 46–64, 2014.

[71] S. Kim, S. Choi, and H. J. Kim, "Aerial manipulation using a quadrotor with a two dof robotic arm," *IEEE International Conference on Intelligent Robots and Systems*, pp. 4990–4995, 2013.

[72] M. Ángel Trujillo, J. R. M.-D. Dios, C. Martín, A. Viguria, and A. Ollero, "Novel aerial manipulator for accurate and robust industrial NDT contact inspection: A new tool for the oil and gas inspection industry," *Sensors*, vol. 19, 2019.

[73] K. Bodie, M. Brunner, M. Pantic, S. Walser, P. Pfändler, U. Angst, R. Siegwart, and J. Nieto, "An Omnidirectional Aerial Manipulation Platform for Contact-Based Inspection," in *Robotics: Science and Systems*, Freiburg im Breisgau, Germany, June 2019.

[74] M. Tognon, H. A. Chavez, E. Gasparin, Q. Sable, D. Bicego, A. Mallet, M. Lany, G. Santi, B. Revaz, J. Cortes, and A. Franchi, "A Truly-Redundant Aerial Manipulator System with Application to Push-and-Slide Inspection in Industrial Plants," *IEEE Robotics and Automation Letters*, vol. 4, pp. 1846–1851, 2019.

[75] G. Garofalo, F. Beck, and C. Ott, "Task-space Tracking Control for Underactuated Aerial Manipulators," in *European Control Conference*, 2018, pp. 628–634.

[76] G. Heredia, A. E. Jimenez-Cano, I. Sanchez, D. Llorente, V. Vega, J. Braga, J. A. Acosta, and A. Ollero, "Control of a multirotor outdoor aerial manipulator," in *IEEE International Conference on Intelligent Robots and Systems*, 2014, pp. 3417–3422.

[77] G. Zhang, Y. He, B. Dai, F. Gu, L. Yang, J. Han, G. Liu, and J. Qi, "Grasp a moving target from the air: System control of an aerial manipulator," *IEEE International Conference on Robotics and Automation*, pp. 1681–1687, 2018.

[78] A. Sharon, N. Hogan, and D. Hardt, "The Macro/Micro Manipulator: An Improved Architecture for Robot Control," *IEEE Transactions on Robotics and Automation*, vol. 10, pp. 209–222, 1988.

[79] A. S. Vempati, M. Kamel, N. Stilinovic, Q. Zhang, D. Reusser, I. Sa, J. Nieto, R. Siegwart, and P. Beardsley, "PaintCopter: An autonomous UAV for spray painting on three-dimensional surfaces," *IEEE Robotics and Automation Letters*, vol. 3, pp. 2862–2869, 2018.

[80] R. Spica, A. Franchi, G. Oriolo, H. H. Bulthoff, and P. R. Giordano, "Aerial grasping of a moving target with a quadrotor UAV," *IEEE International Conference on Intelligent Robots and Systems*, pp. 4985–4992, 2012.

[81] P. J. From, "An Explicit Formulation of Singularity-Free Dynamic Equations of Mechanical Systems in Lagrangian Form - Part Two: Multibody Systems," *Modeling, Identification and Control*, vol. 33, pp. 61–68, 2012.

[82] H. Yang and D. Lee, "Dynamics and control of quadrotor with robotic manipulator," in *IEEE International Conference on Robotics and Automation*. IEEE, 2014, pp. 5544–5549.

[83] D. DeMers and K. Kreutz-Delgado, "Global Regularization of Inverse Kinematics for Redundant Manipulators," *Advances in Neural Information Processing Systems*, vol. 5, pp. 255–262, 1993.

[84] H. K. Khalil, *Nonlinear Systems*, 3rd ed. Prentice Hall, 2002.

[85] H. N. Nguyen, C. Ha, and D. Lee, "Mechanics, control and internal dynamics of quadrotor tool operation," *Automatica*, vol. 61, 2015.

[86] J. C. Ryu, V. Sangwan, and S. K. Agrawal, "Differentially flat designs of underactuated mobile manipulators," *Journal of Dynamic Systems, Measurement and Control, Transactions of the ASME*, vol. 132, pp. 1–6, 2010.

[87] R. Schneider, D. Honerkamp, T. Welschehold, and A. Valada, "Task-driven co-design of mobile manipulators," *IEEE Robotics and Automation Letters*, vol. 10, no. 7, pp. 7158–7165, 2025.

[88] J. Welde and V. Kumar, "Almost Global Asymptotic Trajectory Tracking for Fully-Actuated Mechanical Systems on Homogeneous Riemannian Manifolds," *IEEE Control Systems Letters*, vol. 8, pp. 724–729, 2024.

[89] J. Di Carlo, P. M. Wensing, B. Katz, G. Bledt, and S. Kim, "Dynamic locomotion in the MIT Cheetah 3 through convex model-predictive control," in *IEEE International Conference on Intelligent Robots and Systems*, 2018.

[90] K. Nguyen, S. Schoedel, A. Alavilli, B. Plancher, and Z. Manchester, "TinyMPC: Model-Predictive Control on Resource-Constrained Microcontrollers," in *IEEE International Conference on Robotics and Automation*, 2024.

[91] A. Molchanov, T. Chen, W. Hönig, J. A. Preiss, N. Ayanian, and G. S. Sukhatme, "Sim-to-(Multi)-Real: Transfer of Low-Level Robust Control Policies to Multiple Quadrotors," in *IEEE International Conference on Intelligent Robots and Systems*, 2019, pp. 59–66.

[92] E. Kaufmann, L. Bauersfeld, and D. Scaramuzza, "A Benchmark Comparison of Learned Control Policies for Agile Quadrotor Flight," in *International Conference on Robotics and Automation*, 2022, pp. 10 504–10 510.

[93] K. Huang, R. Rana, A. Spitzer, G. Shi, and B. Boots, "DATT: Deep Adaptive Trajectory Tracking for Quadrotor Control," in *Conference on Robot Learning*, 2023, pp. 326–340.

[94] P. Kunapuli, J. Welde, D. Jayaraman, and V. Kumar, "Leveling the Playing Field: Carefully Comparing Classical and Learned Controllers for Quadrotor Trajectory Tracking," in *Robotics: Science and Systems*, Los Angeles, CA, USA, 2025.

[95] D. S. Maithripala, J. M. Berg, and W. P. Dayawansa, "Almost-global tracking of simple mechanical systems on a general class of Lie groups," *IEEE Transactions on Automatic Control*, vol. 51, no. 2, pp. 216–225, 2006.

[96] T. Lee, M. Leok, and N. H. McClamroch, "Geometric tracking control of a quadrotor UAV on SE(3)," in *IEEE Conference on Decision and Control*, 2010, pp. 5420–5425.

[97] D. E. Koditschek, "The Application of Total Energy as a Lyapunov Function for Mechanical Control Systems," *Contemporary Mathematics*, vol. 97, p. 131, 1989.

[98] A. Nayak and R. N. Banavar, "On Almost-Global Tracking for a Certain Class of Simple Mechanical Systems," *IEEE Transactions on Automatic Control*, vol. 64, no. 1, pp. 412–419, 2019.

[99] E. Bernuau, W. Perruquetti, and E. Moulay, "Retraction obstruction to time-varying stabilization," *Automatica*, vol. 49, no. 6, pp. 1941–1943, 2013.

[100] F. Bullo and R. M. Murray, "Tracking for Fully Actuated Mechanical Systems: A Geometric Framework," *Automatica*, vol. 35, no. 1, pp. 17–34, 1999.

[101] D. Kooijman, A. P. Schoellig, and D. J. Antunes, "Trajectory Tracking for Quadrotors with Attitude Control on $\mathcal{S}^2 \times \mathcal{S}^1$," in *European Control Conference*, 2019, pp. 4002–4009.

[102] K. Gamagedara, M. Bisheban, E. Kaufman, and T. Lee, "Geometric Controls of a Quadrotor UAV with Decoupled Yaw Control," in *American Control Conference*, 2019, pp. 3285–3290.

[103] D. Brescianini and R. D'Andrea, "Tilt-Prioritized Quadrocopter Attitude Control," *IEEE Transactions on Control Systems Technology*, vol. 28, no. 2, pp. 376–387, 2020.

[104] M. Hampsey, P. van Goor, and R. Mahony, "Tracking control on homogeneous spaces: the Equivariant Regulator (EqR)," in *IFAC World Congress*, 2023, pp. 7462–7467.

[105] S. Gudmundsson and E. Kappos, "On the geometry of tangent bundles," *Expositiones Mathematicae*, vol. 20, no. 1, pp. 1–41, 2002.

[106] P. Martin, P. Rouchon, and J. Rudolph, "Invariant tracking," *ESAIM: Control, Optimisation and Calculus of Variations*, vol. 10, no. 1, pp. 1–13, 2004.

[107] T. Lee, "Optimal hybrid controls for global exponential tracking on the two-sphere," in *IEEE Conference on Decision and Control*, 2016, pp. 3331–3337.

[108] N. J. Cowan, "Navigation Functions on Cross Product Spaces," *IEEE Transactions on Automatic Control*, vol. 52, no. 7, pp. 1297–1302, 2007.

[109] R. Mahony, P. Van Goor, and T. Hamel, "Observer Design for Nonlinear Systems with Equivariance," *Annual Review of Control, Robotics, and Autonomous Systems*, vol. 5, no. 1, pp. 221–252, 2022.

[110] O. Kowalski and J. Szenthe, "On the existence of homogeneous geodesics in homogeneous Riemannian manifolds," *Geometriae Dedicata*, vol. 81, no. 1-3, pp. 209–214, 2000.

[111] D. B. A. Epstein and A. Marden, "Convex hulls in hyperbolic space, a theorem of Sullivan, and measured pleated surfaces," in *Fundamentals of Hyperbolic Manifolds: Selected Expositions.* Cambridge Univ. Press, 2006, pp. 117–266.

[112] D. Brescianini and R. D'Andrea, "Design, modeling and control of an omni-directional aerial vehicle," in *IEEE International Conference on Robotics and Automation*, 2016, pp. 3261–3266.

[113] J. Welde, M. D. Kvalheim, and V. Kumar, "A Compositional Approach to Certifying Almost Global Asymptotic Stability of Cascade Systems," *IEEE Control Systems Letters*, vol. 7, pp. 1969–1974, 2023.

[114] P. Kokotović and M. Arcak, "Constructive nonlinear control: a historical perspective," *Automatica*, vol. 37, no. 5, pp. 637–662, 2001.

[115] R. Olfati-Saber, "Cascade normal forms for underactuated mechanical systems," in *IEEE Conference on Decision and Control*, vol. 3, 2000, pp. 2162–2167.

[116] D. Angeli, "An almost global notion of input-to-state stability," *IEEE Transactions on Automatic Control*, vol. 49, no. 6, pp. 866–874, 2004.

[117] R. Sepulchre, M. Jankovic, and P. V. Kokotovic, *Constructive Nonlinear Control.* Springer, 1997.

[118] P. Seibert and R. Suarez, "Global stabilization of nonlinear cascade systems," *Systems & Control Letters*, vol. 14, no. 4, pp. 347–352, 1990.

[119] E. D. Sontag, "Remarks on stabilization and input-to-state stability," in *IEEE Conference on Decision and Control*, vol. 2, 1989, pp. 1376–1378.

[120] C. G. Mayhew and A. R. Teel, "On the topological structure of attraction basins for differential inclusions," *Systems and Control Letters*, vol. 60, no. 12, pp. 1045–1050, 2011.

[121] P. Kokotović, H. K. Khalil, and J. O'reilly, *Singular Perturbation Methods in Control: Analysis and Design.* SIAM, 1999.

[122] F. W. Wilson, Jr., "The structure of the level surfaces of a Lyapunov function," *Journal of Differential Equations*, vol. 3, pp. 323–329, 1967.

[123] S. P. Bhat and D. S. Bernstein, "A topological obstruction to continuous global stabilization of rotational motion and the unwinding phenomenon," *Systems & Control Letters*, vol. 39, no. 1, pp. 63–70, 2000.

[124] D. Angeli and L. Praly, "Stability robustness in the presence of exponentially unstable isolated equilibria," *IEEE Transactions on Automatic Control*, vol. 56, no. 7, pp. 1582–1592, 2010.

[125] K. Mischaikow, H. Smith, and H. R. Thieme, "Asymptotically Autonomous Semiflows: Chain Recurrence and Lyapunov Functions," *Transactions of the American Mathematical Society*, vol. 347, no. 5, pp. 1669–1685, 1995.

[126] C. Robinson, *Dynamical Systems: Stability, Symbolic Dynamics, and Chaos.* CRC press, 1998.

[127] J. J. Palis and W. de Melo, *Geometric Theory of Dynamical Systems: An Introduction.* Springer, 1982.

[128] J. Eldering, M. Kvalheim, and S. Revzen, "Global linearization and fiber bundle structure of invariant manifolds," *Nonlinearity*, vol. 31, no. 9, p. 4202, 2018.

[129] J. Lee, *Introduction to Topological Manifolds.* Springer, 2010, vol. 202.

[130] M. Benaim and M. W. Hirsch, "Dynamics of Morse-Smale urn processes," *Ergodic Theory and Dynamical Systems*, vol. 15, no. 6, pp. 1005–1030, 1995.

[131] V. Santibáñez and R. Kelly, "Strict Lyapunov functions for control of robot manipulators," *Automatica*, vol. 33, no. 4, pp. 675–682, 1997.

[132] J. Welde*, N. Rao*, P. Kunapuli*, D. Jayaraman, and V. Kumar, "Leveraging Symmetry to Accelerate Learning of Trajectory Tracking Controllers for Free-Flying Robotic Systems," in *IEEE International Conference on Robotics and Automation*, 2025, *equal contribution.

[133] J. Hwangbo, I. Sa, R. Y. Siegwart, and M. Hutter, "Control of a Quadrotor With Reinforcement Learning," *IEEE Robotics and Automation Letters*, vol. 2, pp. 2096–2103, 2017.

[134] N. Rudin, D. Hoeller, P. Reist, and M. Hutter, "Learning to Walk in Minutes Using Massively Parallel Deep Reinforcement Learning," in *Conference on Robot Learning*, 2022, pp. 91–100.

[135] J. Ostrowski, "Computing reduced equations for robotic systems with constraints and symmetries," *IEEE Transactions on Robotics and Automation*, vol. 15, no. 1, pp. 111–123, 1999.

[136] D. F. Ordonez-Apraez, M. Martin, A. Agudo, and F. Moreno, "On discrete symmetries of robotics systems: A group-theoretic and data-driven analysis," in *Robotics: Science and Systems*, Daegu, Republic of Korea, July 2023.

[137] R. L. Hatton, Z. Brock, S. Chen, H. Choset, H. Faraji, R. Fu, N. Justus, and S. Ramasamy, "The Geometry of Optimal Gaits for Inertia-Dominated Kinematic Systems," *IEEE Transactions on Robotics*, vol. 38, no. 5, pp. 3279–3299, 2022.

[138] M. Hampsey, P. van Goor, T. Hamel, and R. Mahony, "Exploiting Different Symmetries for Trajectory Tracking Control with Application to Quadrotors," in *IFAC Symposium on Nonlinear Control Systems*, 2023, pp. 132–137.

[139] S. Teng, D. Chen, W. Clark, and M. Ghaffari, "An Error-State Model Predictive Control on Connected Matrix Lie Groups for Legged Robot Control," in *IEEE International Conference on Intelligent Robots and Systems*, 2022, pp. 8850–8857.

[140] D. Wang, R. Walters, X. Zhu, and R. Platt, "Equivariant Q Learning in Spatial Action Spaces," in *Conference on Robot Learning*, 2022, pp. 1713–1723.

[141] E. van der Pol, D. Worrall, H. van Hoof, F. Oliehoek, and M. Welling, "MDP Homomorphic Networks: Group Symmetries in Reinforcement Learning," in *Advances in Neural Information Processing Systems*, 2020, pp. 4199–4210.

[142] B. Ravindran, "An Algebraic Approach to Abstraction in Reinforcement Learning," Ph.D. dissertation, University of Massachusetts Amherst, 2004.

[143] B. Yu and T. Lee, "Equivariant Reinforcement Learning for Quadrotor UAV," in *American Control Conference*, 2023, pp. 2842–2847.

[144] P. Panangaden, S. Rezaei-Shoshtari, R. Zhao, D. Meger, and D. Precup, "Policy Gradient Methods in the Presence of Symmetries and State Abstractions," *Journal of Machine Learning Research*, vol. 25, no. 71, pp. 1–57, 2024.

[145] S. Rezaei-Shoshtari, R. Zhao, P. Panangaden, D. Meger, and D. Precup, "Continuous MDP Homomorphisms and Homomorphic Policy Gradient," in *Advances in Neural Information Processing Systems*, vol. 35, 2022, pp. 20 189–20 204.

[146] R. Y. Zhao, "Continuous Homomorphisms and Leveraging Symmetries in Policy Gradient Algorithms for Markov Decision Processes," Master's thesis, McGill University, 2022.

[147] T. tom Dieck, *Algebraic Topology*. European Mathematical Society, 2008.

[148] M. Bualat, J. Barlow, T. Fong, C. Provencher, and T. Smith, "Astrobee: Developing a free-flying robot for the international space station," in *AIAA SPACE Conference and Exposition*, 2015, p. 4643.

[149] N. A. Rao, "Exploring Symmetries and Equivariance in Robot Learning," Master's thesis, University of Pennsylvania, 2025.

[150] J. Bradbury, R. Frostig, P. Hawkins, M. J. Johnson, C. Leary, D. Maclaurin, G. Necula, A. Paszke, J. VanderPlas, S. Wanderman-Milne, and Q. Zhang, "JAX: composable transformations of Python+NumPy programs," `http://github.com/google/jax`, 2018.

[151] J. Schulman, F. Wolski, P. Dhariwal, A. Radford, and O. Klimov, "Proximal Policy Optimization Algorithms," 2017, `arXiv:1707.06347 [cs.LG]`.

[152] V. Makoviychuk, L. Wawrzyniak, Y. Guo, M. Lu, K. Storey, M. Macklin, D. Hoeller, N. Rudin, A. Allshire, A. Handa, and G. State, "Isaac Gym: High Performance GPU-Based Physics Simulation For Robot Learning," 2021, `arXiv:2108.10470 [cs.RO]`.

[153] J. Campanella, "Integrated Hardware and Software Codesign for Controlling Underactuated Aerial Robots," Master's thesis, University of Pennsylvania, 2025.